

8-2016

## Heparin-Peptide Interactions

Jacqueline Anastasia Morris  
*University of Arkansas, Fayetteville*

Follow this and additional works at: <https://scholarworks.uark.edu/etd>



Part of the [Analytical Chemistry Commons](#), and the [Biochemistry Commons](#)

---

### Citation

Morris, J. A. (2016). Heparin-Peptide Interactions. *Graduate Theses and Dissertations* Retrieved from <https://scholarworks.uark.edu/etd/2645>

This Dissertation is brought to you for free and open access by ScholarWorks@UARK. It has been accepted for inclusion in Graduate Theses and Dissertations by an authorized administrator of ScholarWorks@UARK. For more information, please contact [uarepos@uark.edu](mailto:uarepos@uark.edu).

# Heparin-Peptide Interactions

A dissertation submitted in partial fulfillment  
of the requirements for the degree of  
Doctor of Philosophy in Chemistry

By

Jacqueline Anastasia Morris  
Stephen F. Austin State University  
Bachelor of Science in Biochemistry, 2010

August 2016  
University of Arkansas

This dissertation is approved for recommendation to the Graduate Council.

---

Thallapuram Krishnaswamy Suresh Kumar, Ph.D.  
Committee Chair

---

Jingyi Chen, Ph.D.  
Committee Member

---

Dan Davis, Ph.D.  
Committee Member

---

Roger Koeppe II, Ph.D.  
Committee Member

## **Abstract**

Heparin is a polydispersed sulfated molecule that is part of the family called glycosaminoglycans found in the extracellular matrix and cell surfaces. This molecule is extremely important for the activation of proteins and protein-receptor interactions that are responsible for downstream cell signaling pathways. Heparin has been isolated from porcine intestine and used as an anticoagulant for the prevention of embolisms, heart thrombosis, and clotting during heart surgeries. This so-called miracle drug was in use until 2008, when isolated batches were found to be contaminated with other glycosaminoglycans similar to heparin. From 2008, there has been a dire need for a more cost-effective purification of heparin in good yield, to remove the contaminants.

Heparin has also been used for affinity chromatography to purify heparin-binding proteins. Recombinant protein purification is an important aspect of biotechnology, with a heavy emphasis on developing easy purification systems for large quantities of homogeneously pure therapeutic proteins at low costs. Several affinity tags have been employed to aid in the expression and purification of various proteins. There are, however, various disadvantages, such as interference with the target protein structure, unsuitable elution conditions, multiple-step purification procedures, and many others.

In this context, a novel heparin-binding peptide (HB-peptide) was designed based on the heparin-binding region of acidic fibroblast growth factor (FGF-1). The HB-peptide has been shown to bind to heparin with better affinity than other glycosaminoglycans. A one-step Heparin-Sepharose-based purification procedure was developed for various recombinant proteins using mild elution conditions. Using proteolytic cleavage, the affinity tag was removed to obtain a folded protein. Polyclonal antibodies were also grown against the specific sequence of the HB-

peptide, which then were used to successfully and specifically bind fusion proteins that only contained the HB-peptide even at the nanogram level.

HB-peptide was then coupled onto a solid matrix to be used as an affinity column, in a similar fashion as heparin-Sepharose with HBPs. Glycosaminoglycans that were in a mixture were separated from each other for the most part. In this context, our HB-peptide can be used as a means to separate glycosaminoglycans, yielding pure heparin for future medical use.

©2016 by Jacqueline Morris  
All Rights Reserved

## Acknowledgements

I want to thank my husband, Scott, who has helped me stay in graduate school even when I wanted to give up and drop out. Thank you for your love, spiritual leadership, and discipleship in my walk with Jesus. I want to also thank my family for their support and love to help me “be whatever I want to be.” I guess a chemist pays more than the Broadway star I dreamed of.

I want to thank my true family and body of Christ who has loved Scott and me and prayed for us in the ups and downs. I want to thank my friends that I have met in graduate school who have come alongside me during this time. Keep your eyes on Jesus!

I also want to thank the professors at SFASU, who truly poured into me during my time there. A special shout out to Dr. Michele Harris for your guidance, love, and many prayers during my saved and unsaved life. Thank you Dr. Kefa Onchoke for you always pushing me to do my best in Chemistry. Your laugh and love for students is so wonderful to see!

I want to thank my committee for your suggestions and wonderful attitudes during my committee meetings, and especially outside of lab. You have been a great and not super scary committee that has helped me grow in my graduate school career. I thank the Kumar lab group for helping me when I didn't understand certain aspects of research, especially Beatrice Kachel and Srinivas Jayanthi. You both have encouraged me even during the times research was a nightmare!!! I also thank my advisor, Dr. Kumar, for all of your guidance and help along the way. I also admire your dedication and love for teaching!

Above all else, I want to thank my Lord and Savior, Jesus Christ, for saving me 5 years ago from a life of complete destruction. I am literally eternally grateful for the freedom You have given me through the cross at Calvary. I have now found the purpose and fulfillment of life. Praise the Lord for keeping me in this program and giving me the strength to finish!

## **Dedication**

I dedicate this dissertation to my husband, Scott, and to our two beautiful unborn children who are worshipping Jesus face to face in Heaven right now.

## Table of Contents

	Page
Chapter 1: Introduction.....	1
1.1. Extracellular Matrix.....	2
1.2. Proteoglycans.....	3
1.3. Glycosaminoglycans.....	5
1.4. Significance of Glycosaminoglycans.....	13
1.5. Use of Heparin in Disease.....	17
1.6. Heparin Contamination.....	20
1.7. Heparin-Binding Proteins.....	22
1.8. Heparin-Binding Region of Heparin-Binding Proteins.....	29
1.9. Recombinant DNA Cloning and Protein Expression.....	32
1.10. Chromatography for Protein Purification.....	37
1.11. Affinity Tags.....	40
1.12. Detection of Proteins by Immunoblotting.....	47
1.13. References.....	49
Chapter 2: Use of Heparin-Binding Affinity Tag for Protein Purification.....	83
2.1. Abstract.....	84
2.2. Introduction.....	85
2.3. Materials and Methods.....	86
2.4. Results and Discussion.....	92
2.5. References.....	122



Chapter 3: Detection of HB-Fusion Proteins Using Polyclonal Antibodies.....	127
3.1. Abstract.....	128
3.2. Introduction.....	128
3.3. Materials and Methods.....	130
3.4. Results and Discussion.....	133
3.5. References.....	148
Chapter 4: Separation of Glycosaminoglycans by HB-Affinity Column.....	151
4.1. Abstract.....	152
4.2. Introduction.....	153
4.3. Materials and Methods.....	155
4.4. Results and Discussion.....	160
4.5. References.....	193
Chapter 5: Conclusions.....	198
Biosafety Committee Approval Letter.....	203
Copyright Permission for Figure 1.5.....	204
Copyright Permission for Figure 2.32.....	209

## Abbreviations

**ECM**, extracellular matrix; **PG**, proteoglycan; **CS**, chondroitin sulfate; **HS**, heparan sulfate; **GAG**, glycosaminoglycans; **KS**, keratan sulfate; **DS**, dermatan sulfate; **HA**, hyaluronic acid; **GlcNAc**, N-acetyl-D-glucosamine; **GalNAc**, N-acetyl-D-galactosamine; **GlcA**, glucuronic acid; **IdoA**, iduronic acid; **CNS**, central nervous system; **FGF**, fibroblast growth factor; **FGFR**, fibroblast growth factor receptor; **HBP**, heparin-binding protein; **ATIII**, antithrombin III; **HIV-1**, human immunodeficiency virus-1; **pRBC**, *Plasmodium*-infected red blood cell; **UFH**, unfractionated heparin; **LMWH**, low-molecular-weight heparin; **OSCS**, oversulfated chondroitin sulfate; **FHF**, FGF homologous factor; **HBR**, heparin-binding region; **MAPK**, mitogen-activated protein kinase; **PI3K**, phosphoinositide 3-kinase; **PLC $\gamma$** , phospholipase C $\gamma$ ; **TGF**, transforming growth factor; **YAC**, yeast artificial chromosome; **BAC**, bacterial artificial chromosome; **SDS-PAGE**, sodium dodecylsulfate polyacrylamide gel electrophoresis; **TB**, terrific broth; **IPTG**, isopropyl- $\beta$ -D-1-thiogalactopyranoside; **GST**, glutathione-S-transferase; **MBP**, maltose-binding protein; **His-tag**, polyhistidine tag; **SEC**, size-exclusion chromatography; **SUMO**, small ubiquitin-like modifier; **CBP**, calmodulin-binding peptide; **IMAC**, immobilized metal affinity chromatography; **TEV**, tobacco etch virus; **NBT/BCIP**, nitro-blue tetrazolium and 5-bromo-4-chloro-3'-indolyphosphate; **SOS**, sucrose octasulfate; **LB**, Luria-Bertani; **PBS**, phosphate buffered saline; **GSH**, reduced glutathione; **IPA**, isopropyl alcohol; **ITC**, isothermal titration calorimetry; **CD**, circular dichroism; **HSQC**, heteronuclear single quantum coherence spectroscopy; **NMR**, nuclear magnetic resonance; **MALDI-TOF**, matrix-assisted

desorption/ionization time-of-flight; **DMSO**, dimethyl sulfoxide; **PMSF**, phenylmethylsulfonylfluoride; **TCA**, trichloroacetic acid; **DTT**, dithiothreitol; **PVD**, polyvinylidene difluoride; **KLH**, keyhole limpet hemocyanin; **MBS**, m-maleimidobenzoyl-N-hydroxysuccinimide; **TBS-T**, Tris buffered saline with Tween 20; **BSA**, bovine serum albumin; **NHS**, N-hydroxysuccinimide; **CV**, column volume; **FITC**, fluorescein isothiocyanate

## List of papers

### Chapter 1, published

Thallapuram, S. K.; Jayanthi, S.; Morris, J.; Brown, A.; McNabb, D.; Henry, R. Heparin affinity tag for protein purification. 2014-US12340, 2015112121, 20140121., 2015.

Morris, J.; Jayanthi, S.; Langston, R.; Daily, A.; Kight, A.; McNabb David, S.; Henry, R.; Kumar Thallapuram Krishnaswamy, S., Heparin-binding peptide as a novel affinity tag for purification of recombinant proteins. *Protein Expr Purif* **2016**.

## **Chapter 1**

### **Introduction**

## 1.1. Extracellular Matrix

The cell is a complex system of various organelles working together to achieve homeostasis for the body. Part of this process involves cells communicating with one another to start various downstream processes in order for cells to survive. Cell signaling allows cells to influence each other's fate and behavior<sup>1</sup>. Extracellular and intracellular signals orchestrate the molecular mechanisms involved in signaling. Various signals include proteins, hormones, and neurotransmitters that bind to specific cell-surface receptors for their activity<sup>2</sup>. The receptors can be other proteins or sugar molecules that proteins in the surrounding environment bind to for activity. Every cell type comes in contact with a dynamic molecular scaffold, known as the extracellular matrix (ECM), in order to perform the process of cell signaling and downstream processes<sup>3</sup>.

The ECM initiates crucial biochemical cues necessary for cell signaling and regulates almost all cellular behavior and developmental processes<sup>4,5</sup>. For endothelial cell proliferation, cytokine function, and angiogenesis, adhesion of these cells to the ECM is critical<sup>6</sup>. Cell adhesion to ECM triggers intracellular signaling pathways that regulate various cell processes, such as progression, migration, and differentiation. The biochemical properties of the ECM are highly variable from one tissue to another, within a specific tissue, and even from one physiological state to another<sup>4</sup>. Frequent remodeling processes occur in the ECM, where components are degraded, modified, or synthesized, enabling cellular functions to be regulated tightly<sup>7</sup>. The ECM is a critical source for the growth, survival, and angiogenic factors that also affect tumor progression<sup>8</sup>. Various proteins are present in this matrix that are important for cell adhesion and regulation of growth factor bioavailability of which include (1) fibrous proteins (collagen, elastin, fibronectin, and laminin), (2) proteoglycans (chondroitin sulfate proteoglycans

(CSPG) and heparan sulfate proteoglycans (HSPG)), and (3) other proteins important for development and disease (non-fibrous glycoproteins, hemostatic system proteins, neuronal guidance molecules, and growth factor associated proteins)<sup>9,10</sup>. The various fibrous proteins are present for tensile strength and stabilization, with collagens being the most abundant proteins present in mammals (25% of total protein mass in mammalian animals)<sup>11,12</sup>. The polysaccharide component in PGs form the hydrated gel composition of the ECM, with the fibrous proteins embedded in it<sup>13</sup>. The ECM contains three families of PGs: (1) large aggregating CSPGs (also known as lecticans), (2) small leucine-rich CSPGs, and (3) HSPGs<sup>14</sup>. Examples of the so-called “other” proteins unlike proteoglycans or fibrous proteins include thrombospondins, von Willebrand factor, neutrins, and insulin-like growth factor binding proteins<sup>10</sup>. Through post-translational modifications by enzymatic and non-enzymatic pathways, remodeling of the ECM occurs to release bioactive factors that enable downstream processes such as growth and morphogenesis<sup>15</sup>.

## 1.2. Proteoglycans

As stated previously, one of the major classes of compounds found in the ECM are PGs, which are ubiquitous macromolecules that play important structural and regulatory roles in the ECM<sup>16,17</sup>. PGs are composed of a protein core that is attached to the cell surface and a glycosaminoglycan (GAG) tails, by GPI-linked or membrane proteins<sup>18</sup> (Table 1.1). HS and CS/DS GAGs are attached to their respective core proteins by the same GAG-protein linkage region, which consists of GlcA( $\beta$ 1-3)Gal( $\beta$ 1-3)Gal( $\beta$ 1-4)Xyl $\beta$ 1-*O*-Ser<sup>19</sup>.

Proteoglycan class	Proteoglycan	Glycosaminoglycan chain	Core protein size (kDa)
HSPG	Glypican 1-6	1-3 HS	57-69
	Perlecan	1-4 HS	400
	Agrin	2-3 HS	212
HS/CSPG	Syndecans 1-4	1-3 CS, 1-2 HS	31-45
	$\beta$ -Glycan	1-2 HS/CS	110
	Serglycin	10-15 heparin/CS	10-19
CSPG	Bikunin	1 CS	18
	Decorin	1 DS/CS	36
	Thrombomodulin	1 CS	58
KSPG	Lumican	KS I	37
	Fibromodulin	KS I	59
	Aggrecan	KS II	200

**Table 1.1** – Properties of well-known PGs present in the body, modified from Li et al<sup>17</sup>.

In the ECM, PGs interact with other components of the ECM, such as collagens, adhesion molecules, and growth factors<sup>20</sup>. The main functions of PGs are cell adhesion and migration and a structural role for the ECM<sup>21</sup>. The families of PGs in the ECM include the two CSPGs: (1) large aggregating CSPGs known as lecticans (eg. Aggrecan, neurocan, brevican, versican), (2) small leucine-rich CSPGs (eg. Decorin, biglycan, lumican) and HSPGs (eg. Perlecan, collagen type XVIII, agrins)<sup>14,22,23,24</sup>. Other HSPGs include membrane-spanning syndecans, membrane glycosylphosphatidylinositol-linked glypicans, and serglycin, present in secretory vesicles<sup>25,26,27,28</sup>. PGs are also located on the surface of all animal cells, intracellular granules of certain cell types, and in the basement membrane of various tissues<sup>17</sup>. These molecules are thought to be the key players in disease control and progression by modulating growth factor functions<sup>29</sup>. PGs interact with various proteins and growth factors to regulate signaling pathways that are important for stem cell fate, such as Wnt and BMP<sup>30</sup>. PGs are extremely vital for cell-cell interactions, but are also implicated in numerous diseases, such as arthritis and cancer<sup>31</sup>.



They also function as joint lubricants and structural components in connective tissue<sup>32</sup>. Small PGs, such as decorin and biglycan, help form and modify collagen fibers in connective tissue for example<sup>33</sup>. Also, in the central nervous system, PGs are extremely important for neurite outgrowth in the regeneration of an injured spinal cord<sup>34</sup>. CSPGs are known to be present in the CNS and are responsible for neuronal plasticity, neuroprotection against cell death inducing processes, and homeostasis around neurons<sup>35,36</sup>. The location of HSPGs depends on the core protein present. They can either be free in the ECM or at the cell-ECM interface<sup>37</sup>. The GAG chain is the major constituent responsible for the biological functions of the PGs<sup>38</sup>. This GAG portion can have a molecular weight of 5 to 50 kDa<sup>39</sup>.

### **1.3. Glycosaminoglycans**

These GAGs are polysaccharides with complex structures, and are vital for growth and signaling processes, including differentiation, proliferation, morphogenesis, and bacterial/viral infections<sup>40,41</sup>. GAGs have been shown to be essential for multicellular life and crucial for development from genetic knockout studies in various organisms<sup>42</sup>. Also known as mucopolysaccharides, GAGs have very viscous and lubricating properties<sup>43</sup>. GAGs are present on all surfaces of animal cells in the ECM<sup>43</sup>. There are four major classes that the GAGs fall into: heparin/heparan sulfate (HS), keratan sulfate (KS), chondroitin sulfate (CS)/dermatan sulfate (DS), and hyaluronic acid (HA)/hyaluronan<sup>44</sup>. The overall structure consists of a repeating disaccharide that contains a hexosamine (N-acetyl-D-glucosamine, GlcNAc, or N-acetyl-D-galactosamine, GalNAc) and either uronic acid (glucuronic acid, GlcA, or iduronic acid, IdoA) or galactose<sup>45</sup> (Figure 1.1).

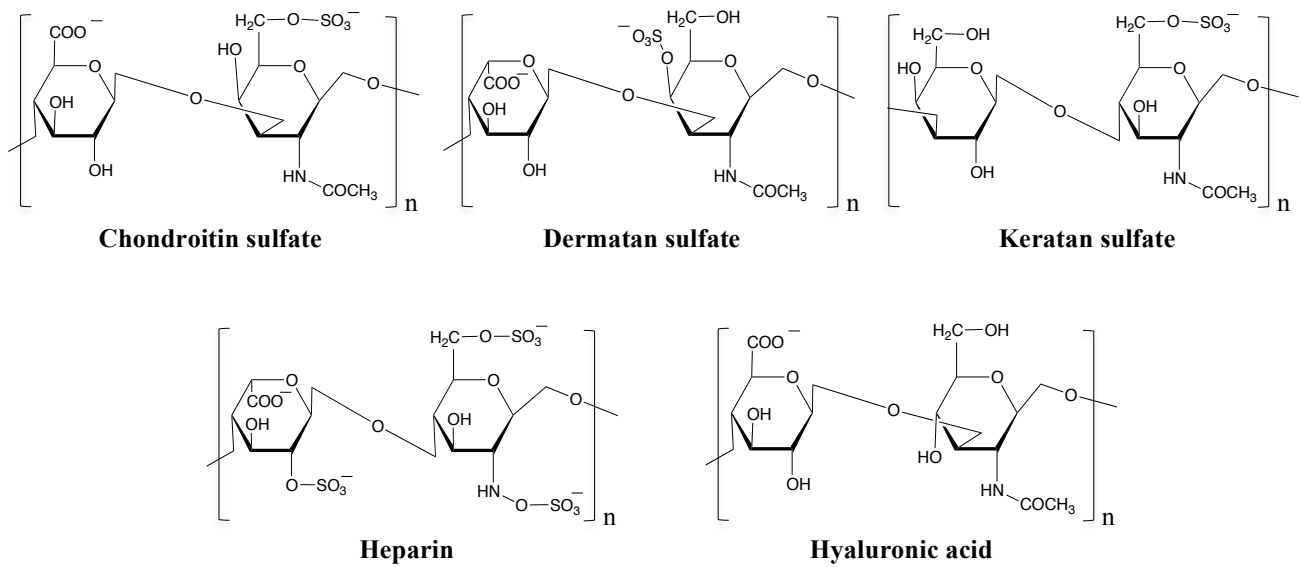


**Figure 1.1** – Structures of the repeating disaccharide units in naturally occurring GAGs present in the body.

Modification by means of sulfation and epimerization occurs in the Golgi, leading to the polydispersity in structure and function of GAGs<sup>42,46</sup>. With the exception of HA, hydroxyl groups on the 2, 4, and 6 positions of the sugar can be sulfated by sulfotransferase enzymes<sup>45</sup>. At least one of the sugars in the repeating unit has a negatively charged carboxylate or sulfate group<sup>32</sup>. The biosynthesis of complex GAGs is highly regulated, and the sulfation patterns are formed in an organ- and tissue-specific manner during development<sup>41</sup>. The sulfate GAGs are ubiquitous to the animal kingdom, whereas in bacteria, these same GAGs are found in the non-sulfated form. For example, in pathogenic bacteria, heparanosan and chondrosan, the non-sulfated version of heparin and chondroitin sulfate, are present to protect the microbe and aid in infection<sup>47</sup>. Sulfated GAGs are also absent in the fungi, plantae, and protista kingdoms. With the exception of hyaluronic acid, GAGs are often covalently attached to a protein core that is found inside cells, on the cell surface, or in the extracellular matrices<sup>48</sup>.

## Chondroitin Sulfate and Dermatan Sulfate

CS and DS are frequently found as hybrid chains in mammalian tissues, which leads to their grouping together in description<sup>49</sup>. When getting into further detail about the individual chains' structures, separation of the two GAG types is called for. Structural stabilization was thought to be their only role until recently. New roles have arisen such as modulation of the CNS environment, cell division and morphogenesis, wound repair, infection, and many others<sup>50,51,52,53,54</sup>. Chondroitin sulfate (CS) chains consist of repeating disaccharides of D-glucuronic acid (GlcA) and N-acetyl-D-galactosamine (GalNAc), with anywhere from 40 to 100 disaccharide units<sup>55</sup>. CS chains are classified as motifs according to their sulfation patterns (O (non-sulfated), A (at GalNAc oxygen-4), C (at GalNAc oxygen-6), D (at GlcA oxygen-2 and GalNAc oxygen-6), E (at GalNAc oxygen-4 and 6))<sup>56,55</sup>. CS-B is not listed because its formal name is actually the DS GAG chain. The enzymes responsible for the sulfation patterns in CS are: 4-O-sulfotransferases 1-3, 6-O-sulfotransferases 1 and 2, and 4-sulfate 6-O-sulfotransferase, which work on the hexosamine moiety. Galactosaminyl uronyl 2-O-sulfotransferase works on the uronic acid moiety<sup>57</sup>. Structures containing C-, D-, and E-units have roles in bone development. CS or HS proteoglycans (CSPGs or HSPGs, respectively) are major components of the ECM in the central nervous system (CNS)<sup>58</sup>. DS chains are extremely similar to CS chains, with iduronic acid (IdoA) instead of glucuronic acid (GlcA). DS can be generated during the CS assembly by epimerization of the GlcA into IdoA by two DS epimerases, DS-epi1 and DS-epi2<sup>59</sup>. Dermatan 4-O-sulfotransferase-1 adds sulfate groups on the IdoA moiety<sup>57</sup>. The presence of IdoA actually likens DS to HS/heparin. DS chains are commonly sulfated at the GalNAc oxygen-4 and 6 (like CS-A and C) and at IdoA oxygen-2 (like HS/heparin)<sup>53</sup>. CS/DS are found bound to at least 32 core proteins to form their subsequence PG<sup>60</sup>. CS/DS, along with

the respective proteoglycan, binds to a wide variety of molecules such as coagulation factors (heparin cofactor II, which then inhibits thrombin), matrix molecules (Type II collagen, involved in primary osteoarthritis), growth factors (fibroblast growth factors (FGF)-2 and 7, mainly DS binds these), chemokines (stromal cell derived factor-1 $\beta$ , SDF-1 $\beta$ ), and pathogen virulence factors (glycoprotein C, responsible for the *herpes simplex* virus infection)<sup>61,62,49,44</sup>. The major GAG synthesized in rat fetal liver is CS, representing over 50% of the sulfated GAGs, but in adult liver, the dominant GAG present becomes HS, comprising over 80% of total GAG<sup>63</sup>. This high level of CS GAG decreases after birth between the 10<sup>th</sup> and 15<sup>th</sup> day of life. The production of CS is cell type dependent as seen by the decrease in levels in differentiated hepatocytes compared to the undifferentiated hepatocytes present in fetuses<sup>63</sup>.

### **Keratan Sulfate**

Keratan sulfate (KS) is a sulfated GAG that is composed of galactose (Gal) and GlcNAc<sup>64</sup>. KS is distinct from the other GAGs because it can be synthesized on N-linked oligosaccharides and on serine/threonine O-linked oligosaccharides<sup>65</sup>. KS is present in various cartilages, the cornea, neural tissue (as seen by its expression at the site of neural injury), and reproductive tissue<sup>66,67,68,16</sup>. KS plays an important role in maintaining transparency in the cornea by providing proper hydration for the ECM in the stroma<sup>69</sup>. Other functions include modulating axonal growth during development and endothelial cell migration<sup>70,71</sup>. KS modulates fibromodulin and osteoadherin in cartilage<sup>72,73</sup>. Inflammation or chronic conditions of the corneal stroma lead to marked decrease or loss of keratan sulfate<sup>74</sup>.

## **Hyaluronic Acid**

Hyaluronic acid (HA) is another GAG that is important for various biochemical processes in the body. HA accounts for roughly 60% of the ECM<sup>75</sup>. HA is a relatively simple GAG that is unsulfated and unbranched, and not attached to protein core<sup>76</sup>. It is synthesized at the inner face of the plasma membrane as a linear chain by integral plasma membrane proteins called hyaluronan synthases (HS1-3), in contrast to the other GAGs that are synthesized in the Golgi and attached to protein cores<sup>77,78</sup>. HA chains consist of alternating (1 → 4)-β linked GlcA and (1 → 3)-β linked GlcNAc residues<sup>79</sup>. This GAG is an extremely large molecule, with a typical molecule ranging from 200-100,000 kDa in size<sup>80</sup>.

Even though HA is not attached to a core protein, it does interact in a noncovalent fashion through its unique hyaluronan-binding motifs<sup>12,47</sup>. CD44 is a major cell-surface receptor that interacts with HA, which is involved in cell proliferation and angiogenesis<sup>81</sup>. This interaction stimulates migration and invasiveness in human melanoma cell lines<sup>82</sup>. HA is ubiquitous and is present in almost all tissues but is most abundant in soft connective tissue<sup>83</sup>. Long thought to be just a lubricating molecule in joints, HA has been shown to have various signaling properties, such as tumor cell migration, wound healing, and apoptosis, depending on its chain length<sup>84,85,86</sup>. HA is found to accumulate in the aortic smooth muscle cells during mitotic stages since it facilitates nuclei separation and cell division<sup>87</sup>. In healthy tissues, HA is high-molecular weight, but smaller fragments are obtained by enzyme-mediated degradation or oxidative stress, and these small fragments have roles unlike the native HA in the body<sup>79</sup>. It has been shown that the low-molecular-weight HA fragments (70-120 kDa) can be used for the delivery of peptides and proteins, useful in chronic wound healing<sup>88</sup>. Native HA is also used in

cosmetics and pharmaceuticals<sup>89</sup>. The specific details of the activity of this GAG are still being studied today.

### **Heparin and Heparan Sulfate**

Heparin, a GAG present in the ECM was discovered in 1916 and has been in the public eye ever since for many amazing roles exogenously and endogenously<sup>90</sup>. It has been found that the highest concentrations of heparin are in lung, liver, and muscle<sup>91</sup>. HSGAGs interact with other ECM components to influence major processes such as normal development, wound healing, and most notably tumor growth<sup>37</sup>. HS is the GAG that is found on all cell surfaces, which is what proteins that interact with GAGs actually interact with instead of heparin. Normally, HSGAG is ushered into the cell in a controlled manner, which is seen by its famous interaction with FGF-2 and FGF receptor (FGFR1). When it binds to these components, this ternary complex is localized to the nucleus to impact cell function<sup>37</sup>. The major repeating disaccharide of heparin and HS consists of IdoA or GlcA attached to GlcNAc. The structures of HS and heparin are very similar, but HS has fewer sulfo groups and is rich in GlcA and GlcNAc<sup>92</sup>. HS is found on all cells, whereas heparin is only found on mast cells near the walls of blood vessels and on the surfaces of endothelial cells<sup>32</sup>. HS is ubiquitously expressed as a proteoglycan on most animal cells and as a component of extracellular matrices and basement membranes<sup>93</sup>. HSGAG is also found in the cell nucleus with possible roles in cell differentiation and proliferation<sup>94</sup>. Heparin, in the dense granules of the mast cells, is released into the extracellular space when the cell is triggered to secrete<sup>32</sup>. Specifically, heparin is produced in the lung, liver, and skin by mast cells<sup>95</sup>. Different numbers of polysaccharide chains can be attached to various serine residues in heparin's core to form the respective proteoglycan<sup>27</sup>. HSPGs are

associated with the surface of epithelial cells at densities of  $10^5$ - $10^6$  molecules/cell<sup>96</sup>. HS has much diversity in its structure based on its tissue location, which in turn affects its activity<sup>97,98</sup>. In this context, in order to adequately study the binding affinities of various proteins that interact with the cell surface, heparin, the highly sulfated analog of HS, is used as an HS model since the sulfate groups on HS are what the proteins interact with<sup>99</sup>.

Heparin/HS is unique in the fact that it is the only GAG that is biosynthesized in the absence of a template<sup>100</sup>. The biosynthesis of heparin begins with the synthesis of a core protein (serglycin) in ER with a tetrasaccharide linker attached to its serine residues in regions rich in Ser-Gly repeats<sup>101</sup>. As it travels through the Golgi, a repeating 1→4-glycosidically-linked copolymer of GlcA and GlcNAc is extended from this linked region through the addition of uridine diphosphate-activated sugars catalyzed by the EXT enzyme<sup>102</sup>. The peptidoglycan heparin is released from serglycin as a small peptide, to which a single polysaccharide chain (100 kDa) is added. This peptidoglycan is short-lived as it is immediately processed by β-endoglucuronidase to a number of smaller polysaccharide chains called GAGs<sup>103</sup>. During its formation, the copolymer is modified by *N*-deacetylase/*N*-sulfotransferase (NDST), C5 epimerase, and 2-, 6-, and 3-*O*-sulfotransferases<sup>104</sup>. Complete modification results in a GAG rich in *N*- and *O*-sulfo-L-iduronic acid, “heparin”. Incomplete or partial modification results in a GAG rich in *O*-sulfo-*N*-acetyl-D-glucosamine and GlcA, “heparan sulfate”<sup>104</sup>. The biosynthetic modification of HS is incomplete, resulting in sequence homogeneity important in the regulation of HS interaction specificity with various cellular proteins<sup>105</sup>. HS is biosynthesized, as a proteoglycan, through the same pathway as heparin, but, unlike heparin, its chain remains attached to its core protein<sup>27</sup>. Although structurally similar, heparin and HS can be distinguished through their different sensitivity towards a family of GAG-degrading microbial enzymes,

heparin lyases<sup>27</sup>. Similar to other natural polysaccharides, heparin is a polydispersed mixture containing chains varying in molecular weights and sulfation patterns<sup>106</sup>. In solution, heparin exists as an extended helical structure with conserved glycosidic bond angles, yet it has a high degree of conformational flexibility<sup>107</sup>. The chair and skew boat conformations of IdoA residues abundant in heparin and S-domains of HS contribute to this flexibility<sup>108,109</sup>. This allows for diverse spatial displays of negative charge thought to aid specific interactions with proteins through induced fit binding mechanisms<sup>107</sup>. Pharmaceutical grade heparin consists of chains ranging in size of 5 to 40 kDa<sup>110</sup>. GAG heparin has the same size range, but an average molecular weight of 15 kDa and an average negative charge of -75<sup>27</sup>. The major component of heparin (75-95%) is the trisulfated disaccharide form by replacing R<sub>1</sub>, R<sub>2</sub>, and R<sub>3</sub> with sulfate groups. HS is known for its ability to modulate the actions of morphogens in the ECM during embryonic development<sup>111</sup>. Heparin interacts with specific proteins that have unique binding sites that recognize heparin among the other GAGs. These proteins are known as heparin-binding proteins (HBPs). The most well-known and first studied in depth role of heparin studied in the science world is its anticoagulation capabilities. In this process, exogenous heparin interacts with antithrombin (ATIII) (a key player in the coagulation pathway) and upon binding, there is an increase in its activity to inhibit thrombin and thus inhibiting blood clot formation<sup>103</sup>. The interaction of ATIII and a pentasaccharide in heparin has marked one of the very few “specific” binding models of heparin with proteins, in which exists a conformational change in the protein and a subsequent increase in activity<sup>103</sup>. This very specific pentasaccharide (DEFGH) makes up one-third of the heparin chains in nature, which is composed of GlcNAc6S→GlcA→GlcNS3S6S→IdoA2S→GlcNS6S<sup>112</sup>. Besides the important biological functions of heparin, it



has also been exploited for better purification techniques for proteins that are known to bind to it, where it is immobilized as a resin (heparin-Sepharose) to be used in affinity chromatography.

### **Heparanase**

The GAG chain of the PG can be degraded and removed from the cell surface for further activity in their free form. Heparanase, an endoglucuronidase, is the only known mammalian endoglycosidase to cleave HS, specifically between the uronic acid and glucosamine<sup>113,114</sup>. It is highly expressed in cancer cells and its activity is associated with high metastasis of cancer. This is thought to be because the disattachment of HS from the ECM surface and basement membrane leads to cell invasion<sup>115</sup>. This degradation of HS leads to disassembly of the EMC, resulting in cancer angiogenesis and metastasis<sup>116</sup>. Once heparanase has degraded the ECM during tumor growth, the liberated HS has molecules still bound to it that are associated with inflammation, metastasis, and angiogenesis. For example, HS-bearing syndecan-1 that is freed from the cell surface binds to and upregulates activity of tumor-derived growth factors, leading to further metastasis<sup>117</sup>. This essential enzyme has positive and negative effects on GAG structure and in turn on the body.

### **1.4. Significance of Glycosaminoglycans**

The most famous use of GAGs, in particular heparin, is for anticoagulation. Most cardiac surgical operations are performed using cardiopulmonary bypass that maintains the systemic blood circulation during cardioplegia<sup>118</sup>. Heparin is used to inhibit coagulation and prevent thrombus formation on the surface of the bypass circuitry and oxygenator<sup>118</sup>. This unique GAG is one of the oldest drugs currently still in widespread use, one of the first biopolymeric drugs,

and one of the few carbohydrate drugs<sup>119</sup>. During anticoagulation, heparin interacts with a protein known as ATIII, which then leads to a multitude of reactions ultimately inhibiting clot formation. ATIII is a member of the serine protease inhibitor superfamily involved in the blood clotting cascade (coagulation), in which it rapidly inhibits proteases, thrombin, factor Xa, and factor IXa<sup>120</sup>. In wound healing, blood clot formation is a major and necessary event for the body. In this process, a key protein known as thrombin directly converts fibrinogen into fibrin, the main component of a blood clot<sup>121</sup>. In order to stop the formation of fibrin, the inhibition of thrombin is needed. ATIII exists in its repressed state able to slowly inhibit the proteins in the cascade, but its interaction with heparin is crucial for anticoagulation to occur during wound healing. Heparin, along with low-molecular-weight heparin (LMWH), binds to and activates ATIII (coagulation protease inhibitor), ultimately inhibiting blood coagulation<sup>92</sup>. The activation process of ATIII by means of heparin is actually very complex and occurs in various stages: (1) ATIII binds a specific pentasaccharide present in heparin, which in turn causes (2) conformational change in the inhibitory loop of ATIII (allosteric activation), (3) increasing the inhibitor activity<sup>122,123</sup>. Binding of ATIII to the pentasaccharide in heparin is enough to inhibit Factor Xa but not for thrombin. In most heparin molecules, the pentasaccharide is flanked on both sides by repeating  $\rightarrow 4$ -(2-O -sulfonato-a-L-idopyrano- syluronate)-(1 $\rightarrow$ 4)-(N-sulfonato-6-O-sulfonato-a-D-glucosaminyl)-(1 $\rightarrow$ disaccharidic sequences<sup>124</sup>. In the case of thrombin, once ATIII is bound to heparin to the pentasaccharide site, thrombin then binds to heparin at a near yet different site. This domino effect thus requires a longer chain of heparin, preferably 18 saccharides in length, instead of just the pentasaccharide for inhibition of Factor Xa<sup>125</sup>. This ternary complex of ATIII-heparin-thrombin is then enough for the inhibition of thrombin<sup>126</sup> (Figure 1.2).

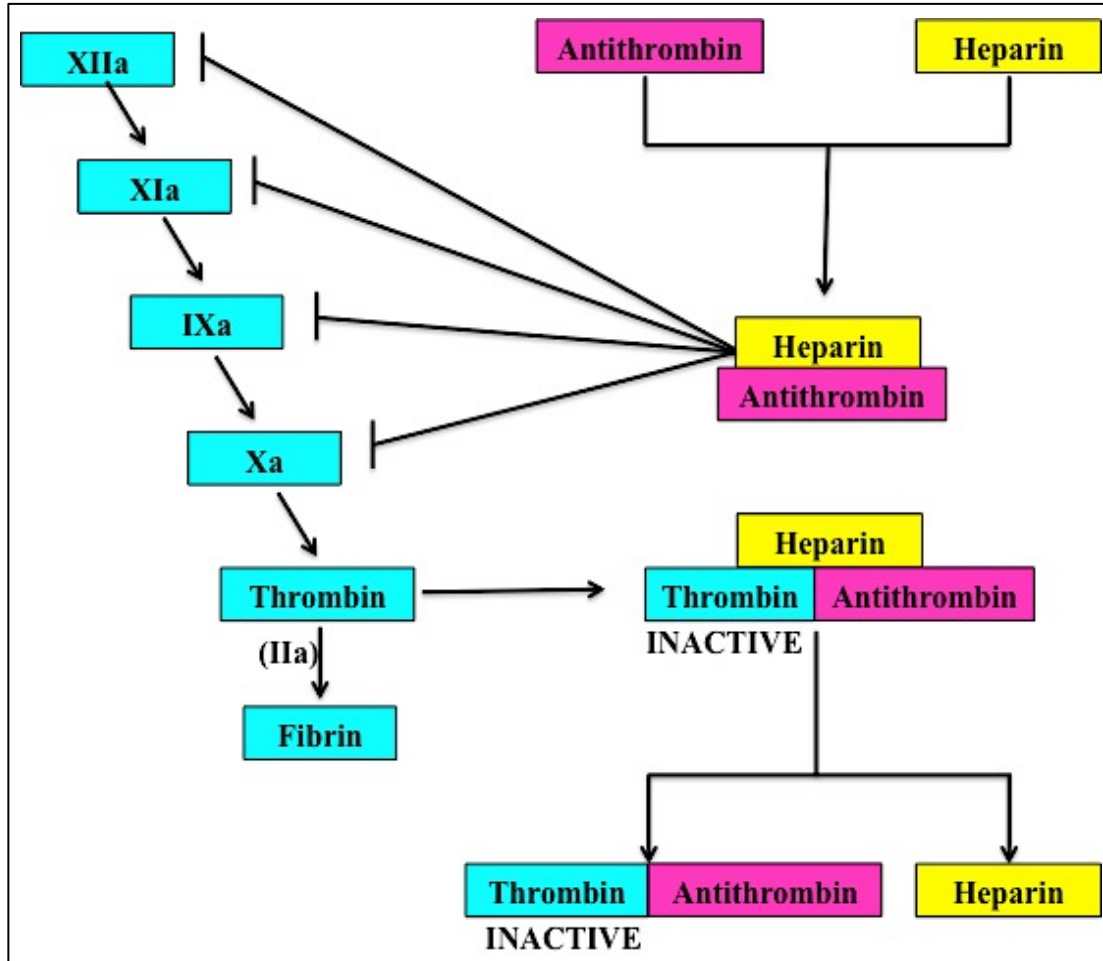


**Figure 1.2** – Blood clotting cascade and the action of heparin as an anticoagulant, modified from Zurawska et al<sup>127</sup>.

In the body, once heparin binds ATIII, the rate of formation of inhibitor-protein complex is increased by at least three orders of magnitude<sup>32,128</sup>. Only a third of the chains found in commercially prepared heparin/HS contain an ATIII binding site. There is a second serpin called heparin cofactor II that selectively inhibits thrombin. This protein is activated by both heparin and DS<sup>129</sup>.

Another role of medicinal importance is the involvement of heparin in cancer.

Components of the ECM change drastically during the progression of cancer. For example, HSPGs known as the syndecan family are known to be involved in tumorigenesis of breast

cancer. In breast cancer cells, SD1 has been shown to promote their proliferation<sup>130</sup>. Of the glypican family, GPC3 is a negative modulator of breast cancer, as seen by its ability to guide breast cancer cells to apoptosis<sup>131</sup>. In breast cancer, this gene is silenced. Exogenous GAGs have regulatory roles on the growth of cultured normal and cancerous cells<sup>20</sup>. For example, in melanoma cells, exogenous CS, DS, and heparin/HS have been shown to inhibit cancer cell growth<sup>132</sup>.

Angiogenesis is the growth of new blood vessels from pre-existing ones. Abnormal angiogenesis leads to the onset of debilitating diseases, such as allergic dermatitis and warts, obesity, cancer, pulmonary hypertension, endometriosis, inflammatory bowel disease, and most famously arthritis<sup>133</sup>. Inflammation is the biological response to injury or harmful stimuli, such as pathogens or damaged cells, in an attempt to heal or repair the organism<sup>134</sup>. In inflammation and arthritis, patients suffer from debilitating pain in joints, especially in the knee. In the incapacitating disease of osteoarthritis, blood vessel invasion allows for the infiltration of osteoblasts in the cartilage, which then ultimately leads to the mineralization of the cartilage<sup>135</sup>. This neurovascular invasion is also implicated in the onset of the pain and cartilage degradation experienced in other debilitating diseases such as rheumatoid arthritis<sup>136</sup>. In short, blood vessel growth leads to nerve growth into the tissue, which then leads to increased sensitivity and pain in joints. Osteoarthritic cartilage has decreased levels of GAGs as compared to normal, healthy cartilage, which allows for more neurovascularization and onset of the disease.

In the case of rheumatoid arthritis, angiogenesis promotes the destruction of cartilage and bone. Heparin-binding growth factors are known to regulate angiogenesis. The systemic administration of heparin, particularly LMWH, reduces the angiogenic activity of these growth factors, which can aid in the inhibition of arthritis and related debilitating diseases. Specifically,

orally administered, partially desulfated heparin pentasaccharide responsible for activating ATIII inhibited articular angiogenesis and bone lesions commonly found in arthritis progression. The pentasaccharide was desulfated and conjugated to deoxycholic acid in order to decrease the concentration of heparin needed for anti-angiogenesis, which is associated with hemorrhage risk<sup>137</sup>.

Aggrecan is a PG composed of CS or KS GAG side chains, which, due to its negative charge, enables water retention and withstands compression in cartilage<sup>138</sup>. Aggrecanase is primarily responsible for the destruction and loss of aggrecan in the early stages of arthritic joint diseases<sup>139</sup>. The addition of exogenous KS was shown to decrease the release of aggrecan after its cleavage in arthritis, showing that KS can be used to ameliorate inflammation in arthritic patients<sup>138</sup>.

### **1.5. Use of Heparin in Disease**

HS has been studied as a receptor for various pathogens such as Dengue virus, Herpes simplex virus, Adeno-associated virus, Respiratory syncytial virus, Human immunodeficiency virus, and many others<sup>140,141,142,143,144</sup>. Initial binding of a virus to its target cell marks the beginning of pathogenesis<sup>145</sup>. This binding may result from a receptor-like interaction between the viral coat protein molecule and the GAG chain of a proteoglycan expressed on cells<sup>27</sup>. Since HS is found on nearly every mammalian cell, it is no surprise that viral proteins would exploit this surface molecule for invasion into its target cell<sup>146,147</sup>. It has been reported though that the addition of soluble GAGs such as heparin and the enzymatic removal of cell-surface GAGs inhibits infection by various viruses such as respiratory syncytial virus and metapneumovirus<sup>148,149</sup>. Recently, Hendricks et al have successfully placed heparin and HS-

polysaccharides of varying sizes in liposomes that act as decoy receptors for various viruses<sup>150</sup>. These decoys bind to viruses like their normal receptors, which gathers them away from their actual cell-surface receptors, not allowing viral penetration into cells, inhibiting the infection in the body. The liposome shell allowed the octasaccharide to be successfully delivered to its target better than if there was the octasaccharide alone. Human immunodeficiency virus type-1 (HIV-1) is a virus of increased interest all over the world that has shown to interact with heparin. This virus targets cells that express a cellular receptor molecule CD4. HIV-1 binds to a loop of 20 amino acids in the first domain of CD4 by interacting with the viral surface glycoprotein gp120<sup>151</sup>. The interaction of gp120 causes a conformational change responsible for the fusion of virus and cell membranes. Heparin exerts anti-HIV activity by binding to the V3 loop, a major epitope (part of antigen recognized by immune system) of gp120<sup>152,153,154</sup>. The V3 loop has an essential role in the membrane fusion by the virus. Chemical studies have shown that O-sulfation is also essential for membrane fusion. Cells lacking the CD4 receptor are still infected by HIV-1 by its interaction with gp120 and cell surface HS<sup>155</sup>. This finding indicates that CD4 dependence by HIV-1 is cell line specific and in some cases, HS can act as another cell surface receptor for HIV-1 to invade cells<sup>27</sup>. Heparin and HS can play another role in HIV-1 invasion. The Tat protein is a protein that binds to cell-surface HS, which is released from cells, has autocrine or paracrine activity, and is essential for HIV-1 replication<sup>156,157,158</sup>. This protein primes the cells for invasion by HIV-1. This shows that heparin is a multi-protein compound capable of affecting different aspects of the HIV-1 infection pathway. Rusnati et al has shown exogenous heparin chains of varying sizes as an antagonistic activity toward Tat protein, meaning heparin is capable of interfering with this deadly protein's interaction with its cell surface receptors as well as its biological activity<sup>159,160</sup>.

The deadliest form of malaria is caused by *Plasmodium falciparum*, a protozoan parasite that is released when female Anopheles mosquitoes bite human flesh. The sporozoites that are released into the host travel through the cytosol of various cells before invading a hepatocyte, liver cell. The invasion of liver cell has been attributed to the interaction of circumsporozoite (CS) protein, 40 kDa antigen that covers the plasma membrane of invading sporozoites, with GAG side chains of proteoglycans on the surface of the hepatocytes<sup>161</sup>. Highly sulfated HS on the surface of liver cells is the GAG of choice and the natural receptor for binding and invasion of CS protein. Heparin, at low concentrations, also enhanced CS binding, suggesting it acts as a cross-linking agent capable of stabilizing multimeric CS complexes. The heparin decasaccharide is the minimum sequence size for CS-protein-binding domain<sup>27</sup>. High concentrations of heparin can also displace CS from the cell surface, inhibiting its invasion into hepatocytes<sup>162</sup>. Heparin can regulate CS binding to HepG2 cells in a dose-dependent manner<sup>161</sup>. *Plasmodium*-infected red blood cells (pRBCs) are the main target for antimalarial medications. One of the main molecules that the pRBCs bind to is cell-surface GAGs, which have become major targets for therapy. Soluble GAGs, especially heparin/HS have shown inhibitory effects against the pRBCs and sporozoites<sup>163</sup>. The high concentrations of heparin that is needed for antimalarial activity posed a significant problem due to the excessive intracranial bleeding<sup>164</sup>. In order to combat these anticoagulation side effects, when heparin is covalently immobilized, by its carboxyl groups, on substrates such as nanoparticles, its binding affinity for ATIII is greatly diminished, leading to lower anticoagulation activity<sup>165</sup>. This immobilized heparin still showed inhibitory effect for pRBC invasion, which could prove heparin to be a promising antimalarial medication as well as an avenue to deliver antimalarial drugs to infected cells, without the undesirable anticoagulant side effects<sup>166</sup>.

## 1.6. Heparin Contamination

Pharmaceutical grade heparin is isolated from pig intestine, sheep intestine, and beef lung, but the existence of mad cow disease and scrapies, has led heparin to be generally isolated only from pig intestine today<sup>112,167</sup>. Warda et al has shown to isolate pharmaceutical grade heparin from camel intestine that has moderately lower anti-factor Xa activity than the commercially available heparin isolated from porcine intestine<sup>168</sup>. This animal source yielded double the heparin per kg of tissue that commercial sources yield. The decrease in activity could be due to the presence of small amounts of HS, so if these contaminating molecules could be removed, greater activity could be achieved. In 2006, this same group isolated HS from camel liver and lung, where they found that the HS from the lung had 50% the anti-factor Xa activity as commercial heparin, which is still much higher than HS from other animal sources<sup>169</sup>. This process is an extremely complicated one, which involves numerous enzymes and harsh chemicals. Commercial heparin is isolated from porcine tissue in tons quantities. There are three types of heparins that are accepted by the FDA: unfractionated heparin (UFH,  $MW_{avg}$  16,000 Da), low-molecular-weight heparin (LMWH,  $MW_{avg}$  3500-6000 Da), and fondaparinux ( $MW_{avg}$  1700 Da)<sup>170</sup>. LMWH has also been introduced by controlled depolymerization and fractionation of heparin for the use as an anticoagulant/antithrombotic agent for over 25 years. These agents have more predictable pharmacological properties, sustained activity, and improved bioavailability, thus replacing heparins as the anticoagulant of choice at the turn of the millennium<sup>171,172,90</sup>. UFH and LMWH give rise to side effects of heparin-induced thromboembolism when given in a prolonged state. Fondaparinux combats that side effect but there is currently no antidote to counter the anticoagulant activity if hemorrhage occurs<sup>173,174</sup>. The raw UF heparin that is isolated is ultimately purified using methods guarded by the Drug



Master file submitted to the FDA. Heparin had been the most widely used clinical intravenous anticoagulation agent for many years until 2008. This year brought with it adverse effects from the use of isolated batches of unintentionally contaminated heparin, which include rash, fainting, racing heart, and above all, hundreds of deaths worldwide<sup>175,176</sup>. During one or more of the concealed processes of isolating heparin, other impurities were recently found in the final product, such as DS and oversulfated chondroitin sulfate (OSCS)<sup>177</sup>. Recent files have shown that several batches of LMWH from the same company are also contaminated with OSCS and DS. DS is not found to contain biological activity that negatively affects the anticoagulation activity of heparin<sup>178</sup>. Before 2008, manufacturers relied on coagulation assays for characterization of heparin and the assessment of its purity<sup>179</sup>. The lack of effective quality tests led to overlooking of the contaminants in the so-called pure heparin samples. OSCS, both the isolated contaminant and synthetic molecule, activated the kinin-kallikrein pathway in human plasma leading to the formation of bradykinin<sup>180,181</sup>. OSCS has also been shown to induce complement protein C3a and C5a generation in the complement cascade<sup>182</sup>. The activation of these pathways is linked to the activation of FXII<sup>183</sup>. This produces the vasoactive mediator bradykinin and its corresponding anaphylatoxins<sup>184</sup>. The activation of all these pathways gave a reasonable theory for why anaphylactic shock and death was seen in patients given contaminated heparin. OSCS also binds to ATIII, but it does not, unlike heparin, induce the conformational change of ATIII, leading to the inactivation of thrombin and FXa. FXIIa can tightly bind OSCS, further boosting bradykinin production<sup>104</sup> (Figure 1.3).

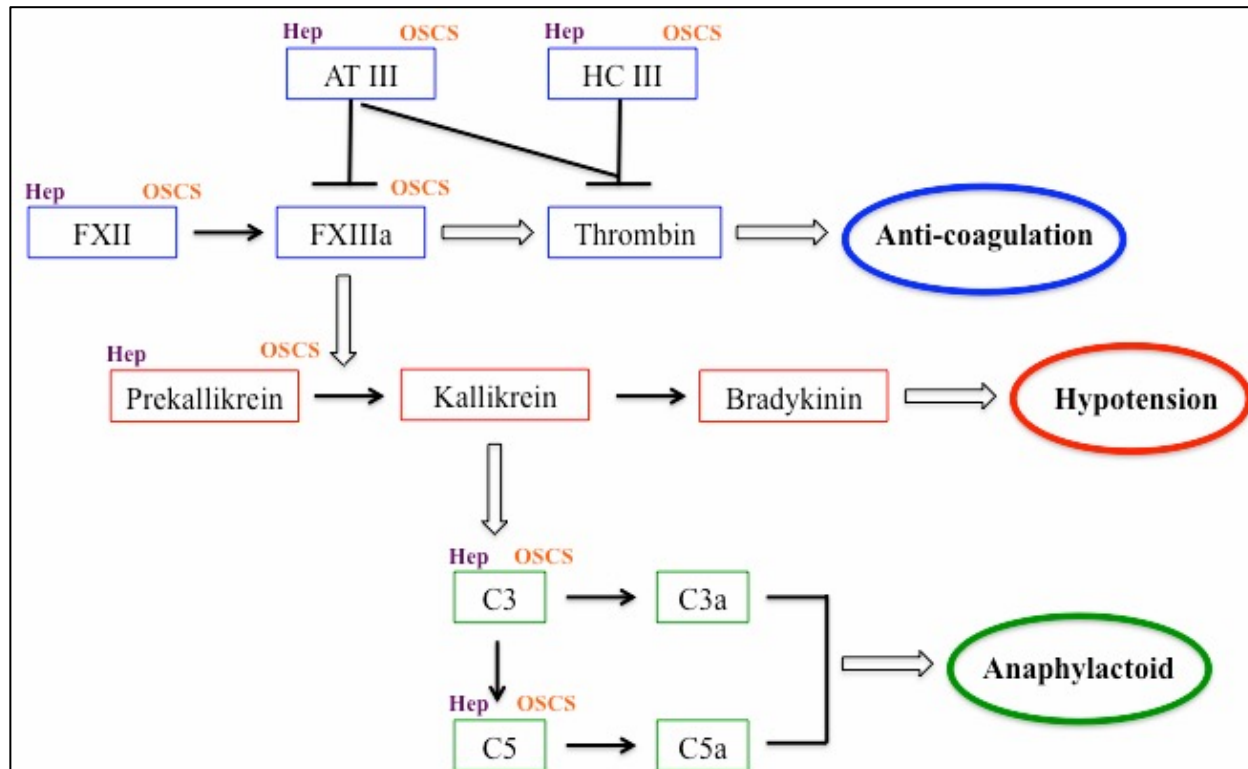


**Figure 1.3** – Pathways that are turned on by the presence of OSCS in contaminated heparin, modified from Liu et al<sup>104</sup>.

Currently, synthetic and other natural methods of purifying heparin are underway, but no effective method has been found and employed worldwide.

### 1.7. Heparin-Binding Proteins

More than 400 proteins interact with heparin/HS at the cell surface and in the ECM<sup>185,186</sup>. These proteins are known as HBPs<sup>103</sup>. These proteins are involved in many biological processes, including cell growth and development, tumor metastasis and angiogenesis, inflammation, viral infection, and fertilization in human seminal fluid<sup>93,187,188,189</sup>. HBPs can also interact with other GAGs, but due to heparin having the most sulfated groups and therefore highest negative charge, the HBPs usually exhibit the highest affinity for this GAG<sup>190</sup>. Many proteins, when they bind to heparin, undergo a conformational change, which is usually necessary for the full expression of

biological properties of the specific protein<sup>38</sup>. HBPs mostly bind to HS instead of heparin in most physiological events, since heparin is released from mast cells at certain inflammatory events<sup>190</sup>. These HBPs include fibronectin, chemokines and cytokines, hepatic and lipoprotein lipases, superoxide dismutase, antithrombin III, various growth factors, and many other less well-known proteins<sup>191,192,193,194,195,196,197</sup> (Table 1.2).

<b>Heparin-Binding Protein</b>	<b>Physiological Role</b>	<b>Binding Affinity (<math>K_d</math>) range</b>
Antithrombin III	Coagulation cascade serpin	nM
Secretory leukocyte protease inhibitor	Inhibits elastase and cathpsin G	nM
C1 esterase inhibitor	Inhibits C1 esterase	nM
Vaccinia complement protein	Protects host cell from complement	nM
Fibroblast growth factors 1 and 2	Proliferation, differentiation, angiogenesis	nM
Platelet factor-4	Inflammation and wound healing	nM
Interleukin-8	Pro-inflammatory cytokine	$\mu$ M
Stromal cell-derived factor-1 $\alpha$	Pro-inflammatory mediator	nM
Annexin II	Receptor for TPA and plasminogen, CMV, and tenascin C	nM
Apolipoprotein E	Lipid transport	nM
HIV-1 glycoprotein 120	Viral entry	nM
HIV-1 Tat protein	Transactivating factor	nM
Malaria circumsporozoite protein	Sporozoite attachment to hepatocytes	nM
Selectins	Adhesion, inflammation, metastasis	$\mu$ M
Vitronectin	Cell adhesion and migration	nM
Fibronectin	Adhesion and traction	$\mu$ M
Amyloid P component	In amyloid plaque	$\mu$ M

**Table 1.2** – Heparin-binding proteins, their role, and binding affinity for heparin, modified from Capila et al<sup>27</sup>. Binding study conditions are not kept constant between the proteins, so binding affinity values are given in ranges not exact values.

## **Fibroblast Growth Factors**

The activity of various growth factors is regulated by their interactions with cell surface HSPGs<sup>198,199</sup>. A specific and very well-known subgroup of HBPs is the family of FGFs. FGFs are known for their roles in tissue repair, organogenesis, embryogenesis, cell proliferation and differentiation, angiogenesis, and wound healing<sup>200,201,202,203</sup>. The biological activities of these secreted growth factors are regulated by their interaction with two types of receptors on the cell surface: high-affinity receptors (FGFRs) and low-affinity receptors (heparin and heparin-like GAGs or HSGAGs)<sup>204</sup>. HSGAGs on the cell surface protect the FGFs from degradation and essentially “hold” the proteins until they are released to bind to the FGFRs<sup>205</sup>. The FGF family consists of 23 members in mammals. There are 18 mammalian FGFs (FGF-1 to FGF-10; FGF-16 to FGF-23) that are grouped into six subfamilies based on differences in sequence homology<sup>200</sup>. The six subfamilies are FGF-1 and FGF-2; FGF-3, 7, 10, and 22; FGF-4, 5, and 6; FGF-8, 17, 18; FGF-9, 16, 20; FGF-19, 21, 23. FGFs-11, 12, 13, and 14 are considered FGF homologous factors (FHF) that have high sequence identity with the FGF family but do not activate the FGF receptors<sup>206</sup>. These FHF are not secreted and act intracellularly<sup>207</sup>. FGF-15 is the mouse ortholog of human FGF-19. FGFs are considered paracrine factors, but it has been recently shown that FGF-19, 21, and 23 function in an endocrine manner, dependent on the presence of Klotho proteins, to regulate bile acid, cholesterol, glucose, vitamin D, and phosphate homeostasis<sup>200</sup>. Most FGFs contain a signal peptide sequence for secretion through the traditional endoplasmic reticulum-Golgi secretory pathway. FGF-1 and FGF-2 lack a signal peptide sequence, are synthesized as cytosolic proteins and are exported from the cell by a non-classical mechanism independent of the endoplasmic reticulum and Golgi apparatus<sup>208</sup>. Soluble

secretory proteins, FGFs excluding FGF-1 and 2, are transported from the ER through the Golgi apparatus to the cell surface. Luminal proteins are then released into the extracellular space by fusion to the plasma membrane<sup>209</sup>. FGF-1 and 2 do, however, possess a nuclear localization motif and have been found associated with the nucleus<sup>210</sup>. This non-classical release of FGF-1 is an inherent protective mechanism developed to regulate the mitogenic potential and widespread expression of FGF-1<sup>211</sup>.

The defining feature of the FGF family is the presence of a central core of 130 amino acids that is highly homologous between the different family members, with 28 residues being highly conserved. This core folds into 12 antiparallel  $\beta$ -strands ( $\beta$ 1- $\beta$ 12) that together form a cylindrical barrel closed by the more variable N- and C-terminal stretches<sup>212</sup>. It is known that 10 of these highly conserved amino acids interact with the fibroblast growth factor receptors (FGFRs) to form functional receptor dimers<sup>213</sup>. The heparin-binding region (HBR) within the core is composed of the  $\beta$ 1- $\beta$ 2 loop and some of the region spanning  $\beta$ 10 and  $\beta$ 12<sup>200</sup>. The amino acid sequence of FGF-1 can be seen below, with the HBR in bold (received from [www.uniprot.org](http://www.uniprot.org)).

MAEGEITTF TALTEKFNLPPGNYKKPKLLYCSNGGHFLRILPDGTVDGTRDRSDQHIQLQ  
LSAESVGEVYIKSTETGQYLAMDTDGLLYGSQTPNEECLFLERLEENHYNTYISKKHAE  
KNWVGL**KKNGSCKRGPRTHYGQ**KAILFLPLPVSSD

The HBS of FGF-1 as well as many other HBPs have been focused on in detail for scientists to fully understand the interaction of heparin with these proteins.

Unlike FGF-1 that is the universal ligand and can bind to all the FGFRs, most of the FGFs require binding to their specific receptors<sup>214</sup>. These FGFRs are members of the receptor tyrosine kinase family (RTK). This family has 58 members and is divided into 20 subfamilies in humans<sup>201</sup>. All members have the common overall structural composition of an extracellular ligand-binding region, a single-pass transmembrane domain, and an intracellular tyrosine kinase domain<sup>215</sup>. Growth factor binding to the ligand-binding region induces RTK activation and the initiation of the intracellular signaling cascades that control vital cellular processes<sup>201</sup>. RTKs play an important role in maintaining tissue homeostasis during the development and adult life of organisms<sup>216,207</sup>. The extracellular domain consists of three immunoglobulin-like (Ig-like) domains termed D1-D3 and an acidic serine-rich region between D1 and D2, termed the acid box (Hung). The D1 domain, together with the acid box, is thought to play a role in receptor auto-inhibition, whereas D2 and D3 domains constitute the FGF ligand binding site<sup>217</sup>. Eswarakumar and coworkers have proposed that an autoinhibition “closed” conformation of FGFR exists in equilibrium with an active “open” state ready for dimerization and autophosphorylation<sup>218</sup>. The D3 domain dictates the specificity of ligand binding, and D2 domain contains the primary sites of binding for both the ligand and heparin<sup>219</sup>. The D1 domain can fold back and interact with D2 in the FGF and HS binding site, functioning as a competitive auto-inhibitor in the interaction of FGFR with FGF and HS<sup>41</sup>. In FGFR1-3, alternative splicing in D3 domain creates isoforms with different ligand-binding specificities<sup>220</sup>. The most common variant involves an alternate exon in the second half of the D3 domain, giving rise to the b and c isoforms<sup>221,222</sup>. The FGFR IIIb isoforms are predominantly epithelial, and the IIIc isoforms are predominantly mesenchymal<sup>223,224</sup>.

## FGF-FGFR Signaling

FGF-FGFR binding specificity is essential for the regulation of FGF signaling and depends on the primary sequence differences in the 18 FGFs and 7 FGFRs<sup>105</sup>. FGF interacts extensively with D2, D3, and the linker between the two domains within one receptor<sup>225</sup>. This constitutes the primary binding site. Receptor signaling and stabilization of the resulting dimer requires the presence of highly sulfated heparin/HS polysaccharide chains of HSPGs to stabilize the FGF/FGFR/HS assembly<sup>226</sup>. HSPG consists of a proteoglycan core that binds two or three linear polysaccharides (heparan sulfate chains). Heparin/HS binds to a positively charged cluster of Lys and Arg residues extending across the D2 domains of the two receptors and the bound FGF molecules<sup>215</sup>. HSPGs protect the FGF ligands from degradation as well as mediate the complex formation between FGF and FGFR<sup>227,228</sup>. FGFs have a high affinity for HS/heparin with dissociation constants in the nanomolar range. The binding of FGFs to FGFRs causes the dimerization of the ternary complex of FGF-FGFR-HS<sup>229,230</sup>. The dimer is stabilized by interactions between FGF and D2 at the secondary binding site in a second receptor. The two FGFs in the 2:2 FGF:FGFR complex surprisingly do not make any contact with one another<sup>231</sup>. There are two main binding models for heparin: 1) HS/heparin binds first to FGF then to FGFR; 2) HS has to bind to FGF-FGFR complex in order for signaling to occur<sup>232,225</sup>. In these experiments, the affinity for HS/heparin of the FGF-FGFR complex is higher than that of a monomer or dimer of FGF alone, suggesting HS binds to the FGF-FGFR complex first<sup>188</sup>. The ternary complex formation causes receptor dimerization and autophosphorylation of specific cytoplasmic tyrosine residues and activation of downstream signaling processes<sup>233,234</sup>. Seven phosphorylation sites have been identified in FGFR1 (Tyr463, Tyr583, Tyr585, Tyr653, Tyr654, Tyr730, and Tyr766)<sup>235,236</sup>. The activated receptor recruits target proteins from the signaling

cascade to its cytoplasmic tail and activates them by phosphorylation<sup>213</sup>. The activation of the receptor initiates transduction via three major intracellular pathways: classic mitogen-activated protein kinase (MAPK), phosphoinositide 3-kinase (PI3K), phospholipase C<sub>γ</sub> (PLC<sub>γ</sub>) activation<sup>237</sup>. The latter two pathways are capable of activating protein kinase C (PKC) and in turn stimulating Erk 1/2 signaling<sup>226</sup>. The FGF/HSPG interaction modulates angiogenesis by the direct activation of PIP2 and PKC-α that eventually leads to activation of MAPKs<sup>110</sup>.

Tight regulation of FGFR activation can be achieved either at the level of extracellular signaling complex assembly or intracellular signaling network<sup>226</sup>. Some examples of extracellular regulatory inputs are the (i) extracellular receptor modulators, such as neural cell adhesion molecule involved in neuronal migration and axon growth, L1, cadherin, and neurofascin, and (ii) receptor auto-inhibitory properties<sup>238,239</sup>. One example of intracellular regulation involves the Sprouty (Spry) protein and MAPK phosphatase family working as negative modulators of FGF signaling through the reduction of downstream signaling<sup>240</sup>. FGF signaling activates Spry proteins, which can then in turn inhibit FGF stimulation of the MAPK pathway by interacting with growth factor receptor bound protein 2, SOS1 or RAF1, preventing their binding to FRS2<sup>241,242</sup>. Spry acts as an inhibitor in a classical negative feedback loop<sup>243</sup>. Besides the classical signaling pathways, other genes can negatively or positively regulate the signaling of FGFs. For example, Sef interacts with FGFRs and prevents FRS2 phosphorylation or blocks FGF signaling downstream of MAPK/ERK (extracellular-signal-regulated kinase) kinase<sup>244,245</sup>. XFLRT3, whose expression is regulated by FGFs, is a novel transmembrane component of the FGF signaling pathway that promotes FGF signaling through the MAPK pathway<sup>246</sup>.



## **Cytokines and Inflammation**

It is necessary for immune cells to migrate and interact with each other for infections to be fought in the immune system. Chemotactic cytokines (chemokines) are mediators of this migration<sup>247</sup>. The main activity of chemokines in inflammation is their recruitment and activation of leukocytes<sup>248</sup>. Like most heparin-binding proteins, these proteins bind to and activate their cell-surface receptors, members of the G-protein-coupled receptor superfamily<sup>249</sup>. Endothelial heparan sulfate binds chemokines and translocates them to the surface of the endothelium during the inflammatory process<sup>250</sup>. The binding of chemokines to heparin/HS is thought to be the key for regulation and modulation of chemokine activity<sup>251</sup>. Once HS immobilizes chemokines on the cell surface, leukocytes are then directed to the site of inflammation<sup>252</sup>. A conserved stretch of residues has been observed in chemokines to be responsible for GAG binding ability that is similar to the binding region of other HBPs.

### **1.8. Heparin-Binding Region of Heparin-Binding Proteins**

The heparin-binding region of each of these proteins is hypothesized to be similar to that of FGF-1, with positive residues adding to the electrostatic interactions with heparin/HS. The first study looking at requirements for GAG-protein interactions was performed by Cardin and Weintraub in 1989, when they compared the heparin-binding regions of four proteins: apolipoprotein B, apolipoprotein E, vitronectin, and platelet factor 4<sup>253</sup>. This study showed that the domains of these proteins contained a conserved sequence of XBBXB and XBBBXXB (B is basic residue and X is neutral and hydrophobic residue)<sup>253</sup>. Molecular modeling results suggested that if the XBBXB sequence was in the  $\beta$ -strand conformation, the basic amino acid residues would be aligned on one face of the strand and the hydrophobic residues would face the

inner core of the protein. If the XBBBXXBX sequence would fold into a  $\alpha$ -helix, the basic residues would face one side of the helix with the other residues facing inside the core of the protein again (Figure 1.4).

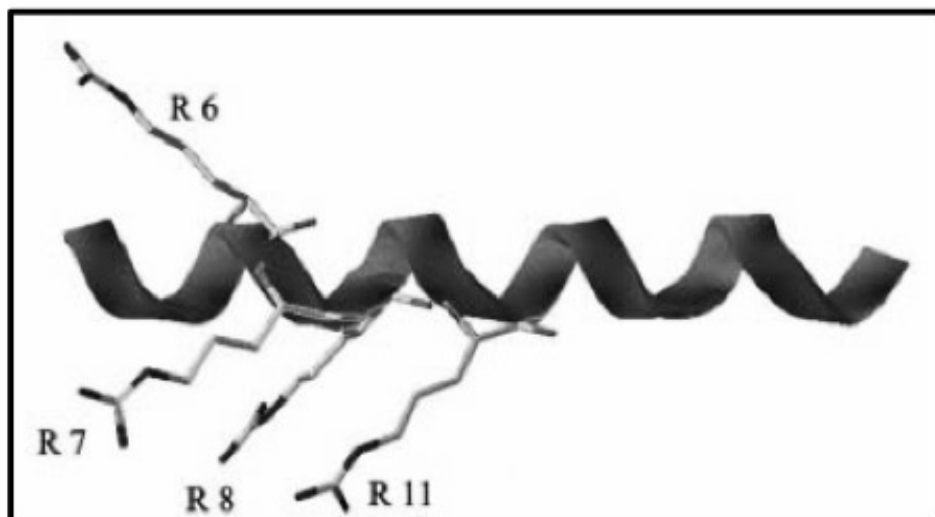


**Figure 1.4** – Helical model of a XBBBXXBX motif built using the software package SYBYL version 6.3, reproduced from Capila et al<sup>27</sup>, with permission from *Angew. Chem. Int. Ed.*

Sobel and co-workers used these findings to propose a new signature sequence, XBBBXXBBBXXBBX, found in another HBP, the von Willebrand factor<sup>254</sup>. This consensus sequence was, however, found in every other HBP.

Spatial orientation, rather than sequence proximity, of the basic residues in signature sequences in a protein is a major factor in determining the binding affinity of the protein to heparin. Margalit and co-workers showed using molecular modeling techniques that a distance of approximately 20 Å between basic amino acids is important for heparin binding<sup>255</sup>. The FGF heparin-binding site contains a peptide backbone that loops back upon itself; three turns are present in the loop<sup>256</sup>. This domain is described as a triangle. By looking at the structures of FGF-1, FGF-2, and transforming growth factor  $\beta$ -1 (TGF  $\beta$ -1), a new motif was implicated:

TXXBXXTBXXXTBB, where B is basic residue, T is a turn, and X is hydrophobic residue<sup>254</sup>  
(Figure 1.5).

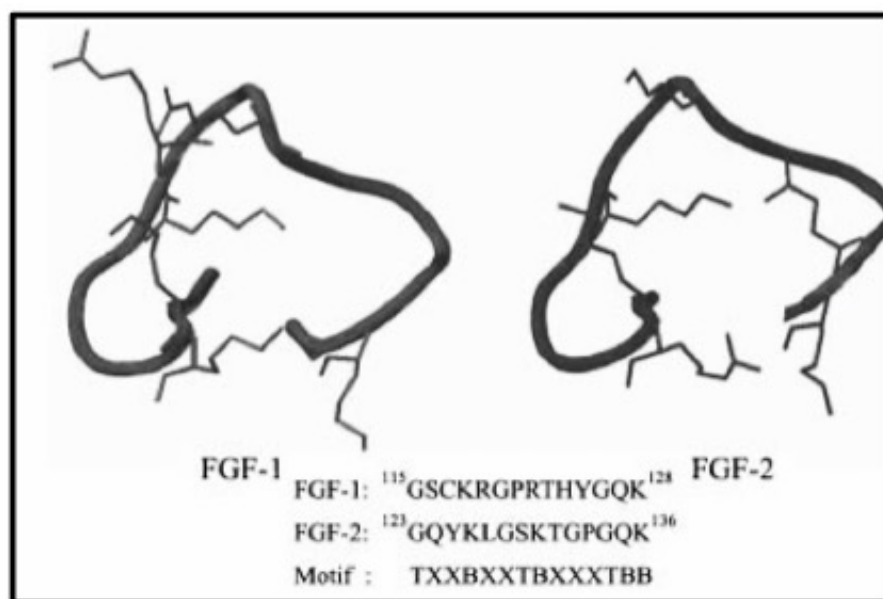


**Figure 1.5** – Turn-rich heparin-binding region in FGF-1 and FGF-2, reproduced with permission from Capila et al<sup>27</sup>, with permission from *Angew. Chem. Int. Ed.*

A cyclic peptide that was designed to resemble the heparin-binding region in the real structures of the proteins, bound more tightly to HS than the acyclic peptide of the same sequence, proving the spatial arrangement of the basic residues is more important for better access and binding to heparin/HS<sup>257</sup>. Capila and Linhardt looked at various libraries of a wide array of peptides and chains of HS and heparin, and concluded that sequences rich in lysine and arginine, but not histidine residues bound more tightly to HS/heparin<sup>27</sup>. Peptides with high affinity for HS/heparin were rich in polar amino acids including serine<sup>258</sup>. It was also observed that known heparin-binding regions contain amino acids (glutamine and asparagine) capable of hydrogen bonding<sup>27</sup>. Arginine binds 2.5 times more strongly than lysine<sup>257</sup>. This tight interaction of arginine results from strong hydrogen bonding between the guanidino group in arginine and a sulfo group in heparin<sup>259</sup>. Bae and coworkers suggested the importance of a tyrosine residue in a synthetic

ATIII peptide. This residue had a specific, hydrophobic interaction with the N-acetyl group in heparin's ATIII pentasaccharide sequence<sup>260</sup>. A single, isolated basic amino acid is commonly found in a heparin-binding site, followed by clusters of two and three basic amino acids<sup>256,257</sup>. Another commonality in heparin-binding sites is a single nonbasic amino acid between basic amino acid clusters<sup>256</sup>. Although various consensus sequences in HBPs have been found, HBPs bind to different sulfo groups in various conformations and orientations in HS and heparin, adding another aspect to the mix of finding a perfect sequence to bind tightly to heparin. Hileman and coworkers used all of these experimental data of synthetic peptides to develop a new type of heparin-binding site having the following characteristics: 1) The peptide backbone that turns back upon itself to form a cup of positive charge to interact with the negatively charged GAG. The majority of the interacting amino acids are contained in this contiguous region with a consensus sequence of TXXBXXTBXXXTBB; 2) Proper spacing and patterns of basic residues partially determine affinity and specificity for GAG interaction; 3) Arginine residues promote tighter interaction of these sites for GAGs than lysine residues. The correct ratio of these two residues defines affinity of the site for GAGs; 4) Other polar amino acids distributed throughout the site, in part, define the specificity and affinity for GAGs<sup>256</sup>.

### **1.9. Recombinant DNA Cloning and Protein Expression**

The biomedical field today is largely controlled by the production of pure proteins that have been expressed using optimized systems. There is greater need year by year for pure proteins that can be used to test pharmaceutical drugs on before they are tested on human beings. Pure recombinant proteins can be obtained from the use of bacterial systems, such as *Escherichia coli* (*E. coli*), due to the ease and low cost of growth<sup>261,262</sup>. Before the protein can be isolated,

the DNA must first be inserted into the cell of choice. Molecular cloning is the insertion of a foreign DNA fragment into the replicating DNA of another type of cell (usually *E. coli*) through the use of a vector<sup>263</sup>. The essential feature of a vector is that it can replicate autonomously in the appropriate host<sup>32</sup>. Plasmids and bacteriophage lambda ( $\lambda$  phage) are choice vectors for cloning in *E. coli*. Plasmids are self-replicating, extrachromosomal, closed circular, double-stranded DNA molecules that occur naturally in some bacteria. They range in size from two to several hundred kilobases. Plasmids carry genes for antibiotic inactivation, production of toxins, and the breakdown of natural products<sup>32</sup>. The lambda phage, a virus, can either destroy or become part of its host<sup>264</sup>. In the lytic pathway, viral DNA and proteins are produced and packaged into virus particles (virions), leading to host cell lysis<sup>32</sup>. In the lysogenic pathway, the phage DNA becomes integrated into the host genome and can be replicated together for many generations, remaining inactive<sup>265</sup>. Certain environmental factors can lead to the activation of the phage DNA, leading to lysis of the host cell. This vector can accept larger DNA fragments of eukaryotic DNA than a plasmid can. Yeast artificial chromosomes (YACs) and bacterial artificial chromosomes (BACs) can hold much larger pieces of DNA. BACs can include inserts as large as 300 kb, which means they can hold the entire genomic locus of most mammalian genes<sup>266,267</sup>. YACs contain a centromere, an autonomously replicating sequence (ARS), a pair of telomeres, selectable marker genes, and a cloning site<sup>32</sup>. They can hold megabase-sized genomic inserts<sup>268</sup>. YACs are then cloned into yeast cells as the name implies. Using these vectors, foreign DNA can be replicated into other host cells, which ultimately leads to the production of the desired product, recombinant proteins.

The main goal of recombinant protein expression is often to obtain a high accumulation of soluble product in the bacterial cell<sup>269</sup>. Various strains of *E. coli* have remained the best organisms to use for cloning techniques due its lack of restriction endonucleases that usually degrade foreign DNA. It remains one of the most attractive systems for heterologous protein production because of its ability to grow on inexpensive carbon sources, its well-characterized genetics, and availability of increasingly large numbers of cloning vectors and mutant host strains<sup>270,271,272</sup>. The most common strain of *E. coli* is BL21 because it is able to grow in minimal media but is non-pathogenic and does not cause disease in host tissues<sup>273</sup>. This strain is also chosen because it is deficient in both *lon* and *ompT* proteases, which interfere with protein isolation downstream<sup>274</sup>.

The common metabolic response in some bacterial strains trying to express recombinant proteins is the accumulation of target proteins into insoluble aggregates known as inclusion bodies because the accumulation of target proteins may not be accepted by the host's metabolism<sup>275,276</sup>. The protein expression commonly saturates the cell folding machinery, leading to formation of aggregates<sup>277,278</sup>. These entities were previously thought to be fully misfolded and thus biologically inactive<sup>269</sup>. Recently, it has been shown that inclusion bodies have intermolecular  $\beta$ -sheet secondary structure, which goes against the previous notion that they are devoid of any molecular structure<sup>279</sup>. These partially folded molecules associate mainly by hydrophobic interactions<sup>280</sup>. Cytoplasmic proteins fold spontaneously under normal conditions, but aggregation prone proteins require the existence of molecular chaperones to prevent misfolding<sup>281</sup>. Molecular chaperones interact with the polypeptide chain to prevent aggregation during the folding process<sup>282</sup>. Aggregation could result from either a large increase in concentration of folding intermediates coming from the ribosome or inefficient processing by

molecular chaperones<sup>283,284</sup>. Depending on the aggregation properties of proteins, different types of inclusion bodies can occur in *E. coli*<sup>285</sup>.

Additional difficulties encountered in *E. coli* include degradation of the protein, toxicity, and production of nonfunctional protein, which generally occurs due to lack of correct eukaryotic post-translational modification<sup>286</sup>. If protein exists in inclusion bodies, strong denaturants may be used such as guanidine hydrochloride or urea in order to solubilize the protein for further purification steps. Urea has advantages over the more harsh denaturant because of its low costs and its ability to be used in sodium dodecylsulfate polyacrylamide gel electrophoresis (SDS-PAGE) unlike guanidine hydrochloride that precipitates in the presence of SDS<sup>287</sup>. The use of mild solubilization agents, not just high concentrations of denaturants, also helps to solubilize aggregates without disturbing the secondary structures of the proteins<sup>288,289,290,291</sup>. Purification of proteins in inclusion bodies has been optimized that greater than 90% purity has been obtained<sup>292,293</sup>. These findings prove the existence of inclusion bodies is not as devastating as previous scientists had believed. After purification, the corresponding denaturant can be removed by dialysis and other methods in order to obtain pure refolded protein<sup>294</sup>.

Several techniques have been proposed to improve the solubility or folding of recombinant proteins in *E. coli*<sup>295</sup>. These include co-expression of chaperone proteins, lowering incubation temperature, use of weak promoters, use of richer media with phosphate buffer such as terrific broth (TB), and the use of fusion tags to aid in the expression and purification process<sup>296,297,298,299</sup>. The activity and expression of a number of *E. coli* chaperones increase at 30°C, as reported by Sorensen and Mortensen<sup>269</sup>. Co-overexpression of molecular chaperones such as DnaK-DnaJ-GrpE and GroEL-GroES systems have proved efficient in soluble expression and decreasing the existence of proteins in inclusion bodies<sup>300</sup>. The partial

elimination of heat shock proteases induced under normal conditions is also a direct result of temperature reduction<sup>301</sup>. The promoters used for transcription of heterologous genes have remained in the *lac* operon family (*lac*-derived regulatory elements). The *lac* promoter and its relative, *lacUV5*, are relatively weak, and are therefore seldom used for high-level production of recombinant proteins<sup>270</sup>. They can, however, be used for expression of helper or toxic proteins, provided that *lacY* mutant hosts are used and that the induction is performed with the non-hydrolyzable lactose analog, isopropyl- $\beta$ -D-1-thiogalactopyranoside (IPTG)<sup>302,303</sup>. The synthetic *tac* and *trc* promoters consist of the -35 region of the *trp* promoter and the -10 region of the *lac* promoter. These promoters are quite strong and commonly allow the accumulation of polypeptides to 30% of the total cell protein<sup>270</sup>. Bacterial growth and expression is controlled by the *lac* operon. When enough lactose is added to the cell, it binds to repressor proteins and causes the induction of the transcription of permease and  $\beta$ -galactosidase because the repressor can no longer bind to operator DNA<sup>304</sup>. Researchers have removed these two genes and have placed their gene of interest in their place. When lactose, or its analog IPTG, is added, the gene of interest is produced through induction, instead of permease and  $\beta$ -galactosidase.

Certain fusion proteins have been constructed and expressed in *E. coli* for use in purification techniques as well as better solubility of proteins in expression systems. These proteins or tags improve the solubility of partner proteins that would otherwise form inclusion bodies in the cytoplasm during expression. Commercially available fusion partners include glutathione-S-transferase (GST), maltose-binding protein (MBP), thioredoxin, or poly-Histidine tag (His-tag)<sup>305</sup>. Improved folding of passenger proteins is most likely obtained by the fusion partner efficiently reaching its native conformation as it exits the ribosome, and promotes the correct structure in downstream folding units by favoring on-pathway isomerization reactions<sup>270</sup>.



For example, unfused MBP requires molecular chaperones such as DnaK-DnaJ-GrpE and GroEL-GroES, which might recruit these molecules to the partner protein during the folding process<sup>270</sup>. It has also been proposed that MBP might actually act as an “intramolecular chaperone” to assist in the correct folding of the fused protein by being in close proximity during the process<sup>306</sup>. Thioredoxins are universal oxido-reductases that reduce disulfide bonds through thio-disulfide exchange<sup>307</sup>. TrxA is an 11.6kDa thioredoxin found in *E. coli* that demonstrates high solubility in the crystallization of proteins and is used to increase expression of recombinant proteins<sup>308</sup>. Small ubiquitin-like modifier (SUMO), when used as an N-terminal carrier protein promotes folding, enhances solubility during expression, and structural stability during protein expression<sup>309,310,311</sup>. In its native system, Smt3, a form of post-translational modification, plays roles in apoptosis, nuclear-cytosolic transport, and protein activation<sup>312,313,314</sup>. These “solubility increasers” are very useful tags during bacterial expression of recombinant proteins, but various tags have also been developed to aid in the purification of the expressed proteins. Some tags, like GST and MBP, have dual roles in expression and purification.

### **1.10. Chromatography for Protein Purification**

After the fusion protein is expressed at high yield, it needs to be removed from the millions of other proteins that are contained in the bacterial cell. The general order of obtaining a protein of interest includes overexpression using solubility tag, lysis of the bacterial cells to bring the proteins into the aqueous phase, and removal of contaminating proteins from the target protein using column chromatography. This purification method employs chromatography techniques that separate the proteins based on various characteristics. The most well-known techniques include size-exclusion, affinity, and ion exchange, with some proteins requiring the

mixture of two or more of these chromatography methods<sup>315</sup>. Proteins that are eluted can be traced using UV-vis spectroscopy attached to the chromatography apparatus because most proteins contain at least one tryptophan that absorbs light at 280 nm. Once fractions containing eluted protein are collected, visualization of distinct proteins occurs using sodium dodecyl sulfate-polyacrylamide gel electrophoresis (SDS-PAGE) and Coomassie Blue staining to determine purity of protein samples.

### **Ion-Exchange Chromatography**

In this technique, proteins interact with charged molecules, either positive or negative, that are bound to a stationary phase by electrostatic interactions<sup>316</sup>. The main advantage of this technique is that it maintains the biological activity of the purified protein<sup>317</sup>. Ligand density has a profound effect on protein binding behavior and purification efficiency, as seen in various experiments performed<sup>318,319,320</sup>. In general, the greater ligand density, the greater binding capacity occurred for a protein. For high ligand densities, physical characteristics of the adsorber such as particle and pore diameter and available adsorber area, also affect elution behavior<sup>321</sup>. This purification mode is often used as a final step of removing any last-minute contaminants after other purification steps have been performed<sup>315</sup>.

### **Size-Exclusion Chromatography (SEC)**

This type of chromatography that is also known as gel filtration chromatography, was first shown in 1955 to be efficient for the separation of biomolecules, in particular the separation of peptides from amino acids and proteins<sup>322,323</sup>. Using SEC has allowed the determination of the molecular weight of an unknown analyte, based on a calibration curve of known

analytes<sup>324,325</sup>. The pore size on the resin is what restricts molecules, depending on their sizes from entering the pores. Larger molecules (larger Stokes radius) do not gain access into the pores, so they elute first. The elution of next largest molecules occurs until the smallest ones come out last<sup>326</sup>. A setback of SEC is that proteins vary in shape, so their Stokes radii do not match up exactly with its actual molecular weight. This usually results in proteins of varying shape and size actually coeluting, which gives rise to the incorrect molecular weight estimation<sup>327</sup>. The average molecular weight of heparin has been studied using various standards, but the mobile phase conditions affected the analysis of its accurate molecular weight<sup>328</sup>. Even though the overall rate of SEC is fast, the desire of any scientist is for improved resolution and separation of biomolecules. This improvement comes with decreased flow rate, which in turn increases the analysis times for SEC. This was demonstrated by Ricker and Sandoval, as better resolution of bovine serum albumin and ovalbumin was observed with decreased flow rate<sup>329</sup>. SEC has become the standard for monitoring protein aggregation and quaternary structure in the biopharmaceutical industry<sup>330,331</sup>. SEC is also used as a polishing step for protein purification in industry, where aggregate impurities could not be removed using previous chromatographic processes<sup>332</sup>.

### **Affinity Chromatography**

One of the most popular methods of purification is the expression of various proteins attached to affinity tags, which allows for a one-step purification process of proteins obtained at high purity<sup>333,334</sup>. Yields over 90% with reduced steps are observed in affinity chromatography<sup>335</sup>. The column consists of beads containing a material or ligand that has a high binding affinity to a protein or small molecule. The protein of interest is attached to a peptide or

large protein that binds in a specific fashion to an immobilized ligand that other proteins do not have affinity for, in a fashion close to antibody-antigen interaction<sup>333</sup>. Advantages of adding an affinity tag to a target protein include improved yield and solubility, increased sensitivity of binding assays, and improved antigenicity<sup>336,337,338,339</sup>. Some disadvantages exist, however, including biological activity being altered<sup>340</sup>. A few examples of affinity chromatography partners include heparin/HBPs, glutathione/GST, nickel/His-tag.

The ligand that is trapped on the column for purifying proteins using affinity tags is of great importance when determining what tag to use. There are many different affinity column materials available but the most well-known include heparin-Sepharose, glutathione-Sepharose, nickel-Sepharose, to name a few. Electrostatic interactions, as well as hydrogen bonding, are the governing forces for the binding of proteins or affinity tags to heparin-Sepharose, with protein eluting using varying salt conditions<sup>341,342</sup>. Due to its high negative character, heparin can also be used as an ion exchanger<sup>315</sup>. Just like the other chromatography techniques, this method can be used in tandem with other techniques for protein purification<sup>343,344,203</sup>.

### **1.11. Affinity Tags**

These affinity tags used as fusion partners for target proteins are efficient tools for their purification from crude extracts<sup>334</sup>. The affinity tags can be small peptides made up of varying or repeating amino acids such as His-tag, or they can be larger proteins such as GST and MBP. Whatever the tag composition is, the ultimate goal in designing or choosing a suitable fusion partner for proteins is the purification technique of choice. A benefit of affinity tags is their ability to hundred- or thousand-fold purification without prior steps to remove cellular material<sup>345</sup>. The affinity-tag systems, when vying for the researchers' attention, should share

similar features, such as minimal steps of purification, minimal effect on the tertiary structure and activity of proteins, specific and easy removal of tag to produce native protein, accurate assay of the recombinant protein during purification, and versatility to different proteins<sup>346,347</sup>. The tags used to increase solubility of proteins during expression include GST, MBP, NusA, thioredoxin, and SUMO. The tags used solely for affinity purification include His-tag, FLAG, Strep II, calmodulin-binding peptide (CBP), and chitin-binding domain. For well-expressed soluble proteins, an affinity tag alone is sufficient for expression and subsequent purification<sup>348</sup>. For poorly soluble proteins that are difficult to express, a solubility and affinity tag might be needed. In order to increase the versatility of the tags with respect to solubility and affinity roles, dual-tagging methods have been applied to various proteins<sup>348</sup>. Tags, such as GST and MBP, have dual roles in expression and purification and have become a highly chosen affinity tag in laboratories today.

The GST tag was first described in 1988 by Smith and Johnson as a 26kDa GST of *Schistosoma japonicum* cloned in an *E. coli* expression vector<sup>349</sup>. In the majority of the cases, the fusion proteins are soluble in aqueous solutions and form dimers<sup>346</sup>. This tag helps protect against intracellular protease cleavage and stabilize the fusion partner<sup>350,351</sup>. GST fusion proteins can be purified on glutathione ( $\gamma$ -glutamylcysteinylglycine)-Sepharose. The resin is affected by  $\gamma$ -glutamyl transpeptidase activity in crude cell lysates<sup>352</sup>. This means that the glutathione resin can only be used up to twenty times. An advantage of glutathione purification is that proteolytic cleavage can be performed while the fusion protein is still bound to the column, which allows fewer steps in the purification process. Glutathione chromatography depends on the proper three-dimensional folding of GST, so insoluble fusion proteins must be refolded and the buffer exchanged before purification is performed<sup>353</sup>. Using a GST tag allows high levels of expression

of the fusion protein in *E. coli* (10-50 mg/liter culture)<sup>354</sup>. A major drawback to using GST-tagged proteins is seen in its slow binding kinetics to glutathione-Sepharose, making purification of large cell culture volumes extremely time consuming<sup>355</sup>. The next fairly large protein molecule used an affinity tag is the 42kDa MBP encoded by *malE* gene of *E. coli* K12<sup>356</sup>. Vectors that facilitate the expression and purification of foreign peptides or proteins in *E. coli* by MBP tags were first described in 1988 by Di Guan and coworkers<sup>357</sup>. MBP-tagged proteins bind to immobilized amylose and are released by 10 mM maltose. This one-step purification process using MBP tags can lead to a fusion protein of 70-90% purity<sup>358</sup>. MBP-tagged proteins have typical yields of 10-40 mg/liter of culture<sup>359</sup>. The large size of this tag, however, may result in aggregation of the target protein after cleavage occurs<sup>360</sup>. Another disadvantage when compared with GST tags is that target proteins cannot be proteolytically cleaved from MBP while still bound to the amylose resin<sup>359</sup>. The MBP tag expression system is widely used in combination with a poly-His tag for better purification<sup>361</sup>.

Very small peptide tags are valued in purification processes due to their ability to not interfere with the biological and structural properties of the fused protein. These small tags include poly-arginine, FLAG, His-tag, Strep II, c-myc, and S tags, which, since so small, may not have to be removed following purification<sup>333</sup>. The poly-arginine tag was first described in 1984 by Sassenfeld and Brewer, which consists of five or six arginine residues<sup>362</sup>. These tagged proteins can be purified by cation exchange resin SP-Sephadex. Proteins elute at a linear sodium chloride gradient at alkaline pH<sup>346</sup>. The downfall of using a poly-arginine tag is that proteins also contain arginine residues, which could then affect the binding capability of the fusion protein containing this tag<sup>363</sup>. The next small peptide tag is a commonly used affinity tag known as His-tag, which consists of roughly six histidine residues that binds to small molecules

immobilized on a column. The process of purifying proteins with His-tags is known as immobilized metal-affinity chromatography (IMAC), which was described in 1975 by Porath and coworkers<sup>364</sup>. This purification technique is based on the interaction between a transition metal ion ( $\text{Co}^{2+}$ ,  $\text{Ni}^{2+}$ ,  $\text{Cu}^{2+}$ ,  $\text{Zn}^{2+}$ , and recently,  $\text{Fe}^{3+}$ ) immobilized on a matrix and specific amino acid side chains (accessible His, Ser, Cys, Glu, and Asp residues)<sup>365, 366</sup>. The electron donor atoms in chelating compounds of the chromatographic support (histidine imidazole ring) are able to coordinate metal ions and form metal chelates, which can be bidentate, tridentate, etc, depending on the number of occupied coordination bonds<sup>367</sup>. In one instance, His-tag showed to improve cell growth rates and protein expression levels in cells containing His-fusion proteins<sup>368</sup>. Also being a short sequence, these tags do not add a significant metabolic load to the protein expression and can easily be incorporated to the protein by simple genetic engineering at the upstream level<sup>369</sup>. Advantages of IMAC include stability of metal chelates over a wide range of buffer conditions and temperatures, ability to exist in denaturing conditions and high protein loading capacities<sup>370,367</sup>. IMAC is also the leading method for purification of denatured proteins<sup>287</sup>. Disadvantages of the His-tag include metal leaching that contaminates the protein, adsorbent binding to other native histidine or amino acid patches resulting in low selectivity or coelution, and altered biological and physiochemical properties of the target protein<sup>371,372,373,374</sup>.

The FLAG peptides are epitope tags, which bind to immobilized monoclonal antibodies, such as M1<sup>375,376,377</sup>. These FLAG-tags can be located at the N- or C-terminal of a fusion protein. The eight-residue Strep II tag binds reversibly to a modified biotin-binding pocket of the engineered streptavidin called Strep-Tactin<sup>378</sup>. It can be released using a biotin analog, in the absence of metal ions during purification<sup>379</sup>. This tag is proteolytically stable, biologically inert, and can be engineered at either terminus of a protein<sup>380</sup>. The murine anti-c-myc antibody 9E10

was developed in 1985 by Evan and coworkers, and is used as an immunochemical reagent today<sup>381</sup>. C-myc tag is an antibody epitope tag of 11 amino acids that can be placed at either end of the desired protein<sup>382</sup>. Tagged proteins of this nature can be purified by coupling mAb 9E10 to divinyl sulphone-activated agarose<sup>346</sup>. This tag is commonly used to monitor expression of proteins in a wide array of cell hosts<sup>383,384,385,386</sup>. The S-tag is a soluble 15 amino acid tag that interacts strongly with the 103 amino-acid S-protein, both derived from RNaseA<sup>387,388</sup>.

There are, however, many other types of affinity tags that are used today but not to the degree of His-tag, GST, and MBP tags. The CBP tag was first described in 1992 by Stofko-Hahn and coworkers as a 26-amino acid tag derived from the C-terminus of skeletal muscle myosin light-chain kinase<sup>389</sup>. The CBP tag forms an  $\alpha$ -helix, which is engulfed by the EF-hand motif of calmodulin<sup>390</sup>. This system has high specificity to purify recombinant proteins in *E. coli* because there are no endogenous proteins that interact with calmodulin in this bacterium<sup>346</sup>. CBP-tagged proteins are released from calmodulin resin by EDTA, which chelates the calcium ions necessary for proper folding of the EF-hand motif<sup>390</sup>. The N-terminal location may reduce the efficiency of translation, whereas the C-terminal location can result in high expression levels<sup>391</sup>. A novel and very innovative tag has been designed called intein-chitin binding domain tag. This tag is the combination of a protein self-splicing element (intein, intervening proteins) and chitin-binding domain<sup>359</sup>. The yield using this tag is roughly 0.5 to 5 mg cleaved protein/liter bacterial culture<sup>345</sup>. Use of this affinity tag is not recommended in eukaryotic cells because endogenous proteins can interfere with the binding affinity based on calcium<sup>392</sup>.

In the industrial and commercial aspect of choosing a good affinity tag for purification, one must consider the ultimate desired outcome. Experiments requiring large amounts of partially purified material in high yields at low cost may find His and GST tags attractive, but for



small amounts of highest purity, FLAG and HPC tags might outweigh their costs and limited capacity<sup>345</sup>. Short peptides have gained the spotlight as excellent ligands for affinity chromatography<sup>393</sup>. Peptide ligands are much more physically and chemically stable than antibody ligands and are more resistant to proteolytic cleavage<sup>394,395</sup>. These peptides can also be easily modified to aid in protein elution under mild conditions. Peptides can be readily synthesized using already established methods at lower cost<sup>396</sup>. Immobilization of these peptides onto a resin can be achieved, and the designed matrices are more durable during protein elution than the protein-based affinity chromatography<sup>397</sup>. Lastly, during protein expression, these affinity peptides have low toxicity and generate low immune responses in the event of cell leakage as compared with proteins and transition metal ligands<sup>394</sup>. No matter what affinity tag is used, there are always advantages and disadvantages to every one (Table 1.3).

Affinity Tag	Size (amino acids)	Advantages	Disadvantages
His-tag	5-15	Low metabolic burden, inexpensive, mild elution conditions, works under native and denaturing conditions	Specificity of IMAC is low
GST	201	Efficient translation initiation, inexpensive, mild elution conditions	High metabolic burden, homodimeric protein
MBP	396	Efficient translation initiation, inexpensive, mild elution conditions	High metabolic burden
Thioredoxin	109	Efficient translation initiation, enhances solubility	Except few derivatives of thioredoxin like His-patch thioredoxin, it does not act as affinity tag
FLAG	8	Low metabolic burden, high specificity	Expensive, harsh elution conditions
S-tag	15	Low metabolic burden, high specificity	Expensive, harsh elution conditions, does not enhance solubility
CBP	27	Low metabolic burden, high specificity	Expensive, does not enhance solubility
STREP II	8	Low metabolic burden, high specificity	Expensive, does not enhance solubility
BAP	51	Low metabolic burden	Expensive, does not enhance solubility
CBD	15	No exogenous proteolytic cleavage is needed	Does not enhance solubility

**Table 1.3** – Well-known affinity tags, their sizes, advantages, and disadvantages, modified from Mondal et al<sup>398</sup>.

Also, various tags can be used in combination on target proteins to increase solubility and yield<sup>399</sup>.

### Cleavage of Affinity Tags

Ultimately, the native pure protein is desired after affinity chromatography is performed, which requires the removal of the affinity tag. This process is performed by enzymatic or chemical cleavage at the junction between the tag and the protein of interest<sup>335,400</sup>. The most

common form of cleavage today is performed enzymatically by proteases, such as thrombin, factor Xa, enterokinase, and tobacco etch virus (TEV) protease<sup>401,402,403,404</sup>. The chemicals most commonly used for cleavage are cyanogen bromide (CNBr), formic acid, and hydroxylamine<sup>348</sup>. Enzymatic cleavage is more specific and milder than chemical cleavage<sup>348</sup>. Thrombin, 37 kDa, is the most well-known endopeptidase and recognizes the specific sequence of Leu-Val-Pro-Arg-Gly-Ser, where it breaks Arg and Gly bond<sup>405</sup>. Thrombin is preferred due to its low cost and optimal physiological pH range of 6-8<sup>406</sup>. The proteases have their own cleavage site that they recognize: thrombin (LVPR/GS), factor Xa (IEGR/), enterokinase (DDDDK/), TEV (ENLYFQ/G)<sup>305</sup>. Various reviews go into more detail on each protease<sup>405,333,407</sup>. The downfall of these endopeptidases, with the exception of TEV protease, is their ability to cleave at sites other than their intended specific cleavage site<sup>408,409,410</sup>. Viral proteases like TEV protease have more specificity for their cleavage sites, which makes TEV protease a solid choice for cleaving affinity tags from target proteins<sup>411</sup>.

### **1.12. Detection of Proteins by Immunoblotting**

Preparation of antibodies to detect specific proteins is an ongoing need in molecular biology<sup>412</sup>. Immunoblotting, also known as Western blotting, originated from the other blotting techniques, Southern for DNA and Northern for RNA<sup>413,414</sup>. WB is a diagnostic tool today for HIV, Lyme disease, and hepatitis B<sup>415</sup>. Towbin et al established a method of transferring proteins from polyacrylamide-urea gel onto a nitrocellulose membrane in 1979, but in 1981, Burnette introduced adaptations to this existing method to coin the new optimized method as Western blotting, in honor of the Southern blotting that already existed<sup>416,417,418</sup>. This Western blotting allows proteins to be transferred from SDS-PAGE gels to nitrocellulose membranes,

since most protein analyses are run on these types of gels not polyacrylamide-urea gels<sup>417</sup>. WB has multiple advantages that include proteins of low abundance can be detected, small amount of chemicals required for transfer, proteins on the membrane are easily accessible to various ligands, and many more<sup>419,420,421</sup>. Electroblotting is the most commonly used technique for transfer of proteins onto the membrane because it is fast and complete compared to conventional ones (diffusion and vacuum). After transfer has occurred milk is used to block unoccupied sites on the membrane<sup>422</sup>. After transfer has occurred, primary antibody grown against a specific peptide sequence is then incubated with the membrane-bound proteins. After this, horseradish peroxidase- or alkaline phosphatase-conjugated secondary antibody, grown against the primary antibody, is incubated as well with multiple washing steps in between. These washing steps remove any unwanted nonspecific antibody-antigen or even antibody-membrane interactions. Most commonly, a substrate composed of nitro-blue tetrazolium (NBT) and 5-bromo-4-chloro-3'-indolyphosphate (BCIP) is added after the secondary antibody is incubated, which when reacted with the alkaline phosphatase, it creates a purple-black precipitate. Since the secondary antibody should only attach to the primary antibody, only the protein of interest that the primary antibody was raised against should make a colored precipitate. It has been shown that to reach a higher sensitivity of detection, heat treatment of the nitrocellulose membrane after blotting can be performed<sup>423</sup>. This method is very effective for detection of protein of interest with high specificity when performed correctly, with the only major drawback of it being a qualitative not quantitative measurement. Antibodies can also be immobilized on a matrix for the purification of proteins by immunoaffinity chromatography<sup>424</sup>.

### 1.13. References

1. Lai, E. C., Notch signaling: control of cell communication and cell fate. *Development (Cambridge, U. K.)* **2004**, *131* (5), 965-973.
2. Thannickal, V. J.; Fanburg, B. L., Reactive oxygen species in cell signaling. *Am J Physiol Lung Cell Mol Physiol* **2000**, *279* (6), L1005-28.
3. Gattazzo, F.; Urciuolo, A.; Bonaldo, P., Extracellular matrix: A dynamic microenvironment for stem cell niche. *Biochim. Biophys. Acta, Gen. Subj.* **2014**, *1840* (8), 2506-2519.
4. Frantz, C.; Stewart, K. M.; Weaver, V. M., The extracellular matrix at a glance. *J. Cell Sci.* **2010**, *123* (24), 4195-4200.
5. Lu, P.; Takai, K.; Weaver, V. M.; Werb, Z., Extracellular matrix degradation and remodeling in development and disease. *Cold Spring Harbor Perspect. Biol.* **2011**, *3* (12), a005058/1-a005058/24.
6. Senger, D. R.; Davis, G. E., Angiogenesis. *Cold Spring Harbor Perspect. Biol.* **2011**, *3* (8), No pp given.
7. Reinhard, J.; Joachim, S. C.; Faissner, A., Extracellular matrix remodeling during retinal development. *Exp. Eye Res.* **2015**, *133*, 132-140.
8. Barkan, D.; Green, J. E.; Chambers, A. F., Extracellular matrix: A gatekeeper in the transition from dormancy to metastatic growth. *Eur. J. Cancer* **2010**, *46* (7), 1181-1188.
9. Brizzi, M. F.; Tarone, G.; Defilippi, P., Extracellular matrix, integrins, and growth factors as tailors of the stem cell niche. *Curr. Opin. Cell Biol.* **2012**, *24* (5), 645-651.
10. Kostourou, V.; Papalazarou, V., Non-collagenous ECM proteins in blood vessel morphogenesis and cancer. *Biochim. Biophys. Acta, Gen. Subj.* **2014**, *1840* (8), 2403-2413.
11. Calabro, N. E.; Kristofik, N. J.; Kyriakides, T. R., Thrombospondin-2 and extracellular matrix assembly. *Biochim. Biophys. Acta, Gen. Subj.* **2014**, *1840* (8), 2396-2402.
12. Esko, J. D.; Kimata, K.; Lindahl, U., Proteoglycans and sulfated glycosaminoglycans. *Essent. Glycobiol. (2nd Ed.)* **2009**, 229-248.
13. Alberts, B.; Alexander, J.; Lewis, J.; Raff, M.; Roberts, K.; Walter, P., *Molecular Biology of the Cell, 4th Edition*. 2004; p 2000 pp.
14. Gill, S.; Wight, T. N.; Frevort, C. W., Proteoglycans: key regulators of pulmonary inflammation and the innate immune response to lung infection. *Anat. Rec.* **2010**, *293* (6), 968-981.

15. Fonovic, M.; Turk, B., Cysteine cathepsins and extracellular matrix degradation. *Biochim. Biophys. Acta, Gen. Subj.* **2014**, *1840* (8), 2560-2570.
16. Weyers, A.; Linhardt, R. J., Neoproteoglycans in tissue engineering. *Febs J.* **2013**, *280* (10), 2511-2522.
17. Li, L.; Ly, M.; Linhardt, R. J., Proteoglycan sequence. *Mol. BioSyst.* **2012**, *8* (6), 1613-1625.
18. Wade, A.; McKinney, A.; Phillips, J. J., Matrix regulators in neural stem cell functions. *Biochim. Biophys. Acta, Gen. Subj.* **2014**, *1840* (8), 2520-2525.
19. Sugahara, K.; Kitagawa, H., Recent advances in the study of the biosynthesis and functions of sulfated glycosaminoglycans. *Curr. Opin. Struct. Biol.* **2000**, *10* (5), 518-527.
20. Chatzinikolaou, G.; Nikitovic, D.; Asimakopoulou, A.; Tsatsakis, A.; Karamanos, N. K.; Tzanakakis, G. N., Heparin-a unique stimulator of human colon cancer cells' growth. *IUBMB Life* **2008**, *60* (5), 333-340.
21. Jackson, R. L.; Busch, S. J.; Cardin, A. D., Glycosaminoglycans: molecular properties, protein interactions, and role in physiological processes. *Physiol. Rev.* **1991**, *71* (2), 481-539.
22. Kinsella, M. G.; Bressler, S. L.; Wight, T. N., The regulated synthesis of versican, decorin, and biglycan: extracellular matrix proteoglycans that influence cellular phenotype. *Crit. Rev. Eukaryotic Gene Expression* **2004**, *14* (3), 203-234.
23. Bosman, F. T.; Stamenkovic, I., Functional structure and composition of the extracellular matrix. *J. Pathol.* **2003**, *200* (4), 423-428.
24. Dolhnikoff, M.; Morin, J.; Roughley, P. J.; Ludwig, M. S., Expression of lumican in human lungs. *Am. J. Respir. Cell Mol. Biol.* **1998**, *19* (4), 582-587.
25. Sarrazin, S.; Lamanna, W. C.; Esko, J. D., Heparan sulfate proteoglycans. *Cold Spring Harbor Perspect. Biol.* **2011**, *3* (7), No pp given.
26. Christianson, H. C.; Belting, M., Heparan sulfate proteoglycan as a cell-surface endocytosis receptor. *Matrix Biol.* **2014**, *35*, 51-55.
27. Capila, I.; Linhardt, R. J., Heparin - protein interactions. *Angew. Chem., Int. Ed.* **2002**, *41* (3), 390-412.
28. Reijmers, R. M.; Spaargaren, M.; Pals, S. T., Heparan sulfate proteoglycans in the control of B cell development and the pathogenesis of multiple myeloma. *Febs J.* **2013**, *280* (10), 2180-2193.
29. Miguez, P. A.; Terajima, M.; Nagaoka, H.; Mochida, Y.; Yamauchi, M., Role of glycosaminoglycans of biglycan in BMP-2 signaling. *Biochem. Biophys. Res. Commun.* **2011**, *405* (2), 262-266.

30. Gasimli, L.; Hickey, A. M.; Yang, B.; Li, G.; dela Rosa, M.; Nairn, A. V.; Kulik, M. J.; Dordick, J. S.; Moremen, K. W.; Dalton, S.; Linhardt, R. J., Changes in glycosaminoglycan structure on differentiation of human embryonic stem cells towards mesoderm and endoderm lineages. *Biochim. Biophys. Acta, Gen. Subj.* **2014**, *1840* (6), 1993-2003.
31. Sattelle, B. M.; Shakeri, J.; Cliff, M. J.; Almond, A., Proteoglycans and Their Heterogeneous Glycosaminoglycans at the Atomic Scale. *Biomacromolecules* **2015**, *16* (3), 951-961.
32. Berg, J.; Tymoczko, J.; Stryer, L., *Biochemistry*. 5th ed.; W H Freeman: New York, 2002.
33. Baasanjav, S.; Al-Gazali, L.; Hashiguchi, T.; Mizumoto, S.; Fischer, B.; Horn, D.; Seelow, D.; Ali, B. R.; Aziz, S. A. A.; Langer, R.; Saleh, A. A. H.; Becker, C.; Nuernberg, G.; Cantagrel, V.; Gleeson, J. G.; Gomez, D.; Michel, J.-B.; Stricker, S.; Lindner, T. H.; Nuernberg, P.; Sugahara, K.; Mundlos, S.; Hoffmann, K., Faulty Initiation of Proteoglycan Synthesis Causes Cardiac and Joint Defects. *Am. J. Hum. Genet.* **2011**, *89* (1), 15-27.
34. Beller, J. A.; Snow, D. M., Proteoglycans: road signs for neurite outgrowth. *Neural Regener. Res.* **2014**, *9* (4), 343-355.
35. Suttkus, A.; Rohn, S.; Weigel, S.; Gloeckner, P.; Arendt, T.; Morawski, M., Aggrecan, link protein and tenascin-R are essential components of the perineuronal net to protect neurons against iron-induced oxidative stress. *Cell Death Dis.* **2014**, *5* (3), e1119.
36. Liu, Z.; Masuko, S.; Solakyildirim, K.; Pu, D.; Linhardt, R. J.; Zhang, F., Glycosaminoglycans of the Porcine Central Nervous System. *Biochemistry* **2010**, *49* (45), 9839-9847.
37. Berry, D.; Lynn, D. M.; Sasisekharan, R.; Langer, R., Poly( $\beta$ -amino ester)s Promote Cellular Uptake of Heparin and Cancer Cell Death. *Chem. Biol.* **2004**, *11* (4), 487-498.
38. Zhao, X.; Yang, B.; Solakyildirim, K.; Solakylidirim, K.; Joo Eun, J.; Toida, T.; Higashi, K.; Linhardt Robert, J.; Li, L., Sequence analysis and domain motifs in the porcine skin decorin glycosaminoglycan chain. *J Biol Chem* **2013**, *288* (13), 9226-37.
39. Ariga, T.; Miyatake, T.; Yu, R. K., Role of proteoglycans and glycosaminoglycans in the pathogenesis of Alzheimer's disease and related disorders: amyloidogenesis and therapeutic strategies-A review. *J. Neurosci. Res.* **2010**, *88* (11), 2303-2315.
40. Raman, R.; Sasisekharan, V.; Sasisekharan, R., Structural insights into biological roles of protein-glycosaminoglycan interactions. *Chem. Biol.* **2005**, *12* (3), 267-277.
41. Yamada, S.; Sugahara, K.; Ozbek, S., Evolution of glycosaminoglycans - comparative biochemical study. *Commun. Integr. Biol.* **2011**, *4* (2), 150-158.

42. DeAngelis, P. L.; Liu, J.; Linhardt, R. J., Chemoenzymatic synthesis of glycosaminoglycans: Re-creating, re-modeling and re-designing nature's longest or most complex carbohydrate chains. *Glycobiology* **2013**, *23* (7), 764-777.
43. Gandhi, N. S.; Mancera, R. L., The structure of glycosaminoglycans and their interactions with proteins. *Chem. Biol. Drug Des.* **2008**, *72* (6), 455-482.
44. Volpi, N., Dermatan sulfate: Recent structural and activity data. *Carbohydr. Polym.* **2010**, *82* (2), 233-239.
45. Hayes, A. J.; Mitchell, R. E.; Bashford, A.; Reynolds, S.; Caterson, B.; Hammond, C. L., Expression of glycosaminoglycan epitopes during zebrafish skeletogenesis. *Dev. Dyn.* **2013**, *242* (6), 778-789.
46. Kramer, K. L.; Yost, H. J., Heparan sulfate core proteins in cell-cell signaling. *Annu. Rev. Genet.* **2003**, *37*, 461-484.
47. Sampaio, L. O.; Tersariol, I. L. S.; Lopes, C. C.; Boucas, R. I.; Nascimento, F. D.; Rocha, H. A. O.; Nader, H. B., Heparins and heparan sulfates. Structure, distribution and protein interactions. *Insights Carbohydr. Struct. Biol. Funct.* **2006**, 1-24.
48. Hardingham, T. E.; Fosang, A. J., Proteoglycans: many forms and many functions. *Faseb J.* **1992**, *6* (3), 861-70.
49. Mizumoto, S.; Fongmoon, D.; Sugahara, K., Interaction of chondroitin sulfate and dermatan sulfate from various biological sources with heparin-binding growth factors and cytokines. *Glycoconjugate J.* **2013**, *30* (6), 619-632.
50. Sugahara, K.; Mikami, T., Chondroitin/dermatan sulfate in the central nervous system. *Curr. Opin. Struct. Biol.* **2007**, *17* (5), 536-545.
51. Mizuguchi, S.; Uyama, T.; Kitagawa, H.; Nomura, K. H.; Dejima, K.; Gengyo-Ando, K.; Mitani, S.; Sugahara, K.; Nomura, K., Chondroitin proteoglycans are involved in cell division of *Caenorhabditis elegans*. *Nature (London, U. K.)* **2003**, *423* (6938), 443-448.
52. Hwang, H.-Y.; Olson, S. K.; Esko, J. D.; Robert Horvitz, H., *Caenorhabditis elegans* early embryogenesis and vulval morphogenesis require chondroitin biosynthesis. *Nature (London, U. K.)* **2003**, *423* (6938), 439-443.
53. Trowbridge, J. M.; Gallo, R. L., Dermatan sulfate: new functions from an old glycosaminoglycan. *Glycobiology* **2002**, *12* (9), 117R-125R.
54. Bergefäll, K.; Trybala, E.; Johansson, M.; Uyama, T.; Naito, S.; Yamada, S.; Kitagawa, H.; Sugahara, K.; Bergström, T., Chondroitin Sulfate Characterized by the E-disaccharide Unit Is a Potent Inhibitor of Herpes Simplex Virus Infectivity and Provides the Virus Binding Sites on gro2C Cells. *J. Biol. Chem.* **2005**, *280* (37), 32193-32199.



55. Faller, C. E.; Guvench, O., Sulfation and Cation Effects on the Conformational Properties of the Glycan Backbone of Chondroitin Sulfate Disaccharides. *J. Phys. Chem. B* **2015**, *119* (20), 6063-6073.
56. Pantazaka, E.; Papadimitriou, E., Chondroitin sulfate-cell membrane effectors as regulators of growth factor-mediated vascular and cancer cell migration. *Biochim. Biophys. Acta, Gen. Subj.* **2014**, *1840* (8), 2643-2650.
57. Kusche-Gullberg, M.; Kjellen, L., Sulfotransferases in glycosaminoglycan biosynthesis. *Curr. Opin. Struct. Biol.* **2003**, *13* (5), 605-611.
58. Miyata, S.; Kitagawa, H., Mechanisms for modulation of neural plasticity and axon regeneration by chondroitin sulphate. *J. Biochem.* **2015**, *157* (1), 13-22.
59. Malmstroem, A.; Bartolini, B.; Thelin, M. A.; Pacheco, B.; Maccarana, M., Iduronic acid in chondroitin/dermatan sulfate: biosynthesis and biological function. *J. Histochem. Cytochem.* **2012**, *60* (12), 916-925, 10 pp.
60. Thelin, M. A.; Bartolini, B.; Axelsson, J.; Gustafsson, R.; Tykesson, E.; Pera, E.; Oldberg, A.; Maccarana, M.; Malmstrom, A., Biological functions of iduronic acid in chondroitin/dermatan sulfate. *Febs J.* **2013**, *280* (10), 2431-2446.
61. Vicente, C. P.; He, L.; Pavao, M. S. G.; Tollefsen, D. M., Antithrombotic activity of dermatan sulfate in heparin cofactor II-deficient mice. *Blood* **2004**, *104* (13), 3965-3970.
62. Taylor, K. R.; Rudisill, J. A.; Gallo, R. L., Structural and Sequence Motifs in Dermatan Sulfate for Promoting Fibroblast Growth Factor-2 (FGF-2) and FGF-7 Activity. *J. Biol. Chem.* **2005**, *280* (7), 5300-5306.
63. Jia, X.-L.; Li, S.-Y.; Dang, S.-S.; Cheng, Y.-A.; Zhang, X.; Wang, W.-J.; Hughes, C. E.; Caterson, B., Increased expression of chondroitin sulphate proteoglycans in rat hepatocellular carcinoma tissues. *World J. Gastroenterol.* **2012**, *18* (30), 3962-3976.
64. Swarup, V. P.; Mencio, C. P.; Hlady, V.; Kuberan, B., Sugar glues for broken neurons. *Biomol. Concepts* **2013**, *4* (3), 233-257.
65. Schaefer, L.; Schaefer, R. M., Proteoglycans: from structural compounds to signaling molecules. *Cell Tissue Res.* **2010**, *339* (1), 237-246.
66. Oguma, T.; Toyoda, H.; Toida, T.; Imanari, T., Analytical method for keratan sulfates by high-performance liquid chromatography/turbo-ionspray tandem mass spectrometry. *Anal. Biochem.* **2001**, *290* (1), 68-73.
67. Ho, L. T. Y.; Harris, A. M.; Tanioka, H.; Yagi, N.; Kinoshita, S.; Caterson, B.; Quantock, A. J.; Young, R. D.; Meek, K. M., A comparison of glycosaminoglycan distributions, keratan sulphate sulphation patterns and collagen fibril architecture from central to peripheral regions of the bovine cornea. *Matrix Biol.* **2014**, *38*, 59-68.

68. Jones, L. L.; Tuszynski, M. H., Spinal cord injury elicits expression of keratan sulfate proteoglycans by macrophages, reactive microglia, and oligodendrocyte progenitors. *J. Neurosci.* **2002**, *22* (11), 4611-4624.
69. Akama, T. O.; Misra, A. K.; Hindsgaul, O.; Fukuda, M. N., Enzymatic Synthesis in Vitro of the Disulfated Disaccharide Unit of Corneal Keratan Sulfate. *J. Biol. Chem.* **2002**, *277* (45), 42505-42513.
70. Schwend, T.; Deaton, R. J.; Zhang, Y.; Caterson, B.; Conrad, G. W., Corneal sulfated glycosaminoglycans and their effects on trigeminal nerve growth cone behavior in vitro: roles for ECM in cornea innervation. *Invest. Ophthalmol. Visual Sci.* **2012**, *53* (13), 8118-8137.
71. Funderburgh, J. L., Keratan sulfate: structure, biosynthesis, and function. *Glycobiology* **2000**, *10* (10), 951-958.
72. Antonsson, P.; Heinegaard, D.; Oldberg, A., Posttranslational modifications of fibromodulin. *J. Biol. Chem.* **1991**, *266* (25), 16859-61.
73. Sommarin, Y.; Wendel, M.; Shen, Z.; Hellman, U.; Heinegaard, D., Osteoadherin, a cell-binding keratan sulfate proteoglycan in bone, belongs to the family of leucine-rich repeat proteins of the extracellular matrix. *J. Biol. Chem.* **1998**, *273* (27), 16723-16729.
74. Funderburgh, J. L.; Funderburgh, M. L.; Rodrigues, M. M.; Krachmer, J. H.; Conrad, G. W., Altered antigenicity of keratan sulfate proteoglycan in selected corneal diseases. *Invest Ophthalmol Vis Sci* **1990**, *31* (3), 419-28.
75. Termeer, C.; Sleeman, J. P.; Simon, J. C., Hyaluronan - magic glue for the regulation of the immune response? *Trends Immunol.* **2003**, *24* (3), 112-114.
76. Vigetti, D.; Karousou, E.; Viola, M.; Deleonibus, S.; De Luca, G.; Passi, A., Hyaluronan: biosynthesis and signaling. *Biochim Biophys Acta* **2014**, *1840* (8), 2452-9.
77. Sironen, R. K.; Tammi, M.; Tammi, R.; Auvinen, P. K.; Anttila, M.; Kosma, V. M., Hyaluronan in human malignancies. *Exp. Cell Res.* **2011**, *317* (4), 383-391.
78. Lee, J. Y.; Spicer, A. P., Hyaluronan: a multifunctional, megaDalton, stealth molecule. *Curr. Opin. Cell Biol.* **2000**, *12* (5), 581-586.
79. Vigetti, D.; Viola, M.; Karousou, E.; Deleonibus, S.; Karamanou, K.; De Luca, G.; Passi, A., Epigenetics in extracellular matrix remodeling and hyaluronan metabolism. *Febs J.* **2014**, *281* (22), 4980-4992.
80. Girish, K. S.; Kemparaju, K., The magic glue hyaluronan and its eraser hyaluronidase: a biological overview. *Life Sci.* **2007**, *80* (21), 1921-1943.
81. Slevin, M.; Krupinski, J.; Gaffney, J.; Matou, S.; West, D.; Delisser, H.; Savani, R. C.; Kumar, S., Hyaluronan-mediated angiogenesis in vascular disease: Uncovering RHAMM and CD44 receptor signaling pathways. *Matrix Biol.* **2007**, *26* (1), 58-68.

82. Ichikawa, T.; Itano, N.; Sawai, T.; Kimata, K.; Koganehira, Y.; Saida, T.; Taniguchi, S. i., Increased synthesis of Hyaluronate enhances motility of human melanoma cells. *J. Invest. Dermatol.* **1999**, *113* (6), 935-939.
83. Fraser, J. R. E.; Appelgren, L. E.; Laurent, T. C., Tissue uptake of circulating hyaluronic acid. A whole body autoradiographic study. *Cell Tissue Res.* **1983**, *233* (2), 285-93.
84. Yang, T.; Witham, T. F.; Villa, L.; Erff, M.; Attanucci, J.; Watkins, S.; Kondziolka, D.; Okada, H.; Pollack, I. F.; Chambers, W. H., Glioma-associated hyaluronan induces apoptosis in dendritic cells via inducible nitric oxide synthase: Implications for the use of dendritic cells for therapy of gliomas. *Cancer Res.* **2002**, *62* (9), 2583-2591.
85. Yuan, P.; Lv, M.; Jin, P.; Wang, M.; Du, G.; Chen, J.; Kang, Z., Enzymatic production of specifically distributed hyaluronan oligosaccharides. *Carbohydr. Polym.* **2015**, *129*, 194-200.
86. Wu, C.-L.; Chou, H.-C.; Li, J.-M.; Chen, Y.-W.; Chen, J.-H.; Chen, Y.-H.; Chan, H.-L., Hyaluronic acid-dependent protection against alkali-burned human corneal cells. *Electrophoresis* **2013**, *34* (3), 388-396.
87. Ramakrishna, S.; Suresh, B.; Baek, K.-H., Biological functions of hyaluronan and cytokine-inducible deubiquitinating enzymes. *Biochim. Biophys. Acta, Rev. Cancer* **2015**, *1855* (1), 83-91.
88. Ferguson, E. L.; Roberts, J. L.; Moseley, R.; Griffiths, P. C.; Thomas, D. W., Evaluation of the physical and biological properties of hyaluronan and hyaluronan fragments. *Int. J. Pharm.* **2011**, *420* (1), 84-92.
89. Stern, R.; Asari, A. A.; Sugahara, K. N., Hyaluronan fragments: an information-rich system. *Eur. J. Cell Biol.* **2006**, *85* (8), 699-715.
90. Linhardt, R. J.; Gunay, N. S., Production and chemical processing of low molecular weight heparins. *Semin. Thromb. Hemostasis* **1999**, *25* (Suppl. 3), 5-16.
91. Middeldorp, S., Heparin: From animal organ extract to designer drug. *Thromb. Res.* **2008**, *122* (6), 753-762.
92. Yang, B.; Solakyildirim, K.; Chang, Y.-Q.; Linhardt, R. J., Hyphenated techniques for the analysis of heparin and heparan sulfate. *Anal. Bioanal. Chem.* **2011**, *399* (2), 541-557.
93. Cochran, S.; Li, C. P.; Ferro, V., A surface plasmon resonance-based solution affinity assay for heparan sulfate-binding proteins. *Glycoconjugate J.* **2009**, *26* (5), 577-587.
94. Kovalszky, I.; Hjerpe, A.; Dobra, K., Nuclear translocation of heparan sulfate proteoglycans and their functional significance. *Biochim. Biophys. Acta, Gen. Subj.* **2014**, *1840* (8), 2491-2497.

95. Shimazaki, K.; Tazume, T.; Uji, K.; Tanaka, M.; Kumura, H.; Mikawa, K.; Shimo-Oka, T., Properties of a heparin-binding peptide derived from bovine lactoferrin. *J. Dairy Sci.* **1998**, *81* (11), 2841-2849.
96. Rusnati, M.; Presta, M., Fibroblast growth factors/fibroblast growth factor receptors as targets for the development of anti-angiogenesis strategies. *Curr. Pharm. Des.* **2007**, *13* (20), 2025-2044.
97. Whitelock, J. M.; Graham, L. D.; Melrose, J.; Murdoch, A. D.; Iozzo, R. V.; Underwood, P. A., Human perlecan immunopurified from different endothelial cell sources has different adhesive properties for vascular cells. *Matrix Biol.* **1999**, *18* (2), 163-178.
98. Knox, S.; Merry, C.; Stringer, S.; Melrose, J.; Whitelock, J., Not all perlecans are created equal. Interactions with fibroblast growth factor (FGF) 2 and FGF receptors. *J. Biol. Chem.* **2002**, *277* (17), 14657-14665.
99. Mulloy, B.; Linhardt, R. J., Order out of complexity - protein structures that interact with heparin. *Curr. Opin. Struct. Biol.* **2001**, *11* (5), 623-628.
100. Mosier, P. D.; Krishnasamy, C.; Kellogg, G. E.; Desai, U. R., On the specificity of heparin/heparan sulfate binding to proteins. Anion-binding sites on antithrombin and thrombin are fundamentally different. *PLoS One* **2012**, *7* (11), e48632.
101. Sequeira, S. J.; McKenna, T. J., Chlorbutol, a new inhibitor of aldosterone biosynthesis, identified during examination of heparin effect on aldosterone production. *J. Clin. Endocrinol. Metab.* **1986**, *63* (3), 780-4.
102. Esko, J. D.; Selleck, S. B., Order out of chaos: assembly of ligand binding sites in heparan sulfate. *Annu. Rev. Biochem.* **2002**, *71*, 435-471.
103. Casu, B.; Naggi, A.; Torri, G., Heparin-derived heparan sulfate mimics to modulate heparan sulfate-protein interaction in inflammation and cancer. *Matrix Biol.* **2010**, *29* (6), 442-452.
104. Liu, H.; Zhang, Z.; Linhardt, R. J., Lessons learned from the contamination of heparin. *Nat. Prod. Rep.* **2009**, *26* (3), 313-321.
105. Zhang, F.; Zhang, Z.; Lin, X.; Beenken, A.; Eliseenkova, A. V.; Mohammadi, M.; Linhardt, R. J., Compositional Analysis of Heparin/Heparan Sulfate Interacting with Fibroblast Growth Factor·Fibroblast Growth Factor Receptor Complexes. *Biochemistry* **2009**, *48* (35), 8379-8386.
106. Cummings, R. D., The repertoire of glycan determinants in the human glycome. *Mol. BioSyst.* **2009**, *5* (10), 1087-1104.
107. Rullo, A.; Nitz, M., Importance of the spatial display of charged residues in heparin-peptide interactions. *Biopolymers* **2010**, *93* (3), 290-298.

108. Mulloy, B.; Forster, M. J.; Jones, C.; Davies, D. B., NMR and molecular-modeling studies of the solution conformation of heparin. *Biochem. J.* **1993**, *293* (3), 849-58.
109. Mulloy, B.; Forster, M. J.; Jones, C.; Drake, A. F.; Johnson, E. A.; Davies, D. B., The effect of variation of substitution on the solution conformation of heparin: a spectroscopic and molecular modeling study. *Carbohydr. Res.* **1994**, *255*, 1-26.
110. Gonzalez-Martinez, D.; Kim, S.-H.; Hu, Y.; Guimond, S.; Schofield, J.; Winyard, P.; Vannelli, G. B.; Turnbull, J.; Bouloux, P.-M., Anosmin-1 modulates fibroblast growth factor receptor 1 signaling in human gonadotropin-releasing hormone olfactory neuroblasts through a heparan sulfate-dependent mechanism. *J. Neurosci.* **2004**, *24* (46), 10384-10392.
111. Khan, S.; Rodriguez, E.; Patel, R.; Gor, J.; Mulloy, B.; Perkins, S. J., The solution structure of heparan sulfate differs from that of heparin: Implications for function. *J. Biol. Chem.* **2011**, *286* (28), 24842-24854.
112. Fu, L.; Li, G.; Yang, B.; Onishi, A.; Li, L.; Sun, P.; Zhang, F.; Linhardt, R. J., Structural characterization of pharmaceutical heparins prepared from different animal tissues. *J. Pharm. Sci.* **2013**, *102* (5), 1447-1457.
113. Kim, S.-H.; Turnbull, J.; Guimond, S., Extracellular matrix and cell signalling: the dynamic cooperation of integrin, proteoglycan and growth factor receptor. *J. Endocrinol.* **2011**, *209* (2), 139-151.
114. Goodall, K. J.; Poon, I. K. H.; Phipps, S.; Hulett, M. D., Soluble heparan sulfate fragments generated by heparanase trigger the release of pro-inflammatory cytokines through TLR-4. *PLoS One* **2014**, *9* (10), e0109596/1-e0109596/13, 13 pp.
115. Fernandes dos Santos Teresa, C.; Gomes Angelica, M.; Stelling Mariana, P.; Paschoal Marcos Eduardo, M.; Rumjanek Vivian Mary Barral, D.; Junior Alyson do, R.; Pereira de Souza Heitor, S.; Valiante Paulo, M.; Madi, K.; Pavao Mauro Sergio, G.; Castelo-Branco Morgana Teixeira, L., Heparanase expression and localization in different types of human lung cancer. *Biochim Biophys Acta* **2014**, *1840* (8), 2599-608.
116. Vlodavsky, I.; Ilan, N.; Nadir, Y.; Brenner, B.; Katz, B.-Z.; Naggi, A.; Torri, G.; Casu, B.; Sasisekharan, R., Heparanase, heparin and the coagulation system in cancer progression. *Thromb Res* **2007**, *120 Suppl 2*, S112-20.
117. Ramani, V. C.; Purushothaman, A.; Stewart, M. D.; Thompson, C. A.; Vlodavsky, I.; Au, J. L. S.; Sanderson, R. D., The heparanase/syndecan-1 axis in cancer: mechanisms and therapies. *Febs J.* **2013**, *280* (10), 2294-2306.
118. Arsenault, K. A.; Paikin, J. S.; Hirsh, J.; Dale, B.; Whitlock, R. P.; Teoh, K.; Young, E.; Ginsberg, J. S.; Weitz, J. I.; Eikelboom, J. W., Subtle differences in commercial heparins can have serious consequences for cardiopulmonary bypass patients: A randomized controlled trial. *J. Thorac. Cardiovasc. Surg.* **2012**, *144* (4), 944-950 e3.

119. Zhang, Z.; Weiwer, M.; Li, B.; Kemp, M. M.; Daman, T. H.; Linhardt, R. J., Oversulfated Chondroitin Sulfate: Impact of a Heparin Impurity, Associated with Adverse Clinical Events, on Low-Molecular-Weight Heparin Preparation. *J. Med. Chem.* **2008**, *51* (18), 5498-5501.
120. Izaguirre, G.; Aguila, S.; Qi, L.; Swanson, R.; Roth, R.; Rezaie, A. R.; Gettins, P. G. W.; Olson, S. T., Conformational activation of antithrombin by heparin involves an altered exosite interaction with protease. *J. Biol. Chem.* **2014**, *289* (49), 34049-34064.
121. Xu, D.; Esko, J. D., Demystifying heparan sulfate-protein interactions. *Annu. Rev. Biochem.* **2014**, *83*, 129-157.
122. Petitou, M.; Herault, J. P.; Bernat, A.; Driguez, P. A.; Duchaussoy, P.; Lormeau, J. C.; Herbert, J. M., New antithrombotic oligosaccharides. *Ann. Pharm. Fr.* **1999**, *57* (3), 232-239.
123. Tyler-Cross, R.; Sobel, M.; Marques, D.; Harris, R. B., Heparin binding domain peptides of antithrombin III: analysis by isothermal titration calorimetry and circular dichroism spectroscopy. *Protein Sci.* **1994**, *3* (4), 620-7.
124. Duchaussoy, P.; Jaurand, G.; Driguez, P. A.; Lederman, I.; Gourvenec, F.; Strassel, J. M.; Sizun, P.; Petitou, M.; Herbert, J. M., Identification of a hexasaccharide sequence able to inhibit thrombin and suitable for 'polymerisation'. *Carbohydr Res* **1999**, *317* (1-4), 63-84.
125. Boneu, B., Low molecular weight heparins: are they superior to unfractionated heparins to prevent and to treat deep vein thrombosis? *Thromb. Res.* **2000**, *100* (2, Vessels 4), V113-V120.
126. Shriver, Z.; Sundaram, M.; Venkataraman, G.; Fareed, J.; Linhardt, R.; Biemann, K.; Sasisekharan, R., Cleavage of the antithrombin III binding site in heparin by heparinases and its implication in the generation of low molecular weight heparin. *Proc. Natl. Acad. Sci. U. S. A.* **2000**, *97* (19), 10365-10370.
127. Zurawska, U.; Parasuraman, S.; Goldhaber Samuel, Z. *Prevention of pulmonary embolism in general surgery patients*; 1524-4539; University of Western Ontario, London, Ontario, Canada: United States FIELD Citation:, 2007; pp e302-7.
128. De Agostini, A. I.; Watkins, S. C.; Slayter, H. S.; Youssoufian, H.; Rosenberg, R. D., Localization of anticoagulant active heparan sulfate proteoglycans in vascular endothelium: antithrombin binding on cultured endothelial cells and perfused rat aorta. *J. Cell Biol.* **1990**, *111* (3), 1293-304.
129. Taylor, G. J.; Yorke, S. C.; Harding, D. R. K., Glycosaminoglycan specificity of a heparin-binding peptide. *Pept. Res.* **1995**, *8* (5), 286-93.
130. Maeda, T.; Alexander, C. M.; Friedl, A., Induction of Syndecan-1 Expression in Stromal Fibroblasts Promotes Proliferation of Human Breast Cancer Cells. *Cancer Res.* **2004**, *64* (2), 612-621.

131. Gonzalez, A. D.; Kaya, M.; Shi, W.; Song, H.; Testa, J. R.; Penn, L. Z.; Filmus, J., OCI-5/GPC3, a glypican encoded by a gene that is mutated in the Simpson-Golabi-Behmel overgrowth syndrome, induces apoptosis in a cell line-specific manner. *J. Cell Biol.* **1998**, *141* (6), 1407-1414.
132. Nikitovic, D.; Assouti, M.; Sifaki, M.; Katonis, P.; Krasagakis, K.; Karamanos, N. K.; Tzanakakis, G. N., Chondroitin sulfate and heparan sulfate-containing proteoglycans are both partners and targets of basic fibroblast growth factor-mediated proliferation in human metastatic melanoma cell lines. *Int. J. Biochem. Cell Biol.* **2008**, *40* (1), 72-83.
133. Carmeliet, P., Angiogenesis in health and disease. *Nat. Med. (N. Y., NY, U. S.)* **2003**, *9* (6), 653-660.
134. Veraldi, N.; Hughes, A. J.; Rudd, T. R.; Thomas, H. B.; Edwards, S. W.; Hadfield, L.; Skidmore, M. A.; Siligardi, G.; Cosentino, C.; Shute, J. K.; Naggi, A.; Yates, E. A., Heparin derivatives for the targeting of multiple activities in the inflammatory response. *Carbohydr. Polym.* **2015**, *117*, 400-407.
135. Bara, J. J.; Johnson, W. E. B.; Caterson, B.; Roberts, S., Articular Cartilage Glycosaminoglycans Inhibit the Adhesion of Endothelial Cells. *Connect. Tissue Res.* **2012**, *53* (3), 220-228.
136. Bonnet, C. S.; Walsh, D. A., Osteoarthritis, angiogenesis and inflammation. *Rheumatology (Oxford)* **2005**, *44* (1), 7-16.
137. Hwang, S. R.; Seo, D.-H.; Al-Hilal, T. A.; Jeon, O.-C.; Kang, J. H.; Kim, S.-H.; Kim, H. S.; Chang, Y.-T.; Kang, Y. M.; Yang, V. C.; Byun, Y., Orally active desulfated low molecular weight heparin and deoxycholic acid conjugate, 6ODS-LHbD, suppresses neovascularization and bone destruction in arthritis. *J. Controlled Release* **2012**, *163* (3), 374-384.
138. Hayashi, M.; Kadomatsu, K.; Ishiguro, N., Keratan sulfate suppresses cartilage damage and ameliorates inflammation in an experimental mice arthritis model. *Biochem. Biophys. Res. Commun.* **2010**, *401* (3), 463-468.
139. Lohmander, L. S.; Neame, P. J.; Sandy, J. D., The structure of aggrecan fragments in human synovial fluid. Evidence that aggrecanase mediates cartilage degradation in inflammatory joint disease, joint injury, and osteoarthritis. *Arthritis Rheum.* **1993**, *36* (9), 1214-22.
140. Chen, Y.; Maguire, T.; Hileman, R. E.; Fromm, J. R.; Esko, J. D.; Linhardt, R. J.; Marks, R. M., Dengue virus infectivity depends on envelope protein binding to target cell heparan sulfate. *Nat. Med. (N. Y.)* **1997**, *3* (8), 866-871.
141. WuDunn, D.; Spear, P. G., Initial interaction of herpes simplex virus with cells is binding to heparan sulfate. *J. Virol.* **1989**, *63* (1), 52-8.
142. Zhang, F.; Aguilera, J.; Beaudet, J. M.; Xie, Q.; Lerch, T. F.; Davulcu, O.; Colon, W.; Chapman, M. S.; Linhardt, R. J., Characterization of Interactions between

Heparin/Glycosaminoglycan and Adeno-Associated Virus. *Biochemistry* **2013**, *52* (36), 6275-6285.

143. Shields, B.; Mills, J.; Ghildyal, R.; Gooley, P.; Meanger, J., Multiple heparin binding domains of respiratory syncytial virus G mediate binding to mammalian cells. *Arch. Virol.* **2003**, *148* (10), 1987-2003.

144. Sandgren, S.; Cheng, F.; Belting, M., Nuclear Targeting of Macromolecular Polyanions by an HIV-Tat Derived Peptide. Role for cell-surface proteoglycans. *J. Biol. Chem.* **2002**, *277* (41), 38877-38883.

145. Tyler, K.; Fields, B., *Fields Virology*. 3rd ed.; Lippincott-Raven: Philadelphia, 1996.

146. Gallagher, J. T.; Turnbull, J. E.; Lyon, M., Heparan sulfate proteoglycans: molecular organization of membrane-associated species and an approach to polysaccharide sequence analysis. *Adv. Exp. Med. Biol.* **1992**, *313* (Heparin Relat. Polysaccharides), 49-57.

147. Bernfield, M.; Kokenyesi, R.; Kato, M.; Hinkes, M. T.; Spring, J.; Gallo, R. L.; Lose, E. J., Biology of the syndecans: A family of transmembrane heparan sulfate proteoglycans. *Annu. Rev. Cell Biol.* **1992**, *8*, 365-93.

148. Hament, J.-M.; Aerts, P. C.; Fleer, A.; Van Dijk, H.; Harmsen, T.; Kimpen, J. L. L.; Wolfs, T. F. W., Direct Binding of Respiratory Syncytial Virus to Pneumococci: A Phenomenon That Enhances Both Pneumococcal Adherence to Human Epithelial Cells and Pneumococcal Invasiveness in a Murine Model. *Pediatr. Res.* **2005**, *58* (6), 1198-1203.

149. Adamson, P.; Thammawat, S.; Muchondo, G.; Sadlon, T.; Gordon, D., Diversity in glycosaminoglycan binding amongst hMPV G protein lineages. *Viruses* **2012**, *4*, 3785-3803.

150. Hendricks, G. L.; Velazquez, L.; Pham, S.; Qaisar, N.; Delaney, J. C.; Viswanathan, K.; Albers, L.; Comolli, J. C.; Shriver, Z.; Knipe, D. M.; Kurt-Jones, E. A.; Fygenon, D. K.; Trevejo, J. M.; Wang, J. P.; Finberg, R. W., Heparin octasaccharide decoy liposomes inhibit replication of multiple viruses. *Antiviral Res.* **2015**, *116*, 34-44.

151. Sweet, R. W.; Truneh, A.; Hendrickson, W. A., CD4: its structure, role in immune function and AIDS pathogenesis, and potential as a pharmacological target. *Curr. Opin. Biotechnol.* **1991**, *2* (4), 622-33.

152. Harrop, H. A.; Coombe, D. R.; Rider, C. C., Heparin specifically inhibits binding of V3 loop antibodies to HIV-1 gp120, an effect potentiated by CD4 binding. *AIDS (London)* **1994**, *8* (2), 183-92.

153. Callahan, L. N.; Phelan, M.; Mallinson, M.; Norcross, M. A., Dextran sulfate blocks antibody binding to the principal neutralizing domain of human immunodeficiency virus type 1 without interfering with gp120-CD4 interactions. *J. Virol.* **1991**, *65* (3), 1543-50.



154. Batinic, D.; Robey, F. A., The V3 region of the envelope glycoprotein of human immunodeficiency virus type 1 binds sulfated polysaccharides and CD4-derived synthetic peptides. *J. Biol. Chem.* **1992**, *267* (10), 6664-71.
155. Mondor, I.; Ugolini, S.; Sattentau, Q. J., Human immunodeficiency virus type 1 attachment to HeLa CD4 cells is CD4 independent and gp120 dependent and requires cell surface heparans. *J. Virol.* **1998**, *72* (5), 3623-3634.
156. Ensoli, B.; Buonaguro, L.; Barillari, G.; Fiorelli, V.; Gendelman, R.; Morgan, R. A.; Wingfield, P.; Gallo, R. C., Release, uptake, and effects of extracellular human immunodeficiency virus type 1 Tat protein on cell growth and viral transactivation. *J. Virol.* **1993**, *67* (1), 277-87.
157. Xie, X.; Colberg-Poley, A. M.; Das, J. R.; Li, J.; Zhang, A.; Tang, P.; Jerebtsova, M.; Gutkind, J. S.; Ray, P. E., The basic domain of HIV-Tat transactivating protein is essential for its targeting to lipid rafts and regulating fibroblast growth factor-2 signaling in podocytes isolated from children with HIV-1-associated nephropathy. *J. Am. Soc. Nephrol.* **2014**, *25* (8), 1800-1813.
158. Chang, H. C.; Samaniego, F.; Nair, B. C.; Buonaguro, L.; Ensoli, B., HIV-1 Tat protein exits from cells via a leaderless secretory pathway and binds to extracellular matrix-associated heparan sulfate proteoglycans through its basic region. *AIDS (London)* **1997**, *11* (12), 1421-1431.
159. Rusnati, M.; Tulipano, G.; Spillmann, D.; Tanghetti, E.; Oreste, P.; Zoppetti, G.; Giacca, M.; Presta, M., Multiple interactions of HIV-I Tat protein with size-defined heparin oligosaccharides. *J. Biol. Chem.* **1999**, *274* (40), 28198-28205.
160. Rusnati, M.; Urbinati, C.; Caputo, A.; Possati, L.; Lortat-Jacob, H.; Giacca, M.; Ribatti, D.; Presta, M., Pentosan polysulfate as an inhibitor of extracellular HIV-1 Tat. *J. Biol. Chem.* **2001**, *276* (25), 22420-22425.
161. Rathore, D.; McCutchan, T. F.; Garboczi, D. N.; Toida, T.; Hernaiz, M. J.; LeBrun, L. A.; Lang, S. C.; Linhardt, R. J., Direct measurement of the interactions of glycosaminoglycans and a heparin decasaccharide with the malaria circumsporozoite protein. *Biochemistry* **2001**, *40* (38), 11518-11524.
162. Frevert, U.; Sinnis, P.; Cerami, C.; Shreffler, W.; Takacs, B.; Nussenzweig, V., Malaria circumsporozoite protein binds to heparan sulfate proteoglycans associated with the surface membrane of hepatocytes. *J. Exp. Med.* **1993**, *177* (5), 1287-98.
163. Marques, J.; Moles, E.; Urban, P.; Prohens, R.; Busquets Maria, A.; Sevrin, C.; Grandfils, C.; Fernandez-Busquets, X., Application of heparin as a dual agent with antimalarial and liposome targeting activities toward Plasmodium-infected red blood cells. *Nanomedicine* **2014**, *10* (8), 1719-28.
164. Rampengan, T. H., Cerebral malaria in children. Comparative study between heparin, dexamethasone and placebo. *Paediatr Indones* **1991**, *31* (1-2), 59-66.

165. Osmond, R. I. W.; Kett, W. C.; Skett, S. E.; Coombe, D. R., Protein-heparin interactions measured by BIAcore 2000 are affected by the method of heparin immobilization. *Anal. Biochem.* **2002**, *310* (2), 199-207.
166. Valle-Delgado, J. J.; Urban, P.; Fernandez-Busquets, X., Demonstration of specific binding of heparin to Plasmodium falciparum-infected vs. non-infected red blood cells by single-molecule force spectroscopy. *Nanoscale* **2013**, *5* (9), 3673-3680.
167. Schonberger, L. B., New variant Creutzfeldt-Jakob disease and bovine spongiform encephalopathy. *Infect Dis Clin North Am* **1998**, *12* (1), 111-21.
168. Warda, M.; Gouda, E. M.; Toida, T.; Chi, L.; Linhardt, R. J., Isolation and characterization of raw heparin from dromedary intestine: evaluation of a new source of pharmaceutical heparin. *Comp. Biochem. Physiol., Part C Toxicol. Pharmacol.* **2003**, *136C* (4), 357-365.
169. Warda, M.; Linhardt, R. J., Dromedary glycosaminoglycans: Molecular characterization of camel lung and liver heparan sulfate. *Comp. Biochem. Physiol., Part B Biochem. Mol. Biol.* **2006**, *143B* (1), 37-43.
170. Liu, J.; Linhardt, R. J., Chemoenzymatic synthesis of heparan sulfate and heparin. *Nat. Prod. Rep.* **2014**, *31* (12), 1676-1685.
171. Fareed, J.; Hoppensteadt, D. A.; Bick, R. L., An update on heparins at the beginning of the new millennium. *Semin. Thromb. Hemostasis* **2000**, *26* (Suppl. 1), 5-21.
172. Fareed, J.; Hoppensteadt, D.; Jeske, W. P., An update on low-molecular-weight heparins. *Hemostasis Thromb.* **2014**, 296-313.
173. Buller, H. R.; Cohen, A. T.; Lensing, A. W. A.; Prins, M. H.; Schulman, S.; Lassen, M. R.; van Amsterdam, R. G. M., A novel long-acting synthetic factor Xa inhibitor (SanOrg34006) to replace warfarin for secondary prevention in deep vein thrombosis. A phase II evaluation. [Erratum to document cited in CA140:368409]. *J. Thromb. Haemostasis* **2004**, *2* (3), 540.
174. Wu, B.; Wei, N.; Thon, V.; Wei, M.; Yu, Z.; Xu, Y.; Chen, X.; Liu, J.; Wang, P. G.; Li, T., Facile chemoenzymatic synthesis of biotinylated heparosan hexasaccharide. *Org. Biomol. Chem.* **2015**, *13* (18), 5098-5101.
175. Beccati, D.; Roy, S.; Yu, F.; Gunay, N. S.; Capila, I.; Lech, M.; Linhardt, R. J.; Venkataraman, G., Identification of a novel structure in heparin generated by potassium permanganate oxidation. *Carbohydr. Polym.* **2010**, *82* (3), 699-705.
176. Pan, J.; Qian, Y.; Zhou, X.; Pazandak, A.; Frazier, S. B.; Weiser, P.; Lu, H.; Zhang, L., Identification of chemically sulfated/desulfated glycosaminoglycans in contaminated heparins and development of a simple assay for the detection of most contaminants in heparin. *Glycobiol. Insights* **2010**, *2*, 1-12.

177. Kishimoto, T. K.; Viswanathan, K.; Ganguly, T.; Elankumaran, S.; Smith, S.; Pelzer, K.; Lansing, J. C.; Sriranganathan, N.; Zhao, G.; Galcheva-Gargova, Z.; Al-Hakim, A.; Bailey, G. S.; Fraser, B.; Roy, S.; Rogers-Cotrone, T.; Buhse, L.; Whary, M.; Fox, J.; Nasr, M.; Dal Pan, G. J.; Shriver, Z.; Langer, R. S.; Venkataraman, G.; Austen, K. F.; Woodcock, J.; Sasisekharan, R., Contaminated heparin associated with adverse clinical events and activation of the contact system. *N. Engl. J. Med.* **2008**, *358* (23), 2457-2467.
178. Beni, S.; Limtiaco, J. F. K.; Larive, C. K., Analysis and characterization of heparin impurities. *Anal. Bioanal. Chem.* **2011**, *399* (2), 527-539.
179. Liu, Z.; Xiao, Z.; Masuko, S.; Zhao, W.; Sterner, E.; Bansal, V.; Fareed, J.; Dordick, J.; Zhang, F.; Linhardt, R. J., Mass balance analysis of contaminated heparin product. *Anal. Biochem.* **2011**, *408* (1), 147-156.
180. Blossom, D. B.; Kallen, A. J.; Patel, P. R.; Elward, A.; Robinson, L.; Gao, G.; Langer, R.; Perkins, K. M.; Jaeger, J. L.; Kurkjian, K. M.; Jones, M.; Schillie, S. F.; Shehab, N.; Ketterer, D.; Venkataraman, G.; Kishimoto, T. K.; Shriver, Z.; McMahon, A. W.; Austen, K. F.; Kozlowski, S.; Srinivasan, A.; Turabelidze, G.; Gould, C. V.; Arduino, M. J.; Sasisekharan, R., Outbreak of adverse reactions associated with contaminated heparin. *N. Engl. J. Med.* **2008**, *359* (25), 2674-2684.
181. Adam, A.; Montpas, N.; Keire, D.; Desormeaux, A.; Brown, N. J.; Marceau, F.; Westenberger, B., Bradykinin forming capacity of oversulfated chondroitin sulfate contaminated heparin in vitro. *Biomaterials* **2010**, *31* (22), 5741-5748.
182. Corbier, A.; Le Berre, N.; Rampe, D.; Meng, H.; Lorenz, M.; Vicat, P.; Potdevin, S.; Doubovetzky, M., Oversulfated Chondroitin Sulfate and OSCS-Contaminated Heparin Cause Dose- and Route-Dependent Hemodynamic Effects in the Rat. *Toxicol. Sci.* **2011**, *121* (2), 417-427.
183. Schwartz, L. B., Heparin comes clean. *N. Engl. J. Med.* **2008**, *358* (23), 2505-2509.
184. Sommers, C. D.; Montpas, N.; Adam, A.; Keire, D. A., Characterization of currently marketed heparin products: Adverse event relevant bioassays. *J. Pharm. Biomed. Anal.* **2012**, *67-68*, 28-35.
185. Peysselon, F.; Ricard-Blum, S., Heparin-protein interactions: From affinity and kinetics to biological roles. Application to an interaction network regulating angiogenesis. *Matrix Biol.* **2014**, *35*, 73-81.
186. Ori, A.; Wilkinson, M. C.; Fernig, D. G., A Systems Biology Approach for the Investigation of the Heparin/Heparan Sulfate Interactome. *J. Biol. Chem.* **2011**, *286* (22), 19892-19904.
187. Batra, S.; Sahi, N.; Mikulcik, K.; Shockley, H.; Turner, C.; Laux, Z.; Badwaik, V. D.; Conte, E.; Rajalingam, D., Efficient and inexpensive method for purification of heparin binding proteins. *J. Chromatogr. B Anal. Technol. Biomed. Life Sci.* **2011**, *879* (24), 2437-2442.

188. Zakrzewska, M.; Marcinkowska, E.; Wiedlocha, A., FGF-1: from biology through engineering to potential medical applications. *Crit. Rev. Clin. Lab. Sci.* **2008**, *45* (1), 91-135.
189. Carlsson, P.; Presto, J.; Spillmann, D.; Lindahl, U.; Kjellen, L., Heparin/Heparan Sulfate Biosynthesis: processive formation of N-sulfated domains. *J. Biol. Chem.* **2008**, *283* (29), 20008-20014.
190. Pomin, V. H., NMR Chemical Shifts in Structural Biology of Glycosaminoglycans. *Anal. Chem. (Washington, DC, U. S.)* **2014**, *86* (1), 65-94.
191. Stewart, M. D.; Sanderson, R. D., Heparan sulfate in the nucleus and its control of cellular functions. *Matrix Biol.* **2014**, *35*, 56-59.
192. Lortat-Jacob, H.; Grosdidier, A.; Imberty, A., Structural diversity of heparan sulfate binding domains in chemokines. *Proc. Natl. Acad. Sci. U. S. A.* **2002**, *99* (3), 1229-1234.
193. Strand, M. E.; Herum, K. M.; Rana, Z. A.; Skrbic, B.; Askevold, E. T.; Dahl, C. P.; Vistnes, M.; Hasic, A.; Kvaloy, H.; Sjaastad, I.; Carlson, C. R.; Tonnessen, T.; Gullestad, L.; Christensen, G.; Lunde, I. G., Innate immune signaling induces expression and shedding of the heparan sulfate proteoglycan syndecan-4 in cardiac fibroblasts and myocytes, affecting inflammation in the pressure-overloaded heart. *Febs J.* **2013**, *280* (10), 2228-2247.
194. Wong, H.; Schotz, M. C., The lipase gene family. *J. Lipid Res.* **2002**, *43* (7), 993-999.
195. Enghild, J. J.; Thogersen, I. B.; Oury, T. D.; Valnickova, Z.; Hojrup, P.; Crapo, J. D., The heparin-binding domain of extracellular superoxide dismutase is proteolytically processed intracellularly during biosynthesis. *J. Biol. Chem.* **1999**, *274* (21), 14818-14822.
196. Desai, U. R.; Petitou, M.; Bjork, I.; Olson, S. T., Mechanism of heparin activation of antithrombin, Role of individual residues of the pentasaccharide activating sequence in the recognition of native and activated states of antithrombin. *J. Biol. Chem.* **1998**, *273* (13), 7478-7487.
197. Nagaoka, M.; Jiang, H.-L.; Hoshiba, T.; Akaike, T.; Cho, C.-S., Application of recombinant fusion proteins for tissue engineering. *Ann Biomed Eng* **2010**, *38* (3), 683-93.
198. Gitay-Goren, H.; Soker, S.; Vlodaysky, I.; Neufeld, G., The binding of vascular endothelial growth factor to its receptors is dependent on cell surface-associated heparin-like molecules. *J. Biol. Chem.* **1992**, *267* (9), 6093-8.
199. Chu, C. L.; Buczek-Thomas, J. A.; Nugent, M. A., Heparan sulphate proteoglycans modulate fibroblast growth factor-2 binding through a lipid raft-mediated mechanism. *Biochem. J.* **2004**, *379* (2), 331-341.
200. Beenken, A.; Mohammadi, M., The FGF family: biology, pathophysiology and therapy. *Nat. Rev. Drug Discovery* **2009**, *8* (3), 235-253.

201. Wesche, J.; Haglund, K.; Haugsten, E. M., Fibroblast growth factors and their receptors in cancer. *Biochem. J.* **2011**, *437* (2), 199-213.
202. Barrientos, S.; Stojadinovic, O.; Golinko Michael, S.; Brem, H.; Tomic-Canic, M., Growth factors and cytokines in wound healing. *Wound Repair Regen* **2008**, *16* (5), 585-601.
203. Arunkumar, A. I.; Kumar, T. K. S.; Kathir, K. M.; Srisailam, S.; Wang, H.-M.; Leena, P. S. T.; Chi, Y.-H.; Chen, H.-C.; Wu, C.-H.; Wu, R.-T.; Chang, G.-G.; Chiu, I.-M.; Yu, C., Oligomerization of acidic fibroblast growth factor is not a prerequisite for its cell proliferation activity. *Protein Sci.* **2002**, *11* (5), 1050-1061.
204. Forsten-Williams, K.; Chu Chia, L.; Fannon, M.; Buczek-Thomas Jo, A.; Nugent Matthew, A., Control of growth factor networks by heparan sulfate proteoglycans. *Ann Biomed Eng* **2008**, *36* (12), 2134-48.
205. Xie, B.; Tassi, E.; Swift, M. R.; McDonnell, K.; Bowden, E. T.; Wang, S.; Ueda, Y.; Tomita, Y.; Riegel, A. T.; Wellstein, A., Identification of the Fibroblast Growth Factor (FGF)-interacting Domain in a Secreted FGF-binding Protein by Phage Display. *J. Biol. Chem.* **2006**, *281* (2), 1137-1144.
206. Olsen, S. K.; Garbi, M.; Zampieri, N.; Eliseenkova, A. V.; Ornitz, D. M.; Goldfarb, M.; Mohammadi, M., Fibroblast growth factor (FGF) homologous factors share structural but not functional homol. with FGFs. *J. Biol. Chem.* **2003**, *278* (36), 34226-34236.
207. Freier, K.; Schwaenen, C.; Sticht, C.; Flechtenmacher, C.; Muehling, J.; Hofele, C.; Radlwimmer, B.; Lichter, P.; Joos, S., Recurrent FGFR1 amplification and high FGFR1 protein expression in oral squamous cell carcinoma (OSCC). *Oral Oncol.* **2007**, *43* (1), 60-66.
208. Rajalingam, D.; Kumar, T. K. S.; Soldi, R.; Graziani, I.; Prudovsky, I.; Yu, C., Molecular mechanism of inhibition of nonclassical FGF-1 export. *Biochemistry* **2005**, *44* (47), 15472-15479.
209. Mohan, S. K.; Rani, S. G.; Yu, C., The Heterohexameric Complex Structure, a Component in the Non-classical Pathway for Fibroblast Growth Factor 1 (FGF1) Secretion. *J. Biol. Chem.* **2010**, *285* (20), 15464-15475.
210. Powers, C. J.; McLeskey, S. W.; Wellstein, A., Fibroblast growth factors, their receptors and signaling. *Endocr.-Relat. Cancer* **2000**, *7* (3), 165-197.
211. Prudovsky, I.; Mandinova, A.; Soldi, R.; Bagala, C.; Graziani, I.; Landriscina, M.; Tarantini, F.; Duarte, M.; Bellum, S.; Doherty, H.; Maciag, T., The non-classical export routes: FGF1 and IL-1 $\alpha$  point the way. *J. Cell Sci.* **2003**, *116* (24), 4871-4881.
212. Ago, H.; Kitagawa, Y.; Fujishima, A.; Matsuura, Y.; Katsube, Y., Crystal structure of basic fibroblast growth factor at 1.6 Å resolution. *J. Biochem.* **1991**, *110* (3), 360-3.
213. Jin, M.; Du, X.; Chen, L., Cross-talk between FGF and other cytokine signalling pathways during endochondral bone development. *Cell Biol. Int.* **2012**, *36* (8), 691-696.

214. Hung, K.-W.; Kumar, T. K. S.; Kathir, K. M.; Xu, P.; Ni, F.; Ji, H.-H.; Chen, M.-C.; Yang, C.-C.; Lin, F.-P.; Chiu, I.-M.; Yu, C., Solution Structure of the Ligand Binding Domain of the Fibroblast Growth Factor Receptor: Role of Heparin in the Activation of the Receptor. *Biochemistry* **2005**, *44* (48), 15787-15798.
215. Schlessinger, J., Cell signaling by receptor tyrosine kinases. *Cell (Cambridge, Mass.)* **2000**, *103* (2), 211-225.
216. Douwes Dekker, P. B.; Kuipers-Dijkshoorn, N. J.; Baelde, H. J.; van der Mey, A. G. L.; Hogendoorn, P. C. W.; Cornelisse, C. J., Basic fibroblast growth factor and fibroblastic growth factor receptor-1 may contribute to head and neck paraganglioma development by an autocrine or paracrine mechanism. *Hum. Pathol.* **2007**, *38* (1), 79-85.
217. Olsen, S. K.; Ibrahimi, O. A.; Raucci, A.; Zhang, F.; Eliseenkova, A. V.; Yayon, A.; Basilico, C.; Linhardt, R. J.; Schlessinger, J.; Mohammadi, M., Insights into the molecular basis for fibroblast growth factor receptor autoinhibition and ligand-binding promiscuity. *Proc. Natl. Acad. Sci. U. S. A.* **2004**, *101* (4), 935-940.
218. Eswarakumar, V. P.; Lax, I.; Schlessinger, J., Cellular signaling by fibroblast growth factor receptors. *Cytokine Growth Factor Rev.* **2005**, *16* (2), 139-149.
219. Yeh, B. K.; Igarashi, M.; Eliseenkova, A. V.; Plotnikov, A. N.; Sher, I.; Ron, D.; Aaronson, S. A.; Mohammadi, M., Structural basis by which alternative splicing confers specificity in fibroblast growth factor receptors. *Proc. Natl. Acad. Sci. U. S. A.* **2003**, *100* (5), 2266-2271.
220. Johnson, D. E.; Williams, L. T., Structural and functional diversity in the FGF receptor multigene family. *Adv. Cancer Res.* **1993**, *60*, 1-41.
221. Guimond, S. E.; Rudd, T. R.; Skidmore, M. A.; Ori, A.; Gaudesi, D.; Cosentino, C.; Guerrini, M.; Edge, R.; Collison, D.; McInnes, E.; Torri, G.; Turnbull, J. E.; Fernig, D. G.; Yates, E. A., Cations Modulate Polysaccharide Structure To Determine FGF-FGFR Signaling: A Comparison of Signaling and Inhibitory Polysaccharide Interactions with FGF-1 in Solution. *Biochemistry* **2009**, *48* (22), 4772-4779.
222. Jang, J.-H.; Chung, C.-P., Loss of ligand-binding specificity of fibroblast growth factor receptor 2 by RNA splicing in human chondrosarcoma cells. *Cancer Lett. (Shannon, Irel.)* **2003**, *191* (2), 215-222.
223. Shi, D.-L.; Launay, C.; Fromentoux, V.; Feige, J.-J.; Boucaut, J.-C., Expression of fibroblast growth factor receptor-2 splice variants is developmentally and tissue-specifically regulated in the amphibian embryo. *Dev. Biol.* **1994**, *164* (1), 173-82.
224. Lu, W.; Luo, Y.; Kan, M.; McKeehan, W. L., Fibroblast growth factor-10. A second candidate stromal to epithelial cell andromedin in prostate. *J Biol Chem* **1999**, *274* (18), 12827-34.

225. Schlessinger, J.; Plotnikov, A. N.; Ibrahimi, O. A.; Eliseenkova, A. V.; Yeh, B. K.; Yayon, A.; Linhardt, R. J.; Mohammadi, M., Crystal structure of a ternary FGF-FGFR-heparin complex reveals a dual role for heparin in FGFR binding and dimerization. *Mol. Cell* **2000**, *6* (3), 743-750.
226. Hu, Y.; Bouloux, P.-M., Novel insights in FGFR1 regulation: lessons from Kallmann syndrome. *Trends Endocrinol. Metab.* **2010**, *21* (6), 385-393.
227. Shute, J., Glycosaminoglycan and chemokine/growth factor interactions. *Handb. Exp. Pharmacol.* **2012**, *207* (Heparin), 307-324.
228. Harmer, N. J., Insights into the role of heparan sulphate in fibroblast growth factor signaling. *Biochem. Soc. Trans.* **2006**, *34* (3), 442-445.
229. Schlessinger, J., Common and distinct elements in cellular signaling via EGF and FGF receptors. *Science (Washington, DC, U. S.)* **2004**, *306* (5701), 1506-1507.
230. Yeh, B. K.; Eliseenkova, A. V.; Plotnikov, A. N.; Green, D.; Pinnell, J.; Polat, T.; Gritli-Linde, A.; Linhardt, R. J.; Mohammadi, M., Structural basis for activation of fibroblast growth factor signaling by sucrose octasulfate. *Mol. Cell. Biol.* **2002**, *22* (20), 7184-7192.
231. Goodger, S. J.; Robinson, C. J.; Murphy, K. J.; Gasiunas, N.; Harmer, N. J.; Blundell, T. L.; Pye, D. A.; Gallagher, J. T., Evidence That Heparin Saccharides Promote FGF2 Mitogenesis through Two Distinct Mechanisms. *J. Biol. Chem.* **2008**, *283* (19), 13001-13008.
232. Pellegrini, L.; Burke, D. F.; Von Delft, F.; Mulloy, B.; Blundell, T. L., Crystal structure of fibroblast growth factor receptor ectodomain bound to ligand and heparin. *Nature (London)* **2000**, *407* (6807), 1029-1034.
233. Cadman, S. M.; Kim, S.-H.; Hu, Y.; Gonzalez-Martinez, D.; Bouloux, P.-M., Molecular Pathogenesis of Kallmann's Syndrome. *Horm. Res.* **2007**, *67* (5), 231-242.
234. Cariboni, A.; Maggi, R., Kallmann's syndrome, a neuronal migration defect. *Cell. Mol. Life Sci.* **2006**, *63* (21), 2512-2526.
235. Mohammadi, M.; Honegger, A. M.; Rotin, D.; Fischer, R.; Bellot, F.; Li, W.; Dionne, C. A.; Jaye, M.; Rubinstein, M.; Schlessinger, J., A tyrosine-phosphorylated carboxy-terminal peptide of the fibroblast growth factor receptor (Flg) is a binding site for the SH2 domain of phospholipase C- $\gamma$ 1. *Mol. Cell. Biol.* **1991**, *11* (10), 5068-78.
236. Mohammadi, M.; Dikic, I.; Sorokin, A.; Burgess, W. H.; Jaye, M.; Schlessinger, J., Identification of six novel autophosphorylation sites on fibroblast growth factor receptor 1 and elucidation of their importance in receptor activation and signal transduction. *Mol. Cell. Biol.* **1996**, *16* (3), 977-89.
237. Boilly, B.; Vercoutter-Edouart, A. S.; Hondermarck, H.; Nurcombe, V.; Le Bourhis, X., FGF signals for cell proliferation and migration through different pathways. *Cytokine Growth Factor Rev.* **2000**, *11* (4), 295-302.

238. Cavallaro, U.; Niedermeyer, J.; Fuxa, M.; Christofori, G., N-CAM modulates tumour-cell adhesion to matrix by inducing FGF-receptor signalling. *Nat. Cell Biol.* **2001**, *3* (7), 650-657.
239. Wiedlocha, A.; Sorensen, V., Signaling, internalization, and intracellular activity of fibroblast growth factor. *Curr. Top. Microbiol. Immunol.* **2004**, *286* (Signalling from Internalized Growth Factor Receptors), 45-79.
240. Hanafusa, H.; Torii, S.; Yasunaga, T.; Nishida, E., Sprouty1 and Sprouty2 provide a control mechanism for the Ras/MAPK signalling pathway. *Nat. Cell Biol.* **2002**, *4* (11), 850-858.
241. Christofori, G., Split personalities: the agonistic antagonist Sprouty. *Nat. Cell Biol.* **2003**, *5* (5), 377-379.
242. Cabrita, M. A.; Christofori, G., Sprouty proteins, masterminds of receptor tyrosine kinase signaling. *Angiogenesis* **2008**, *11* (1), 53-62.
243. Hacoen, N.; Kramer, S.; Sutherland, D.; Hiromi, Y.; Krasnow, M. A., sprouty encodes a novel antagonist of FGF signaling that patterns apical branching of the Drosophila airways. *Cell (Cambridge, Mass.)* **1998**, *92* (2), 253-263.
244. Furthauer, M.; Lin, W.; Ang, S.-L.; Thisse, B.; Thisse, C., Sef is a feedback-induced antagonist of Ras/MAPK-mediated FGF signaling. *Nat. Cell Biol.* **2002**, *4* (2), 170-174.
245. Tsang, M.; Friesel, R.; Kudoh, T.; Dawid, I. B., Identification of Sef, a novel modulator of FGF signalling. *Nat. Cell Biol.* **2002**, *4* (2), 165-169.
246. Bottcher Ralph, T.; Pollet, N.; Delius, H.; Niehrs, C., The transmembrane protein XFLRT3 forms a complex with FGF receptors and promotes FGF signalling. *Nat Cell Biol* **2004**, *6* (1), 38-44.
247. Groom, J. R., Chemokines in cellular positioning and human disease. *Immunol. Cell Biol.* **2015**, *93* (4), 328-329.
248. Zimmermann, H. W.; Sterzer, V.; Sahin, H., CCR1 and CCR2 Antagonists. *Curr. Top. Med. Chem. (Sharjah, United Arab Emirates)* **2014**, *14* (13), 1539-1552.
249. Ziarek, J. J.; Veldkamp, C. T.; Zhang, F.; Murray, N. J.; Kartz, G. A.; Liang, X.; Su, J.; Baker, J. E.; Linhardt, R. J.; Volkman, B. F., Heparin Oligosaccharides Inhibit Chemokine (CXC Motif) Ligand 12 (CXCL12) Cardioprotection by Binding Orthogonal to the Dimerization Interface, Promoting Oligomerization, and Competing with the Chemokine (CXC Motif) Receptor 4 (CXCR4) N Terminus. *J. Biol. Chem.* **2013**, *288* (1), 737-746.
250. De Paz, J. L.; Moseman, E. A.; Noti, C.; Polito, L.; Von Andrian, U. H.; Seeberger, P. H., Profiling Heparin-Chemokine Interactions Using Synthetic Tools. *ACS Chem. Biol.* **2007**, *2* (11), 735-744.



251. Culley, F. J.; Fadlon, E. J.; Kirchem, A.; Williams, T. J.; Jose, P. J.; Pease, J. E., Proteoglycans are potent modulators of the biological responses of eosinophils to chemokines. *Eur. J. Immunol.* **2003**, *33* (5), 1302-1310.
252. Severin, I. C.; Gaudry, J.-P.; Johnson, Z.; Kungl, A.; Jansma, A.; Gesslbauer, B.; Mulloy, B.; Power, C.; Proudfoot, A. E. I.; Handel, T., Characterization of the Chemokine CXCL11-Heparin Interaction Suggests two Different Affinities for Glycosaminoglycans. *J. Biol. Chem.* **2010**, *285* (23), 17713-17724.
253. Cardin, A. D.; Weintraub, H. J. R., Molecular modeling of protein-glycosaminoglycan interactions. *Arteriosclerosis (Dallas)* **1989**, *9* (1), 21-32.
254. Sobel, M.; Soler, D. F.; Kermode, J. C.; Harris, R. B., Localization and characterization of a heparin binding domain peptide of human von Willebrand factor. *J. Biol. Chem.* **1992**, *267* (13), 8857-62.
255. Margalit, H.; Fischer, N.; Ben-Sasson, S. A., Comparative analysis of structurally defined heparin binding sequences reveals a distinct spatial distribution of basic residues. *J. Biol. Chem.* **1993**, *268* (26), 19228-31.
256. Hileman, R. E.; Fromm, J. R.; Weiler, J. M.; Linhardt, R. J., Glycosaminoglycan-protein interactions: definition of consensus sites in glycosaminoglycan binding proteins. *Bioessays* **1998**, *20* (2), 156-67.
257. Fromm, J. R.; Hileman, R. E.; Caldwell, E. E. O.; Weiler, J. M.; Linhardt, R. J., Pattern and spacing of basic amino acids in heparin binding sites. *Arch. Biochem. Biophys.* **1997**, *343* (1), 92-100.
258. Caldwell, E. E. O.; Nadkarni, V. D.; Fromm, J. R.; Linhardt, R. J.; Weiler, J. M., Importance of specific amino acids in protein binding sites for heparin and heparan sulfate. *Int. J. Biochem. Cell Biol.* **1996**, *28* (2), 203-16.
259. Fromm, J. R.; Hileman, R. E.; Caldwell, E. E. O.; Weiler, J. M.; Linhardt, R. J., Differences in the interaction of heparin with arginine and lysine and the importance of these basic amino acids in the binding of heparin to acidic fibroblast growth factor. *Arch. Biochem. Biophys.* **1995**, *323* (2), 279-87.
260. Bae, J.; Desai, U. R.; Pervin, A.; Caldwell, E. E. O.; Weiler, J. M.; Linhardt, R. J., Interaction of heparin with synthetic antithrombin III peptide analogs. *Biochem. J.* **1994**, *301* (1), 121-9.
261. Frank, E. G.; McDonald, J. P.; Karata, K.; Huston, D.; Woodgate, R., A strategy for the expression of recombinant proteins traditionally hard to purify. *Anal. Biochem.* **2012**, *429* (2), 132-139.
262. Fakruddin, M.; Mazumdar, R. M.; Bin Mannan, K. S.; Chowdhury, A.; Hossain, M. N., Critical factors affecting the success of cloning, expression, and mass production of enzymes by recombinant E. coli. *ISRN Biotechnol.* **2013**, 590587, 8 pp.

263. Schumann, W.; Ferreira, L. C. S., Production of recombinant proteins in *Escherichia coli*. *Genet. Mol. Biol.* **2004**, *27* (3), 442-453.
264. Engelberg-Kulka, H.; Kumar, S., Yet another way that phage  $\lambda$  manipulates its *Escherichia coli* host:  $\lambda$ rexB is involved in the lysogenic-lytic switch. *Mol. Microbiol.* **2015**, *96* (4), 689-693.
265. Feiner, R.; Argov, T.; Rabinovich, L.; Sigal, N.; Borovok, I.; Herskovits, A. A., A new perspective on lysogeny: prophages as active regulatory switches of bacteria. *Nat. Rev. Microbiol.* **2015**, *13* (10), 641-650.
266. Devoy, A.; Bunton-Stasyshyn, R. K. A.; Tybulewicz, V. L. J.; Smith, A. J. H.; Fisher, E. M. C., Genomically humanized mice: technologies and promises. *Nat. Rev. Genet.* **2012**, *13* (1), 14-20.
267. Johnson, S. J.; Wade-Martins, R., A BACwards glance at neurodegeneration: molecular insights into disease from LRRK2, SNCA and MAPT BAC-transgenic mice. *Biochem. Soc. Trans.* **2011**, *39* (4), 862-867.
268. Copeland, N. G.; Jenkins, N. A.; Court, D. L., Recombineering: a powerful new tool for mouse functional genomics. *Nat Rev Genet* **2001**, *2* (10), 769-79.
269. Sorensen, H. P.; Mortensen, K. K., Soluble expression of recombinant proteins in the cytoplasm of *Escherichia coli*. *Microb. Cell Fact.* **2005**, *4*, No pp given.
270. Baneyx, F., Recombinant protein expression in *Escherichia coli*. *Curr. Opin. Biotechnol.* **1999**, *10* (5), 411-421.
271. Berrow, N. S.; Buessow, K.; Coutard, B.; Diprose, J.; Ekberg, M.; Folkers, G. E.; Levy, N.; Lieu, V.; Owens, R. J.; Peleg, Y.; Pinaglia, C.; Quevillon-Cheruel, S.; Salim, L.; Scheich, C.; Vincentelli, R.; Busso, D., Recombinant protein expression and solubility screening in *Escherichia coli*: A comparative study. *Acta Crystallogr., Sect. D Biol. Crystallogr.* **2006**, *D62* (10), 1218-1226.
272. Macinkovic, I. S.; Abughren, M.; Mrkic, I.; Grozdanovic, M. M.; Prodanovic, R.; Gavrovic-Jankulovic, M., Employment of colorimetric enzyme assay for monitoring expression and solubility of GST fusion proteins targeted to inclusion bodies. *J. Biotechnol.* **2013**, *168* (4), 506-510.
273. Chart, H.; Smith, H. R.; La Ragione, R. M.; Woodward, M. J., An investigation into the pathogenic properties of *Escherichia coli* strains BLR, BL21, DH5 $\alpha$  and EQ1. *J. Appl. Microbiol.* **2000**, *89* (6), 1048-1058.
274. Graslund, S.; Nordlund, P.; Weigelt, J.; Hallberg, B. M.; Bray, J.; Gileadi, O.; Knapp, S.; Oppermann, U.; Arrowsmith, C.; Hui, R.; Ming, J.; dhe-Paganon, S.; Park, H.-w.; Savchenko, A.; Yee, A.; Edwards, A.; Vincentelli, R.; Cambillau, C.; Kim, R.; Kim, S.-H.; Rao, Z.; Shi, Y.; Terwilliger Thomas, C.; Kim, C.-Y.; Hung, L.-W.; Waldo Geoffrey, S.; Peleg, Y.; Albeck, S.; Unger, T.; Dym, O.; Prilusky, J.; Sussman Joel, L.; Stevens Ray, C.; Lesley Scott, A.; Wilson

Ian, A.; Joachimiak, A.; Collart, F.; Dementieva, I.; Donnelly Mark, I.; Eschenfeldt William, H.; Kim, Y.; Stols, L.; Wu, R.; Zhou, M.; Burley Stephen, K.; Emtage, J. S.; Sauder, J. M.; Thompson, D.; Bain, K.; Luz, J.; Gheyi, T.; Zhang, F.; Atwell, S.; Almo Steven, C.; Bonanno Jeffrey, B.; Fiser, A.; Swaminathan, S.; Studier, F. W.; Chance Mark, R.; Sali, A.; Acton Thomas, B.; Xiao, R.; Zhao, L.; Ma Li, C.; Hunt John, F.; Tong, L.; Cunningham, K.; Inouye, M.; Anderson, S.; Janjua, H.; Shastry, R.; Ho Chi, K.; Wang, D.; Wang, H.; Jiang, M.; Montelione Gaetano, T.; Stuart David, I.; Owens Raymond, J.; Daenke, S.; Schutz, A.; Heinemann, U.; Yokoyama, S.; Bussow, K.; Gunsalus Kristin, C., Protein production and purification. *Nat Methods* **2008**, 5 (2), 135-46.

275. Villaverde, A.; Mar Carrio, M., Protein aggregation in recombinant bacteria: biological role of inclusion bodies. *Biotechnol. Lett.* **2003**, 25 (17), 1385-1395.

276. Lebendiker, M.; Danieli, T., Production of prone-to-aggregate proteins. *FEBS Lett.* **2014**, 588 (2), 236-246.

277. Ventura, S.; Villaverde, A., Protein quality in bacterial inclusion bodies. *Trends Biotechnol.* **2006**, 24 (4), 179-185.

278. Morell, M.; Bravo, R.; Espargaro, A.; Sisquella, X.; Aviles, F. X.; Fernandez-Busquets, X.; Ventura, S., Inclusion bodies: Specificity in their aggregation process and amyloid-like structure. *Biochim. Biophys. Acta, Mol. Cell Res.* **2008**, 1783 (10), 1815-1825.

279. Ami, D.; Natalello, A.; Taylor, G.; Tonon, G.; Maria Doglia, S., Structural analysis of protein inclusion bodies by Fourier transform infrared microspectroscopy. *Biochim. Biophys. Acta, Proteins Proteomics* **2006**, 1764 (4), 793-799.

280. Burgess, R. R., Refolding solubilized inclusion body proteins. *Methods Enzymol.* **2009**, 463 (Guide to Protein Purification), 259-282.

281. Hartl, F. U.; Hayer-Hart, M., Molecular chaperones in the cytosol: from nascent chain to folded protein. *Science (Washington, DC, U. S.)* **2002**, 295 (5561), 1852-1858.

282. Frydman, J., Folding of newly translated proteins in vivo: the role of molecular chaperones. *Annu. Rev. Biochem.* **2001**, 70, 603-647.

283. Ventura, S., Sequence determinants of protein aggregation: Tools to increase protein solubility. *Microb. Cell Fact.* **2005**, 4, No pp given.

284. Rinas, U.; Bailey, J. E., Protein compositional analysis of inclusion bodies produced in recombinant *Escherichia coli*. *Appl. Microbiol. Biotechnol.* **1992**, 37 (5), 609-14.

285. Upadhyay, A. K.; Murmu, A.; Singh, A.; Panda, A. K., Kinetics of inclusion body formation and its correlation with the characteristics of protein aggregates in *Escherichia coli*. *PLoS One* **2012**, 7 (3), e33951.

286. Peleg, Y.; Unger, T., Resolving bottlenecks for recombinant protein expression in *E. coli*. *Methods Mol. Biol. (N. Y., NY, U. S.)* **2012**, 800 (Chemical Genomics and Proteomics), 173-186.

287. Hwang, P. M.; Pan, J. S.; Sykes, B. D., Targeted expression, purification, and cleavage of fusion proteins from inclusion bodies in *Escherichia coli*. *FEBS Lett.* **2014**, *588* (2), 247-252.
288. Patra, A. K.; Gahlay, G. K.; Reddy, B. V. V.; Gupta, S. K.; Panda, A. K., Refolding, structural transition and spermatozoa-binding of recombinant bonnet monkey (*Macaca radiata*) zona pellucida glycoprotein-C expressed in *Escherichia coli*. *Eur. J. Biochem.* **2000**, *267* (24), 7075-7081.
289. Umetsu, M.; Tsumoto, K.; Nitta, S.; Adschiri, T.; Ejima, D.; Arakawa, T.; Kumagai, I., Nondenaturing solubilization of  $\beta 2$  microglobulin from inclusion bodies by L-arginine. *Biochem. Biophys. Res. Commun.* **2005**, *328* (1), 189-197.
290. Singh, S. M.; Panda, A. K., Solubilization and refolding of bacterial inclusion body proteins. *J. Biosci. Bioeng.* **2005**, *99* (4), 303-310.
291. Singh, S. M.; Sharma, A.; Upadhyay, A. K.; Singh, A.; Garg, L. C.; Panda, A. K., Solubilization of inclusion body proteins using n-propanol and its refolding into bioactive form. *Protein Expression Purif.* **2012**, *81* (1), 75-82.
292. Patra, A. K.; Mukhopadhyay, R.; Mukhija, R.; Krishnan, A.; Garg, L. C.; Panda, A. K., Optimization of inclusion body solubilization and renaturation of recombinant human growth hormone from *Escherichia coli*. *Protein Expression Purif.* **2000**, *18* (2), 182-192.
293. Upadhyay, V.; Singh, A.; Panda, A. K., Purification of recombinant ovalbumin from inclusion bodies of *Escherichia coli*. *Protein Expression Purif.* **2016**, *117*, 52-58.
294. Misawa, S.; Kumagai, I., Refolding of therapeutic proteins produced in *Escherichia coli* as inclusion bodies. *Biopolymers* **1999**, *51* (4), 297-307.
295. Das, K. M. P.; Banerjee, S.; Shekhar, N.; Damodaran, K.; Nair, R.; Somani, S.; Raiker, V. P.; Jain, S.; Padmanabhan, S., Cloning, soluble expression and purification of high yield recombinant hGMCSF in *Escherichia coli*. *Int. J. Mol. Sci.* **2011**, *12*, 2064-2076.
296. Smith, H. E., The transcriptional response of *Escherichia coli* to recombinant protein insolubility. *J. Struct. Funct. Genomics* **2007**, *8* (1), 27-35.
297. De Marco, V.; Stier, G.; Blandin, S.; de Marco, A., The solubility and stability of recombinant proteins are increased by their fusion to NusA. *Biochem. Biophys. Res. Commun.* **2004**, *322* (3), 766-771.
298. Banerjee, S.; Salunkhe Shardul, S.; Apte-Deshpande Anjali, D.; Mandi Naganath, S.; Mandal, G.; Padmanabhan, S., Over-expression of proteins using a modified pBAD24 vector in *E. coli* expression system. *Biotechnol Lett* **2009**, *31* (7), 1031-6.
299. Salunkhe, S.; Prasad, B.; Sabnis-Prasad, K.; Apte-Deshpande, A.; Padmanabhan, S., Expression and purification of SAK-fused human Interferon alpha in *Escherichia coli*. *J. Microb. Biochem. Technol.* **2009**, *1* (1), 005-010.

300. Nishihara, K.; Kanemori, M.; Yanagi, H.; Yura, T., Overexpression of trigger factor prevents aggregation of recombinant proteins in Escherichia coli. *Appl. Environ. Microbiol.* **2000**, *66* (3), 884-889.
301. Chesshyre, J. A.; Hipkiss, A. R., Low temperatures stabilize interferon  $\alpha$ -2 against proteolysis in Methylophilus methylotrophus and Escherichia coli. *Appl. Microbiol. Biotechnol.* **1989**, *31* (2), 158-62.
302. Hashemzadeh-Bonehi, L.; Mehraein-Ghomi, F.; Mitsopoulos, C.; Jacob, J. P.; Hennessey, E. S.; Broome-Smith, J. K., Importance of using lac rather than ara promoter vectors for modulating the levels of toxic gene products in Escherichia coli. *Mol. Microbiol.* **1998**, *30* (3), 676-678.
303. Siegele, D. A.; Hu, J. C., Gene expression from plasmids containing the araBAD promoter at subsaturating inducer concentrations represents mixed populations. *Proc. Natl. Acad. Sci. U. S. A.* **1997**, *94* (15), 8168-8172.
304. van Hoek, M.; Hogeweg, P., The effect of stochasticity on the Lac operon: an evolutionary perspective. *PLoS Comput. Biol.* **2007**, *3* (6), 1071-1082.
305. Sheibani, N., Prokaryotic gene fusion expression systems and their use in structural and functional studies of proteins. *Prep. Biochem. Biotechnol.* **1999**, *29* (1), 77-90.
306. Kapust, R. B.; Waugh, D. S., Escherichia coli maltose-binding protein is uncommonly effective at promoting the solubility of polypeptides to which it is fused. *Protein Sci.* **1999**, *8* (8), 1668-1674.
307. Young, C. L.; Britton, Z. T.; Robinson, A. S., Recombinant protein expression and purification: A comprehensive review of affinity tags and microbial applications. *Biotechnol. J.* **2012**, *7* (5), 620-634.
308. LaVallie, E. R.; Lu, Z.; Diblasio-Smith, E. A.; Collins-Racie, L. A.; McCoy, J. M., Thioredoxin as a fusion partner for production of soluble recombinant proteins in Escherichia coli. *Methods Enzymol* **2000**, *326*, 322-40.
309. Malakhov, M. P.; Mattern, M. R.; Malakhova, O. A.; Drinker, M.; Weeks, S. D.; Butt, T. R., SUMO fusions and SUMO-specific protease for efficient expression and purification of proteins. *J. Struct. Funct. Genomics* **2004**, *5* (1-2), 75-86.
310. Zuo, X.; Li, S.; Hall, J.; Mattern, M. R.; Tran, H.; Shoo, J.; Tan, R.; Weiss, S. R.; Butt, T. R., Enhanced Expression and Purification of Membrane Proteins by SUMO Fusion in Escherichia coli. *J. Struct. Funct. Genomics* **2005**, *6* (2-3), 103-111.
311. Marblestone, J. G.; Edavettal, S. C.; Lim, Y.; Lim, P.; Zuo, X.; Butt, T. R., Comparison of SUMO fusion technology with traditional gene fusion systems: Enhanced expression and solubility with SUMO. *Protein Sci.* **2006**, *15* (1), 182-189.

312. Meinecke, I.; Cinski, A.; Baier, A.; Peters, M. A.; Dankbar, B.; Wille, A.; Drynda, A.; Mendoza, H.; Gay, R. E.; Hay, R. T.; Ink, B.; Gay, S.; Pap, T., Modification of nuclear PML protein by SUMO-1 regulates Fas-induced apoptosis in rheumatoid arthritis synovial fibroblasts. *Proc. Natl. Acad. Sci. U. S. A.* **2007**, *104* (12), 5073-5078.
313. Seeler, J. S.; Bischof, O.; Nacerddine, K.; Dejean, A., SUMO, the three Rs and cancer. *Curr. Top. Microbiol. Immunol.* **2007**, *313* (Acute Promyelocytic Leukemia), 49-71.
314. Rajan, S.; Plant, L. D.; Rabin, M. L.; Butler, M. H.; Goldstein, S. A. N., Sumoylation silences the plasma membrane leak K<sup>+</sup> channel K2P1. *Cell (Cambridge, MA, U. S.)* **2005**, *121* (1), 37-47.
315. Guan, D.; Chen, Z., Challenges and recent advances in affinity purification of tag-free proteins. *Biotechnol. Lett.* **2014**, *36* (7), 1391-1406.
316. Lang, K. M. H.; Kittelmann, J.; Pilgram, F.; Osberghaus, A.; Hubbuch, J., Custom-tailored adsorbers: A molecular dynamics study on optimal design of ion exchange chromatography material. *J. Chromatogr. A* **2015**, *1413*, 60-67.
317. Stahlberg, J., Retention models for ions in chromatography. *J. Chromatogr. A* **1999**, *855* (1), 3-55.
318. Hardin, A. M.; Harinarayan, C.; Malmquist, G.; Axen, A.; van Reis, R., Ion exchange chromatography of monoclonal antibodies: Effect of resin ligand density on dynamic binding capacity. *J. Chromatogr. A* **2009**, *1216* (20), 4366-4371.
319. Franke, A.; Forrer, N.; Butte, A.; Cvijetic, B.; Morbidelli, M.; Johnck, M.; Schulte, M., Role of the ligand density in cation exchange materials for the purification of proteins. *J. Chromatogr. A* **2010**, *1217* (15), 2216-2225.
320. Fogle, J.; Persson, J., Effects of resin ligand density on yield and impurity clearance in preparative cation exchange chromatography. II. Process characterization. *J. Chromatogr. A* **2012**, *1225*, 70-78.
321. Lang, K. M. H.; Kittelmann, J.; Duerr, C.; Osberghaus, A.; Hubbuch, J., A comprehensive molecular dynamics approach to protein retention modeling in ion exchange chromatography. *J. Chromatogr. A* **2015**, *1381*, 184-193.
322. Lindqvist, B.; Storgards, T., Molecular-sieving properties of starch. *Nature (London, U. K.)* **1955**, *175*, 511-12.
323. Lathe, G. H.; Ruthven, C. R., The separation of substances on the basis of their molecular weights, using columns of starch and water. *Biochem J* **1955**, *60* (4), xxxiv.
324. Kunji, E. R. S.; Harding, M.; Butler, P. J. G.; Akamine, P., Determination of the molecular mass and dimensions of membrane proteins by size exclusion chromatography. *Methods (Amsterdam, Neth.)* **2008**, *46* (2), 62-72.

325. Heyden, Y. V.; Popovici, S. T.; Schoenmaker, P. J., Evaluation of size-exclusion chromatography and size-exclusion electrochromatography calibration curves. *J Chromatogr A* **2002**, *957* (2), 127-37.
326. Hong, P.; Koza, S.; Bouvier, E. S. P., A review size-exclusion chromatography for the analysis of protein biotherapeutics and their aggregates. *J. Liq. Chromatogr. Relat. Technol.* **2012**, *35* (20), 2923-2950.
327. Berek, D., Size exclusion chromatography - a blessing and a curse of science and technology of synthetic polymers. *J. Sep. Sci.* **2010**, *33* (3), 315-335.
328. Guo, X.; Condra, M.; Kimura, K.; Berth, G.; Dautzenberg, H.; Dubin, P. L., Determination of molecular weight of heparin by size exclusion chromatography with universal calibration. *Anal. Biochem.* **2003**, *312* (1), 33-39.
329. Ricker, R. D.; Sandoval, L. A., Fast, reproducible size-exclusion chromatography of biological macromolecules. *J. Chromatogr. A* **1996**, *743* (1), 43-50.
330. Cordoba-Rodriguez, R. V., Aggregates in MAbs and recombinant therapeutic proteins: a regulatory perspective. *BioPharm Int.* **2008**, *21* (11), 44-46, 48-50, 52-53.
331. Staub, A.; Guillarme, D.; Schappler, J.; Veuthey, J.-L.; Rudaz, S., Intact protein analysis in the biopharmaceutical field. *J. Pharm. Biomed. Anal.* **2011**, *55* (4), 810-822.
332. Suda, E. J.; Thomas, K. E.; Pabst, T. M.; Mensah, P.; Ramasubramanian, N.; Gustafson, M. E.; Hunter, A. K., Comparison of agarose and dextran-grafted agarose strong ion exchangers for the separation of protein aggregates. *J. Chromatogr. A* **2009**, *1216* (27), 5256-5264.
333. Zhao, X.; Li, G.; Liang, S., Several affinity tags commonly used in chromatographic purification. *J. Anal. Methods Chem.* **2013**, 581093/1-581093/9, 9 pp.
334. Park, N.; Ryu, J.; Jang, S.; Lee, H. S., Metal ion affinity purification of proteins by genetically incorporating metal-chelating amino acids. *Tetrahedron* **2012**, *68* (24), 4649-4654.
335. Arnau, J.; Lauritzen, C.; Petersen, G. E.; Pedersen, J., Current strategies for the use of affinity tags and tag removal for the purification of recombinant proteins. *Protein Expression Purif.* **2006**, *48* (1), 1-13.
336. Sun, Q.-M.; Chen, L.-L.; Cao, L.; Fang, L.; Chen, C.; Hua, Z.-C., An improved strategy for high-level production of human vasostatin120-180. *Biotechnol Prog* **2005**, *21* (4), 1048-52.
337. Chen, H.; Xu, Z.; Xu, N.; Cen, P., Efficient production of a soluble fusion protein containing human beta-defensin-2 in E. coli cell-free system. *J. Biotechnol.* **2005**, *115* (3), 307-315.
338. Wang, X.; Campoli, M.; Ko, E.; Luo, W.; Ferrone, S., Enhancement of scFv fragment reactivity with target antigens in binding assays following mixing with anti-tag monoclonal antibodies. *J. Immunol. Methods* **2004**, *294* (1-2), 23-35.

339. Mayer, A.; Sharma, S. K.; Tolner, B.; Minton, N. P.; Purdy, D.; Amlot, P.; Tharakan, G.; Begent, R. H. J.; Chester, K. A., Modifying an immunogenic epitope on a therapeutic protein: a step towards an improved system for antibody-directed enzyme prodrug therapy (ADEPT). *Br. J. Cancer* **2004**, *90* (12), 2402-2410.
340. Fonda, I.; Kenig, M.; Gaberc-Porekar, V.; Pristovsek, P.; Menart, V., Attachment of histidine tags to recombinant tumor necrosis factor-alpha drastically changes its properties. *TheScientificWorld* **2002**, *2*, 1312-1325.
341. Xiong, S.; Zhang, L.; He, Q.-Y., Fractionation of proteins by heparin chromatography. *Methods Mol. Biol. (Totowa, NJ, U. S.)* **2008**, *424* (2D PAGE: Sample Preparation and Fractionation, Volume 1), 213-221.
342. Iida, T.; Kamo, M.; Uozumi, N.; Inui, T.; Imai, K., Further application of a two-step heparin affinity chromatography method using divalent cations as eluents: Purification and identification of membrane-bound heparin binding proteins from the mitochondrial fraction of HL-60 cells. *J. Chromatogr. B Anal. Technol. Biomed. Life Sci.* **2005**, *823* (2), 209-212.
343. Gao, N.; Shearwin, K.; Mack, J.; Finzi, L.; Dunlap, D., Purification of bacteriophage lambda repressor. *Protein Expression Purif.* **2013**, *91* (1), 30-36.
344. Kumar, V.; Hassan, M. I.; Kashav, T.; Singh, T. P.; Yadav, S., Heparin-binding proteins of human seminal plasma: purification and characterization. *Mol. Reprod. Dev.* **2008**, *75* (12), 1767-1774.
345. Lichty, J. J.; Malecki, J. L.; Agnew, H. D.; Michelson-Horowitz, D. J.; Tan, S., Comparison of affinity tags for protein purification. *Protein Expression Purif.* **2005**, *41* (1), 98-105.
346. Terpe, K., Overview of tag protein fusions: from molecular and biochemical fundamentals to commercial systems. *Appl. Microbiol. Biotechnol.* **2003**, *60* (5), 523-533.
347. Khan, K. H., Gene expression systems and recombinant protein purification. *Res. J. Pharm., Biol. Chem. Sci.* **2014**, *5* (6), 450-463.
348. Li, Y., The tandem affinity purification technology: an overview. *Biotechnol. Lett.* **2011**, *33* (8), 1487-1499.
349. Smith, D. B.; Johnson, K. S., Single-step purification of polypeptides expressed in *Escherichia coli* as fusions with glutathione S-transferase. *Gene* **1988**, *67* (1), 31-40.
350. Lim, K.; Ho, J. X.; Keeling, K.; Gilliland, G. L.; Ji, X.; Rueker, F.; Carter, D. C., Three-dimensional structure of *Schistosoma japonicum* glutathione S-transferase fused with a six-amino acid conserved neutralizing epitope of gp41 from HIV. *Protein Sci.* **1994**, *3* (12), 2233-44.
351. Kaplan, W.; Husler, P.; Klump, H.; Erhardt, J.; Sluis-Cremer, N.; Dirr, H., Conformational stability of pGEX-expressed *Schistosoma japonicum* glutathione S-transferase: A detoxification enzyme and fusion-protein affinity tag. *Protein Sci.* **1997**, *6* (2), 399-406.



352. Kimple Michelle, E.; Sondek, J., Overview of affinity tags for protein purification. *Curr Protoc Protein Sci* **2004**, Chapter 9, Unit 9 9.
353. Frangioni, J. V.; Neel, B. G., Use of a general purpose mammalian expression vector for studying intracellular protein targeting: identification of critical residues in the nuclear lamin A/C nuclear localization signal. *J. Cell Sci.* **1993**, *105* (2), 481-8.
354. Harper, S.; Speicher, D. W., Purification of proteins fused to glutathione S-transferase. *Methods Mol. Biol. (N. Y., NY, U. S.)* **2011**, *681* (Protein Chromatography), 259-280.
355. Hunt, I., From gene to protein: a review of new and enabling technologies for multi-parallel protein expression. *Protein Expression Purif.* **2005**, *40* (1), 1-22.
356. Duplay, P.; Bedouelle, H.; Fowler, A.; Zabin, I.; Saurin, W.; Hofnung, M., Sequences of the malE gene and of its product, the maltose-binding protein of Escherichia coli K12. *J. Biol. Chem.* **1984**, *259* (16), 10606-13.
357. Di Guan, C.; Li, P.; Riggs, P. D.; Inouye, H., Vectors that facilitate the expression and purification of foreign peptides in Escherichia coli by fusion to maltose-binding protein. *Gene* **1988**, *67* (1), 21-30.
358. Pattenden, L. K.; Thomas, W. G., Amylose affinity chromatography of maltose-binding protein. Purification by both native and novel matrix-assisted dialysis refolding methods. *Methods Mol. Biol. (Totowa, NJ, U. S.)* **2008**, *421* (Affinity Chromatography (2nd Edition)), 169-189.
359. Kimple Michelle, E.; Brill Allison, L.; Pasker Renee, L., Overview of affinity tags for protein purification. *Curr Protoc Protein Sci* **2013**, *73*, Unit 9 9.
360. Malhotra, A., Tagging for protein expression. *Methods Enzymol.* **2009**, *463* (Guide to Protein Purification), 239-258.
361. Nallamsetty, S.; Waugh, D. S., A generic protocol for the expression and purification of recombinant proteins in Escherichia coli using a combinatorial His6-maltose binding protein fusion tag. *Nat. Protoc.* **2007**, *2* (2), 383-391.
362. Sassenfeld, H. M.; Brewer, S. J., A polypeptide fusion designed for the purification of recombinant proteins. *Bio/Technology* **1984**, *2* (1), 76-81.
363. Nock, S.; Spudich, J. A.; Wagner, P., Reversible, site-specific immobilization of polyarginine-tagged fusion proteins on mica surfaces. *FEBS Lett* **1997**, *414* (2), 233-8.
364. Porath, J.; Carlsson, J.; Olsson, I.; Belfrage, G., Metal chelate affinity chromatography, a new approach to protein fractionation. *Nature (London)* **1975**, *258* (5536), 598-9.
365. Swain, J. H.; Tabatabai, L. B.; Reddy, M. B., Histidine content of low-molecular-weight beef proteins influences nonheme iron bioavailability in Caco-2 cells. *J. Nutr.* **2002**, *132* (2), 245-251.

366. Storcksdieck, S.; Bonsmann, G.; Hurrell, R. F., Iron-binding properties, amino acid composition, and structure of muscle tissue peptides from in vitro digestion of different meat sources. *J. Food Sci.* **2007**, *72* (1), S19-S29.
367. Gaberc-Porekar, V.; Menart, V., Perspectives of immobilized-metal affinity chromatography. *J. Biochem. Biophys. Methods* **2001**, *49* (1-3), 335-360.
368. Svensson, J.; Andersson, C.; Reseland, J. E.; Lyngstadaas, P.; Buelow, L., Histidine tag fusion increases expression levels of active recombinant amelogenin in *Escherichia coli*. *Protein Expression Purif.* **2006**, *48* (1), 134-141.
369. Ferrer-Miralles, N.; Corchero, J. L.; Kumar, P.; Cedano, J. A.; Gupta, K. C.; Villaverde, A.; Vazquez, E., Biological activities of histidine-rich peptides; merging biotechnology and nanomedicine. *Microb. Cell Fact.* **2011**, *10*, 101.
370. Kuo, W.-H. K.; Chase, H. A., Exploiting the interactions between poly-histidine fusion tags and immobilized metal ions. *Biotechnol. Lett.* **2011**, *33* (6), 1075-1084.
371. Sulkowski, E., The saga of IMAC and MIT. *BioEssays* **1989**, *10* (5), 170-5.
372. Petzold, M.; Coghlan, C. J.; Hearn, M. T. W., Studies with an immobilized metal affinity chromatography cassette system involving binuclear triazacyclononane-derived ligands: Automation of batch adsorption measurements with tagged recombinant proteins. *J. Chromatogr. A* **2014**, *1351*, 61-69.
373. Bornhorst, J. A.; Falke, J. J., Purification of proteins using polyhistidine affinity tags. *Methods Enzymol.* **2000**, *326* (Applications of Chimeric Genes and Hybrid Proteins, Pt. A), 245-254.
374. Gaberc-Porekar, V.; Menart, V., Potential for using histidine tags in purification of proteins at large scale. *Chem. Eng. Technol.* **2005**, *28* (11), 1306-1314.
375. Hopp, T. P.; Prickett, K. S.; Price, V. L.; Libby, R. T.; March, C. J.; Cerretti, D. P.; Urdal, D. L.; Conlon, P. J., A short polypeptide marker sequence useful for recombinant protein identification and purification. *Bio/Technology* **1988**, *6* (10), 1204-10.
376. Knappik, A.; Plueckthun, A., An improved affinity tag based on the FLAG peptide for the detection and purification of recombinant antibody fragments. *BioTechniques* **1994**, *17* (4), 754-61.
377. Brizzard, B. L.; Chubet, R. G.; Vizard, D. L., Immunoaffinity purification of FLAG epitope-tagged bacterial alkaline phosphatase using a novel monoclonal antibody and peptide elution. *BioTechniques* **1994**, *16* (4), 730-2, 734-5.
378. Voss, S.; Skerra, A., Mutagenesis of a flexible loop in streptavidin leads to higher affinity for the Strep-tag II peptide and improved performance in recombinant protein purification. *Protein Eng.* **1997**, *10* (8), 975-982.

379. Skerra, A.; Schmidt, T. G. M., Use of the Strep-tag and streptavidin for detection and purification of recombinant proteins. *Methods Enzymol.* **2000**, *326* (Applications of Chimeric Genes and Hybrid Proteins, Pt. A), 271-304.
380. Walls, D.; Loughran, S. T., Tagging recombinant proteins to enhance solubility and aid purification. *Methods Mol. Biol. (N. Y., NY, U. S.)* **2011**, *681* (Protein Chromatography), 151-175.
381. Evan, G. I.; Lewis, G. K.; Ramsay, G.; Bishop, J. M., Isolation of monoclonal antibodies specific for human c-myc proto-oncogene product. *Mol. Cell. Biol.* **1985**, *5* (12), 3610-16.
382. Manstein, D. J.; Schuster, H.-P.; Morandini, P.; Hunt, D. M., Cloning vectors for the production of proteins in *Dictyostelium discoideum*. *Gene* **1995**, *162* (1), 129-34.
383. Vaughan, T. J.; Williams, A. J.; Pritchard, K.; Osbourn, J. K.; Pope, A. R.; Earnshaw, J. C.; McCafferty, J.; Hodits, R. A.; Wilton, J.; Johnson, K. S., Human antibodies with sub-nanomolar affinities isolated from a large non-immunized phage display library. *Nat. Biotechnol.* **1996**, *14* (3), 309-14.
384. Wiese, A.; Wilms, B.; Syltatk, C.; Mattes, R.; Altenbuchner, J., Cloning, nucleotide sequence and expression of a hydantoinase and carbamoylase gene from *Arthrobacter aurescens* DSM 3745 in *Escherichia coli* and comparison with the corresponding genes from *Arthrobacter aurescens* DSM 3747. *Appl. Microbiol. Biotechnol.* **2001**, *55* (6), 750-757.
385. Schioth, H. B.; Muceniece, R.; Szardenings, M.; Prusis, P.; Wikberg, J. E., Evidence indicating that the TM4, EL2, and TM5 of the melanocortin 3 receptor Do not participate in ligand binding. *Biochem Biophys Res Commun* **1996**, *229* (3), 687-92.
386. Moorby, C. D.; Gherardi, E., Expression of a Cx43 Deletion Mutant in 3T3 A31 Fibroblasts Prevents PDGF-Induced Inhibition of Cell Communication and Suppresses Cell Growth. *Exp. Cell Res.* **1999**, *249* (2), 367-376.
387. Karpeisky, M. Y.; Senchenko, V. N.; Dianova, M. V.; Kanevsky, V. Y., Formation and properties of S-protein complex with S-peptide-containing fusion protein. *FEBS Lett.* **1994**, *339* (3), 209-12.
388. Kim, J.-S.; Raines, R. T., A misfolded but active dimer of bovine seminal ribonuclease. *Eur. J. Biochem.* **1994**, *224* (1), 109-14.
389. Stofko-Hahn, R.; Carr, D. W.; Scott, J. D., A single step purification for recombinant proteins: characterization of a microtubule associated protein (MAP2) fragment which associates with the type II cAMP-dependent protein kinase. *FEBS Lett.* **1992**, *302* (3), 274-8.
390. Meador, W. E.; Means, A. R.; Quijcho, F. A., Target enzyme recognition by calmodulin: 2.4 Å structure of a calmodulin-peptide complex. *Science (Washington, D. C., 1883-)* **1992**, *257* (5074), 1251-5.

391. Zheng, C.-F.; Simcox, T.; Xu, L.; Vaillancourt, P., A new expression vector for high level protein production, one step purification and direct isotopic labeling of calmodulin-binding peptide fusion proteins. *Gene* **1997**, *186* (1), 55-60.
392. Head, J. F., A better grip on calmodulin. *Curr. Biol.* **1992**, *2* (11), 609-11.
393. Hearn, M. T. W.; Acosta, D., Applications of novel affinity cassette methods: use of peptide fusion handles for the purification of recombinant proteins. *J. Mol. Recognit.* **2001**, *14* (6), 323-369.
394. Martinez-Ceron, M. C.; Targovnik, A. M.; Urtasun, N.; Cascone, O.; Miranda, M. V.; Camperi, S. A., Recombinant protein purification using complementary peptides as affinity tags. *New Biotechnol.* **2012**, *29* (2), 206-210.
395. Kikot, P.; Polat, A.; Achilli, E.; Fernandez Lahore, M.; Grasselli, M., Immobilized palladium(II) ion affinity chromatography for recovery of recombinant proteins with peptide tags containing histidine and cysteine. *J. Mol. Recognit.* **2014**, *27* (11), 659-668.
396. Van Hijfte, L.; Marciniak, G.; Froloff, N., Combinatorial chemistry, automation and molecular diversity: new trends in the pharmaceutical industry. *J. Chromatogr. B Biomed. Sci. Appl.* **1999**, *725* (1), 3-15.
397. Tozzi, C.; Anfossi, L.; Giraudi, G., Affinity chromatography techniques based on the immobilization of peptides exhibiting specific binding activity. *J. Chromatogr. B Anal. Technol. Biomed. Life Sci.* **2003**, *797* (1-2), 289-304.
398. Mondal, S.; Shet, D.; Prasanna, C.; Atreya, H. S., High yield expression of proteins in *E. coli* for NMR studies. *Adv. Biosci. Biotechnol.* **2013**, *4* (6), 751-767.
399. Sivashanmugam, A.; Murray, V.; Cui, C.; Zhang, Y.; Wang, J.; Li, Q., Practical protocols for production of very high yields of recombinant proteins using *Escherichia coli*. *Protein Sci.* **2009**, *18* (5), 936-948.
400. McCoy, J.; Lavallie, E., Expression and purification of thioredoxin fusion proteins. *Curr Protoc Mol Biol* **2001**, *Chapter 16*, Unit16 8.
401. Rajalingam, D.; Kumar, T. K. S.; Yu, C., The C2A Domain of Synaptotagmin Exhibits a High Binding Affinity for Copper: Implications in the Formation of the Multiprotein FGF Release Complex. *Biochemistry* **2005**, *44* (44), 14431-14442.
402. Nallamsetty, S.; Kapust, R. B.; Toezser, J.; Cherry, S.; Tropea, J. E.; Copeland, T. D.; Waugh, D. S., Efficient site-specific processing of fusion proteins by tobacco vein mottling virus protease in vivo and in vitro. *Protein Expression Purif.* **2004**, *38* (1), 108-115.
403. Bulani, S. I.; Moleleki, L.; Albertyn, J.; Moleleki, N., Development of a novel rDNA based plasmid for enhanced cell surface display on *Yarrowia lipolytica*. *AMB Express* **2012**, *2* (1), 27/1-27/8, 8 pp.

404. Jung, A. S.; Koo, B.-K.; Chong, S.-H.; Kim, K.; Choi, D. K.; Vu, T. T. T.; Nguyen, M. T.; Jeong, B.; Ryu, H.-B.; Kim, I.; Jang, Y. J.; Robinson, R. C.; Choe, H., Soluble expression of human leukemia inhibitory factor with protein disulfide isomerase in *Escherichia coli* and its simple purification. *PLoS One* **2013**, *8* (12), e83781/1-e83781/12, 12 pp.
405. Amarasinghe, C.; Jin, J.-P., The Use of Affinity Tags to Overcome Obstacles in Recombinant Protein Expression and Purification. *Protein Pept. Lett.* **2015**, *22* (10), 885-892.
406. Rajalingam, D.; Kathir, K. M.; Ananthamurthy, K.; Adams, P. D.; Kumar, T. K. S., A method for the prevention of thrombin-induced degradation of recombinant proteins. *Anal. Biochem.* **2008**, *375* (2), 361-363.
407. Charlton, A.; Zachariou, M., Tag removal by site-specific cleavage of recombinant fusion proteins. *Methods Mol. Biol. (N. Y., NY, U. S.)* **2011**, *681* (Protein Chromatography), 349-367.
408. Liew, O. W.; Chong, J. P. C.; Yandle, T. G.; Brennan, S. O., Preparation of recombinant thioredoxin fused N-terminal proCNP: Analysis of enterokinase cleavage products reveals new enterokinase cleavage sites. *Protein Expression Purif.* **2005**, *41* (2), 332-340.
409. Eaton, D.; Rodriguez, H.; Vehar, G. A., Proteolytic processing of human factor VIII. Correlation of specific cleavages by thrombin, factor Xa, and activated protein C with activation and inactivation of factor VIII coagulant activity. *Biochemistry* **1986**, *25* (2), 505-12.
410. Jenny, R. J.; Mann, K. G.; Lundblad, R. L., A critical review of the methods for cleavage of fusion proteins with thrombin and factor Xa. *Protein Expression Purif.* **2003**, *31* (1), 1-11.
411. Kapust, R. B.; Tozser, J.; Copeland, T. D.; Waugh, D. S., The P1' specificity of tobacco etch virus protease. *Biochem. Biophys. Res. Commun.* **2002**, *294* (5), 949-955.
412. Hancock, D. C.; O'Reilly, N. J., Production of polyclonal antibodies in rabbits. *Methods Mol. Biol. (Totowa, NJ, U. S.)* **2005**, *295* (Immunochemical Protocols (3rd Edition)), 27-39.
413. Southern, E. M., Detection of specific sequences among DNA fragments separated by gel electrophoresis. *J. Mol. Biol.* **1975**, *98* (3), 503-17.
414. Alwine, J. C.; Kemp, D. J.; Stark, G. R., Method for detection of specific RNAs in agarose gels by transfer to diazobenzyloxymethyl-paper and hybridization with DNA probes. *Proc. Natl. Acad. Sci. U. S. A.* **1977**, *74* (12), 5350-4.
415. Jin, S.; Kennedy, R. T., New developments in Western blot technology. *Chin. Chem. Lett.* **2015**, *26* (4), 416-418.
416. Towbin, H.; Staehelin, T.; Gordon, J., Electrophoretic transfer of proteins from polyacrylamide gels to nitrocellulose sheets: Procedure and some applications. *Proc. Natl. Acad. Sci. U. S. A.* **1979**, *76* (9), 4350-4.

417. Burnette, W. N., "Western blotting": electrophoretic transfer of proteins from sodium dodecyl sulfate-polyacrylamide gels to unmodified nitrocellulose and radiographic detection with antibody and radioiodinated protein A. *Anal. Biochem.* **1981**, *112* (2), 195-203.
418. Kurien, B. T.; Scofield, R. H., Western blotting. *Methods (San Diego, CA, U. S.)* **2006**, *38* (4), 283-293.
419. Kost, J.; Liu, L. S.; Ferreira, J.; Langer, R., Enhanced protein blotting from PhastGel media to membranes by irradiation of low-intensity ultrasound. *Anal. Biochem.* **1994**, *216* (1), 27-32.
420. Gershoni, J. M.; Palade, G. E., Electrophoretic transfer of proteins from sodium dodecyl sulfate-polyacrylamide gels to a positively charged membrane filter. *Anal. Biochem.* **1982**, *124* (2), 396-405.
421. Gershoni, J. M., Protein blotting: a manual. *Methods Biochem. Anal.* **1988**, *33*, 1-58.
422. Kenna, J. G.; Major, G. N.; Williams, R. S., Methods for reducing non-specific antibody binding in enzyme-linked immunosorbent assays. *J. Immunol. Methods* **1985**, *85* (2), 409-19.
423. Ida, N.; Hartmann, T.; Pantel, J.; Schroeder, J.; Zerfass, R.; Foerstl, H.; Sandbrink, R.; Masters, C. L.; Beyreuther, K., Analysis of heterogeneous  $\beta$ A4 peptides in human cerebrospinal fluid and blood by a newly developed sensitive Western blot assay. *J. Biol. Chem.* **1996**, *271* (37), 22908-22914.
424. Cao, J.; Fernandez, M.; Villamarin, J. A., A method for the purification of cAMP-dependent protein kinase using immunoaffinity chromatography. *Protein Expression Purif.* **1998**, *14* (3), 418-424.

## **Chapter 2**

### **Use of Heparin-Binding Affinity Tag for Protein Purification**

## 2.1. Abstract

Recombinant proteins are useful in a variety of settings in biotechnology. These proteins need to be purified to homogeneity, however, before they can be used for further experiments. Affinity tags have become common avenues for protein purification. Several affinity tags available today include GST, His-tag, MBP, and several others. Despite being commonly used, they have multiple downfalls that include their bulky size interfering with target protein structure and folding, aggregation, and expensive and harsh conditions needed for purification. We have designed a 34-amino acid residue heparin-binding (HB) peptide based on structural features from the heparin-binding region of various HBPs, which are known to naturally bind to heparin. HB-peptide has good binding affinity for heparin and HS in a two-site binding model ( $K_d$  in high nM to low  $\mu$ M for both GAGs). In the presence of heparin or its analog SOS, HB-peptide gains helical secondary structure from a random coil structure, does not undergo an extreme change in its tertiary structure, but is perturbed in its overall backbone conformation. This peptide has also successfully been exploited as an affinity tag for the expression and purification of three different non-heparin-binding proteins (C2A, CA1b3, and S100A13). Using a step-wise NaCl gradient on heparin-Sepharose, the fusion proteins were purified to homogeneity (HB-C2A elutes at 500 mM NaCl, and HB-CA1b3 and HB-S100A13 elutes at 1 M NaCl). These mild conditions using various pH and buffers allowed for successful purification of these fusion proteins. Following purification, enzymatic cleavage was successful for all three proteins using thrombin and TEV protease. Subsequent separation of the target protein from the HB-peptide was then achieved by additional heparin-Sepharose affinity chromatography.



## 2.2. Introduction

Pure recombinant proteins have become extremely important in a commercial aspect such as therapeutics, diagnostic tools, and drug design<sup>1,2</sup>. These target proteins are expressed in large yields in bacterial cell lines such as *E. coli*, and are then purified to homogeneity. Various types of purification methods exist such as ion-exchange, size exclusion, and affinity chromatography. Affinity chromatography has become one of the most widely used methods to purify recombinant proteins due to high yields and high purity that can be achieved<sup>3</sup>. Typically, an affinity tag of any desired size (protein or peptide) is attached to the target protein of choice. The affinity tag then binds to its partner that is immobilized on a resin, aiding in the efficient purification of the desired protein. In general, affinity tags used for protein purification are expected to possess the following properties: (a) high binding specificity during purification; (b) wide range of target proteins as their partner; (c) no interference with the target protein's structure or and (d) ability to be removed from the target protein<sup>4,5,6,7,8,9</sup>. Common affinity tags include His-tag, GST, MBP, thioredoxin, and several others<sup>10,11</sup>. The current affinity tags have some downsides, which include conditions or the presence of the tag interfering with the target protein's structure/activity, aggregation during purification, lack of purification under denaturing, and expensive conditions of purification required<sup>12,13,14,15</sup>. Peptides, however, have become popular in their use as affinity tags due to their stability<sup>16</sup>. Most small peptide tags added to a target protein will not affect the protein activity<sup>17</sup>.

Numerous proteins have exhibited heparin-binding capability that are involved in extremely diverse processes<sup>18,19,20,21,22,23</sup>. The regions called HBRs that exist in the proteins demonstrating this binding affinity contain an expanse of positively charged residues that bind to the negatively charged heparin molecule<sup>24</sup>. Cardin and Weintraub have shown that HBPs

contain specific consensus sequences that are responsible for their specific interaction with heparin, most commonly including XBBXBX, XBBBXXBX, and XBBXXBBBXXBBX, where B is one of the three basic amino acids (arginine, lysine or histidine) and X is any of the other 17 natural amino acids<sup>25,26,27,28</sup>. Spatial arrangement of the HBR is just as important for heparin-binding capability as the sequence itself. Heparin binding is also known to increase  $\alpha$ -helix conformation of specifically designed short-chained peptides, increasing their stability<sup>29</sup>.

HBPs, such as FGFs, ATIII, fibronectin, cytokines, and others exhibit high binding affinity for heparin<sup>30,31,32,33,34</sup>. Heparin-Sepharose is especially important for the purification of these HBPs, which naturally bind to heparin-Sepharose without the aid of an affinity tag<sup>35</sup>. If a non-heparin-binding protein needs to be purified, the addition of an affinity tag that binds to heparin would be beneficial in order to use the mild elution conditions and simple steps that heparin-Sepharose provides. We have fashioned a heparin-binding peptide after various sequence and structural features in HBPs that is used as an affinity tag for the purification of various recombinant proteins by heparin-Sepharose affinity chromatography.

### **2.3. Materials and Methods**

#### ***Expression and Purification of GST-HB***

In order to acquire large amounts of the HB-peptide, a GST-fused-HB-peptide was designed for characterization studies. The recombinant GST-fused-HB-peptide (GST-HB) was transformed into BL21 *E. coli* strain. Bacteria were grown under shaking conditions (250 rpm) at 37°C for in Luria-Bertani (LB) broth containing ampicillin (100 mg/mL). Once the OD of 0.6 was reached IPTG was used to induce the cells, which grew an additional 4 hours in the same environment. The cells were later harvested at 6000 rpm at 4°C. Expression cell samples in phosphate

buffered saline (1X PBS) (10 mM Na<sub>2</sub>HPO<sub>4</sub>, 1.8 mM KH<sub>2</sub>PO<sub>4</sub>, 2.7 mM KCl, 137 mM NaCl), pH 7.2 were lysed (10 minutes, 10-second pulse with 10-second rest) on ice using a Microson XL sonicator with a power setting of 15. The cell lysate was centrifuged at 20,000 rpm for 30 minutes at 4°C. The supernatant was loaded onto equilibrated glutathione-Sepharose at a flow rate of 1 mL/minute and eluted using 10 mM reduced glutathione (GSH) in 1X PBS. Protein elution was monitored at 280 nm using a BioRad UV-visible detector. The eluted protein was dialyzed against 1X PBS, pH 7.2 to be used for further experiments. The GST affinity tag was cleaved from the HB-peptide using thrombin (1 unit thrombin/250 µg GST-HB for 16 hours at 25°C) while gently rocking. The HB-peptide was removed from GST using heat treatment method established by the Kumar lab (data not published yet). The supernatant from this method was HB-peptide, which was then desalted using precipitation by isopropyl alcohol (IPA). Varying amounts (percentage) of IPA was added to the HB-peptide solution, which was then incubated at -20°C for 4 hours. This mixture was then centrifuged at 13,000 rpm for 10 minutes, and the resulting pellet (HB-peptide) was dried with nitrogen and heated if IPA was still present.

### ***Isothermal Titration Calorimetry of HB-peptide***

Isothermal titration calorimetry (ITC) measurements were performed using iTC200 (MicroCal Inc., Northampton, MA) at 25°C. The concentration of HB-peptide was maintained at 1:10 the concentration of LMWH and HS in 10 mM phosphate buffer, 100 mM NaCl, pH 7.2. All samples were centrifuged at 13,000 rpm to remove particulates and later degassed under vacuum. The corresponding GAG was titrated into HB-peptide at 1.3 µL injections with 12 sec intervals. The raw data was fit using binding models in the Origin Version 7.0 software supplied by MicroCal Inc. The accuracy of the fitting was assessed using the given X<sup>2</sup> values.

### ***Far UV Circular Dichroism of HB-peptide***

All circular dichroism (CD) measurements were performed on a Jasco-720 spectropolarimeter at 25°C in Milli-Q H<sub>2</sub>O. The concentration of HB-peptide was 100 μM, with LMWH and SOS of 500 μM. Wavelength scans were from 190-250 nm in a 0.02 cm path length cuvette. CD spectra are average of 10 scans at a scan speed of 50 nm/minute.

### ***Intrinsic Fluorescence of HB-peptide***

All intrinsic fluorescence measurements were performed on a Hitachi F2500 fluorimeter using a 1.0 cm path length cuvette. Concentration of HB-peptide was 25 μM, whereas LMWH and SOS were 250 μM. The excitation wavelength was 280 nm with acquisition of 300-450 nm.

### ***NMR Spectroscopy of HB-peptide***

<sup>1</sup>H-<sup>15</sup>N heteronuclear single quantum coherence spectroscopy (HSQC) measurements were performed on Bruker Avance 500 MHz nuclear magnetic resonance (NMR) at 25°C.

Concentration of HB-peptide was 500 μM and heparin was 2.5 mM in 10 mM phosphate buffer, 100 mM NaCl, pH 7.2 (90% H<sub>2</sub>O + 10% D<sub>2</sub>O). All <sup>1</sup>H data were referenced to the resonance frequency of H<sub>2</sub>O (~ 4.7-4.8 ppm)

### ***Expression and Purification of the First HB-fusion Protein (HB-C2A)***

The previously obtained recombinant pET-28a-HB fusion construct (HB-C2A) was transformed into BL21\* *E. coli* strain. In short, the C2A domain of mouse synaptotagmin-1 was cloned into the pET-28a-HB vector. Bacteria were grown under shaking conditions (250 rpm) at 37°C in LB and TB containing kanamycin (50 μg/mL) for HB-C2A and both ampicillin (100 μg/mL) and

chloramphenicol (35 µg/mL) for HB-S100A13 and HB-CA1b3. Once the OD of 0.6 was reached, IPTG was used to induce the cells, which grew an additional 4 hours in the same environment. The cells were later harvested by centrifugation at 4°C at 6000 rpm. For <sup>15</sup>N-labeled HB-C2A, M9 minimal medium with <sup>15</sup>NH<sub>4</sub>Cl as the sole source of nitrogen was used.

Expression samples in 10 mM Tris-HCl, pH 8 were lysed (10 minutes, 10-second pulse, 10-second rest) on ice using a Microson XL sonicator with a power setting of 15. The cell lysate was centrifuged at 20,000 rpm for 30 minutes at 4°C. The supernatant was loaded onto equilibrated heparin-Sepharose (6% highly cross linked spherical agarose) at a flow rate of 1 mL/minute and eluted using a salt gradient of 100 mM to 500 mM NaCl in 10 mM Tris-HCl. Protein elution was monitored at 280 nm using a BioRad UV-visible detector. Purifications were also performed in 10 mM Tris-HCl, pH 7.2 and 10 mM phosphate buffer, pH 6.5, pH 7.2, and pH 8. The purity of each eluted protein was assessed on a 15% SDS-PAGE gel. All protein concentrations were measured using an Agilent spectrophotometer at 280 nm in 10 mM Tris-HCl, pH 8.

### ***Cloning, Expression, and Purification of Other HB-fusion Proteins***

Mouse S100A13, heparin-affinity tag vector, and the C-terminal domain of Albino-3 from *Arabidopsis thaliana* (CA1b3) were each transformed into DH5α cells using ampicillin as the antibiotic of choice. A colony from each transformed product was inoculated 16 hours, and plasmid isolation was performed using Qiagen Miniprep Plasmid Purification kit. Primers of 30 bp in length were designed that contained restriction site bases for BamHI and XhoI. Preparative PCR was then performed using the designed primers, Phusion Mastermix, and

dimethyl sulfoxide (DMSO). Double digestion of the inserts and the affinity tag vector was performed using BamHI and XhoI as the restriction enzymes after gel extraction was performed using Qiagen Gel Extraction kit. Antarctic phosphatase was added to the affinity tag vector for dephosphorylation before ligation occurred. HB-vector and target inserts were ligated using T4 ligase at 22°C for 20 minutes. The ligation product was transformed into DH5 $\alpha$  cells with ampicillin as the antibiotic of choice. Colony PCR was performed using Taq polymerase. Double digestion using BamHI and XhoI was performed on the ligated product to ensure successful ligation. The pET-22b-HB fusion constructs were transformed into BL21 (DE3) *E. coli* strain for S100A13 and Rosetta DE3 *E. coli* strain for CA1b3. Expression was performed in a similar fashion as HB-C2A.

Expression samples in 10 mM Tris-HCl, pH 8 were lysed (10 minutes, 10-second pulse with 10-second rest) on ice using a Microson XL sonicator with a power setting of 15. The cell lysate was centrifuged at 20,000 rpm for 30 minutes at 4°C. The supernatant was loaded onto equilibrated heparin-Sepharose at a flow rate of 1 mL/min and eluted using a salt gradient of 100 mM to 2 M NaCl in 10 mM Tris-HCl. Protein elution was monitored at 280 nm using a BioRad UV-visible detector. The purity of each eluted protein was assessed on a 15% SDS-PAGE gel.

### ***Purification of Denatured HB-fusion Proteins***

The expression samples in 10 mM Tris-HCl, pH 8 containing either 8 M urea or 6 M guanidine hydrochloride were lysed (10 minutes, 10-second pulse with 10-second rest) on ice using a Microson XL sonicator with a power setting of 15. The cell lysate was centrifuged at 20,000 rpm for 30 minutes at 4°C. The supernatant was loaded onto heparin-Sepharose at a flow rate of

1 mL/min, and protein was eluted using a salt gradient of 100 mM to 2 M NaCl in 10 mM Tris-HCl containing corresponding denaturant. Protein elution was monitored at 280 nm using a BioRad UV-visible detector.

### ***Proteolytic Cleavage of HB-Fusion Proteins***

Dialysis (10 mM Tris-HCl, 100 mM NaCl, pH 8) was performed immediately following elution. The sample was concentrated down to 5 mL (Macrosep Advance Centrifugal Device, MWCO 10K), and the amount of protein present was determined using Agilent spectrophotometer at 280 nm. Thrombin cleavage then occurred for HB-C2A (1 unit thrombin/25 ug HB-C2A for 20-24 hours at 37°C) and HB-CA1b3 (1 unit thrombin/10 ug HB-CA1b3 for 24 hours at 37°C). ProTEV Plus was used for cleavage of HB-S100A13 (1 unit ProTEV Plus/200 ug HB-S100A13 for 18 hours at 30°C in presence of 1 mM DTT in 1X ProTEV Plus buffer). Recombinant TEV protease was used under similar conditions (1  $\mu$ L TEV/2  $\mu$ g HB-S100A13 for 9 hours). Phenylmethylsulfonylfluoride (PMSF) was used to inhibit thrombin cleavage, and trichloroacetic acid (TCA) for TEV protease cleavage. The cleaved sample of HB-C2A was passed onto heparin-Sepharose using the salt gradient of 100 mM to 2 M NaCl in 10 mM Tris-HCl, pH 8 to separate the target protein from the HB-peptide. Cleavage of HB-C2A was also performed in 10 mM Tris-HCl, pH 7.2 and 10 mM phosphate buffer, pH 6.5, pH 7.2, and pH 8.

### ***NMR Spectroscopy of Target Protein (C2A)***

$^1\text{H}$ - $^{15}\text{N}$  HSQC measurements were performed on Bruker Avance 500 MHz NMR at 25°C. Concentration of C2A was 320  $\mu$ M in 1X PBS, pH 7.2 (90%  $\text{H}_2\text{O}$ , 10%  $\text{D}_2\text{O}$ ). All  $^1\text{H}$  data were referenced to the resonance frequency of  $\text{H}_2\text{O}$  (~ 4.7-4.8 ppm).

### ***Comparison of Affinity Tags***

Two simultaneous transformations into BL21 cells, followed with over-expression of 1L culture in LB broth were performed for both HB-C2A and GST-C2A. The expression pellet of HB-C2A was resuspended in 10 mM Tris-HCl, pH 8, whereas GST-C2A was in 1X PBS, pH 7.2. Both cell samples were lysed (10 minutes, 10-second pulse with 10-second rest) on ice using a Microson XL sonicator with a power setting of 15. Both cell lysates were centrifuged at 20,000 rpm for 30 minutes at 4°C. The supernatant was loaded onto heparin-Sepharose column for HB-C2A and a GSH-Sepharose column for GST-C2A.

### **2.4. Results and Discussion**

***HB-peptide is designed to contain similar features as HBPs:*** Consensus sequences discovered in the HBR of HBPs are responsible for their binding affinity for heparin. In helical wheel plots of these motifs, the positively-charged amino acid residues (mainly Lys and Arg) face the outside of the protein in order to interact in a mainly electrostatic manner with the negatively-charged heparin molecule. Another important factor responsible for heparin-binding capability is the protein's ability to hydrogen bond (mainly Gln and Asn). The ability for the designed HB-peptide to form a helix and have the positively-charged residues face the outside of the helix enables the peptide to bind strongly to heparin (Figure 2.1).



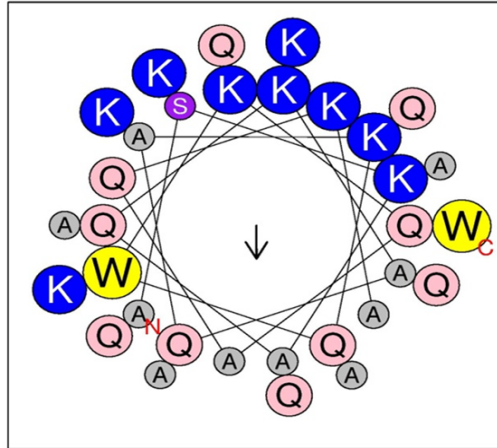


**Figure 2.1** – Helical wheel plot of HB-peptide. As seen here, positively-charged lysine residues face the outside of the helix to interact with heparin.

***Good yield of HB-peptide is achieved from purification of GST-HB:*** Characterization of the peptide in the presence of heparin, such as its binding affinity for heparin, needs to be established before it is used as an affinity tag by heparin-Sepharose chromatography. In order to obtain high yields of the peptide, a GST affinity tag was attached to the N-terminal end of the peptide. Since the thrombin cleavage site would then be on the N-terminal end of the peptide, once cleavage has occurred, only the amino acids glycine and serine would be present on the peptide. These two residues are not expected to interfere with heparin-binding capability since it is only two residues. GST-HB contains 256 amino acid residues with ~ 30 kDa molecular weight (Figure 2.2).

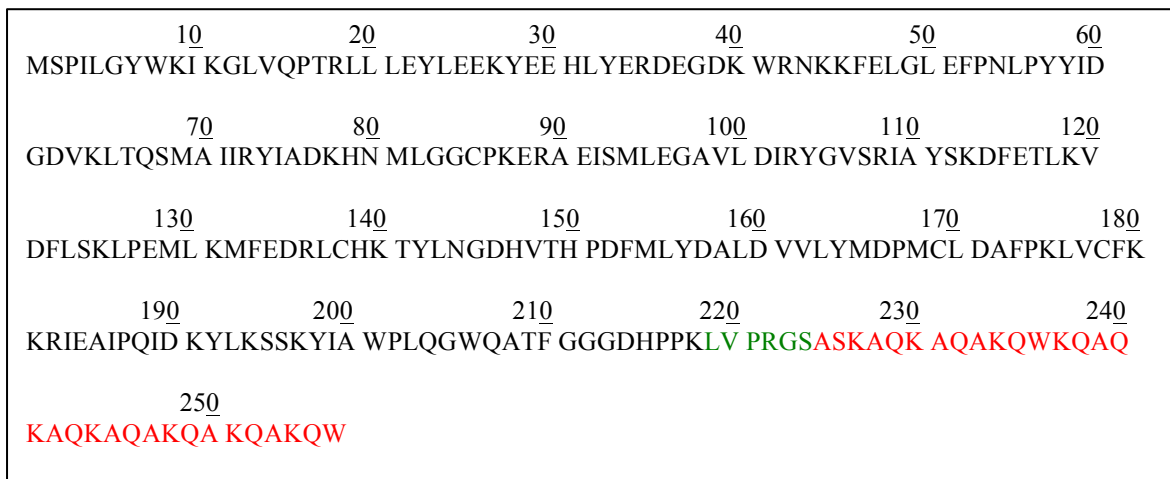


**Figure 2.2** – Amino acid sequence of GST-HB (256 residues, 30 kDa). HB-peptide portion is in red, and thrombin cleavage site is in green.

Large yields of GST-HB (as high as 40 mg) can be expressed and further purified by Glutathione-Sepharose affinity chromatography (Figure 2.3). Due to the large amount of GST-HB expressed, some of the protein is aggregated on the column (lane 6). In this circumstance, it is not a problem because good yield of protein is still acquired for experiments.

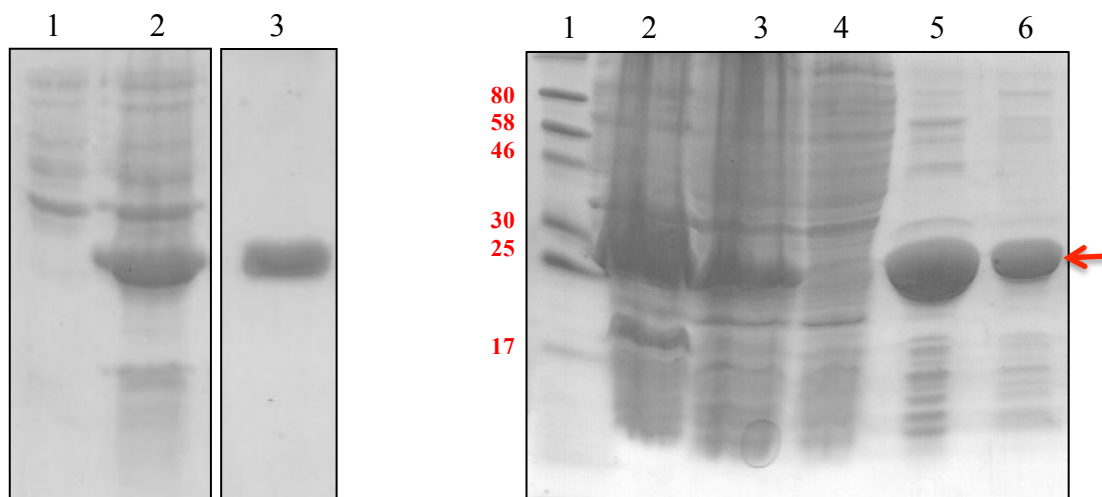


**Figure 2.3** – Expression (Panel-A) and purification (Panel-B) of GST-HB by glutathione-Sepharose affinity chromatography. Panel-A: Lane 1, uninduced; Lane 2, induced; Lane 3, GST-HB (positive control, 30 kDa). Panel-B: Lane 1, protein marker; Lane 2, post-sonication pellet; Lane 3, clear cell lysate; Lane 4, 1X PBS flow-through; Lane 5, 10 mM GSH (eluted GST-HB); Lane 6, 6 M guanidine hydrochloride.

This is a bottleneck to be avoided for other target proteins attached to GST tag. On occasion, impurities are seen after purification, but these are removed when separation by heat treatment is performed.

The Kumar lab has optimized separation of target proteins from GST affinity tag by heat treatment (data not published). This approach proved to be beneficial for the peptide since the molecular weight cutoff for the heat treatment procedure is 10 kDa or less. Even though a small portion of the peptide is lost in the heat treatment technique, the most important aspect is the purity of the peptide (Figure 2.4). As seen in lane 9, no GST is present in the heat treatment supernatant. Consistently, 5 mg of HB-peptide is obtained from 2 L culture.

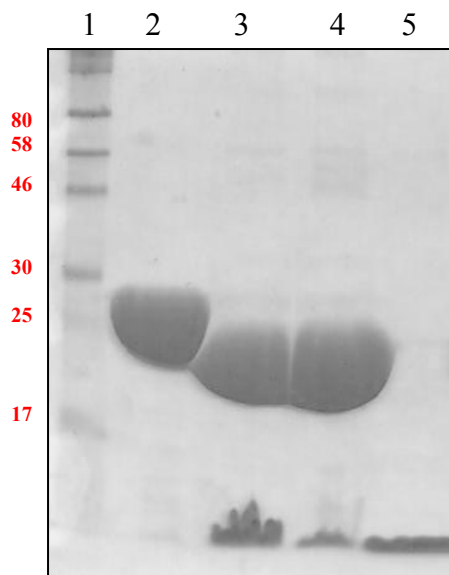


**Figure 2.4** – Thrombin cleavage of GST-HB followed by the heat treatment at 65°C to obtain the HB-peptide separated from GST tag. Lane 1, protein marker; Lane 2, GST-HB; Lane 3, cleaved GST-HB; Lane 4, heat treatment pellet (GST); Lane 5, heat treatment supernatant (HB-peptide).

In order to obtain concentrated peptide, lyophilization was employed in the beginning, but this posed a problem when the lyophilized peptide needed to be in a different buffer than before. The desalting method by IPA (at least 80% v/v) was previously optimized in the Kumar lab (unpublished data), where a peptide or protein can be precipitated free from buffer. The pellet

can then be dissolved in any volume of the buffer of choice when needed. As the amount of IPA is increased to 95%, there is no increase in yield of peptide because all of the peptide gets precipitated at 80% IPA (Figure 2.5). Therefore, 80% IPA has been established as the condition of choice when a peptide or protein needs to be desalted and concentrated without using centrifugal filter/membrane units.

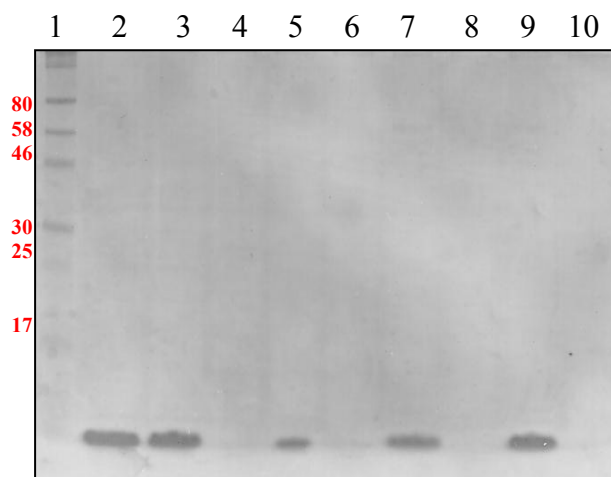


**Figure 2.5** – Precipitation of HB-peptide using varying amounts of isopropyl alcohol at  $-20^{\circ}\text{C}$  to obtain the desalted and concentrated HB-peptide. Lane 1, protein marker; Lane 2, untreated HB-peptide; Lane 3, 80%-pellet; Lane 4, 80%-supernatant; Lane 5, 85%-pellet; Lane 6, 85%-supernatant; Lane 7, 90%-pellet; Lane 8, 90%-supernatant; Lane 9, 95%-pellet; Lane 10, 95%-supernatant.

This method also saves on time and reagents compared to dialysis or concentration. Peptides are also very susceptible to degradation due to their residues being readily accessible to proteases and other enzymes, so stable storage includes lyophilization and not freezing. This method of precipitation allows for the desired storage without using an expensive lyophilizing instrument.

***HB-peptide exhibits good heparin-binding affinity:*** Since the peptide was fashioned after the heparin-binding region of FGF-1 that exhibits good binding affinity for heparin, it is expected that the peptide should also have good binding affinity for heparin. ITC is a beneficial

technique, used for the measurement of the binding affinity for protein-ligand interactions<sup>36,37</sup>.

The binding affinities of the HB-peptide for heparin and HS were measured using ITC. HS was used in this study as well because it is the universal ligand that exists on every cell surface, on which it is the ligand of choice for growth factors and other HBPs<sup>38</sup>. In order to determine if the peptide functions in a similar fashion as the HBR of other HBPs, the cell surface HS was chosen as the ligand for this peptide before heparin was introduced. The isothermograms representing the interaction of HB-peptide with HS and heparin are exothermic and sigmoidal (Figure 2.6). HB-peptide binds to both ligands in a 1:2 stoichiometry. The binding affinities for HS are 0.15 and 3.3  $\mu\text{M}$ , whereas for heparin, the affinities are 176 and 14 nM.

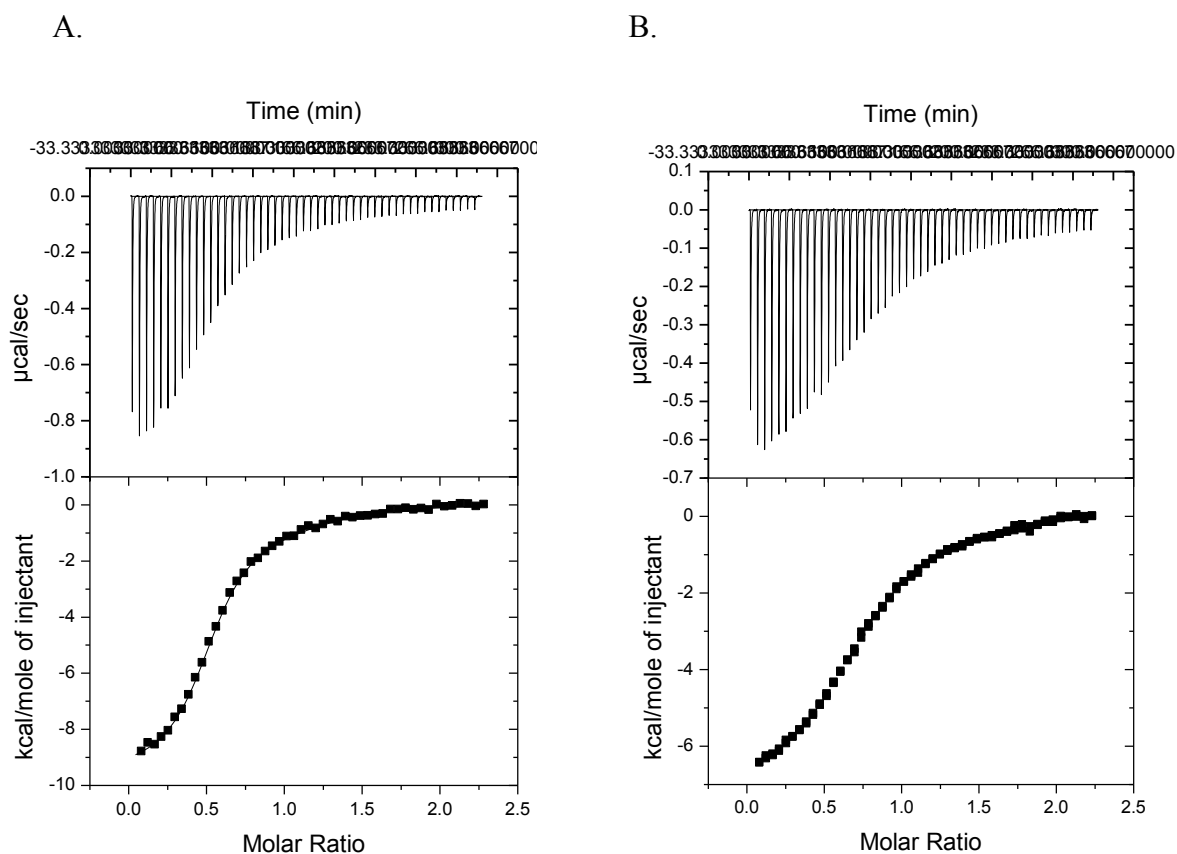


**Figure 2.6** – Isothermograms for the titrations of HB-peptide with heparan sulfate (Panel-A) and heparin (Panel-B). The top panel is the raw data, whereas the bottom panel is the integrated data from the raw data. The peptide binds to both GAGs in a 1:2 binding fashion and has good binding affinity for heparan sulfate ( $K_d \sim 0.15$  and  $3.3 \mu\text{M}$ ) and heparin (176 and 14 nM).

Heparin does show slightly better binding affinity for this peptide, which is promising for the subsequent purification of proteins by the binding of this peptide to heparin-Sepharose. The binding of the peptide to heparin is crucial for other heparin-binding applications. Due to this good binding affinity, the peptide shows promise for use in downstream heparin-related applications. In order for the peptide to have selective affinity for heparin over the other GAGs, future mutations need to be performed on the peptide.

***Secondary structure changes when bound to heparin/SOS:*** FGF-1 and other HBPs undergo a conformational change when binding to heparin occurs. This change is expected for the peptide due to its ability to bind to heparin with good affinity. Far-UV CD is a useful tool for determining the overall secondary structure of proteins and peptides<sup>39</sup>. The spectra of HB-peptide in the presence and absence of heparin and SOS, a functional mimic of heparin used for binding studies, are in Figure 2.7. SOS is used occasionally in the place of heparin because it has been shown to interact with heparin-binding growth factors in a similar fashion as heparin<sup>40</sup>.

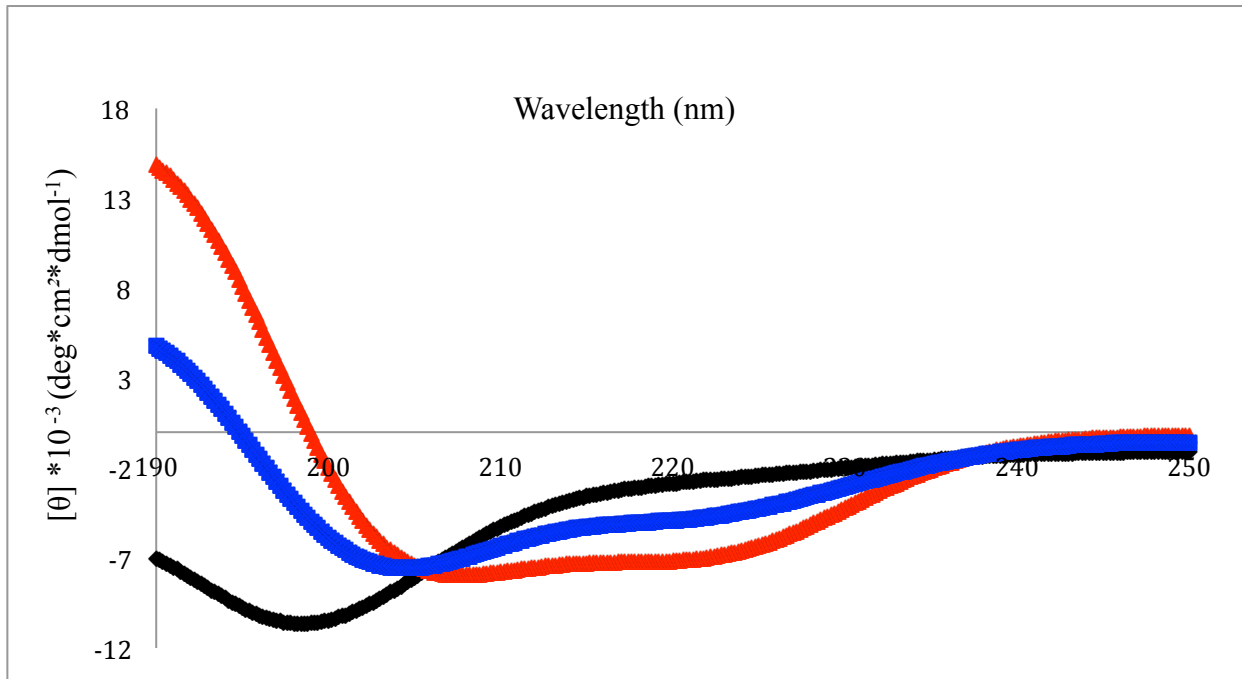


**Figure 2.7** – Overlay of the far-UV circular dichroism spectra of HB-peptide in the absence (black) and presence of heparin (red) and SOS (blue). The peptide adopts an alpha helical nature upon binding to heparin/SOS.

In the absence of heparin/SOS, the peptide adopts a random coil-like structure, which is seen by the negative band around 200 nm, but the corresponding positive band at 212 nm is not present. The peptide could adopt a slight overall structure that is more similar to random coil than the other two secondary structures. Peptides are short chains of amino acid residues, which usually are not long enough to adopt any significant secondary or tertiary structure like larger proteins. This is seen in the spectrum for the peptide not bound to any molecule. In the presence of heparin/SOS, the peptide then becomes more alpha helical in nature with the negative bands at 208 nm and 222 nm, characteristic of an alpha helix. Heparin gives a more pronounced shift in conformation due to its character being more alpha helical than SOS.

***Subtle tertiary structural changes are seen when bound to heparin/SOS:*** Changes in structural changes at the tertiary level can be monitored by intrinsic fluorescence spectroscopy<sup>41</sup>.

Tryptophan residues in proteins are studied because their quantum yields are high, and they give an efficient fluorescence signal. Changes in the emission of tryptophan residues monitor protein folding because their quantum yields are sensitive to their microenvironment<sup>42</sup>. The peptide is in the unfolded state, as seen by the emission maximum at 355 nm. In this instance, the tryptophan is completely solvent exposed. When bound to heparin/SOS, it gains some structure, as seen by the increase in relative fluorescence intensity, but the peptide does not become fully folded (Figure 2.8). If the peptide became fully folded, the tryptophan would now be on the interior of the fold in a hydrophobic environment, which would be accompanied by a blue shift to shorter wavelengths. Since the tryptophan would not be completely buried, a shift of emission maximum would not be expected.

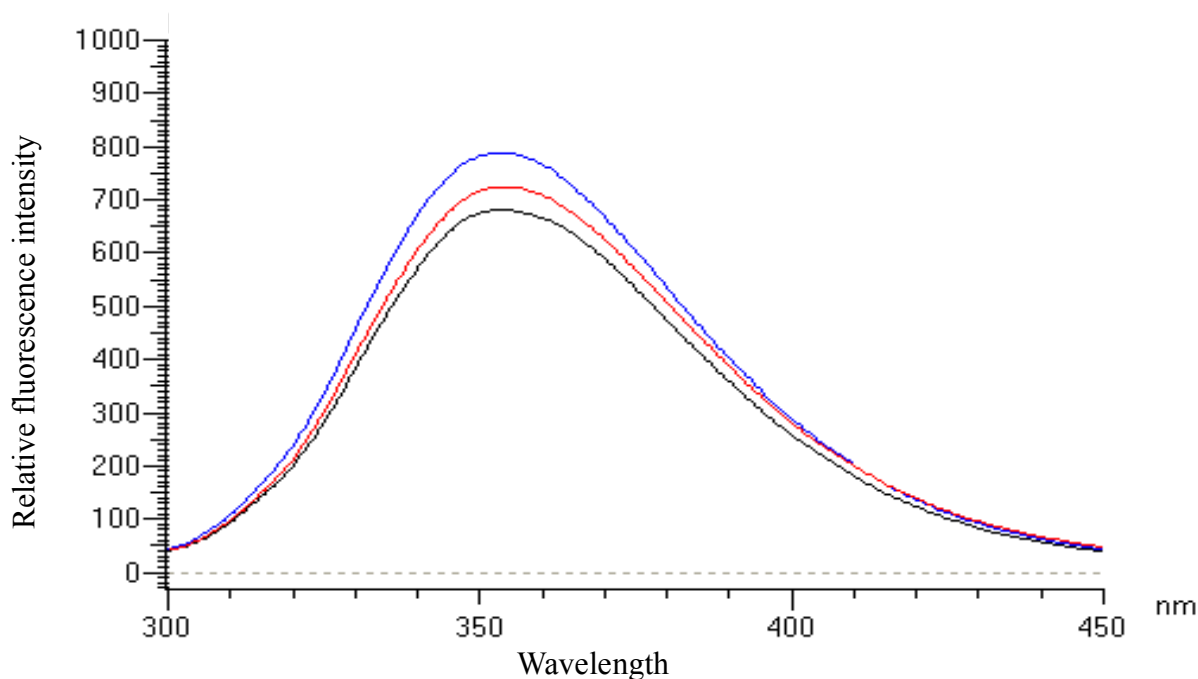


**Figure 2.8** – Intrinsic tryptophan fluorescence spectra of the peptide (black) and upon binding to heparin (red) and SOS (blue). Only a minor conformational change in the tertiary structure is seen by the slight intensity increase.



***Interaction with heparin causes chemical shift perturbation:*** Two-dimensional  $^1\text{H}$ - $^{15}\text{N}$  HSQC spectroscopy provides useful information about the backbone conformation of a protein or peptide. Each crosspeak represents an amino acid residue that is in a specific backbone conformation of the protein<sup>43</sup>. When structural changes occur, the conformation of the backbone is perturbed, leading to shifts in the corresponding crosspeaks or particular amino acids affected by the structural change<sup>44</sup>. The conformational change of the backbone for the peptide was studied upon the binding of heparin by the chemical shifts of the crosspeaks. The peptide is not well structured, as indicated by the clustering of peaks in the spectrum (Figure 2.9). Well-structured proteins have crosspeaks that are spread out in the spectrum normally. Once the peptide is bound to heparin, a significant shift in almost every crosspeak is observed, proving that a structural change has occurred. The binding of heparin probably changes the conformation of the individual amino acids but does not completely fold the peptide, since the intrinsic tryptophan fluorescence does not show a red shift. This hypothesis is also confirmed by the continued clustering of crosspeaks in the  $^1\text{H}$ - $^{15}\text{N}$  HSQC spectrum even upon the binding to heparin.

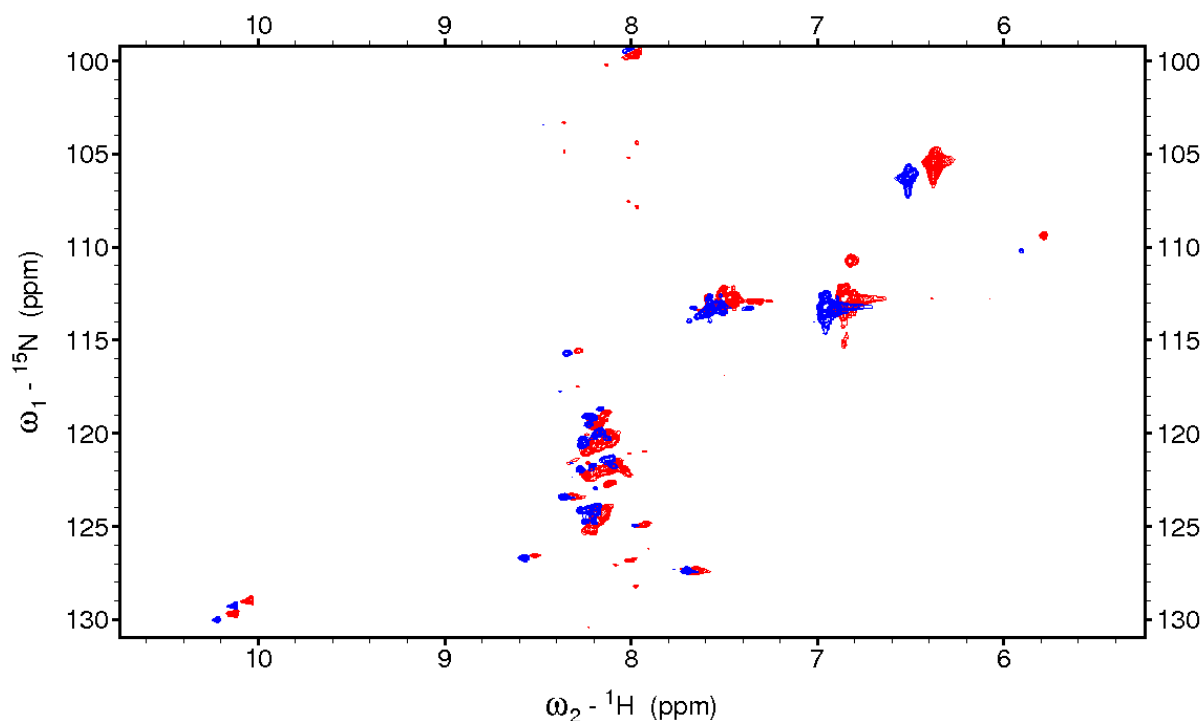


**Figure 2.9** –  $^1\text{H}$ - $^{15}\text{N}$  HSQC spectrum of the peptide bound to heparin (red) overlaid on the peptide (blue). There is a shift in the cross peaks upon binding to heparin, showing a conformational change occurs.

***HB-fusion proteins are expressed and purified in good yields:*** Once HB-C2A is successfully cloned into pET-28a, the fusion protein is successfully expressed in the soluble form at good yield in LB broth. The amino acid sequence of this fusion protein shows the HB-peptide in the N-terminal position, followed by the thrombin cleavage site (LVPRGS), the C2A portion, ending with a C-terminal His-tag (Figure 2.10). The strong band around 20 kDa in the induced lane (lane 3) and supernatant lane (lane 5) after sonication occurs is indicative of a successful expression of this fusion protein (Figure 2.11).

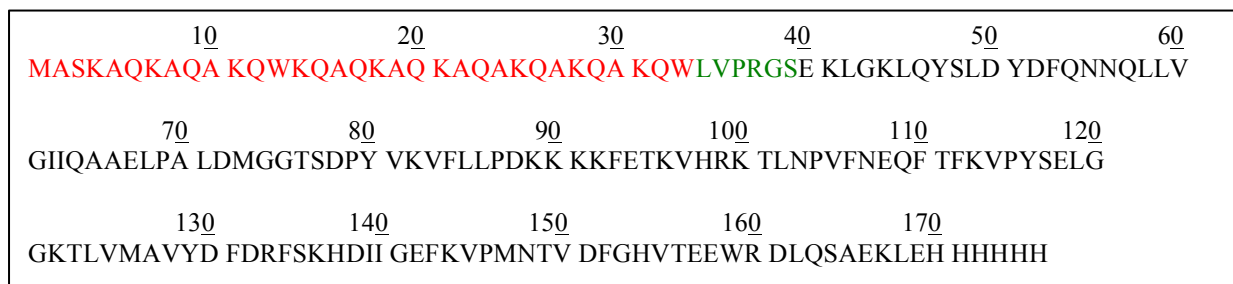


**Figure 2.10** – Amino acid sequence of HB-C2A (175 residues, 20 kDa). HB-peptide portion is in red, and thrombin cleavage site is in green.

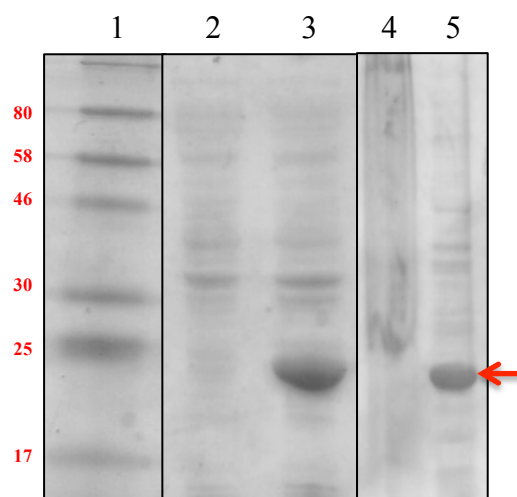


**Figure 2.11** – Overexpression and sonication of HB-C2A. Lane 1, protein marker; Lane 2, uninduced; Lane 3, induced; Lane 4, post-sonication pellet; Lane 5, post-sonication supernatant/cell lysate.

This protein is then purified to homogeneity in Tris buffers within the acceptable pH values using one-step heparin-Sepharose affinity chromatography (Figure 2.12). Tris-HCl buffer has a pKa of 8.1, which means the buffering capacity is from pH 7-9. HB-C2A has a pI of 9.44, which means the pH needs to be 8.4 or 10.4. Since pH 10.4 is outside the range of Tris buffer, the pH of 8 was chosen. The majority of HB-C2A elutes in 500 mM NaCl (lane 7) extremely pure every time, even at both pH conditions. Even though this protein does not bind to heparin as tightly as FGF-1 (this protein elutes at 1.5 M NaCl), at 500 mM NaCl, the majority of contaminants are already removed.

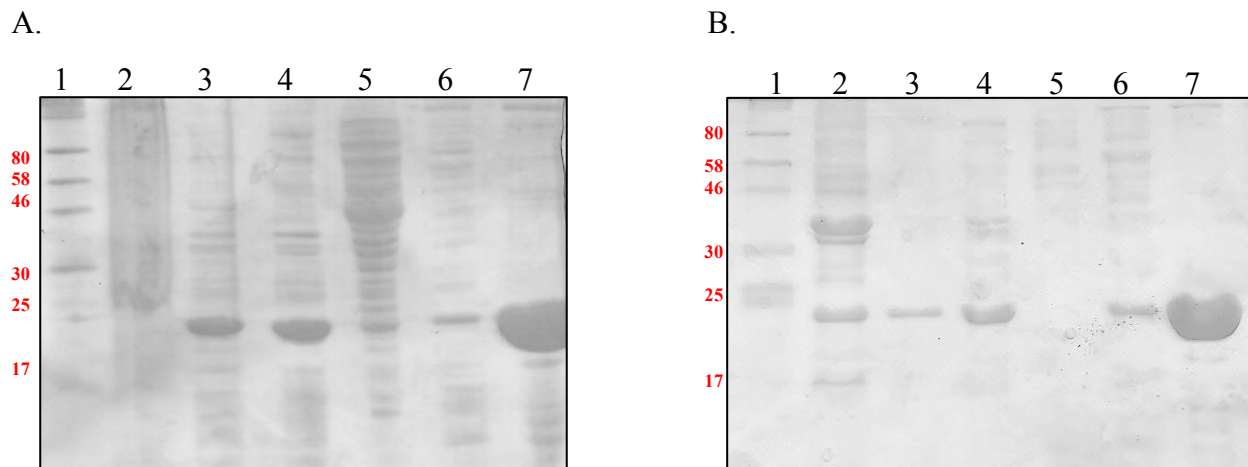


**Figure 2.12** – Purification of HB-C2A in 10 mM Tris, pH 7.2 (Panel-A) and pH 8 (Panel-B) with step-wise NaCl gradient using heparin-Sepharose affinity chromatography. Lane 1, protein marker; Lane 2, post-sonication pellet; Lane 3, clear cell lysate; Lane 4, 0 mM NaCl; Lane 5, 100 mM NaCl; Lane 6, 350 mM NaCl; Lane 7, 500 mM NaCl (eluted HB-C2A).

Oftentimes, GST-tagged proteins have a tendency to aggregate on the glutathione-Sepharose resin, leading to a loss of protein, but this does not occur using the HB-affinity tag. Normally, 20 mg of HB-C2A is obtained from 1 L culture. This high yield leads the target protein, C2A, to be in high yield as well since the small HB-peptide does not add any significant portion to the overall yield. Other buffer conditions are employed in order to determine the efficacy of the HB-tag in various environments (Figure 2.13). Sodium phosphate buffer is also used at pH 6.5-8 because the pKa of this buffer is 6.8, which means its buffering capacity is from pH 5.8 to pH 7.8. Again, HB-C2A is eluted at 500 mM NaCl (lane 7), although some protein is lost in the lower salt concentrations, due to overloading the column. A larger column can be used for more accumulation of fusion protein in the future.

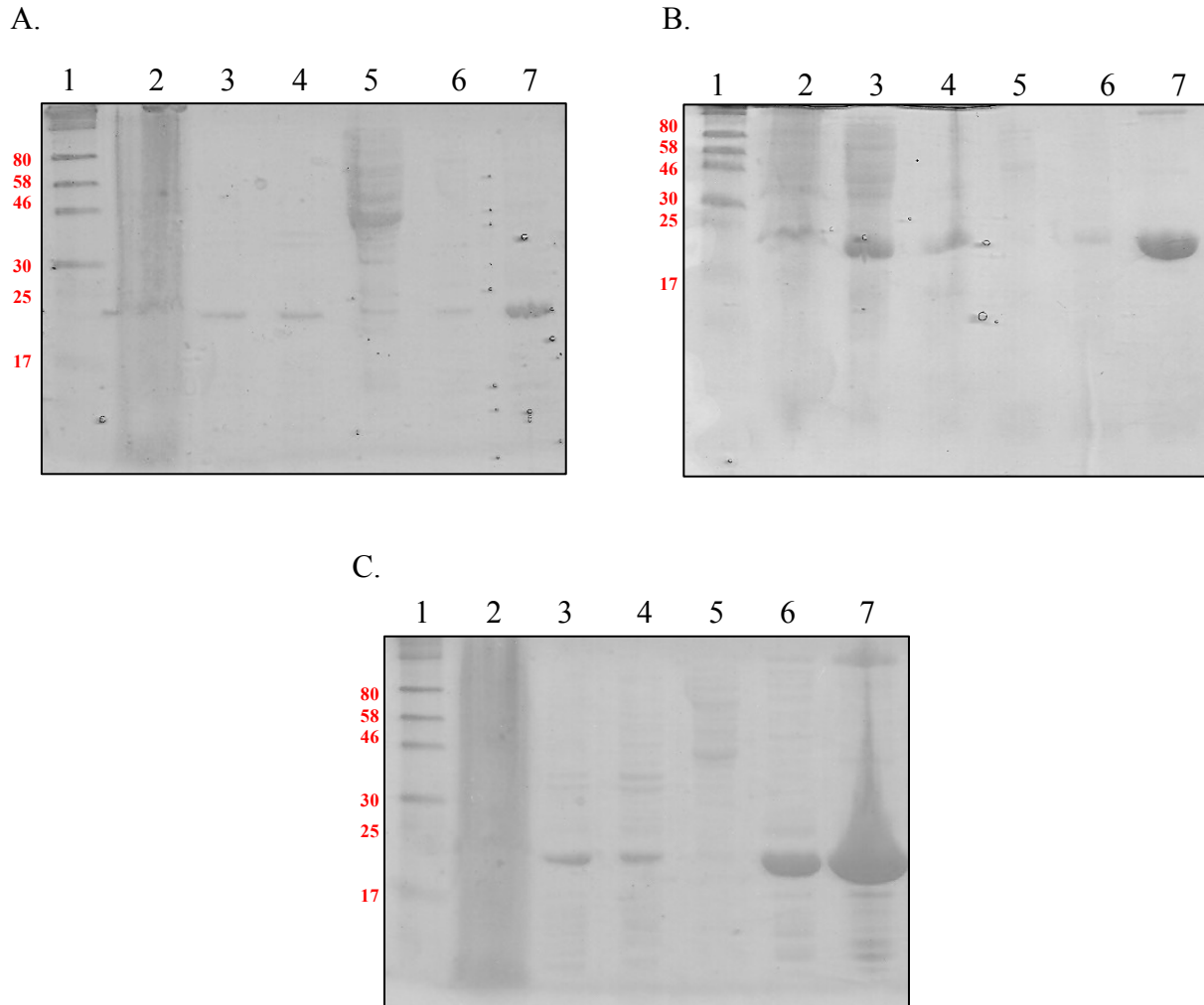


**Figure 2.13** – Purification of HB-C2A in 10 mM sodium phosphate buffer, pH 6.5 (Panel-A), pH 7.2 (Panel-B), and 8 (Panel-C) with step-wise NaCl gradient using heparin-Sepharose affinity chromatography. Lane 1, protein marker; Lane 2, post-sonication pellet; Lane 3, clear cell lysate; Lane 4, 0 mM NaCl; Lane 5, 100 mM NaCl; Lane 6, 350 mM NaCl; Lane 7, 500 mM NaCl (eluted HB-C2A).

Since this peptide has acted as a successful affinity tag, other non-heparin-binding proteins (CALb3 and S100A13) have been selected and ligated successfully into the HB-vector. The inserts are first amplified by PCR, followed by the double digestion of the inserts and HB-vector (Figure 2.14).

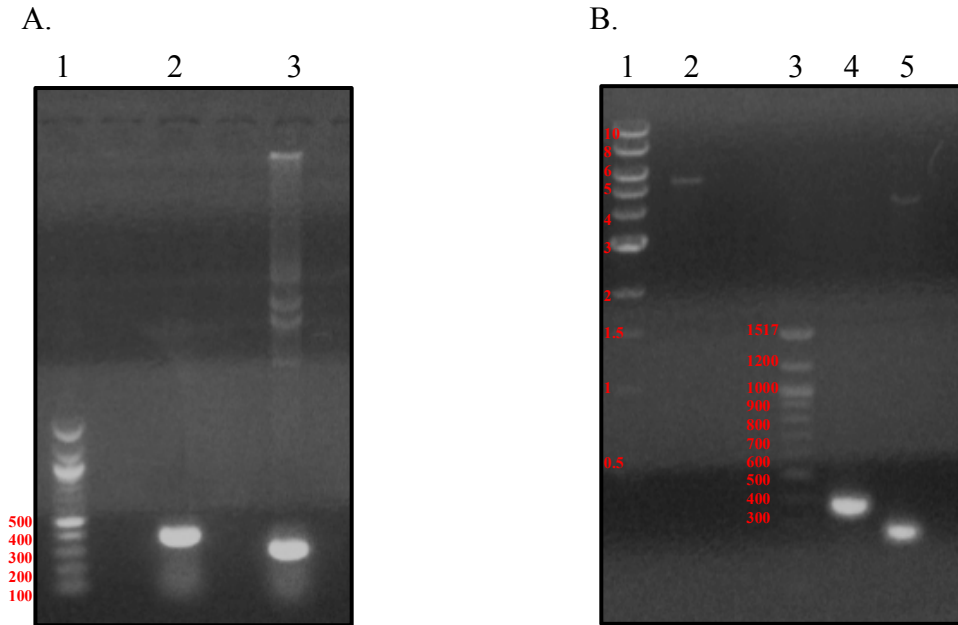


**Figure 2.14** – Amplification of inserts, CALb3 and S100A13 (Panel-A) and double digestion of inserts and HB-vector (Panel-B). Panel-A: Lane 1, DNA marker; Lane 2, CALb3 PCR product (375 bp); Lane 3, S100A13 PCR product (294 bp). Panel-B: Lane 1, DNA marker; Lane 2, digested HB-vector; Lane 3, DNA marker; Lane 4, digested CALb3; Lane 5, digested S100A13.

The digested components are then combined in a ligation reaction that has to be determined if the reaction is successful. Once ligation has occurred, colony PCR of the ligation products are performed in order to determine which colonies are positive ligation products (Figure 2.15).

Since PCR only amplifies the inserts in the vector, a band at approximately 400 Da (CALb3) and 300 Da (S100A13) is seen, proving the insert is present as the plasmid is transformed into DH5 $\alpha$  cells and had antibiotic resistance. Only the vector has antibiotic resistant, so since the insert band is seen from a grown colony (lanes 1, 2, and 4), it can be concluded that the insert is actually ligated into the vector.

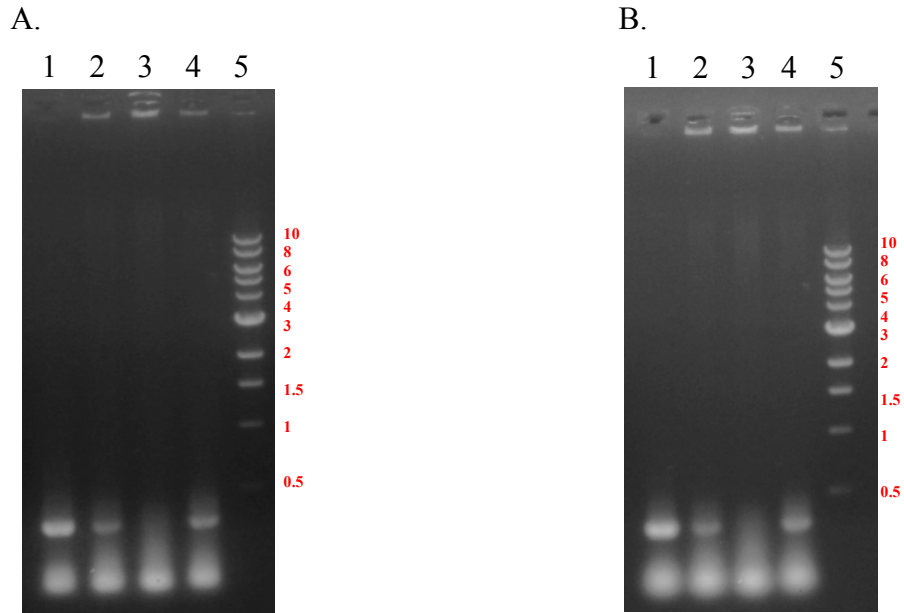


**Figure 2.15** – Colony PCR of HB-S100A13 (Panel-A) and HB-CALb3 (Panel-B) after ligation occurred. Lane 1, colony 1; Lane 2, colony 2; Lane 3, colony 3; Lane 4, colony 4; Lane 5, DNA marker.

In order to be completely assured, double digestion proves the ligation is successful (Figure 2.16).

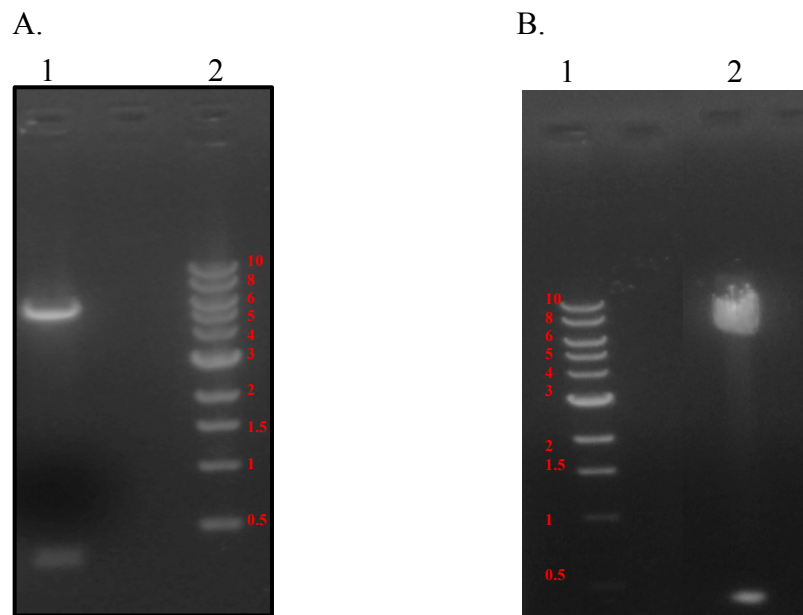


**Figure 2.16** – Double digestion of ligated HB-S100A13 (Panel-A) and HB-CALb3 (Panel-B). Panel-A: Lane 1, digested HB-S100A13; Lane 2, DNA marker. Panel-B: Lane 1, DNA marker; Lane 2, digested HB-CALb3.

The amino acid sequence of HB-S100A13 (Figure 2.17) and HB-CA1b3 (Figure 2.18) has similar order as HB-C2A, except HB-S100A13 has TEV protease cleavage site (ENLYFQG) instead of thrombin cleavage site. They also do not contain a His-tag like HB-C2A.

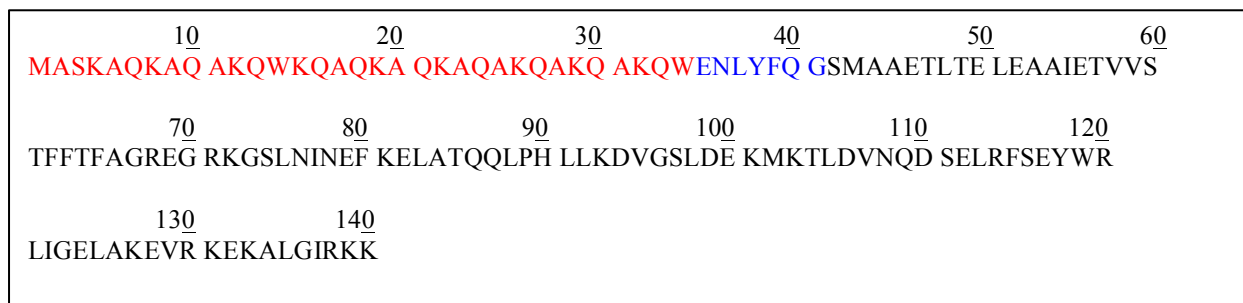


**Figure 2.17** – Amino acid sequence of HB-S100A13 (140 residues, 16 kDa). HB-peptide is in red, and the TEV protease cleavage site is in blue.

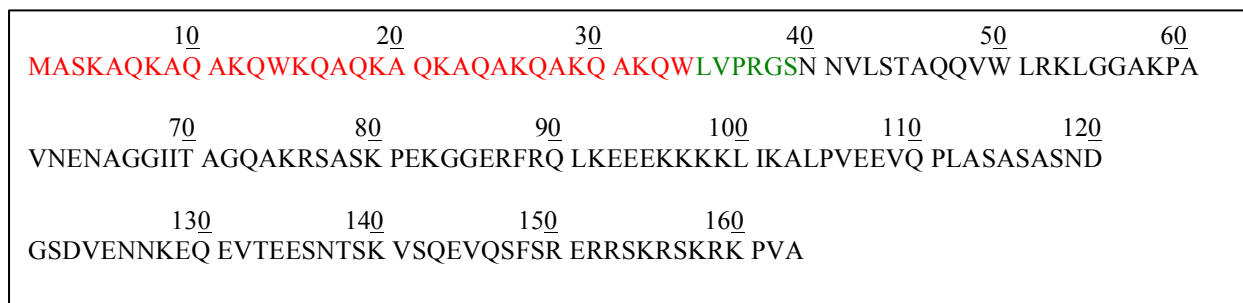


**Figure 2.18** – Amino acid sequence of HB-CA1b3 (163 residues, 18 kDa). HB-peptide is in red, and the thrombin cleavage site is in green.

These clones are successfully expressed in LB broth (Figure 2.19), as seen by the bands of appropriate molecular weight in the induced lane, lane 2 (HB-CA1b3 ~ 18 kDa; HB-S100A13 ~ 16 kDa) indicated by arrows. Interestingly enough, HB-CA1b3 is always seen to migrate lower than its expected molecular weight (right below the 17 kDa band in the protein marker) on 15% SDS-PAGE. HB antibodies bind to this protein in Western blotting, proving this protein band indeed belongs to HB-CA1b3. The lower migration is likely due to the positively charged protein binding more negatively charged SDS molecules, leading to faster migration through the gel.



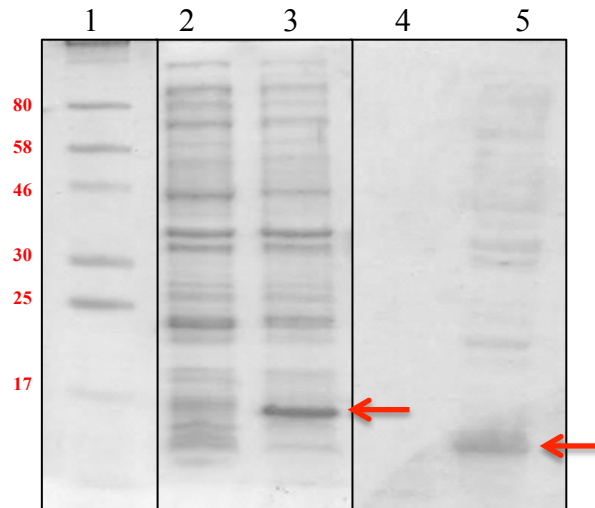


**Figure 2.19** – Expression of HB-CALb3 and HB-S100A13 in LB broth. Lane 1, protein marker; Lane 2, uninduced HB-CALb3; Lane 3, induced HB-CALb3; Lane 4, uninduced HB-S100A13; Lane 5, induced HB-S100A13.

The Kumar lab has been unsuccessful in expressing CALb3 using solely a His or GST tag, so it is rewarding that by the use of the HB-tag, this protein can be expressed. CALb3 being a difficult protein, it is not surprising that the overall yield of HB-CALb3 is much lower than C2A and S100A13.

***Other HB-fusion proteins can be purified to homogeneity using heparin-Sepharose affinity***

***chromatography:*** Since HB-peptide is an effective affinity tag for C2A, its reputation continues by aiding in the purification of CALb3 and S100A13, two more non-heparin-binding proteins.

The fusion proteins elute at 1 M NaCl, as indicated in lane 8 by the arrows, as compared to 500 mM NaCl for HB-C2A (Figure 2.20). HB-CALb3 and HB-S100A13 have pI values of 10.3 and 9.6-9.7, respectively, compared to that of HB-C2A of 9.4. These greater pI values could contribute to the greater binding affinity for heparin-Sepharose because the positively charged residues could be in a better orientation for interaction with the negatively charged heparin molecule. The linear amino acid sequence does not play as much of a role in binding capability

as does the overall fold of the protein, as seen by the consensus sequences in heparin-binding proteins. Target proteins are also known at times to contribute to the binding capability of the affinity tag<sup>45,46</sup>.

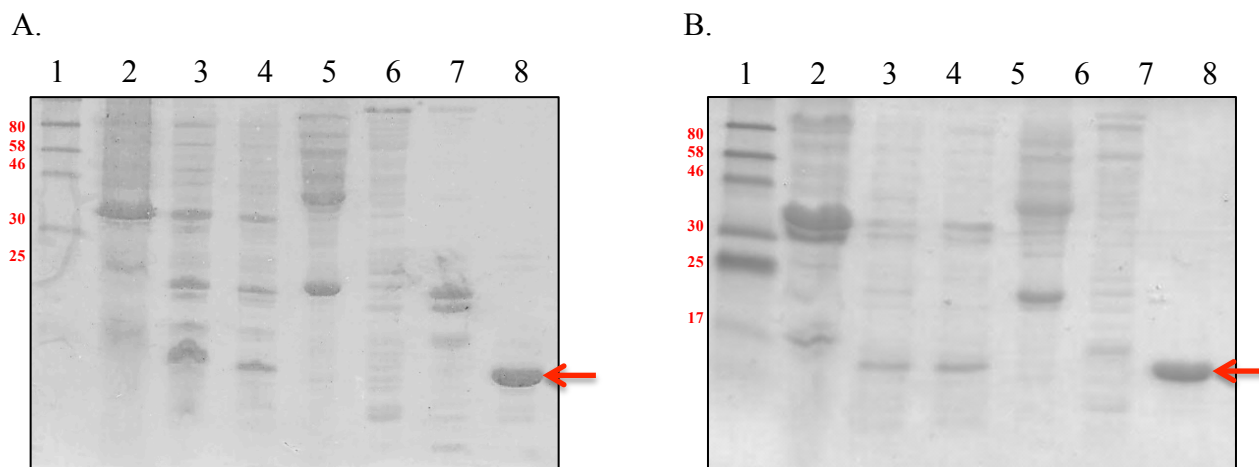


**Figure 2.20** – Purification of HB-CALb3 (Panel-A) and HB-S100A13 (Panel-B) by heparin-Sepharose affinity chromatography. Lane 1, protein marker; Lane 2, post-sonication pellet; Lane 3, clear cell lysate; Lane 4, 0 mM NaCl; Lane 5, 100 mM NaCl; Lane 6, 350 mM NaCl; Lane 7, 500 mM NaCl; Lane 8, 1 M NaCl.

At times, HB-CALb3 does elute around 1 M to 2 M NaCl, but still in a pure state. The majority of the fusion protein elutes at 1 M NaCl but there is residual protein at 2 M NaCl. Both fractions are normally combined for further experiments if enough protein is observed in the 2 M NaCl fraction. The yield of HB-CALb3 is approximately 2 mg protein/L culture, whereas HB-S100A13 is 3-4 mg protein/L culture. CALb3 has also not been purified to homogeneity successfully in the past attempts in the Kumar lab, so being able to purify this protein by means of HB-affinity tag is quite gratifying. In the future, it would be interesting to investigate the efficacy of HB-affinity tag with other proteins that do not possess as high of a pI value as these proteins to determine their effect on binding capability to heparin-Sepharose.

***HB-fusion proteins can be purified in a mild denatured state:*** On occasion, it is reported that certain proteins are expressed in insoluble form, which are known as inclusion bodies<sup>47,48,49</sup>. Denaturants are needed to isolate proteins from inclusion bodies in order to perform their purification effectively. Urea, unlike guanidine hydrochloride, is a non-ionic denaturant commonly used in purification<sup>50,51,52</sup>. HB-C2A and HB-S100A13 are successfully purified in 8 M urea (Figure 2.21).

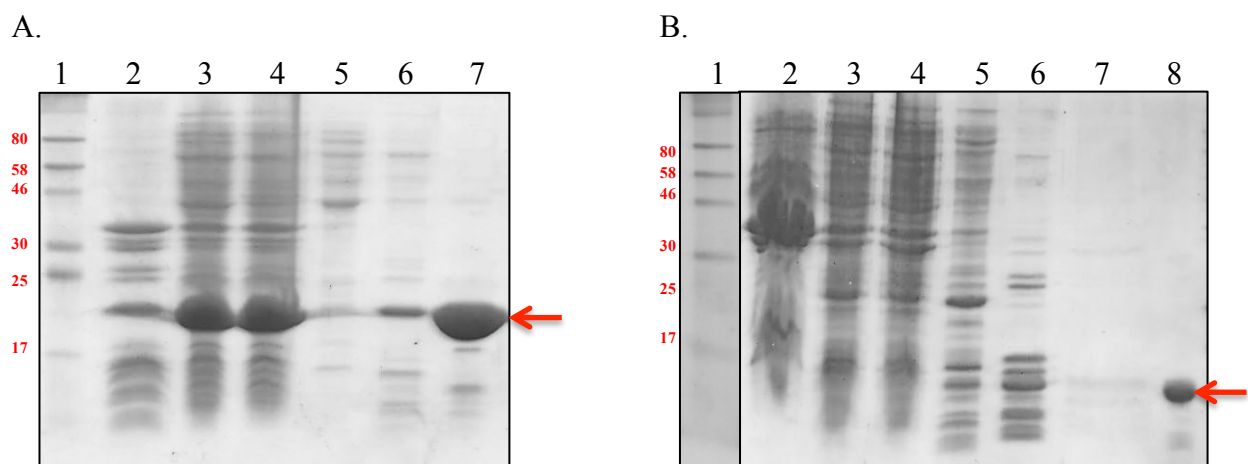


**Figure 2.21** – Purification of HB-C2A (Panel-A) and HB-S100A13 (Panel-B) in 8 M urea. Panel-A: Lane 1, protein marker; Lane 2, post-sonication pellet; Lane 3, clear cell lysate; Lane 4, 0 mM NaCl; Lane 5, 100 mM NaCl; Lane 6, 350 mM NaCl; Lane 7, 500 mM NaCl (eluted HB-C2A). Panel-B: Lane 1, protein marker; Lane 2, post-sonication pellet; Lane 3, clear cell lysate; Lane 4, 0 mM NaCl; Lane 5, 100 mM NaCl; Lane 6, 350 mM NaCl; Lane 7, 500 mM NaCl; Lane 8, 1 M NaCl (eluted HB-S100A13).

There is some HB-C2A that is present in the flow-through (lane 4), probably resulting from an overloaded resin. This is likely because the majority, if not all, of HB-S100A13 is present in 1 M NaCl, not the flow-through, and this fusion protein gives less yield than HB-C2A. The HB-affinity tag cannot, however, be used in 6 M guanidine hydrochloride (Figure 2.22). All of the HB-C2A is eluted in 0 mM NaCl (lane 3), as seen by the band at the same molecular weight as the positive control (HB-C2A, 20 kDa) with arrow. This is expected because guanidine hydrochloride is an ionic denaturant that breaks all electrostatic interactions present. HB-peptide

and heparin bind to each other based mainly on electrostatic interactions, which are completely interrupted by this denaturant.

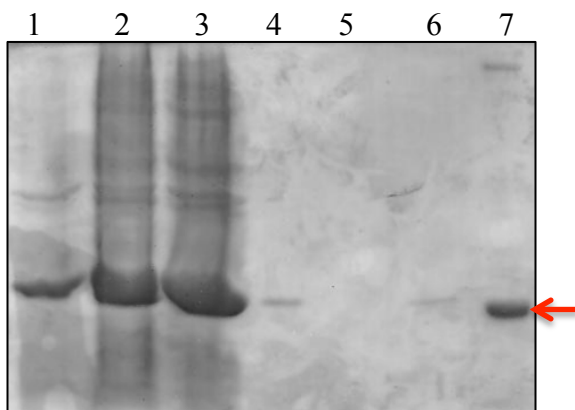


**Figure 2.22** – Purification of HB-C2A in 6 M guanidine hydrochloride using heparin-Sepharose affinity chromatography. Lane 1, post-sonication pellet; Lane 2, clear cell lysate; Lane 3, 0 mM NaCl (eluted HB-C2A); Lane 4, 100 mM NaCl; Lane 5, 350 mM NaCl; Lane 6, 500 mM NaCl; Lane 7, HB-C2A (positive control).

If HB-fusion proteins need to be purified using a denaturant, a non-ionic one is preferred for efficient purification by heparin-Sepharose. Proteins that generally express as inclusion bodies can be attached to the HB-affinity tag, solubilized in urea, and purified by heparin-Sepharose affinity chromatography in the future.

***Target protein can be obtained from HB-fusion proteins through proteolytic cleavage:***

Enzymatic cleavage is a useful tool to remove target proteins from their corresponding affinity tags. In this case, thrombin and TEV protease sites were added to the HB-fusion clones, in order to later detach C2A, CA1b3, and S100A13 from the HB-affinity tag. The cleavage reaction is optimized, and the corresponding target protein can be removed from the peptide via another round of heparin-Sepharose affinity chromatography. Once cleaved, the target protein contains the last two residues of the thrombin or TEV protease cleavage site, which should not interfere with the activity or structure of the target protein. The best cleavage conditions for HB-C2A

include 1 unit thrombin per 25  $\mu\text{g}$  protein overnight at 37°C. The cleavage reaction is complete after 20 hours, but the reaction was let go 24 hours for feasible wait times in the lab (Figure 2.23). Even at longer times such as 24 hours, no additional cleavage products/degradation of C2A is observed (only two product bands are seen in lane 3). The HB-peptide (~ 4 kDa) is indicated by the red arrow. If less thrombin is preferred, the incubation time needs to be increased to approximately 48 hours.

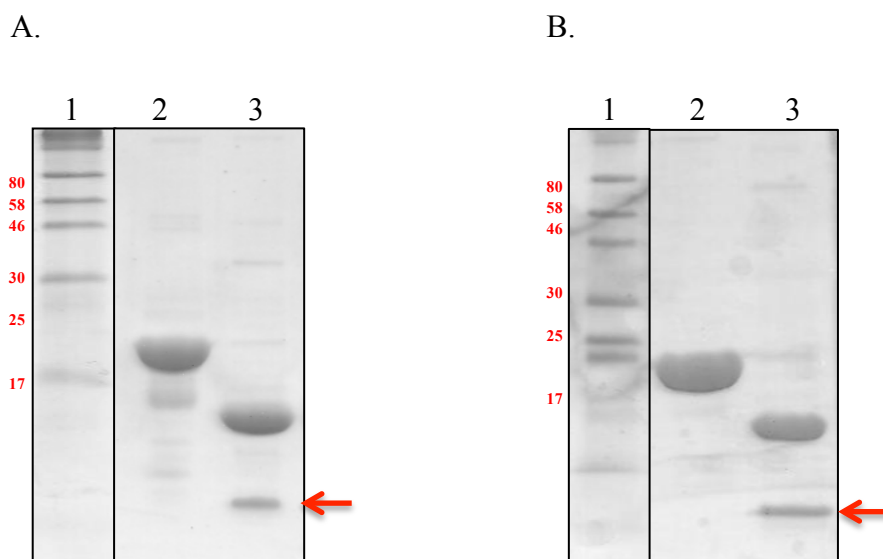


**Figure 2.23** – Thrombin cleavage of HB-C2A using 25  $\mu\text{g}$  (Panel-A) and 50  $\mu\text{g}$  (Panel-B) of fusion protein. Lane 1, protein marker; Lane 2, HB-C2A; Lane 3, thrombin-cleaved HB-C2A.

The cleavage reaction of HB-C2A, like the purification, has also been optimized for other buffer conditions (Figure 2.24). Sometimes, HB-peptide is not in high yield so a strong band is not observed on the gel, but its position is indicated by the red arrow. In order to stabilize thrombin, calcium ions are normally used during thrombin cleavage reactions. It has been shown in the Kumar lab that 2.5 mM calcium chloride is a good condition for efficient thrombin cleavage to occur. Interestingly enough, for HB-C2A, calcium chloride is not required for suitable cleavage to happen. As seen in lanes 2 and 3, both with and without the calcium ions work for good cleavage of HB-C2A. The downside of using phosphate buffer is that calcium chloride cannot

be used in this buffer because the negatively charged phosphate groups do a double displacement reaction with chloride ions to produce calcium phosphate, instead of free calcium ions. Calcium phosphate, the product of calcium chloride in phosphate buffer, precipitates out of solution as well, which is extremely undesirable. Only Tris buffer should be used in this instance.

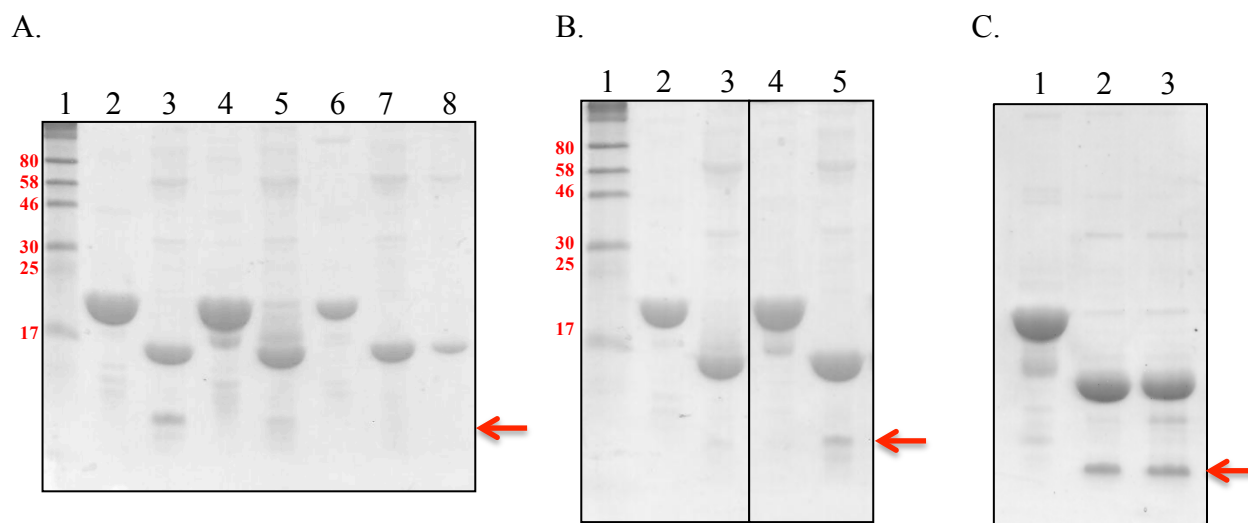


**Figure 2.24** – Thrombin cleavage of HB-C2A in 10 mM phosphate buffer (Panel-A) and 10 mM Tris-HCl (Panel-B) with and without CaCl<sub>2</sub> (Panel-C) for 24 hr. Panel-A: Lane 1, protein marker; Lane 2, HB-C2A (20 kDa); Lane 3, cleaved at pH 6.5; Lane 4, HB-C2A; Lane 5, cleaved at pH 7.2; Lane 6, HB-C2A; Lane 7, cleaved at pH 8; Lane 8, C2A (16 kDa). Panel-B: Lane 1, protein marker; Lane 2, HB-C2A; Lane 3, cleaved at pH 7.2; Lane 4, HB-C2A; Lane 5, cleaved at pH 8. Panel-C: Lane 1, HB-C2A; Lane 2, cleaved without CaCl<sub>2</sub>; Lane 3, cleaved with CaCl<sub>2</sub>.

HB-CAIb3 is also cleaved with thrombin, but the greater number of positively charged residues makes the cleavage reaction not as efficient using similar conditions as HB-C2A (Figure 2.25).

A ratio of 1 unit thrombin per 25 µg HB-CAIb3 is used for 48 hours, and calcium chloride is essential, unlike HB-C2A, for this cleavage reaction to successfully transpire. Since calcium chloride is required for this cleavage reaction, phosphate buffer cannot be used in this instance.

HB-peptide is not in high yield so only a faint band is observed on the gel, as indicated by the red arrow.

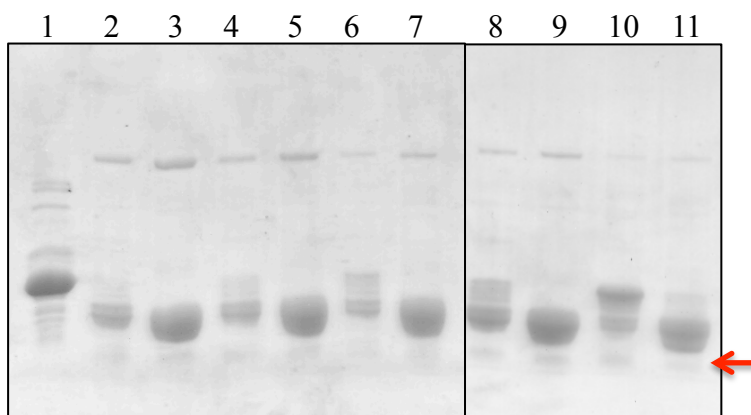


**Figure 2.25** – Optimization of thrombin cleavage of HB-CAlb3. Lane 1, HB-CAlb3; Lane 2, 1/5-24 hours; Lane 3, 1/5-48 hours; Lane 4, 1/10-24 hours; Lane 5, 1/10-48 hours; Lane 6, 1/20-24 hours; Lane 7, 1/20-48 hours; Lane 8, 1/25-24 hours; Lane 9, 1/25-48 hours; Lane 10, 1/50-24 hours; Lane 11, 1/50-48 hours.

TEV protease is a more stringent protease than thrombin and the others, which means it is more specific to its cleavage site, resulting in less nonspecific cleavage products sometimes seen from thrombin or chymotrypsin<sup>53,54,55</sup>. For this reason, a TEV protease cleavage site is added to HB-S100A13, but also to determine the efficacy of HB-affinity tag when other proteases are used. The cleavage reaction has been optimized for HB-S100A13 using the protocol given by the ProTEV Plus provider (Promega Corp.). The Kumar lab has been successful in purifying recombinant TEV protease, so its activity is compared to that of ProTEV Plus in a small-scale reaction in the presence and absence of dithiothreitol (DTT) (Figure 2.26). DTT is used as a reducing agent to protect the cysteine residues in TEV protease from being oxidized, thus reducing the enzyme activity. However, ProTEV Plus works to cleave HB-S100A13 even in absence of DTT, whereas the recombinant TEV protease does not start partially cleaving until 6 hours of incubation with a 1  $\mu$ L TEV/10  $\mu$ g protein ratio only in the presence of DTT (lane 9). The very lowest band is HB-peptide, as indicated by the red arrow.

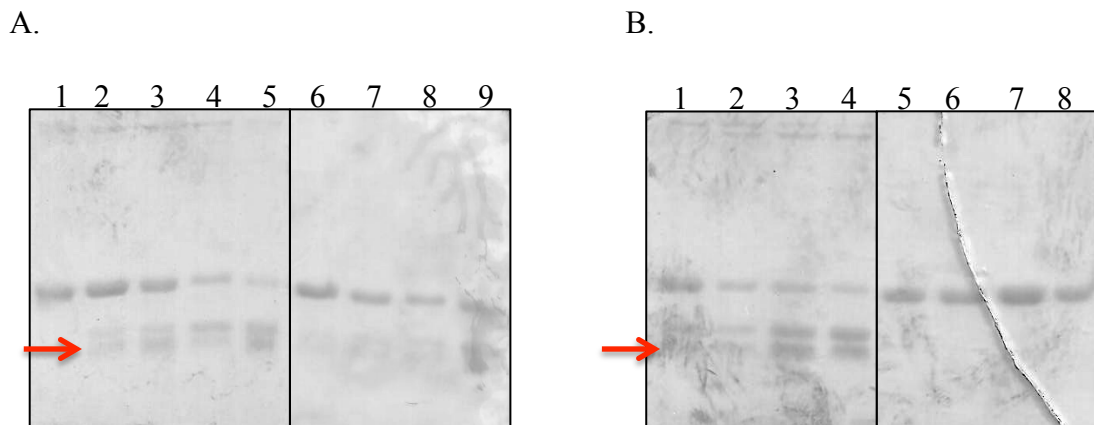


**Figure 2.26** – Small-scale cleavage of HB-S100A13 by ProTEV Plus (PT) and recombinant TEV protease (RT) in the presence (Panel-A) and absence (Panel-B) of 1 mM DTT. Panel-A: Lane 1, 0 hour; Lane 2, PT-1 hour; Lane 3, PT-2 hours; Lane 4, PT-4 hours; Lane 5, PT-6 hours; Lane 6, RT-1 hour; Lane 7, RT-2 hours; Lane 8, RT-4 hours; Lane 9, RT-6 hours. Panel-B: Lane 1, PT-1 hour; Lane 2, PT-2 hours; Lane 3, PT-4 hours; Lane 4, PT-6 hours; Lane 5, RT-1 hours; Lane 6, RT-2 hours; Lane 7, RT-4 hours; Lane 8, RT-6 hours.

The large-scale reaction of cleavage of HB-S10013 is successful using ProTEV Plus in a greater ratio than the manufacturer suggests (1 unit ProTEV Plus/100  $\mu$ g protein), allowing less enzyme to be wasted on one reaction (Figure 2.27). Longer incubation time is required for this new ratio, but it is the same time as HB-C2A. HB-peptide is indicated with the red arrow. The upper-most band in lane is ProTEV Plus (48 kDa molecular weight on SDS-PAGE, information from Promega Corp.).

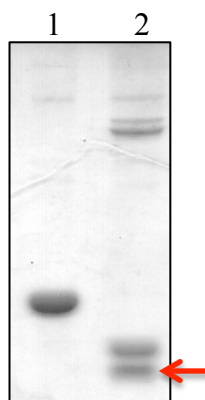


**Figure 2.27** – Large-scale cleavage of HB-S100A13 by ProTEV Plus at 30°C. Lane 1, HB-S100A13; Lane 2, 20-hour cleaved HB-S100A13.



A more in-depth examination of the recombinant TEV protease reveals that cleavage is successful after 9 hours when a 1  $\mu$ L TEV/2  $\mu$ g protein ratio is applied (Figure 2.28). The red arrow again indicates HB-peptide. This ratio is not cost-effective so longer incubation time could allow for lower amount of TEV protease to be used.

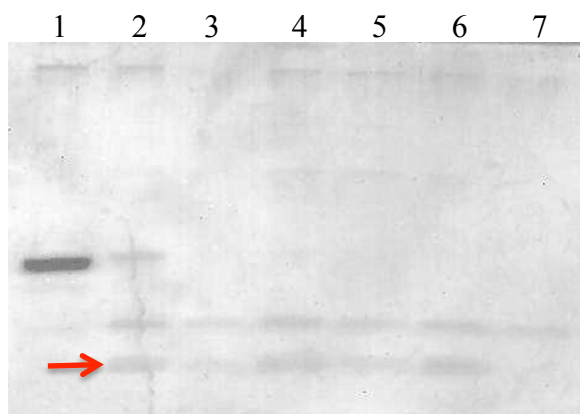


**Figure 2.28** – Optimization of cleavage of HB-S100A13 by recombinant TEV protease at 30°C. Lane 1, HB-S100A13; Lane 2, 6 hours; Lane 3, 9 hours; Lane 4, 15 hours; Lane 5, 18 hours; Lane 6, 21 hours; Lane 7, 24 hours.

Expressing and purifying the recombinant TEV protease seems more cost-effective due to its endless supply and lack of dependence on supplier. The purified TEV protease produced in the Kumar lab is currently being used as the protease of choice by designing clones with a TEV protease cleavage site instead of thrombin.

***Target protein can be removed from HB-affinity tag by heparin-Sepharose:*** The target protein, once cleaved from HB-peptide, is not a heparin-binding protein, so it does not bind with as high affinity to heparin-Sepharose as HB-peptide. Thrombin, however, is an HBP, which means it should bind tightly to heparin-Sepharose, only eluting with very high concentrations of NaCl. The target protein would have already eluted before this stage. The target protein is seen eluted at low NaCl concentration (100 mM NaCl), completely separated from the peptide and thrombin

(Figure 2.29). The HB-peptide is indicated by the red arrow. The upper-most band in lanes 1 and 2 are more than likely an oligomer of C2A and not thrombin because thrombin is 37 kDa, and this band is a little lower than the 30-kDa band in the protein marker. Since thrombin is supposed to elute at greater NaCl concentration than HB-peptide, it is highly unlikely it would elute at such an early stage as 100 mM NaCl.

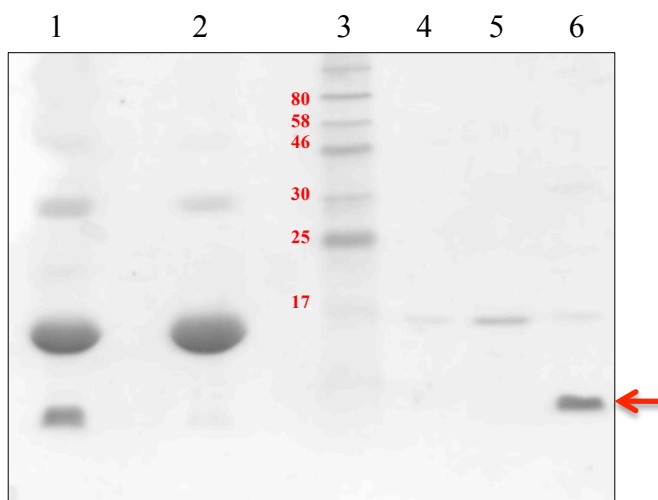


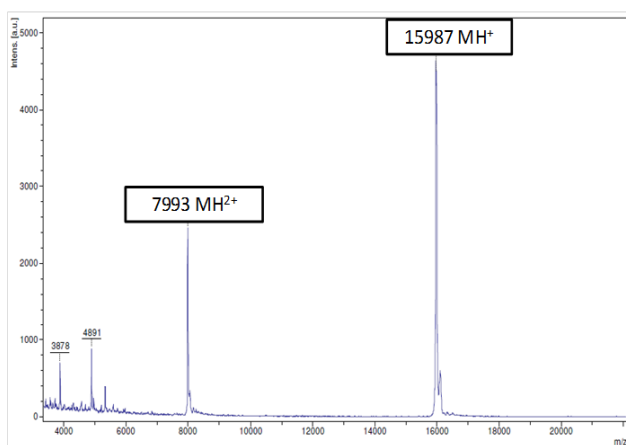
**Figure 2.29** – Separation of C2A from HB-peptide by heparin-Sepharose affinity chromatography. Lane 1, cleaved HB-C2A; Lane 2, 100 mM NaCl; Lane 3, protein marker; Lane 4, 250 mM NaCl; Lane 5, 350 mM NaCl; Lane 6, 500 mM NaCl.

TEV protease on the other hand, does not bind to heparin, so this enzyme can be removed by metal affinity chromatography, which can then be followed by passing the cleaved sample (HB and S100A13) onto heparin-Sepharose. The target protein would then elute at low NaCl (0 mM and 100 mM) concentration, whereas HB-peptide would elute at 500 mM NaCl.

Matrix-assisted laser desorption/ionization time-of-flight mass spectrometry (MALDI-TOF) provides useful information on molecular weights of proteins and peptides. After separation on heparin-Sepharose, C2A and HB-peptide individually show purity at the relatively accurate molecular weights (Figure 2.30). The molecular weights of HB-peptide and C2A are

approximately 4 kDa and 16 kDa, respectively. The peak given around 8 kDa is the  $[M-H]^{2+}$ , basically  $m/z$  where  $z=2$ . The separation of HB-peptide from C2A results in C2A in the absence of any residual HB-peptide.

A.



B.

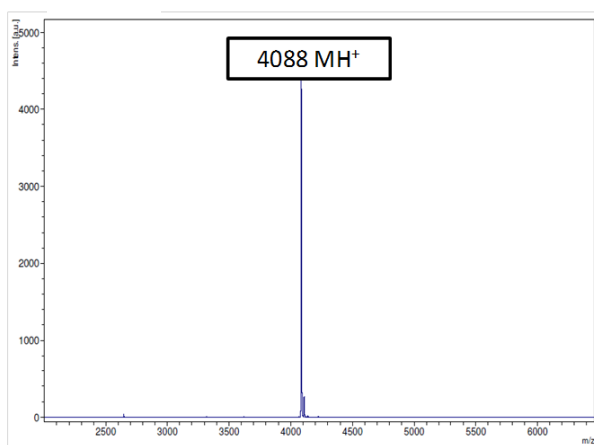


**Figure 2.30** – Mass spectra of C2A (Panel-A) and HB-peptide (Panel-B) after thrombin cleavage and separation by heparin-Sepharose affinity chromatography.

***Target protein, once cleaved from HB-affinity tag, retains its overall backbone conformation:***

Two-dimensional  $^1\text{H}$ - $^{15}\text{N}$  heteronuclear single quantum coherence spectroscopy (HSQC) is a useful tool for the backbone conformation of proteins<sup>56,57</sup>. Each peak corresponds to a particular amino acid residue in the protein sequence. Previously, the spectrum of C2A, after cleavage from its GST affinity tag, was obtained, and each peak was assigned, giving a “standard” for comparison of this C2A to the one from HB-affinity tag<sup>58,59</sup>. A well-folded native protein has a well-dispersed spectrum, which is what is seen on the spectrum of C2A after cleavage from HB-peptide (Figure 2.31). The overall spatial pattern of the peaks on this spectrum is in agreement with the published spectrum from Rajalingam et al<sup>59</sup> (Figure 2.32). The small size of the HB-

affinity tag was promising for no interference with the target protein's native structure, as seen with some other affinity tags.

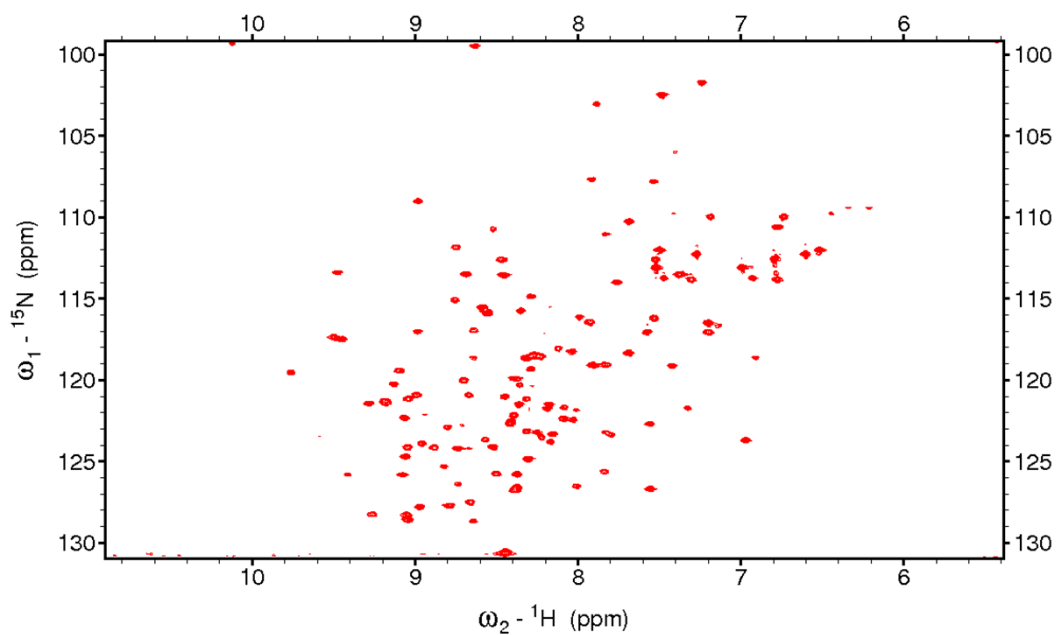


**Figure 2.31** –  ${}^1\text{H}$ - ${}^{15}\text{N}$  HSQC spectrum of C2A after thrombin cleavage and separation from the HB-peptide.

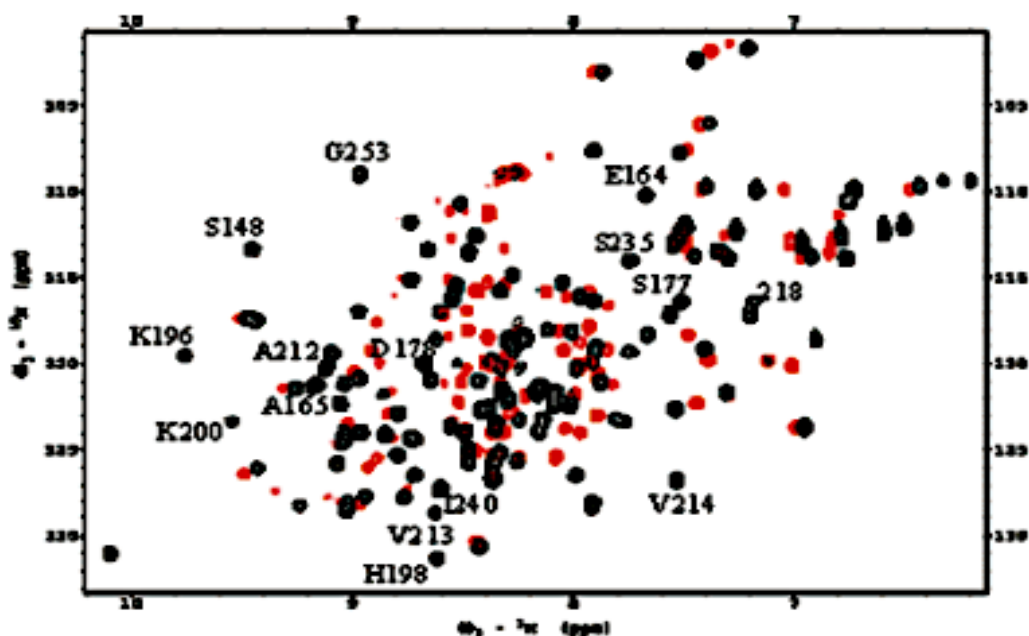


**Figure 2.32** –  $^1\text{H}$ - $^{15}\text{N}$  HSQC spectrum of C2A after cleavage from GST, reproduced from Rajalingam et al, with permission from *Biochemistry*<sup>59</sup>. Red peaks correspond to C2A in pH 3.4, whereas black peaks are in pH 6.

The black peaks are for C2A that is in its native conformation at a more neutral pH, which is similar to the conditions used for C2A from HB-peptide (pH 7.2). As the pH drops to 3.4, there is some perturbation seen in the peaks, leading to partially unfolded state.

This HB-peptide is successfully used as an affinity tag for recombinant proteins using heparin-Sepharose. In the future, proteins of biological importance can be used in conjunction with HB-affinity in the future to determine if their cleavage from HB-peptide interferes with their biological activity. It is not expected that this peptide would interfere at all with protein function, structure, or folding capability. Work involving the HB-peptide has been published as a patent and manuscript<sup>60,61</sup>.

## 2.5. References

1. Arnau, J.; Lauritzen, C.; Petersen, G. E.; Pedersen, J., Current strategies for the use of affinity tags and tag removal for the purification of recombinant proteins. *Protein Expression Purif.* **2006**, *48* (1), 1-13.
2. Ferrer-Miralles, N.; Corchero, J. L.; Kumar, P.; Cedano, J. A.; Gupta, K. C.; Villaverde, A.; Vazquez, E., Biological activities of histidine-rich peptides; merging biotechnology and nanomedicine. *Microb. Cell Fact.* **2011**, *10*, 101.
3. Bornhorst, J. A.; Falke, J. J., Purification of proteins using polyhistidine affinity tags. *Methods Enzymol.* **2000**, *326* (Applications of Chimeric Genes and Hybrid Proteins, Pt. A), 245-254.
4. Einhauer, A.; Jungbauer, A., The FLAG peptide, a versatile fusion tag for the purification of recombinant proteins. *J. Biochem. Biophys. Methods* **2001**, *49* (1-3), 455-465.
5. Vaillancourt, P.; Zheng, C.-F.; Hoang, D. Q.; Breister, L., Affinity purification of recombinant proteins fused to calmodulin or to calmodulin-binding peptides. *Methods Enzymol.* **2000**, *326* (Applications of Chimeric Genes and Hybrid Proteins, Pt. A), 340-362.
6. Lichty, J. J.; Malecki, J. L.; Agnew, H. D.; Michelson-Horowitz, D. J.; Tan, S., Comparison of affinity tags for protein purification. *Protein Expression Purif.* **2005**, *41* (1), 98-105.
7. Kaur, J.; Reinhardt, D. P., Immobilized metal affinity chromatography co-purifies TGF- $\beta$ 1 with histidine-tagged recombinant extracellular proteins. *PLoS One* **2012**, *7* (10), e48629.
8. Bradshaw, R. A.; Brickey, W. W.; Walker, K. W., N-terminal processing: the methionine aminopeptidase and N $\alpha$ -acetyl transferase families. *Trends Biochem. Sci.* **1998**, *23* (7), 263-267.
9. Hearn, M. T. W.; Acosta, D., Applications of novel affinity cassette methods: use of peptide fusion handles for the purification of recombinant proteins. *J. Mol. Recognit.* **2001**, *14* (6), 323-369.
10. Park, N.; Ryu, J.; Jang, S.; Lee, H. S., Metal ion affinity purification of proteins by genetically incorporating metal-chelating amino acids. *Tetrahedron* **2012**, *68* (24), 4649-4654.
11. Terpe, K., Overview of tag protein fusions: from molecular and biochemical fundamentals to commercial systems. *Appl. Microbiol. Biotechnol.* **2003**, *60* (5), 523-533.
12. Fong, B. A.; Wu, W.-Y.; Wood, D. W., The potential role of self-cleaving purification tags in commercial-scale processes. *Trends Biotechnol.* **2010**, *28* (5), 272-279.
13. Kaplan, W.; Husler, P.; Klump, H.; Erhardt, J.; Sluis-Cremer, N.; Dirr, H., Conformational stability of pGEX-expressed *Schistosoma japonicum* glutathione S-transferase: A detoxification enzyme and fusion-protein affinity tag. *Protein Sci.* **1997**, *6* (2), 399-406.

14. Tagwerker, C.; Flick, K.; Cui, M.; Guerrero, C.; Dou, Y.; Auer, B.; Baldi, P.; Huang, L.; Kaiser, P., A tandem affinity tag for two-step purification under fully denaturing conditions: application in ubiquitin profiling and protein complex identification combined with in vivo cross-linking. *Mol. Cell. Proteomics* **2006**, *5* (4), 737-748.
15. Banki, M. R.; Wood, D. W., Inteins and affinity resin substitutes for protein purification and scale up. *Microb. Cell Fact.* **2005**, *4*, No pp given.
16. Martinez-Ceron, M. C.; Targovnik, A. M.; Urtasun, N.; Cascone, O.; Miranda, M. V.; Camperi, S. A., Recombinant protein purification using complementary peptides as affinity tags. *New Biotechnol.* **2012**, *29* (2), 206-210.
17. Guan, D.; Chen, Z., Challenges and recent advances in affinity purification of tag-free proteins. *Biotechnol. Lett.* **2014**, *36* (7), 1391-1406.
18. Batra, S.; Sahi, N.; Mikulcik, K.; Shockley, H.; Turner, C.; Laux, Z.; Badwaik, V. D.; Conte, E.; Rajalingam, D., Efficient and inexpensive method for purification of heparin binding proteins. *J. Chromatogr. B Anal. Technol. Biomed. Life Sci.* **2011**, *879* (24), 2437-2442.
19. Launay, G.; Salza, R.; Multedo, D.; Ricard-Blum, S.; Thierry-Mieg, N., MatrixDB, the extracellular matrix interaction database: updated content, a new navigator and expanded functionalities. *Nucleic Acids Res* **2015**, *43* (Database issue), D321-7.
20. Esko, J. D.; Kimata, K.; Lindahl, U., Proteoglycans and sulfated glycosaminoglycans. *Essent. Glycobiol. (2nd Ed.)* **2009**, 229-248.
21. Fang, J.; Dong, Y.; Salamat-Miller, N.; Middaugh, C. R., DB-PABP: a database of polyanion-binding proteins. *Nucleic Acids Res.* **2008**, *36* (Database Iss), D303-D306.
22. Peysselon, F.; Ricard-Blum, S., Heparin-protein interactions: From affinity and kinetics to biological roles. Application to an interaction network regulating angiogenesis. *Matrix Biol.* **2014**, *35*, 73-81.
23. Someya, S.; Kakuta, M.; Morita, M.; Sumikoshi, K.; Cao, W.; Ge, Z.; Hirose, O.; Nakamura, S.; Terada, T.; Shimizu, K., Prediction of carbohydrate-binding proteins from sequences using support vector machines. *Adv Bioinformatics* **2010**.
24. Crim, R. L.; Audet, S. A.; Feldman, S. A.; Mostowski, H. S.; Beeler, J. A., Identification of linear heparin-binding peptides derived from human respiratory syncytial virus fusion glycoprotein that inhibit infectivity. *J. Virol.* **2007**, *81* (1), 261-271.
25. Cardin, A. D.; Weintraub, H. J. R., Molecular modeling of protein-glycosaminoglycan interactions. *Arteriosclerosis (Dallas)* **1989**, *9* (1), 21-32.
26. Sobel, M.; Soler, D. F.; Kermode, J. C.; Harris, R. B., Localization and characterization of a heparin binding domain peptide of human von Willebrand factor. *J. Biol. Chem.* **1992**, *267* (13), 8857-62.

27. Margalit, H.; Fischer, N.; Ben-Sasson, S. A., Comparative analysis of structurally defined heparin binding sequences reveals a distinct spatial distribution of basic residues. *J. Biol. Chem.* **1993**, *268* (26), 19228-31.
28. Fromm, J. R.; Hileman, R. E.; Caldwell, E. E. O.; Weiler, J. M.; Linhardt, R. J., Pattern and spacing of basic amino acids in heparin binding sites. *Arch. Biochem. Biophys.* **1997**, *343* (1), 92-100.
29. Tyler-Cross, R.; Sobel, M.; Marques, D.; Soler, D. F.; Harris, R. B., Heparin-von Willebrand factor binding as assessed by isothermal titration calorimetry and by affinity fractionation of heparins using synthetic peptides. *Arch. Biochem. Biophys.* **1993**, *306* (2), 528-33.
30. Raman, R.; Sasisekharan, V.; Sasisekharan, R., Structural insights into biological roles of protein-glycosaminoglycan interactions. *Chem. Biol.* **2005**, *12* (3), 267-277.
31. Tyler-Cross, R.; Sobel, M.; Marques, D.; Harris, R. B., Heparin binding domain peptides of antithrombin III: analysis by isothermal titration calorimetry and circular dichroism spectroscopy. *Protein Sci.* **1994**, *3* (4), 620-7.
32. Mitsi, M.; Forsten-Williams, K.; Gopalakrishnan, M.; Nugent, M. A., A Catalytic Role of Heparin within the Extracellular Matrix. *J. Biol. Chem.* **2008**, *283* (50), 34796-34807.
33. De Paz, J. L.; Moseman, E. A.; Noti, C.; Polito, L.; Von Andrian, U. H.; Seeberger, P. H., Profiling Heparin-Chemokine Interactions Using Synthetic Tools. *ACS Chem. Biol.* **2007**, *2* (11), 735-744.
34. Culley, F. J.; Fadlon, E. J.; Kirchem, A.; Williams, T. J.; Jose, P. J.; Pease, J. E., Proteoglycans are potent modulators of the biological responses of eosinophils to chemokines. *Eur. J. Immunol.* **2003**, *33* (5), 1302-1310.
35. Ye, S.; Luo, Y.; Lu, W.; Jones, R. B.; Linhardt, R. J.; Capila, I.; Toida, T.; Kan, M.; Pelletier, H.; McKeehan, W. L., Structural Basis for Interaction of FGF-1, FGF-2, and FGF-7 with Different Heparan Sulfate Motifs. *Biochemistry* **2001**, *40* (48), 14429-14439.
36. Pierce, M. M.; Raman, C. S.; Nall, B. T., Isothermal Titration Calorimetry of Protein-Protein Interactions. *Methods (Orlando, Fla.)* **1999**, *19* (2), 213-221.
37. Velazquez-Campoy, A.; Leavitt, S. A.; Freire, E., Characterization of protein-protein interactions by isothermal titration calorimetry. *Methods Mol. Biol. (Totowa, NJ, U. S.)* **2004**, *261* (Protein-Protein Interactions), 35-54.
38. Lindahl, U.; Kjellen, L., Pathophysiology of heparan sulphate: many diseases, few drugs. *J. Intern. Med.* **2013**, *273* (6), 555-571.
39. Li, C. H.; Nguyen, X.; Narhi, L.; Chemmalil, L.; Towers, E.; Muzammil, S.; Gabrielson, J.; Jiang, Y., Applications of circular dichroism (CD) for structural analysis of proteins:



qualification of near- and far-UV CD for protein higher order structural analysis. *J. Pharm. Sci.* **2011**, *100* (11), 4642-4654.

40. Fannon, M.; Forsten-Williams, K.; Nugent, M. A.; Gregory, K. J.; Chu, C. L.; Goerges-Wildt, A. L.; Panigrahy, D.; Kaipainen, A.; Barnes, C.; Lapp, C.; Shing, Y., Sucrose octasulfate regulates fibroblast growth factor-2 binding, transport, and activity: potential for regulation of tumor growth. *J. Cell. Physiol.* **2008**, *215* (2), 434-441.

41. Royer, C. A., Probing protein folding and conformational transitions with fluorescence. *Chem. Rev. (Washington, DC, U. S.)* **2006**, *106* (5), 1769-1784.

42. Vivian, J. T.; Callis, P. R., Mechanisms of tryptophan fluorescence shifts in proteins. *Biophys. J.* **2001**, *80* (5), 2093-2109.

43. Kwan, A. H.; Mobli, M.; Gooley, P. R.; King, G. F.; Mackay, J. P., Macromolecular NMR spectroscopy for the non-spectroscopist. *Febs J.* **2011**, *278* (5), 687-703.

44. Bieri, M.; Kwan, A. H.; Mobli, M.; King, G. F.; Mackay, J. P.; Gooley, P. R., Macromolecular NMR spectroscopy for the non-spectroscopist: beyond macromolecular solution structure determination. *Febs J.* **2011**, *278* (5), 704-715.

45. Westra, D. F.; Welling, G. W.; Koedijk, D. G. A. M.; Scheffer, A. J.; The, T. H.; Welling-Wester, S., Immobilized metal-ion affinity chromatography purification of histidine-tagged recombinant proteins: a wash step with a low concentration of EDTA. *J. Chromatogr. B Biomed. Sci. Appl.* **2001**, *760* (1), 129-136.

46. Franken, K. L. M. C.; Hiemstra, H. S.; van Meijgaarden, K. E.; Subronto, Y.; den Hartigh, J.; Ottenhoff, T. H. M.; Drijfhout, J. W., Purification of His-Tagged Proteins by Immobilized Chelate Affinity Chromatography: The Benefits from the Use of Organic Solvent. *Protein Expression Purif.* **2000**, *18* (1), 95-99.

47. Mondal, S.; Shet, D.; Prasanna, C.; Atreya, H. S., High yield expression of proteins in *E. coli* for NMR studies. *Adv. Biosci. Biotechnol.* **2013**, *4* (6), 751-767.

48. Pina, A. S.; Lowe, C. R.; Roque, A. C. A., Challenges and opportunities in the purification of recombinant tagged proteins. *Biotechnol. Adv.* **2014**, Ahead of Print.

49. Garcia-Fruitos, E.; Vazquez, E.; Diez-Gil, C.; Corchero, J. L.; Seras-Franzoso, J.; Ratera, I.; Veciana, J.; Villaverde, A., Bacterial inclusion bodies: making gold from waste. *Trends Biotechnol.* **2012**, *30* (2), 65-70.

50. Boonyuen, U.; Promnares, K.; Junkree, S.; Day, N. P. J.; Imwong, M., Efficient in vitro refolding and functional characterization of recombinant human liver carboxylesterase (CES1) expressed in *E. coli*. *Protein Expression Purif.* **2015**, *107*, 68-75.

51. Macinkovic, I. S.; Abughren, M.; Mrkic, I.; Grozdanovic, M. M.; Prodanovic, R.; Gavrovic-Jankulovic, M., Employment of colorimetric enzyme assay for monitoring expression

and solubility of GST fusion proteins targeted to inclusion bodies. *J. Biotechnol.* **2013**, *168* (4), 506-510.

52. Wang, G.; Han, J.; Wang, S.; Li, P., Expression and purification of recombinant human bone morphogenetic protein-7 in *Escherichia coli*. *Prep. Biochem. Biotechnol.* **2014**, *44* (1), 16-25.
53. Parks, T. D.; Howard, E. D.; Wolpert, T. J.; Arp, D. J.; Dougherty, W. G., Expression and purification of a recombinant tobacco etch virus NIa proteinase: biochemical analyses of the full-length and a naturally occurring truncated proteinase form. *Virology* **1995**, *210* (1), 194-201.
54. Blommel, P. G.; Fox, B. G., Fluorescence anisotropy assay for proteolysis of specifically labeled fusion proteins. *Anal. Biochem.* **2005**, *336* (1), 75-86.
55. Blommel, P. G.; Fox, B. G., A combined approach to improving large-scale production of tobacco etch virus protease. *Protein Expression Purif.* **2007**, *55* (1), 53-68.
56. Meyer, B.; Peters, T., NMR spectroscopy techniques for screening and identifying ligand binding to protein receptors. *Angew. Chem., Int. Ed.* **2003**, *42* (8), 864-890.
57. Pomin, V. H.; Sharp, J. S.; Li, X.; Wang, L.; Prestegard, J. H., Characterization of Glycosaminoglycans by <sup>15</sup>N NMR Spectroscopy and in Vivo Isotopic Labeling. *Anal. Chem. (Washington, DC, U. S.)* **2010**, *82* (10), 4078-4088.
58. Rajalingam, D.; Kumar, T. K. S.; Yu, C., The C2A Domain of Synaptotagmin Exhibits a High Binding Affinity for Copper: Implications in the Formation of the Multiprotein FGF Release Complex. *Biochemistry* **2005**, *44* (44), 14431-14442.
59. Rajalingam, D.; Graziani, I.; Prudovsky, I.; Yu, C.; Kumar, T. K. S., Relevance of Partially Structured States in the Non-Classical Secretion of Acidic Fibroblast Growth Factor. *Biochemistry* **2007**, *46* (32), 9225-9238.
60. Thallapuranam, S. K.; Jayanthi, S.; Morris, J.; Brown, A.; McNabb, D.; Henry, R. Heparin affinity tag for protein purification. 2014-US12340, 2015112121, 20140121., 2015.
61. Morris, J.; Jayanthi, S.; Langston, R.; Daily, A.; Kight, A.; McNabb David, S.; Henry, R.; Kumar Thallapuranam Krishnaswamy, S., Heparin-binding peptide as a novel affinity tag for purification of recombinant proteins. *Protein Expr Purif* **2016**.

## **Chapter 3**

### **Detection of HB-Fusion Proteins Using Polyclonal Antibodies**

### **3.1. Abstract**

Recombinant protein production is an important field for biotechnology and pharmaceutical research. In order to determine if the appropriate proteins are expressed and purified, antibodies are used for detection of these recombinant proteins. In our study, the use of HB-peptide as an affinity tag has caused the need for specific detection of the HB-fusion proteins. The detection method of choice for most laboratories is protein immunoblotting or Western blotting. This method involves the resolution of the proteins on a SDS-PAGE gel, electrophoretic transfer to a nitrocellulose, and detection using primary and secondary antibodies. The primary antibodies that were used in this chapter were generated against a specific sequence (first 12 amino acid residues) in the HB-peptide. They are, however, polyclonal antibodies, which recognize multiple epitopes in an antigen, resulting in less specific interactions. These antibodies are advantageous for amplifying signals of target proteins, tolerance to changes in the protein conformation or denaturation, and more efficient detection across cell types.

### **3.2. Introduction**

Recombinant protein expression and purification are traced by separating proteins based on molecular weight using gel electrophoresis. In some cases, recombinant proteins do not express in high yields and are usually difficult to visualize on a SDS-PAGE gel<sup>1</sup>. In other cases, proteins with similar molecular weights as the protein of interest may co-elute with the desired protein during purification, causing ambiguity regarding the identity of the target protein of interest<sup>2</sup>. Gel electrophoresis is not sufficient for all instances to detect proteins of interest. Protein immunoblotting or Western blotting, first discovered in 1979, helps circumvent these

problems in protein chemistry<sup>3</sup>. This simple, sensitive, and effective biochemical technique has been modified and optimized to remain as a key method in biotechnology<sup>4</sup>. It is useful for the detection of proteins with specific sequences that antibodies are raised against, particularly proteins of low abundance<sup>5</sup>. It is also possible to characterize new proteins with unknown biological activity by their reaction with specific antibodies<sup>6</sup>. Western blotting has been used for a wide array of applications, such as a diagnostic tool for prion diseases, yeast infections, parasitic infections, viral infections, diseases, cancer progression, and several others<sup>7,8,9,10,11,12,13</sup>. The most well-known application is the detection of anti-HIV antibody in human serum samples<sup>14</sup>.

Macromolecules are resolved on an electrophoresis gel, which are then electrophoretically transferred to either a nitrocellulose or polyvinylidene difluoride (PVD) membrane. It is hypothesized that proteins interact with the membranes in mainly a hydrophobic manner, as observed by the elution of bound proteins when nonionic detergents are used<sup>15</sup>. The membrane is then blocked to prevent any nonspecific antibody binding to the membrane. Bovine serum albumin or non-fat milk is the blocking agent of choice because the protein binds to areas on the membrane where the target protein is not found. This leads to less likelihood that the primary antibody would bind to open areas on the membrane, leading to less background noise. Polyoxyethylenesorbitan monolaureate (Tween 20) is also used in the wash buffer to continually remove nonspecific antibody binding<sup>16</sup>. A primary antibody binds to the target protein that contains the epitope to which it was raised against in an animal of choice. A secondary antibody that is generated against the animal of choice, in which the primary antibody was raised, is modified with a reporter enzyme such as alkaline phosphatase or horseradish

peroxidase. The enzyme, upon exposure to its substrate, produces a colorimetric response of insoluble dye, indicative of the target protein<sup>17</sup>.

Antibodies, or immunoglobulins, are naturally occurring molecules that are produced from specialized B lymphocytes called plasma cells when a foreign molecule (i.e. bacterial toxins) invades the body, to which the antibody will specifically bind<sup>18,19</sup>. In 1890, Emil von Behring applied his finding (when rabbits were injected with tetanus toxin, they produced tetanus antibodies) to treat diphtheria in children<sup>20</sup>. Researchers have produced antibodies from either multiple B cell clones (polyclonal antibodies) or a single clone (monoclonal antibodies)<sup>20</sup>. Monoclonal antibodies result from splenic B cells being fused with myeloma cells to form hybridomas, each one producing a unique antibody<sup>21</sup>. These antibodies recognize only one epitope on each antigen, making the antigen-antibody interaction more specific. Polyclonal antibodies do recognize more than one epitope, resulting in more nonspecific interactions, but these are less expensive and more tolerant of changes in protein structure such as denaturation required in SDS-PAGE<sup>22</sup>. We have used this method for the specific detection of HB-fusion proteins by anti-HB polyclonal antibodies.

### **3.3. Materials and Methods**

#### ***Western blotting of HB-fusion proteins***

HB-antibodies (HB-Ab) were generated by Genescript, NJ, USA using our specifications. The segment of the HB-peptide possessing the highest antigenicity was designed using the Optimum Antigen design program at the vendor site (<http://www.genscript.com/PolyExpress.html>). HB-Ab was raised in rabbit against the first 14 amino acids in the HB-peptide (QKAQKAQAKQAKQA). A cysteine residue was added to the C-terminal end of the peptide to

couple the N-terminus amino group of the carrier protein like thyroglobulin or Keyhole limpet hemocyanin (KLH) to the thiol group of the peptide using m-maleimidobenzoyl-N-hydroxysuccinimide ester (MBS) as a cross linking agent. This residue is also known to increase immunogenicity. The detailed protocol for the generation of HB-Ab can be obtained at the vendor website (<http://www.genscript.com/PolyExpress.html>).

Western blotting for all experiments was performed by making adaptations of the protocol from Burnette et al<sup>23</sup>. Proteins were resolved on a 15% SDS-PAGE gel and were then transferred to a nitrocellulose membrane for 2 hours at 150 V and 75 mA. The nitrocellulose membrane was blocked using 5% skim milk in Tris buffered saline with Tween 20 (1X TBS-T) (10 mM Tris, 150 mM NaCl, 0.05% Tween-20, pH 7.4) at 25°C for 30 minutes. The membrane was then washed with 0.2% bovine serum albumin (BSA) in 1X TBS-T and the primary antibody, raised in rabbit against the HB-peptide, was added at 1:2500 dilution and incubated for 16 hours at 25°C. Three washes of the membrane were performed using 1X TBS-T\* (varying NaCl concentrations of 150 mM, 500 mM, and 750 mM NaCl). Alkaline phosphatase-conjugated secondary antibody was added to the membrane at 1:2500 dilution and incubated for 2 hours at 25°C. Nitrocellulose-immobilized protein was detected using the NBT/BCIP substrate.

#### ***Limit of Detection of HB-C2A Using Dot Blotting***

Dot blotting was performed similarly to Western blotting without the use of electrophoretic transfer. Varying amounts of fusion protein (1 ug to 0.5 ng) were spotted on the nitrocellulose membrane. For the dot blot washed with 150 mM NaCl, the negative control was BSA in varying amounts of protein as well. Antibody response was calculated by imaging densitometry

using UN-SCAN-IT Gel Analysis Software (Silk Scientific, Orem, UT). Appropriate background subtractions were made.

### ***Western Blotting to Detect and Monitor Protein Expression and Purification***

The expressed cell pellets were resuspended in 5 mL of 10 mM Tris-HCl, pH 8. All three HB-fusion cell samples were sonicated (10 minutes, 10-second pulse with 10-second rest) on ice using a Microson XL unit with power setting at 15. The cell lysate was centrifuged at 20,000 rpm for 30 minutes at 4°C to remove cell debris. These samples were resolved on a 15% SDS-PAGE gel, and were then transferred electrophoretically to a nitrocellulose membrane. Normal Western blotting was performed as described previously using varying concentrations of NaCl (150 mM, 500 mM, 750 mM) in TBS-T\* for secondary antibody incubation. Each eluted protein sample from the heparin-Sepharose purification of the HB-fusion proteins was also TCA precipitated as previously described, and Western blotting occurred. During this technique, 750 mM NaCl in the TBS-T\* was used for secondary antibody incubation. Another Western blotting was performed on the pure HB-fusion proteins using the same procedure.

### ***Western Blotting of GST-HB and HB-S100A13 Cleavage Products***

GST-HB was cleaved, and after separation of GST from HB-peptide by the established heat treatment method, the samples resolved on a tricine gel. HB-S100A13 underwent cleavage by TEV protease, and these cleaved samples were resolved on a 15% SDS-PAGE gel. They were then transferred to a nitrocellulose membrane for 3 hours at 150 V and 100 mA for tricine gel and 2 hours at 150 V and 80 mA for SDS-PAGE gel. The Western blotting protocol stated above was performed.



### ***Spiking of HB-C2A in Different Cell Lines***

*Mus musculus* NIH-3T3 cells, *Pichia pastoris* KM71H cells, and *E. coli* Rosetta (DE3) cells were resuspended in small volume of 1X PBS. These samples were sonicated for 45 seconds (5 second-pulse with 5-second rest) on ice and centrifuged at 13,000 rpm for 5 minutes. The total protein present in the supernatant was estimated using Bradford assay at 595 nm. The total cell sample required was 100 µg, to which 10 µg HB-C2A was added. The cell samples were spotted on the nitrocellulose membrane in order to have 160 ng HB-C2A present. Varying NaCl concentrations in the TBS-T (150 mM, 500 mM, and 750 mM NaCl) were used. Similar dot blotting technique was used as stated above to detect the HB-C2A in the crude mixture before Western blotting occurred. Antibody response was calculated by imaging densitometry using UN-SCAN-IT Gel Analysis Software (Silk Scientific, Orem, UT). Appropriate background subtractions were made. The cell samples (1.25 µg HB-C2A) were then TCA precipitated and resolved on a 15% SDS-PAGE gel, from which Western blotting occurred as previously stated.

### **3.4. Results and Discussion**

***HB-C2A is detected at nanogram levels using polyclonal antibodies:*** Optimization of the use of these antibodies needs to be established before they can be used efficiently in a commercial setting. These antibodies should recognize a specific sequence in the HB-peptide (first 12 amino acids), which in turn should give a fairly specific response on the nitrocellulose membrane. In order to detect proteins containing the HB-affinity tag, their limit of detection needs to be established first. Dot blotting is a technique useful for determination of the presence of a protein to conclude if Western blotting is required. If low amounts of protein/antigen are present, it might not be transferred efficiently to the nitrocellulose membrane, which results in a blank

membrane. Another use of dot blotting is for establishing if the amount of protein required for adequate antibody binding is at an acceptable level for experimental purposes. If the amount required were too high, it would not be feasible to use these antibodies for Western blotting. Varying amounts of NaCl were used in the dot blotting to determine if this affects the antibody-antigen interaction (Figure 3.1). HB-C2A can be detected as low as 10 ng in 150 mM NaCl, which is a promising result for commercial use of these antibodies (A). BSA is used as a negative standard because it is a protein that is not similar to the HB-peptide, not a heparin-binding protein. This protein should not exhibit any binding affinity to antibodies. No antibody response is observed on the membrane (circles 9-13). When 500 mM NaCl (B) and 750 mM NaCl (C) are used, HB-C2A is detected down to only 50 ng instead of 10 ng. The increase in salt concentration slightly disrupts the interaction between HB-peptide and the antibodies. The level is still in the nanogram range, which means the antibodies can be used for detection in low-level protein production.

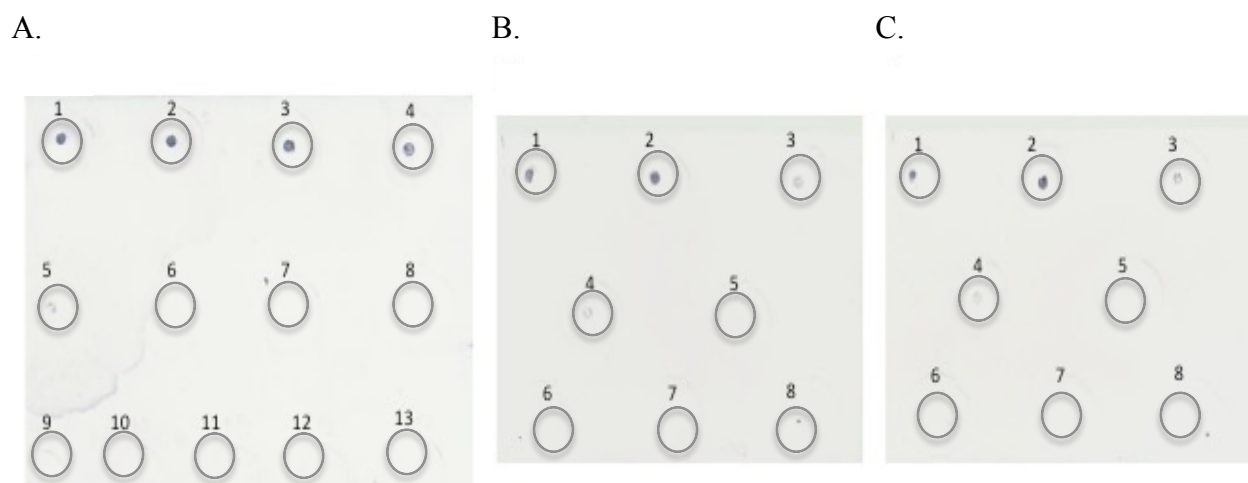


**Figure 3.1** – Dot blot analysis of HB-C2A in TBS-T containing 150 mM NaCl (Panel-A), 500 mM NaCl (Panel-B), and 750 mM NaCl (Panel-C). Circles 1-8 are HB-C2A; Circles 9-13 are BSA in the same amounts as circles 1-5. Circle 1, 1  $\mu$ g; Circle 2, 500 ng; Circle 3, 100 ng; Circle 4, 50 ng; Circle 5, 10 ng; Circle 6, 5 ng; Circle 7, 1 ng; Circle 8, 0.5 ng.

Densitometry shows the increase in antibody response as the amount of HB-C2A blotted is increased for all three conditions (Figure 3.2). This is expected because more antigen (more epitopes) is present for the antibodies to bind to, leading to greater detection.

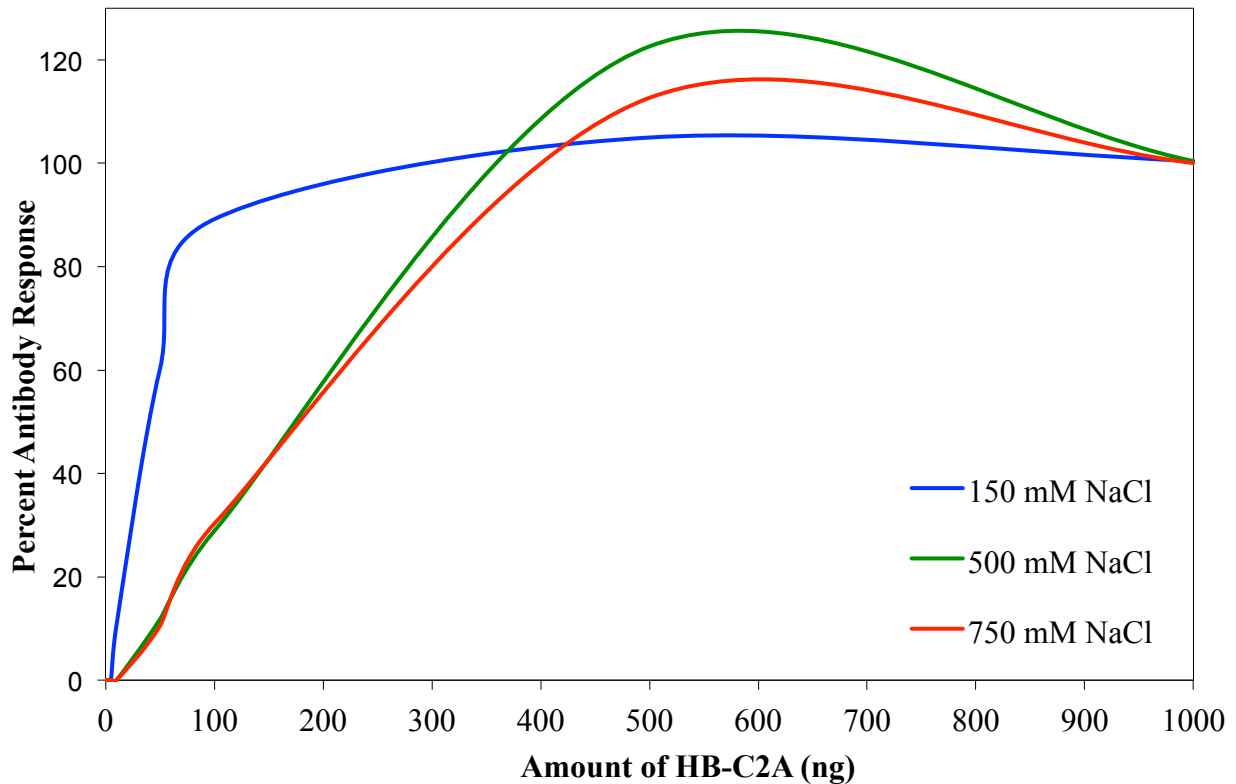


**Figure 3.2** – Plot of densitometric scan of dot blot analysis of HB-C2A. The blue curve represents 150 mM NaCl, green is 500 mM NaCl, and red is 750 mM NaCl.

The pure fusion proteins were then transferred to a nitrocellulose membrane and detected using Western blotting (Figure 3.3). The fusion protein HB-S100A13 migrated slightly higher than what its expected molecular weight is (~ 16 kDa), but it is still detected using the polyclonal antibodies.

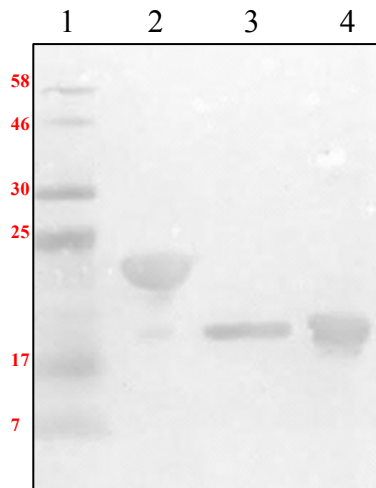


**Figure 3.3** – Western blot analysis of pure HB-fusion proteins. Lane 1, protein marker; Lane 2, HB-C2A; Lane 3, HB-CAlb3; Lane 4, HB-S100A13.

***HB-antibodies detect fusion proteins in crude cell samples and during purification:*** Even though the antibodies bind to HB-C2A when in pure form during dot blotting, one must examine their specificity for the fusion proteins in the presence of other proteins. When proteins are not expressed in high yields, bands normally do not appear on SDS-PAGE gels in cell lysates where hundreds of other *E. coli* proteins are present. There is also a chance of other proteins that are relatively the same size as the protein of interest at higher yield than the protein of interest, which could result in false positives on the gels occurring. There is a need for sensitive and specific detection in cell lysates before further purification is performed. Western blotting is a highly specific technique that can be used for low-level detection of antigens using specific antibodies grown against a specific sequence. Since the antibodies were grown against the specific sequence in HB-peptide, which was specially designed and expressed in much higher yield than *E. coli* proteins, it is likely that the antibodies would bind to proteins that contain the HB-affinity tag. In order to test this hypothesis, Western blotting is performed on lysed cells that contain the proteins of interest, HB-fusion proteins (Figure 3.4).

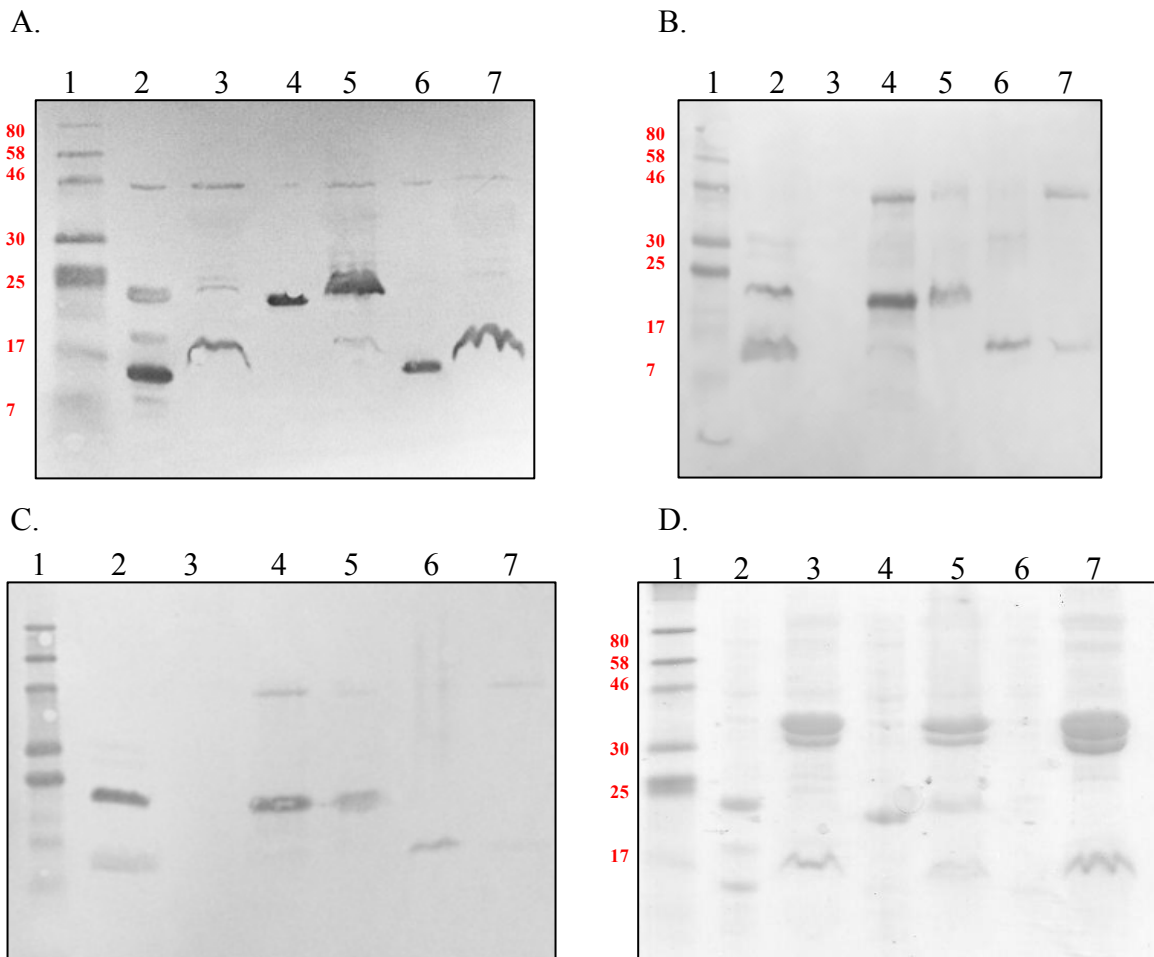


**Figure 3.4** – Western blot analysis of crude cell samples in TBS-T containing 150 mM NaCl (Panel-A), 500 mM NaCl (Panel-B), and 750 mM NaCl (Panel-C) after SDS-PAGE is performed (Panel-D). Lane 1, protein marker; Lane 2, HB-CALb3-clear cell lysate; Lane 3, HB-CALb3-post-sonication pellet; Lane 4, HB-C2A-clear cell lysate; Lane 5, HB-C2A-post-sonication pellet; Lane 6, HB-S100A13-clear cell lysate; Lane 7, HB-S100A13-post-sonication pellet.

It is more advantageous to use secondary antibodies that are conjugated with alkaline phosphatase instead of horseradish peroxidase because this commercially available enzyme (alkaline phosphatase) exists in high purity<sup>24</sup>. In 150 mM NaCl, the HB-fusion proteins are detected extremely well in the lysate and pellet, as seen by the darker bands on the membrane (Panel-A). There are, however, other proteins that are detected as well, which is probably due to the nonspecific manner of binding of the secondary antibodies. In addition, polyclonal

antibodies are known to be less specific and more variable than monoclonal, so there is that risk of cross-reactivity when using these antibodies for Western blotting<sup>25</sup>. Polyclonal antibodies recognize more than one epitope on an antigen, but can also recognize other proteins that have high homology with the HB-fusion proteins<sup>26</sup>. This finding could plausibly explain the presence of other protein bands along with the HB-fusion proteins on the membrane. Since the HB-fusion proteins are expressed in higher yield than the other *E. coli* proteins, antibodies should give a greater response when bound to these concentrated HB-proteins. In this context, the salt concentration was increased to 500 mM NaCl to remove nonspecific interactions, which aids in the removal of other protein bands (Panel-B). Still, other protein bands are present, so 750 mM NaCl is preferred because it removes the majority of the nonspecific interactions (Panel-C). Multimers of various proteins can be observed as well, which would contain the epitope of interest that the antibodies bind to. This could result in other proteins being detected on the membrane. The HB-peptide is composed of a repeating sequence of the epitope that was used in raising the antibodies, which means the interaction between antibodies and HB-fusion proteins is strong and amplified. When proteins do not express in large amounts and high sensitivity is required, polyclonal over monoclonal antibodies are preferred.

Once the salt concentration for specific detection is optimized, Western blotting of the purification fractions is performed. Using 750 mM NaCl, only the bands corresponding to the HB-fusion proteins HB-C2A (Figure 3.5), HB-CA1b3 (Figure 3.6), and HB-S100A13 (Figure 3.7) appear on the membrane. Even in the presence of contaminants, such as in 0 mM to 350 mM NaCl fractions, a pure band of interest is observed. From these results, it is clear that the

antibodies are specific to HB-fusion proteins, as the bands align with the marker at their known molecular weights (HB-C2A is 20 kDa, HB-CAlb3 is 18 kDa, HB-S100A13 is 16 kDa).

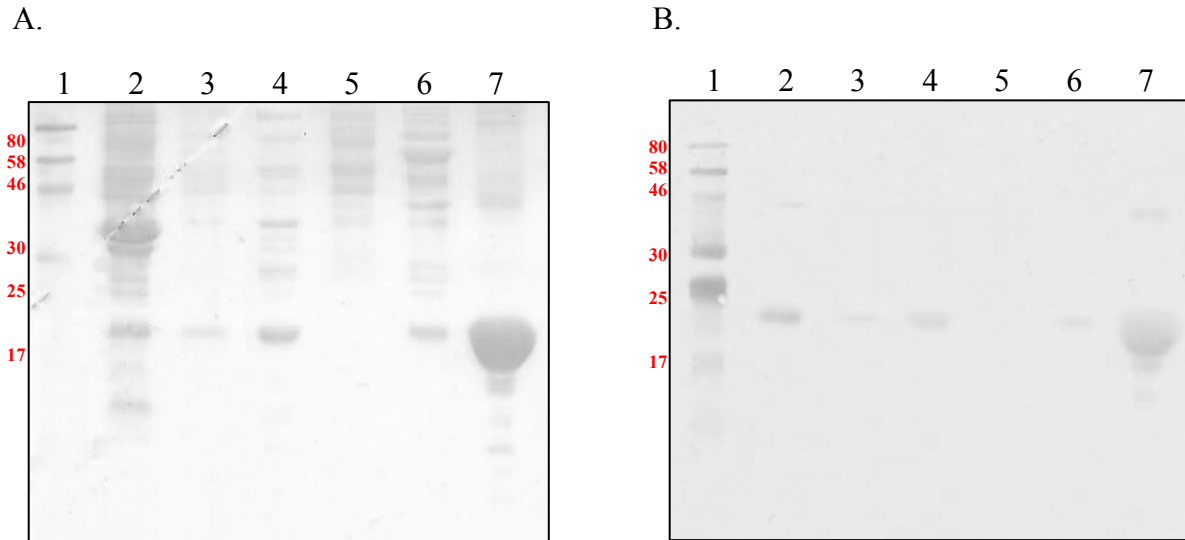


**Figure 3.5** – SDS-PAGE (Panel-A) and Western blot analysis (Panel-B) of fractions collected from the purification of HB-C2A using heparin-Sepharose affinity chromatography. Lane 1, protein marker; Lane 2, post-sonication pellet; Lane 3, clear cell lysate; Lane 4, 0 mM NaCl; Lane 5, 100 mM NaCl; Lane 6, 350 mM NaCl; Lane 7, 500 mM NaCl.

Despite being polyclonal antibodies, they show specific interaction with the fusion proteins containing the HB-sequence when 750 mM NaCl is used.

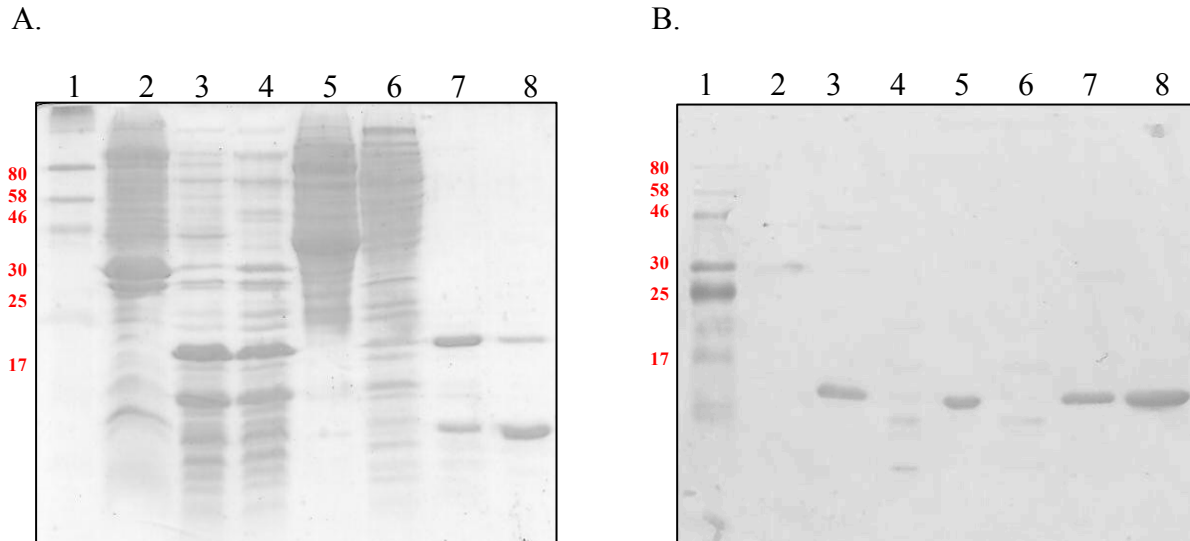


**Figure 3.6** – SDS-PAGE (Panel-A) and Western blot analysis (Panel-B) of fractions collected from the purification of HB-CALb3 using heparin-Sepharose affinity chromatography. Lane 1, protein marker; Lane 2, post-sonication pellet; Lane 3, clear cell lysate; Lane 4, 0 mM NaCl; Lane 5, 100 mM NaCl; Lane 6, 350 mM NaCl; Lane 7, 1 M NaCl; Lane 8, 2 M NaCl.

HB-CALb3, however, migrates at a slightly lower molecular weight compared to the marker, as seen by its band migrating near the 17-kDa band. This is possibly due the protein not being fully reduced by  $\beta$ -mercaptoethanol, which in turn does not reduce all disulfide bonds causing the protein to migrate faster on the gel. In other instances, HB-CALb3 migrates near the 17-kDa marker band, but other times migrates faster. If a protein does not have its structure completely disrupted by reducing agents, the resolving rate is skewed. Since the antibodies do bind to this protein alone on the membrane, it can be inferred that it is indeed HB-CALb3 regardless of how it resolves on the gel. As the amount of contaminants are decreased in each fraction, the signal on the membrane corresponding to the fusion protein increases. Another positive finding is that even in low yield, proteins of interest (HB-fusion proteins) can be detected via Western blotting using these antibodies. In the future, if higher specificity is required, anti-HB monoclonal antibodies need to be generated. However, to circumvent the use of expensive monoclonal



antibodies, the salt conditions for immunoblotting have been successfully optimized to reduce any nonspecific interactions and cross reactivity.

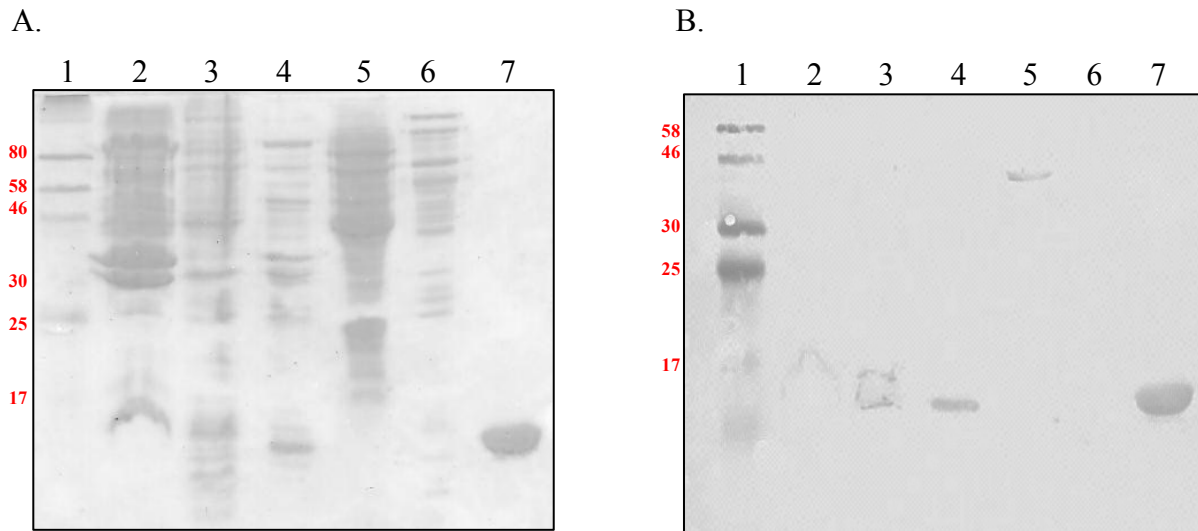


**Figure 3.7** – SDS-PAGE (Panel-A) and Western blot analysis (Panel-B) of fractions collected from the purification of HB-S100A13 using heparin-Sepharose affinity chromatography. Lane 1, protein marker; Lane 2, post-sonication pellet; Lane 3, clear cell lysate; Lane 4, 0 mM NaCl; Lane 5, 100 mM NaCl; Lane 6, 350 mM NaCl; Lane 7, 1 M NaCl.

***HB-peptide, not the target protein, contributes to antibody response:*** Antibodies are specific to HB-fusion proteins, but should only bind to the epitope present in the peptide and not the partner protein. HB-peptide is fused to GST, which is a 26 kDa protein that is not known to be a heparin-binding protein, and therefore should not contain the specific epitope that is recognized by the antibodies<sup>27</sup>. It is therefore expected that GST should not contribute to antibody response. In order to examine this possibility, GST-HB, GST, and HB-peptide were analyzed by SDS-PAGE and Western blotting (Figure 3.8). Only the fusion protein (lane 1) and HB-peptide (lane 3) are detected on the membrane, which demonstrates the antibodies are specific to only HB-peptide and proteins that contain this affinity tag. The large molecular weight of GST does not contribute to the antibody response elicited on the membrane.

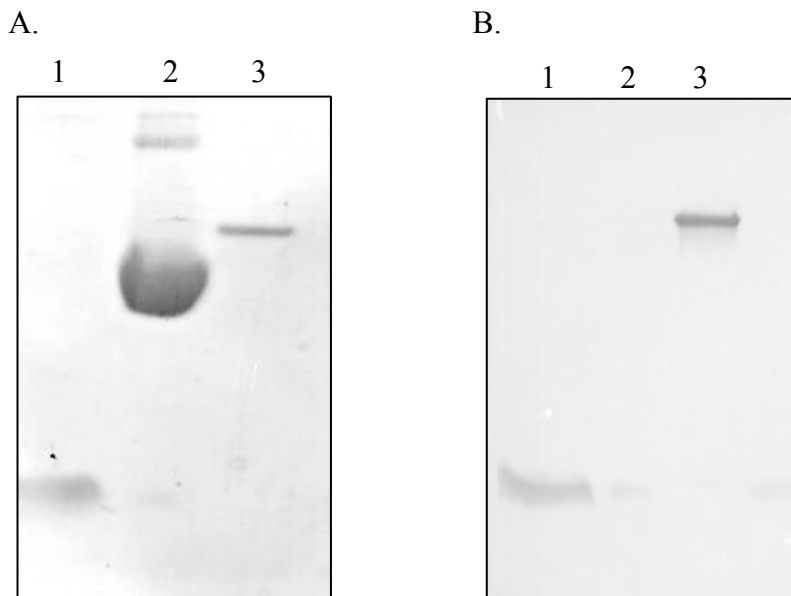


**Figure 3.8** – SDS-PAGE (Panel-A) and Western blot analysis (Panel-B) of GST-HB cleavage samples. Lane 1, HB-peptide; Lane 2, GST; Lane 3, GST-HB.

Cleaved HB-S100A13 has a similar result, in which only the HB-peptide is detected on the membrane (Figure 3.9). The target protein does not contain any structural similarities (heparin-binding capability), which removes any possibility of it binding to the antibodies. These antibodies can be used to detect fusion proteins that contain the HB-affinity tag.

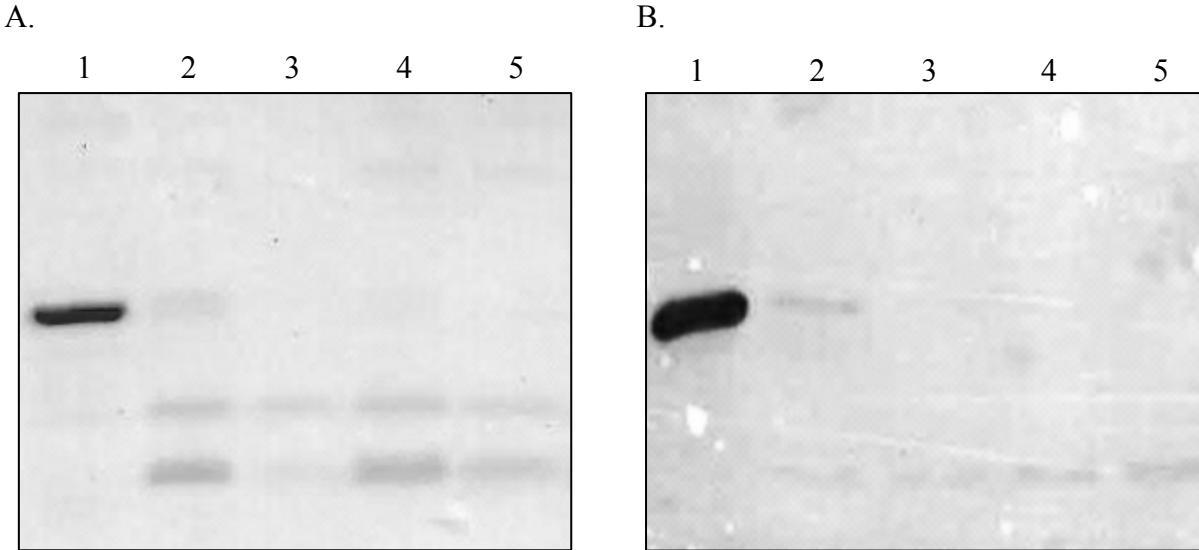


**Figure 3.9** – SDS-PAGE (Panel-A) and Western blot analysis (Panel-B) of cleaved HB-S100A13. Lane 1, HB-S100A13; Lane 2, 6-hour cleavage; Lane 3, 9-hour cleavage; Lane 4, 15-hour cleavage; Lane 5, 18-hour cleavage.

In the previous Western blotting of the expression clones (Figure 3.4), the contaminating proteins that interacted with HB-antibodies are possibly other proteins that have similar sequences as HB-peptide, perhaps even heparin-binding proteins present in the bacterial cells. Since the S100A13 and GST are not considered heparin-binding proteins, they would not contain epitopes similar to HB-peptide, which shows that the detected proteins have to, in fact, be similar to HB-peptide. Proteins that do not exhibit heparin-binding qualities would not bind to the antibodies.

***HB-antibodies can interact with fusion proteins in other cell lines:*** Many eukaryotic proteins do not fold properly during expression in bacteria, which calls for their expression in other cells, such as yeast or mammal. When expression occurs, post-translational modification occurs that is not found in bacterial expression systems<sup>28</sup>. These modifications change the structural features of the target protein in these cell lines, resulting in the original epitope being altered. Once the

epitope changes, monoclonal antibodies cannot bind to the target protein of interest. This is due to monoclonal antibodies only recognizing one epitope on an antigen, which is too specific for fusion proteins expressed in other cell lines. Polyclonal antibodies are more tolerant to changes across cell lines, which is beneficial for proteins that are expressed in other cell lines. However, cross reactivity of polyclonal antibodies occurs on occasion, with the antibodies binding to other cell host proteins, as stated previously. This spiking experiment is to determine the efficacy of the antibodies binding to HB-fusion proteins in any host of choice. Dot blotting shows the detection of the fusion protein is successful in crude cell samples (Figure 3.10). The various salt concentrations are used in order to reduce the nonspecific interactions that occur as previously stated in crude cell samples. Even in 750 mM NaCl, the antibodies still bind to the fusion protein in all the cell lines. The presence of different non-heparin-binding proteins produced in the host cells do not appear to interfere with the antibody-antigen response generated on the membrane.

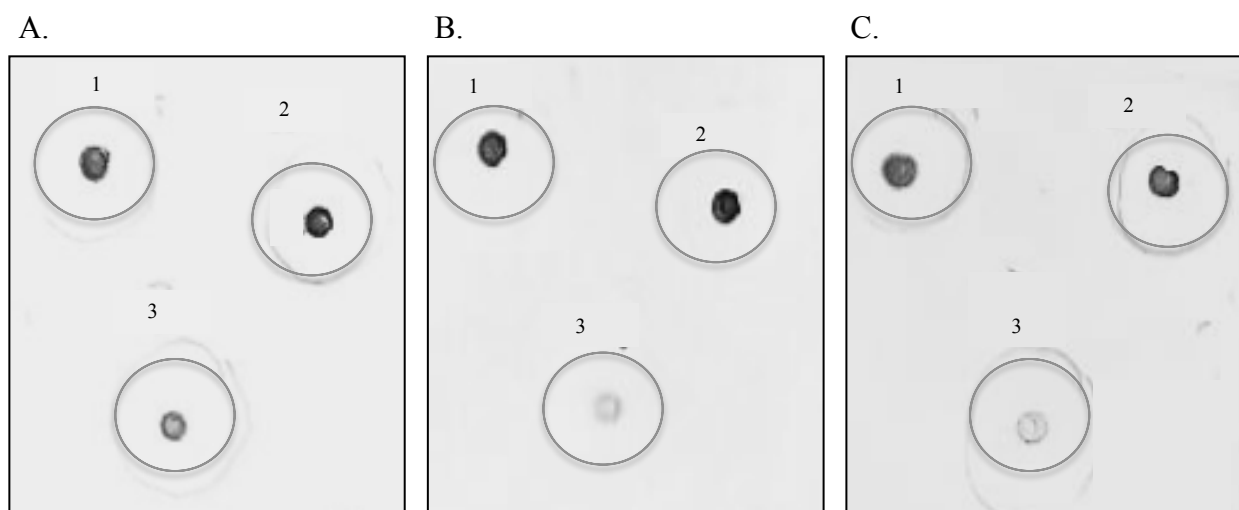


**Figure 3.10** – Dot blot analysis of HB-C2A spiked in bacterial, mammalian, and yeast cell lines in TBS-T containing 150 mM NaCl (Panel-A), 500 mM NaCl (Panel-B), and 750 mM NaCl (Panel-C). Circle 1, bacteria; Circle 2, mammal; Circle 3, yeast.

Quantification by densitometry shows a decrease in antibody response (expressed as a percentage) from 150 mM to 750 mM NaCl (Figure 3.11). This salt concentration was set to 100% because this is the normal blotting condition. No interference of antibody binding should occur using this concentration. There is not a large decrease in antibody response for bacterial and mammalian cells when the salt concentration is increased from 150 mM NaCl. Similar to the expression clones, 750 mM NaCl was the salt concentration of choice used for the subsequent Western blotting of the spiking experiment.

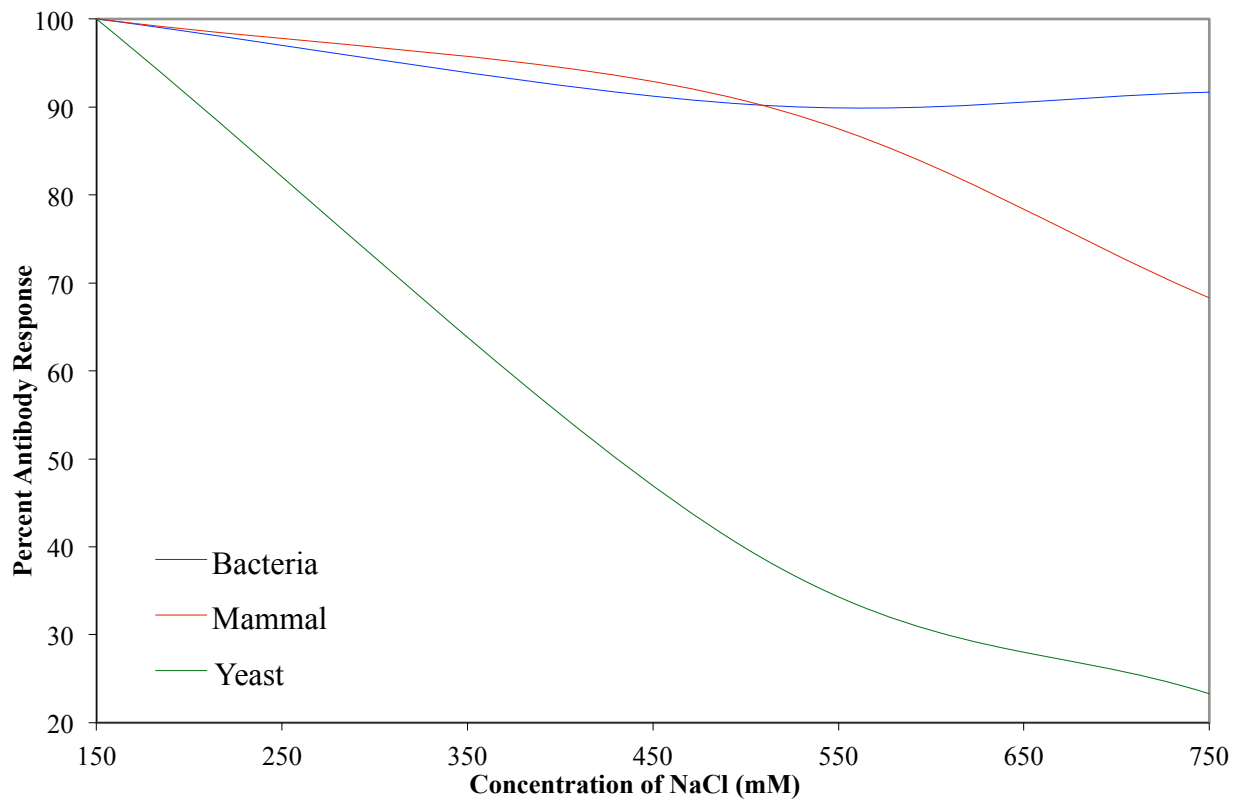


**Figure 3.11** – Plot of densitometric scan of dot blot analysis of HB-C2A spiked in bacterial (blue), mammalian (red), and yeast (green) cell lines.

All three cell samples, after undergoing TCA precipitation, were resolved on SDS-PAGE and transferred to nitrocellulose membrane (Figure 3.12). Even in the cell lysates, in which many

other contaminating proteins are present, the antibodies are still specific to HB-C2A. Bacteria produce much higher amounts of protein during expression, which can then “drown out” the presence of HB-C2A. For Western blotting, TCA precipitation is required of the cell lysate, which for the bacteria sample produced an extremely large pellet. The use of urea did not completely dissolve the bacterial pellet due to its large size, compared to the yeast and mammalian cell pellets. Some of the HB-C2A could have been lost in this pellet and not been resolved on the SDS-PAGE gel. This can then lead to a decrease in signal on the membrane. In dot blotting, however, no precipitation of the cell lysate was required, leading to the full, uninterrupted interaction between the antibodies and HB-C2A. Based on this experiment, these polyclonal antibodies prove, once again, to be beneficial for the detection of HB-fusion proteins.

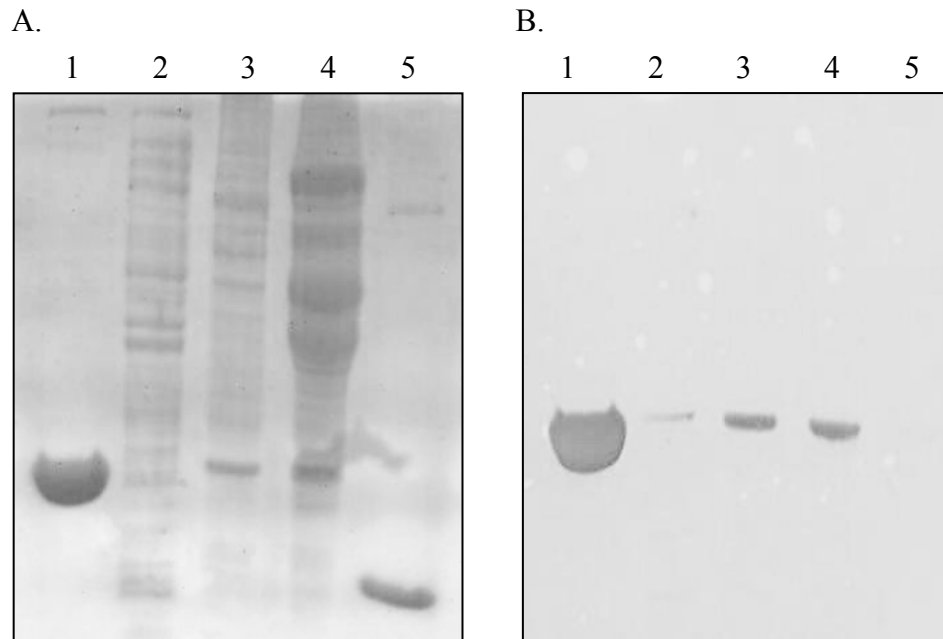


**Figure 3.12** – SDS-PAGE (Panel-A) and Western blot analysis (Panel-B) of HB-C2A spiked in different cell lines. Lane 1, HB-C2A; Lane 2, bacterial cells; Lane 3, mammalian cells; Lane 4, yeast cells.

The use of polyclonal antibodies that are generated against HB-affinity peptide has shown great promise for the detection of HB-fusion proteins. The cell line does not play a large role in the binding capability of the antibodies to their target protein of interest. Even though polyclonal antibodies have been shown to bind in a nonspecific manner at times, increasing the salt concentration during the washing steps decreases these nonspecific interactions. These antibodies can be used commercially to detect any protein that contains the HB-affinity tag no matter the cell of choice. Some work in this chapter has been published as a manuscript<sup>29</sup>.

### 3.5. References

1. Wang, G.; Han, J.; Wang, S.; Li, P., Expression and purification of recombinant human bone morphogenetic protein-7 in Escherichia coli. *Prep. Biochem. Biotechnol.* **2014**, *44* (1), 16-25.
2. Hartinger, D.; Heintl, S.; Schwartz, H. E.; Grabherr, R.; Schatzmayr, G.; Haltrich, D.; Moll, W.-D., Enhancement of solubility in Escherichia coli and purification of an aminotransferase from Sphingopyxis sp. MTA144 for deamination of hydrolyzed fumonisin B1. *Microb. Cell Fact.* **2010**, *9*, No pp given.
3. Towbin, H.; Staehelin, T.; Gordon, J., Electrophoretic transfer of proteins from polyacrylamide gels to nitrocellulose sheets: Procedure and some applications. *Proc. Natl. Acad. Sci. U. S. A.* **1979**, *76* (9), 4350-4.
4. Kaufman, P. B.; Kirakosyan, A.; Cseke, L. J.; Seymour, E. M., Western blot hybridization. *Handb. Mol. Cell. Methods Biol. Med. (3rd Ed.)* **2011**, 313-330.
5. Kurien, B. T.; Scofield, R. H., Western blotting. *Methods (San Diego, CA, U. S.)* **2006**, *38* (4), 283-293.
6. Falkenberg, F. W.; Pierard, D.; Mai, U.; Kantwerk, G., Polyclonal and monoclonal antibodies as reagents in biochemical and in clinical chemical analysis. *J. Clin. Chem. Clin. Biochem.* **1984**, *22* (12), 867-82.
7. Ikegami, Y.; Ito, M.; Isomura, H.; Momotani, E.; Sasaki, K.; Muramatsu, Y.; Ishiguro, N.; Shinagawa, M., Pre-clinical and clinical diagnosis of scrapie by detection of PrP protein in tissues of sheep. *Vet Rec* **1991**, *128* (12), 271-5.
8. Pitarch, A.; Pardo, M.; Jimenez, A.; Pla, J.; Gil, C.; Sanchez, M.; Nombela, C., Two-dimensional gel electrophoresis as analytical tool for identifying Candida albicans immunogenic proteins. *Electrophoresis* **1999**, *20* (4-5), 1001-1010.
9. Magi, B.; Migliorini, L., Western blotting for the diagnosis of congenital toxoplasmosis. *New Microbiol* **2011**, *34* (1), 93-5.
10. Gierer, S.; Bertram, S.; Kaup, F.; Wrensch, F.; Heurich, A.; Kraemer-Kuehl, A.; Welsch, K.; Winkler, M.; Meyer, B.; Drosten, C.; Dittmer, U.; von Hahn, T.; Simmons, G.; Hofmann, H.; Poehlmann, S., The spike protein of the emerging betacoronavirus EMC uses a novel coronavirus receptor for entry, can be activated by TMPRSS2, and is targeted by neutralizing antibodies. *J. Virol.* **2013**, *87* (10), 5502-5511.
11. Hoxha, E.; Harendza, S.; Zahner, G.; Panzer, U.; Steinmetz, O.; Fechner, K.; Helmchen, U.; Stahl, R. A. K., An immunofluorescence test for phospholipase-A2-receptor antibodies and its clinical usefulness in patients with membranous glomerulonephritis. *Nephrol., Dial., Transplant.* **2011**, *26* (8), 2526-2532.



12. Jin, S.; Kennedy, R. T., New developments in Western blot technology. *Chin. Chem. Lett.* **2015**, *26* (4), 416-418.
13. Du, L.; Wang, H.; He, L.; Zhang, J.; Ni, B.; Wang, X.; Jin, H.; Cahuzac, N.; Mehrpour, M.; Lu, Y.; Chen, Q., CD44 is of Functional Importance for Colorectal Cancer Stem Cells. *Clin. Cancer Res.* **2008**, *14* (21), 6751-6760.
14. Kapadiya, G. M.; Parmar, A. M.; Sen, D. J., Western blotting: an unique technology for detection of proteins by antigen-antibody interaction. *World J. Pharm. Pharm. Sci.* **2014**, *3* (10), 1810-1824, 15 pp.
15. Van Oss, C. J.; Good, R. J.; Chaudhury, M. K., Mechanism of DNA (Southern) and protein (Western) blotting on cellulose nitrate and other membranes. *J. Chromatogr.* **1987**, *391* (1), 53-65.
16. Welinder, C.; Ekblad, L., Coomassie staining as loading control in western blot analysis. *J. Proteome Res.* **2011**, *10* (3), 1416-1419.
17. Blake, M. S.; Johnston, K. H.; Russell-Jones, G. J.; Gotschlich, E. C., A rapid, sensitive method for detection of alkaline phosphatase-conjugated anti-antibody on Western blots. *Anal. Biochem.* **1984**, *136* (1), 175-9.
18. Drenckhahn, D.; Joens, T.; Schmitz, F., Production of polyclonal antibodies against proteins and peptides. *Methods Cell Biol.* **1993**, *37* (Antibodies in Cell Biology), 7-56.
19. Lipman, N. S.; Jackson, L. R.; Trudel, L. J.; Weis-Garcia, F., Monoclonal versus polyclonal antibodies: Distinguishing characteristics, applications, and information resources. *Ilar J.* **2005**, *46* (3), 258-268.
20. Wootla, B.; Denic, A.; Rodriguez, M., Polyclonal and Monoclonal Antibodies in Clinic. *Methods Mol. Biol. (N. Y., NY, U. S.)* **2013**, *1060* (Human Monoclonal Antibodies), 79-110.
21. Kohler, G.; Milstein, C., Continuous cultures of fused cells secreting antibody of predefined specificity. *Nature* **1975**, *256* (5517), 495-7.
22. Gorr, T. A.; Vogel, J., Western blotting revisited: Critical perusal of underappreciated technical issues. *Proteomics Clin. Appl.* **2015**, *9* (3-4), 396-405.
23. Burnette, W. N., "Western blotting": electrophoretic transfer of proteins from sodium dodecyl sulfate-polyacrylamide gels to unmodified nitrocellulose and radiographic detection with antibody and radioiodinated protein A. *Anal. Biochem.* **1981**, *112* (2), 195-203.
24. Holtzhauer, M., Immunochemical Protocols. In *Basic Methods for the Biochemical Lab*, 1 ed.; Springer-Verlag Berlin Heidelberg: 2006; pp 129-160.
25. Magdeldin, S.; Moser, A., Affinity Chromatography: Principles and Applications. In *Affinity Chromatography*, Magdeldin, S., Ed. InTech: 2012.

26. Michnick, S. W.; Sidhu, S. S., Submitting antibodies to binding arbitration. *Nat. Chem. Biol.* **2008**, *4* (6), 326-329.
27. Rusnati, M.; Coltrini, D.; Oreste, P.; Zoppetti, G.; Albini, A.; Noonan, D.; Di Fagagna, F. D. a.; Giacca, M.; Presta, M., Interaction of HIV-1 Tat protein with heparin. Role of the backbone structure, sulfation, and size. *J. Biol. Chem.* **1997**, *272* (17), 11313-11320.
28. Nadeau, J., *Introduction to Experimental Biophysics: Biological Methods for Physical Scientists*. Taylor and Francis Group: Boca Raton, FL, 2011.
29. Morris, J.; Jayanthi, S.; Langston, R.; Daily, A.; Kight, A.; McNabb David, S.; Henry, R.; Kumar Thallapuram Krishnaswamy, S., Heparin-binding peptide as a novel affinity tag for purification of recombinant proteins. *Protein Expr Purif* **2016**.

## **Chapter 4**

### **Separation of Glycosaminoglycans by HB-Affinity Column**

#### 4.1. Abstract

Heparin is an important drug used for the treatment and cure of blood clots. In 2008, molecules that are similar to heparin (OSCS and DS) were detected in batches of heparin that resulted in numerous deaths worldwide. The contamination of heparin in 2008 has spurred on a global approach to develop pure heparin either from existing animal sources or synthesize oligosaccharides that have anticoagulation activity. We have designed a heparin-binding (HB) peptide that has shown to bind with greater binding affinity to heparin than to dermatan sulfate, chondroitin sulfate, and hyaluronic acid. Based on this finding, the HB-peptide was then coupled onto NHS-Sepharose, which is a resin commonly used for the immobilization of peptides and antibodies. The HB-coupled affinity column was applied in a similar fashion as heparin-Sepharose is used to purify heparin-binding proteins, such as fibroblast growth factors. A mixture of GAGs that included heparin, DS, and CS was applied to the HB-affinity column. Using a step-wise NaCl gradient, fractions of GAGs were collected. The <sup>1</sup>H NMR spectrum of each fraction was analyzed and compared to standard GAG samples, and using this, we discovered that heparin can in fact be separated from the majority of the other GAGs. Some “impurities”, however, still remained when heparin was eluted, in higher salt concentrations. Based on this result, we concluded that the “impurity” peak actually belonged to DS because chondroitin sulfate did not show significant binding affinity to the peptide to stay bound to the column for this long. These results are very promising for the preliminary use of this peptide for the isolation of GAGs. We have also successfully isolated GAGs from chicken intestines on a small-scale level using a simple method of enzymatic treatment. Azure A assay was used to show close to 5 μg of GAGs was obtained, which was not enough to purify using the HB-affinity

column. The HB-peptide is a very promising molecule, when future modifications are implemented, for the commercial application of the isolation of heparin.

## 4.2. Introduction

Heparin, a glycosaminoglycan, was discovered in 1916 by McLean and Howell, but first used as an anticoagulant in 1935 in clinical trials<sup>1</sup>. Heparin has also shown promise in therapy for rheumatoid arthritis (RA). It works by reducing angiogenesis by HBPs, which promotes the destruction of cartilage and bone in the course of RA<sup>2</sup>. This remarkable drug is normally isolated in high yields (tons) from porcine intestines, but in 2008, contaminants of OSCS and DS were present in the isolated batch. This oversight caused over 200 deaths<sup>3</sup>. Anaphylactic shock and vasodilation were the results of the activation of the kinin-kallikrein and complementary cascade<sup>4,5,6</sup>. OSCS is a semisynthetic molecule containing four sulfate groups per one building block, not normally present in animal tissue<sup>7</sup>.

The major challenge in the analysis of adulterated heparin samples is the detection and identification of the structurally similar impurities<sup>3</sup>. GAGs are extremely similar in structure but there are certain aspects of each one that is unique from the others. For example, each GAG has a unique NMR fingerprint that can be used for its detection and separation from the other GAGs<sup>8,9,10</sup>. Heparin and contaminated heparin have different NMR spectra, due to the presence of DS and OSCS<sup>3</sup>. These impurities actually have their own unique proton signals in NMR<sup>11,12</sup>. Proton NMR has been established as the major analytical method to detect contaminants in adulterated heparin samples<sup>13,14,15,16</sup>. Despite these analytical procedures for the identification of contaminated heparin samples, there is still a need for pure heparin samples for use in medicine.

Synthetic pathways have been proposed for the production of pure heparin, but these processes have not shown to be efficient. The main bottleneck of this method is the poor yield (milligram scale) obtained of the desired product as well the incessantly large amounts of synthesis steps and cost<sup>17</sup>. A chemoenzymatically prepared alternative to heparin has been made by using enzymes and substrates found in the biosynthetic pathway in the body. In 2013, the number of steps required to obtain fondaparinux was decreased from the 50 steps to 36 steps<sup>18</sup>. Another pentasaccharide of heparin called Idraparinux was synthesized in a total of 51 steps with only 4% overall yield from D-glucose and  $\alpha$ -D-glucopyranoside<sup>19</sup>. In addition, although the risk of thromboembolism is reduced from that of heparin, the costly and increased number of steps outweighs the benefit of synthesis. The biosynthesis of heparin in nature produces the most accurate molecules for anticoagulation, whereas you run the risk of not enough or incorrect sulfation patterns on the synthesized heparin oligosaccharides. Bhaskar et al recently have proposed a bioengineered approach to the synthesis of heparin from recombinant heparosan in *E. coli*, which resembles a non-sulfated heparin backbone<sup>20</sup>. The synthesis needs to be optimized further for low cost and efficient yield. Other groups have proposed a similar process to the isolation from porcine and bovine intestine in other animal sources. Saravanan et al have isolated a LMWH of 6500-7500 Da from Marine Mollusc *Amussium pleuronectus* in decent yield that showed good anticoagulation activity. This analog is sulfated like porcine heparin and contains equivalent uronic acid and hexosamine<sup>21</sup>. The most cost and time effective method for obtaining pure heparin or LMWH appears to be purifying already existing contaminated samples using affinity chromatography, but optimized methods for this protocol have not yet been reported. In order for this highly needed anticoagulant to be used again, a new method for its isolation is required.

FGF-1 is a heparin-binding protein that uses heparin proteoglycans to activate its cell signaling pathways. In the absence of heparin/HS present, FGF-1 cannot bind to its tyrosine kinase receptor with high affinity<sup>22,23,24</sup>. Based on structural features and sequence information present in HBPs, such as FGF-1, a heparin-binding (HB) peptide was designed that is capable of binding to heparin. This peptide, like other small molecules, can be immobilized on a solid matrix for binding of its partner molecule, heparin. Peptides and antibodies have shown promise in their coupling to NHS-Sepharose for protein partner or antigen binding studies<sup>25,26</sup>. Using this method, we have designed an HB-affinity column that should tightly bind heparin. This method enables heparin to be separated from other contaminating GAGs to achieve pure heparin for future biomedical applications. In this study, there is a pressing need for a simple and cost-effective isolation of pure heparin.

### **4.3. Materials and Methods**

#### ***Isothermal Titration Calorimetry***

ITC measurements were performed using iTC200 (MicroCal Inc., Northampton, MA) at 25°C. Concentration of HB-peptide was maintained at 1:10 the concentration of the GAGs in 10 mM phosphate buffer, 100 mM NaCl, pH 7.2. Unfractionated GAGs chosen were heparin sodium salt from porcine intestinal mucosa (Sigma-Aldrich), hyaluronic acid sodium salt from bovine vitreous humor (Sigma-Aldrich), dermatan sulfate from porcine intestinal mucosa (Sigma-Aldrich), and chondroitin sulfate hydrogen sulfate (Chem-Impex Int'l). All samples were centrifuged at 13,000 rpm to remove insoluble particulates and later degasses under vacuum. The corresponding GAG was titrated into HB-peptide at 1.3  $\mu$ L injections with 12 sec intervals.

The raw data was fit using binding models in the Origin Version 7.0 software supplied by MicroCal Inc. The accuracy of the fitting was assessed using the given  $X^2$  values.

### ***Coupling to NHS-Sepharose***

N-hydroxysuccinimide (NHS)-activated Sepharose 4 Fast Flow resin (GE Healthcare Life Sciences, Pittsburgh, PA) is a pre-activated agarose matrix that is designed for efficient immobilization of small proteins and peptides. Preliminary coupling procedures were performed using GSH. The coupling protocol provided by GE Healthcare Life Sciences ([www.gelifesciences.com](http://www.gelifesciences.com)) was followed precisely with only one minor change. In short, resin was washed with 10-15 column volumes (CV) of cold 1 mM HCl. The resin was then washed with 10 CV of coupling buffer (0.2 M NaHCO<sub>3</sub>, 0.5 M NaCl, pH 8.3) before the addition of the ligand. Ligand was incubated with resin at 25°C for 4 hours or at 4°C for 16 hours. Coupling efficiency was determined by using absorbance of sample before and after coupling at 205 nm by following the protocol published by Scopes<sup>27</sup>. The pH of the coupling buffer was also varied (pH 6, pH 8.3, and pH 8.8) to determine the best coupling conditions. After coupling occurred, the activated groups were blocked using ethanolamine for 2-3 hours. The resin was then regenerated using alternating solutions of 0.1 M Tris buffer, pH 8 and 0.1 M acetate buffer, pH 4.5. The resin was then stored at 4°C in 20% ethanol.

This same protocol was followed for the coupling of HB-peptide to NHS-Sepharose. Ligand (2 mg to 10 mg HB-peptide) was incubated in coupling buffer (0.2 M NaHCO<sub>3</sub>, 0.5 M NaCl, pH 8.3) at varying temperatures as previously described. A column (labeled “negative”) was prepared by following the same protocol without the addition of ligand.



### ***Fluoroisothiocyanate (FITC)-Heparin Binding***

FITC-heparin obtained from Dr. David Zaharoff (University of Arkansas) was used to determine the binding capability of heparin to HB-peptide that was coupled to NHS-Sepharose.

Fluorescence spectroscopy was performed on fractions collected from the binding experiment using Hitachi F2500 fluorimeter, with an excitation wavelength of 488 nm and emission range of 500-600 nm. The emission maximum for FITC-heparin was 525 nm. The provided FITC-heparin sample was diluted in 10 mM Tris-HCl, pH 8 to obtain a total volume of 1 mL (same as the column volume). The fluorescence spectrum of this sample was obtained for both the HB-Sepharose and the negative control (without HB-peptide). The resins were equilibrated with 10 CV of 10 mM Tris-HCl, pH 8. After equilibration, FITC-heparin was incubated with the resin in a gentle rocking motion at 4°C for 2-3 hours. After centrifuging the resin at 3500 rpm, the supernatant was then decanted and centrifuged again at 13,000 rpm for 1 minute to remove any resin particulates. After the supernatant was decanted, the resin was incubated with 10 mM Tris-HCl with increasing concentrations of salt (100 mM to 2 M NaCl) for 10 minutes at 25°C for each concentration. The initial binding of FITC-heparin was then performed at 25°C for 1 hour as well to compare binding efficiency with that at 4°C. The preparation of FITC-heparin was attempted but resulted in only a few molecules of FITC coupled to heparin. The protocol produced by Nagasawa et al<sup>28</sup>, was modified. In short, 10 mg LMWH dissolved in 100 µL of 0.5 M carbonate buffer, pH 8.5. This mixture was added to a solution of 1.9 mL of DMSO containing 13 mg FITC. A 1:10 heparin: FITC molar ratio was obtained to ensure efficient FITC coupling. This solution was incubated at 37°C for 2 hours without rocking. The DMSO and free FITC was dialyzed in Milli-Q H<sub>2</sub>O every hour for 12 hours. After dialysis, no color was observed for the coupled FITC-heparin.

### ***NMR Spectroscopy of Glycosaminoglycans***

Proton NMR experiments were performed using Bruker Avance 700 MHz NMR at 25°C.

Measurements were performed on unfractionated heparin, CS, and DS in Milli-Q H<sub>2</sub>O (90% H<sub>2</sub>O + 10% D<sub>2</sub>O). All <sup>1</sup>H data were referenced to the resonance frequency of H<sub>2</sub>O (~ 4.7-4.8 ppm).

### ***Glycosaminoglycan Binding to HB-Sepharose***

HB-peptide was coupled to NHS-Sepharose (70% HB-peptide coupled) by the protocol stated above. The coupled HB resin was equilibrated extensively (10-15 CV) using 10 mM phosphate buffer, pH 7.2. The three GAGs chosen were DS, CS, and UFH. Each of these GAGs (5 mg) was dissolved in 10 mM phosphate buffer, pH 7.2, and the solutions were mixed together. This GAG mixture was incubated with the coupled resin at 4°C for 4 hours with gentle rocking. After incubation, phosphate buffer containing 100 mM to 2 M NaCl was used (2 CV each) to elute the GAGs. Each elution occurred after 15 minutes rocking at 25°C. The resin was centrifuged at 4500 rpm to settle the beads from which the liquid portions were dialyzed (MWCO 3 kDa) into 10 mM phosphate buffer, 100 mM NaCl, pH 7.2. The samples were then concentrated to 1 mL and were then analyzed by <sup>1</sup>H NMR spectroscopy on a Bruker Avance 700 MHz NMR at 25°C. These spectra were compared to the standard spectra of the GAGs in Milli-Q water previously acquired.

### ***Isolation of Glycosaminoglycans from Chicken Intestines***

Chicken intestines (obtained from Dr. Doug Rhoads, University of Arkansas) were mixed with 10 mM phosphate buffer, 100 mM NaCl, pH 7.2 and then blended using a high-speed blender provided by Dr. Frank Millett. After homogenizing the sample, it was centrifuged at 6,000 rpm,

and the solid layer (pellet) was first frozen in liquid nitrogen and then crushed using mortar and pestle. The crushed solid was added to the liquid layer and centrifuged again at the same speed. The resulting liquid layer (supernatant) was used for GAG isolation. To this sample, 2% sodium metabisulfite was added as a preservative for future storage. A control sample was prepared in similar fashion, but no enzyme addition occurred. To the liquid sample, DNase (0.5 mg/mL) was added and incubated with slow shaking (50 rpm) at 37°C for 6 hours or 0.1 mg/mL for 16 hours. The sample was again centrifuged, and the two layers (pellet and supernatant) were separated. Thermolysin (0.2 mg/mL) was then added to both layers and incubated at 70°C for 10 hours. The sample was again centrifuged, and two layers were separated. The liquid layer was dialyzed against 10 mM phosphate buffer, pH 7.2.

#### ***Quantification of Glycosaminoglycan Content Using Azure A Assay***

A 2 mg/100 mL solution of Azure A chloride (Sigma-Aldrich) in 1X PBS was used for the assay. Varying amounts of unfractionated heparin were prepared (1-500 µg) using 1X PBS. Absorbance measurements were acquired on an Agilent 8453 spectrophotometer at 620 nm after 30 min incubation. A solution containing 1 mL of Azure A and 1 mL of 1X PBS was measured as the 100% absorbance reading. This standard curve was developed using the absorbance reading given compared to the starting reading of 100% for the buffer and dye solution. The GAG amount in chicken intestines was calculated by measuring the absorbance at 620 nm using Azure A assay.

#### 4.4. Results and Discussion

***HB-peptide has greater binding affinity for heparin than other GAGs:*** GAGs are polydispersed polysaccharides, existing in various chain lengths of differing molecular weights. In this instance, it is extremely difficult to identify a specific molecular weight for experiments. However, average molecular weights for the GAGs have been reported, which are used for calculating binding affinities for the peptide and different GAGs. Using different average molecular weights, concentrations of the GAGs can be estimated and used for calculating the binding affinities through ITC experiments. HA is a large polysaccharide with average molecular weights in the thousands (kDa)<sup>29,30</sup>. In this context, a logical concentration for ITC could not be obtained for appropriate binding. The peptide binds to the various unfractionated GAGs in a 1:1 stoichiometry, and the spectra are hyperbolic (Figure 4.1). This change in binding from LMWH and HS (3 kDa) is probably due to the extreme polydispersity of the unfractionated polysaccharides. Large chains interact with the small peptide in a very different manner than the smaller chains found in LMWH and HS. There are also small chains present in the unfractionated GAGs as well that would interact with the peptide differently than the large chains, compromising the exact binding mechanism. The dissociation constants that exhibited the best  $X^2$  values were chosen for each GAG-peptide interaction, which are represented by the curves shown below (Figure 4.1). UFH binds with the best affinity for the peptide (nM) followed by DS (low  $\mu\text{M}$ ) then CS (higher  $\mu\text{M}$ ) and then HA that had no binding. It is expected that this peptide bind best to heparin because it has similar structural features as other HBPs that have good affinity for heparin.

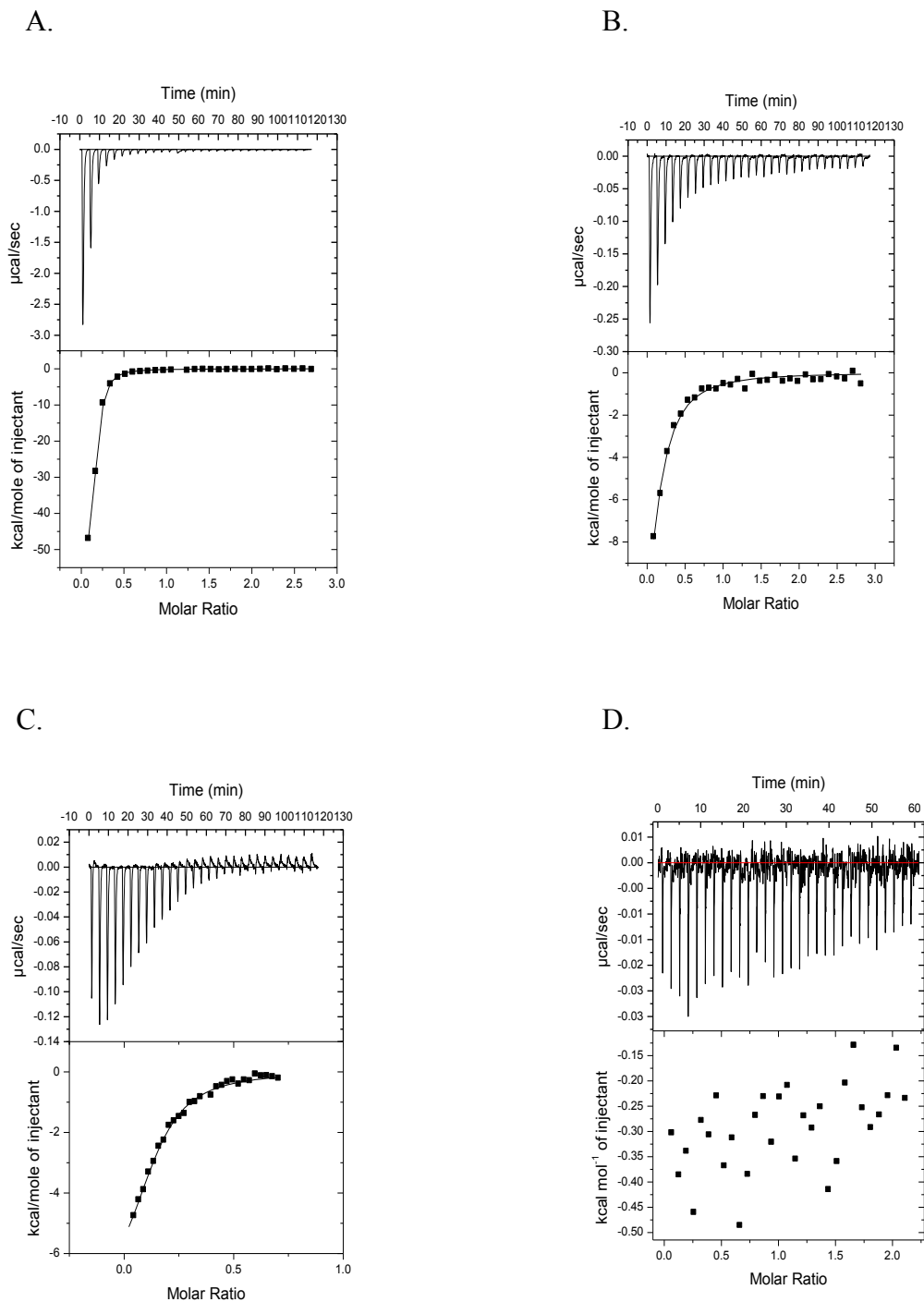


**Figure 4.1** – Isothermograms of the titrations of HB-peptide with UFH (Panel-A), DS (Panel-B), CS (Panel-C), and HA (Panel-B). A one-site binding model was used to fit the raw data from the titration, which is shown in the top panel. The bottom panel shows the integrated data from the raw data.

The molecular weights that exhibited the best binding curves and number of binding sites, not just dissociation constants, were chosen for analysis. As the estimated molecular weight drifts farther from the actual average molecular weight (less accurate estimated molecular weight), the binding curves do not fit the data as well. All of these variables were taken into account before the dissociation constants were determined. Heparin contains the most sulfation content among the GAGs, which gives it the highest negative charge. This greater negative character contributes to its better binding affinity for positively charged molecules (i.e. HBPs and the HB-peptide). HB-peptide would then be expected to bind more specifically to heparin because 1) it has similar structural features as the HBR of HBPs and 2) heparin contains more sulfate groups (i.e. negative charge), which would bind tighter to this positively charged peptide. DS has been shown to bind various heparin-binding proteins such as certain FGFs, which might explain the similarly shaped curve as heparin<sup>31,32</sup>. This phenomenon is thought to be due to the flexibility of the iduronic acid group present in heparin and DS, but not in CS<sup>33</sup>. The flexibility of these groups, usually modified with sulfate groups, orient the negative charges in such a position for ideal interaction with positively charged proteins. Even though DS possesses this ability, it does not displace heparin/HS in the body naturally. DS does not however compete with HS in the body for binding to FGF-2, which is probably due to the lack of kink or loop found in FGF-bound HS<sup>34</sup>. CS is also a negatively-charged molecule because it contains sulfate groups. These groups would interact with the positively charged peptide, causing some binding to occur. Chondroitin sulfate does exhibit some binding affinity for the HB-peptide but the dissociation constant is in the micromolar range, showing HB-peptide does bind with greater affinity to heparin. HA did not show any binding for the peptide, probably due to HA lacking sulfate groups. Other GAGs contain sulfate groups leading to their highly negative charge. HA does,

however, contain carboxylate groups so some negative charge exists for this molecule but not as much as the other sulfated GAGs. This property of HA could explain the lack of binding for the positively charged peptide. As stated earlier, GAGs consist of chains of varying length, resulting in high heterogeneity with regards to molecular weight. An average molecular weight is a value that takes into account the various chain sizes for an overall estimation. In the literature, DS is reported to be approximately 30 kDa to 50 kDa, whereas CS is close to 15 kDa, similar to heparin<sup>35,36,37,38</sup>. For this reason, an average molecular weight of 50 kDa is used as the maximum value for both GAGs; the molecular weight has not been reported to exceed this value. In the literature, heparin shows an average molecular weight of 13 kDa to 15 kDa<sup>39,40</sup>. As the estimated molecular weight of heparin draws near to 25 kDa, the dissociation constant falls in the nanomolar range. No matter what molecular weight is used for calculation of dissociation constants, based on the binding curves (Figure 4.1), heparin displays better binding affinity for the HB-peptide. As the average molecular weight of each GAG is increased, the dissociation constant,  $K_d$ , decreases (Figure 4.2).

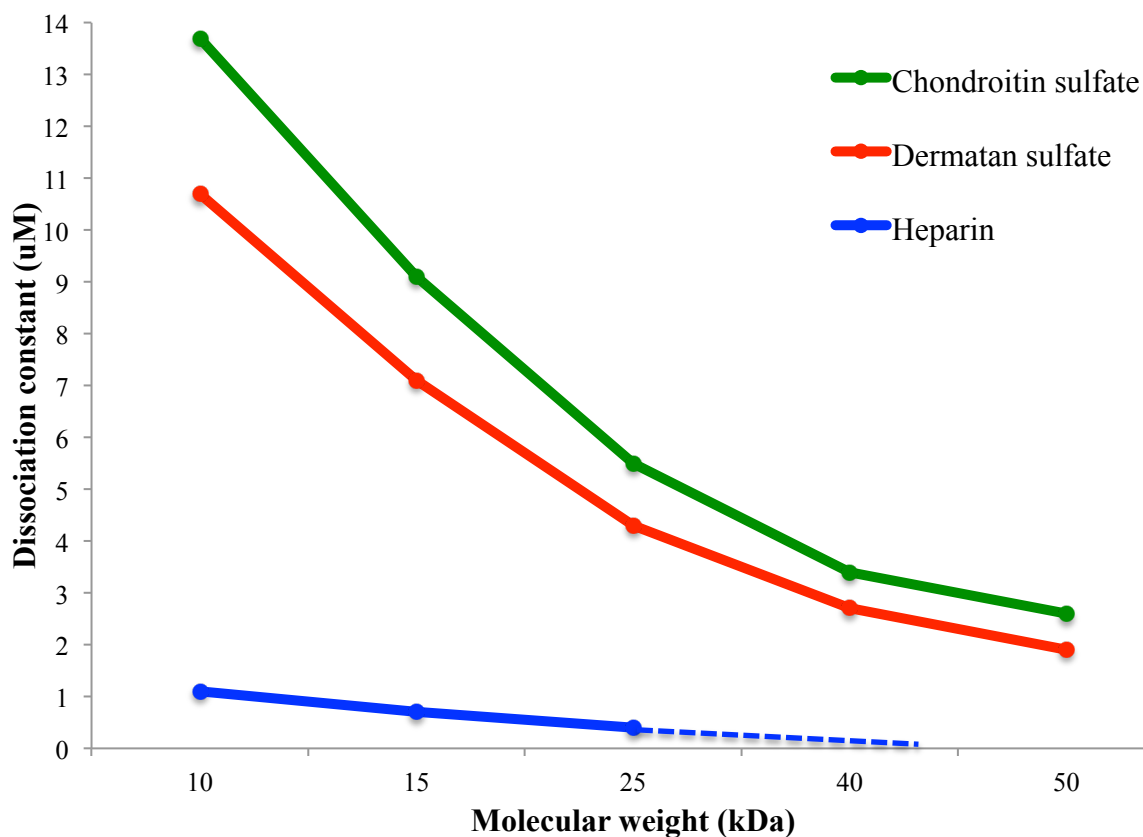


**Figure 4.2** – Plot of change in dissociation constants ( $K_d$ ) as a function of the molecular weights of CS (green), DS (red), and UFH (blue).

The blue dashed line represents the estimated effect that increasing molecular weight of heparin has on the corresponding dissociation constant. No matter what the exact molecular weight for each of the GAGs is, the binding affinity of the peptide for heparin continues to be better compared to the other GAGs. The binding affinity of HB-peptide is better for heparin than that of the other GAGs, as seen by the dissociation constant falling into the low nanomolar range (blue dashed line). These binding study results show promise for using HB-peptide as an affinity column for the separation of GAGs. Based on the binding curves, a table has been generated displaying the dissociation constants as a function of average molecular weight of the GAGs (Table 4.1).



	10 kDa	15 kDa	25 kDa	40 kDa	50 kDa
UFH	1.1	0.7	0.4	X	X
DS	10.7	7.1	4.3	2.7	1.9
CS	13.7	9.1	5.5	3.4	2.6

**Table 4.1** – Binding affinities ( $K_d$  in  $\mu\text{M}$ ) of HB-peptide for the various GAGs in 10 mM phosphate buffer, 100 mM NaCl, pH 7.2 as their estimated average molecular weights are varied.

The number of binding sites (N),  $X^2$  value, enthalpy, and entropy produced from the binding of HB-peptide to each of these GAGs is not shown but has been calculated for all interactions (MicroCal Inc.). From these results, it appears that the HB-peptide can be used to separate the GAGs from each other.

***NHS-Sepharose can be used for successful immobilization of HB-peptide:*** Since the peptide has good binding affinity for heparin compared to the other GAGs, it can be used as an affinity resin in order to separate heparin from the other GAGs. NHS-Sepharose is a resin that is capable of immobilizing small molecules such as peptides and antibodies onto which ligands and antigens bind to their desired target. This activated resin is prepared by coupling Sepharose with 6-aminohexanoic acid, which is then activated by esterification with NHS. Ligands that have primary amino groups are easily coupled to this ester group to form amide linkage, after which the peptide amino groups displace the NHS group. Before coupling HB-peptide, GSH is successfully coupled to NHS-Sepharose with yields up to roughly 70% coupling efficiency (Table 4.2). This efficiency is achieved by using GSH in excess of 5:1 of the NHS groups present.

GSH:NHS	pH	Temp (°C)	Time (hour)	Blocking time (hour)	Coupling efficiency (%)	GST amount (ug)	pH of 1X PBS	Temp (°C)	Time (hour)	Protein binding
5:1	6	25	4	none	50	10	7.2	25	4	
5:1	6	25	4	none	50	10	6	25	4	
5:1	6	25	4	none	15	10	7.2	25	4	
5:1	8.3	25	4	1	40	500	7.2	25	0.5	
5:1	8.3	25	16	1	50	500	7.2	25	0.5	
5:1	8.3	25	4	2	50	200	7.2	25	0.5	
5:1	8.3	25	4	1	50	350	7.2	4C then 25C	1 hour at 4C then 1 hour at 25C	✓
5:1	8.3	25	4	1	50	300	7.2	gravity flow at 25C	Abs at 280nm used to detect	✓
5:1	8.3	25	3	none	40	100	6	25	1	
25:1	8.3	25	3	none	20	100	6	25	1	
5:1	8.8	25	3	none	20	100	6	25	1	
100:1	8.8	4	16	none	40	100	7.2	25	2	
commercial GSH						10	7.2	25	4	✓
none						200	7.2	25	0.5	
none						500	7.2	25	0.5	

**Table 4.2** – Conditions of GSH coupling to NHS-Sepharose. The buffer pH, temperature and time of incubation, and mole-to-mole ratio of target ligand to NHS groups were varied to obtain the most optimal coupling efficiency and subsequent protein binding.

Purification of GST-tagged proteins is currently accomplished by affinity chromatography using commercially available GSH-Sepharose<sup>41,42</sup>. This method is applied to the experimentally prepared GSH-Sepharose for the binding studies of GST and GST-C2A. Both proteins bind to the prepared resin and only elute using excess GSH. It could be questioned whether or not uncoupled NHS groups on the resin might nonselectively bind GST and allow it to bind to the prepared GSH column. This problem is circumvented by blocking all uncoupled groups with ethanolamine, which also removes excess GSH that did not couple to the resin. Both proteins elute in 10 mM GSH, but some protein also elutes in 1X PBS (Figure 4.3). This finding is

probably due to the number of GSH groups present on the experimentally coupled GSH resin is less than the commercial GSH-Sepharose resin, which means less protein can be bound.

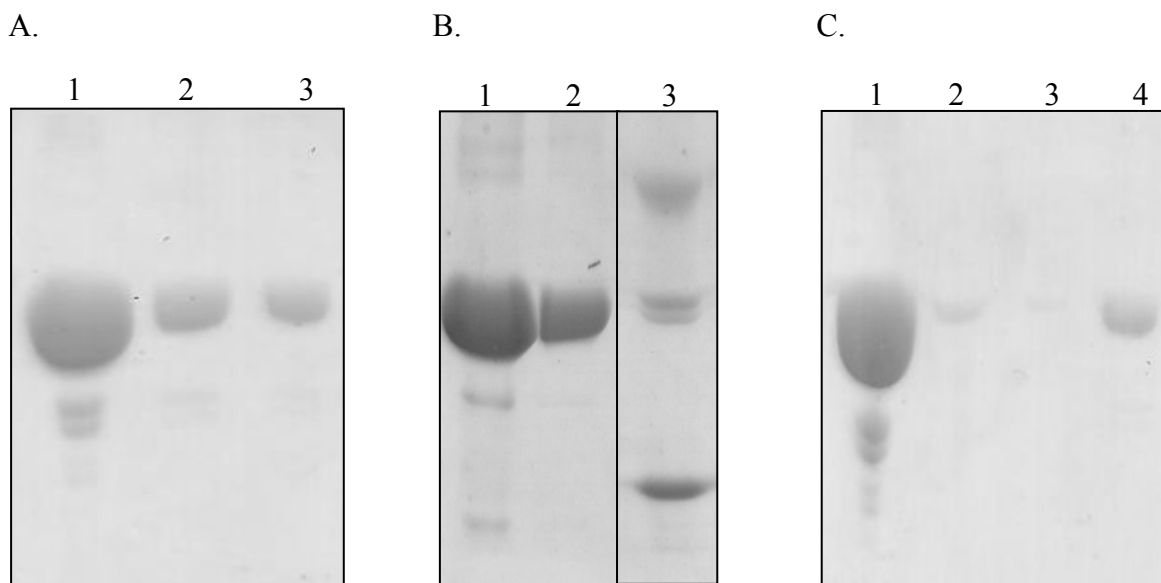


**Figure 4.3** – Binding studies of GST-C2A (Panel-A) and GST (Panel-B) to GSH-coupled Sepharose and GST-C2A to commercially available GSH-Sepharose (Panel-C). Panel-A, Lane 1, unbound GST-C2A; Lane 2, flow-through; Lane 3, 10 mM GSH (eluted GST-C2A); Panel-B (GST): Lane 1, unbound GST; Lane 6, 10 mM GSH (eluted GST); Panel-C (GST-C2A on commercial GSH-Sepharose): Lane 1, GST-C2A; Lane 2, unbound GST-C2A; Lane 3, flow-through; Lane 4, 10 mM GSH (eluted GST-C2A).

If the same amount of GST-tagged protein is loaded onto a resin with less available GSH, an excess of a GST-tagged protein to available GSH groups occurs. There is always a chance of such a small ligand as GSH getting buried in the beads due to their small size, which limits the accessibility of the ligand (GSH) for its target (GST-tagged proteins). Using larger ligands such as the HB-peptide that has 34 amino acid residues can circumvent this problem. Successful binding and elution of GST-tagged proteins using GST-coupled NHS-Sepharose did occur. HB-peptide is also successfully coupled on NHS-Sepharose using the similar method as GSH. The primary amino group at the N-terminal end of the peptide rapidly forms a stable amide linkage with the 6-aminohexanoic acid, allowing the successful coupling onto Sepharose beads for

further use as an affinity column for purifying heparin. The incubation temperature and time did not cause a significant change in coupling efficiency (percentage) when the experimental conditions were varied. The longer incubation time caused an increase of only 5-10% efficiency. It would seem more appealing to save on time of coupling than to gain 5-10% yield. As the amount of peptide (mg) that is loaded is increased, the corresponding amount of peptide (mg) retained on the resin is also increased, as expected (Figures 4.4 and 4.5). No matter what amount of peptide is applied to the resin, the efficiency (percentage) remains constant; with the corresponding amount of peptide (mg) increasing that has adhered to the column. This efficiency (percentage) is comparable to reported values in the literature for several other proteins<sup>26,43</sup>.

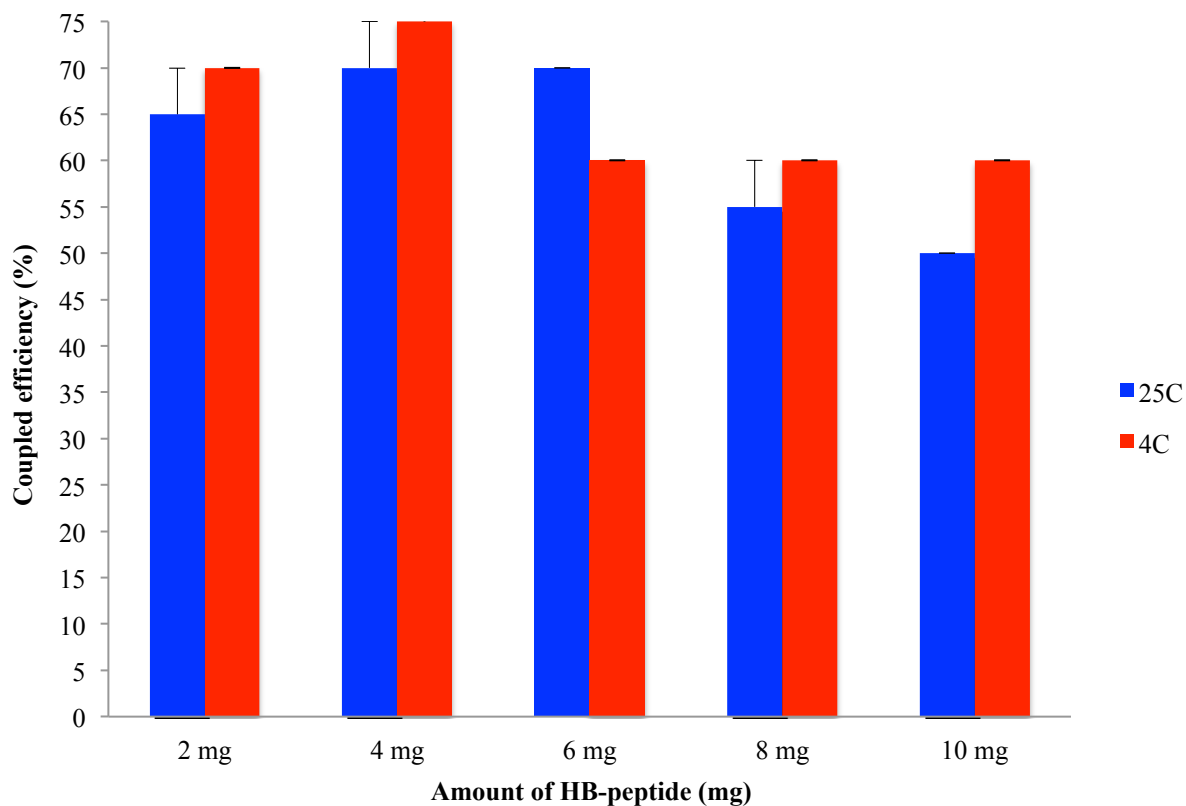


**Figure 4.4** – Plot of the coupling efficiency (percentage) for the coupling reaction of HB-peptide to NHS-Sepharose as a function of the amount of HB-peptide (mg) used at at 25°C (blue) and 4°C (red).

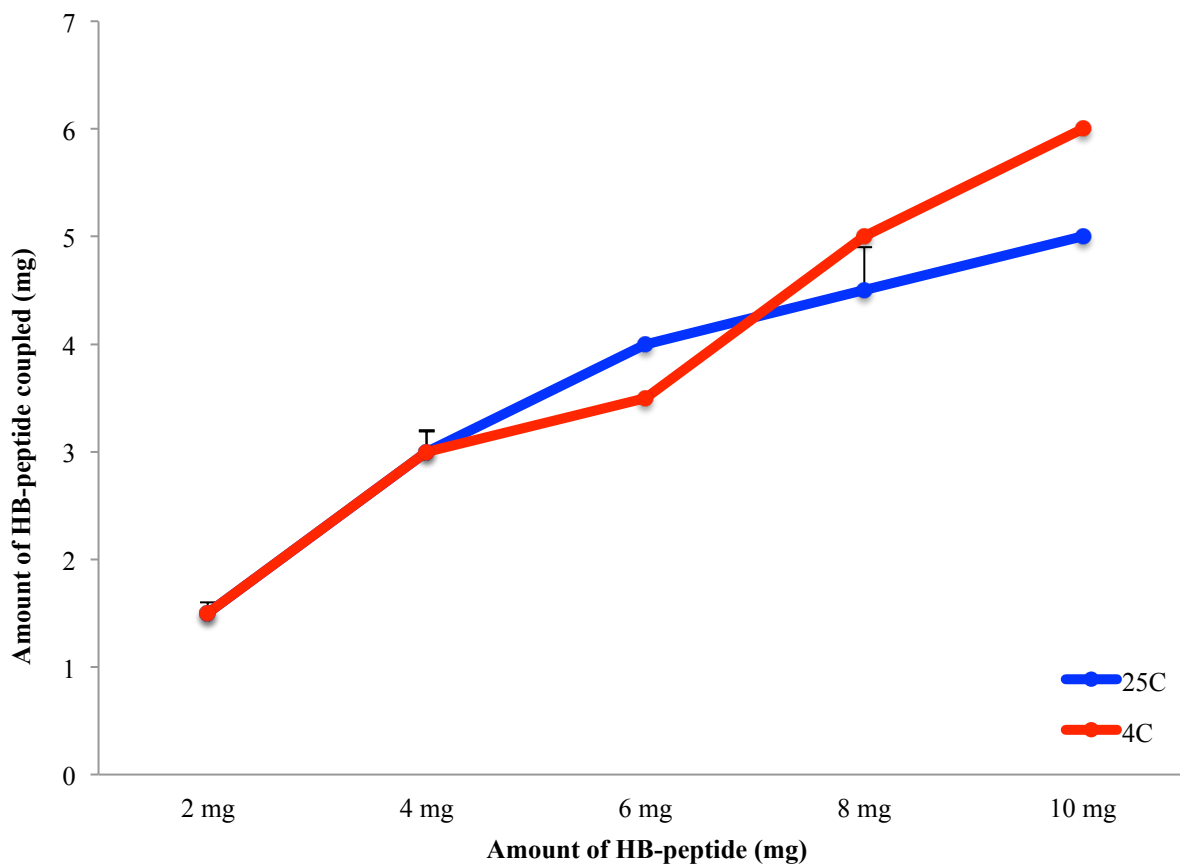


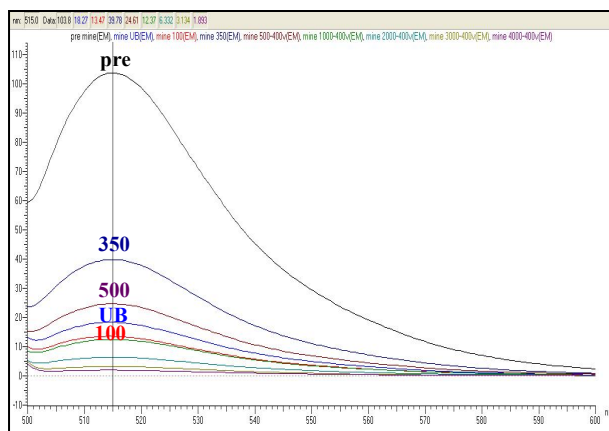
**Figure 4.5** – Plot of the amount of HB-peptide (mg) coupled to NHS-Sepharose as a function of increasing the amount of HB-peptide (mg) used at 25°C (blue) and 4°C (red).

The highest efficiency obtained for this coupling method is about 75% for 4°C and 70% for 25°C. In 1 mL of resin, the highest amount of peptide coupled is about 6 mg. There is a good chance that if more peptide were added to this small amount of resin, overcrowding of the groups would occur, resulting in steric hindrance. This would then cause less accessibility of groups to bind to their ligand, heparin, and consequently leading to a decrease in heparin binding.

***FITC-heparin has strong binding affinity for prepared HB-affinity column:*** Heparin is not easily identified spectroscopically except for NMR, but this method is very susceptible to changes in proton chemical shift values due to high salt concentrations. To bypass this problem,

heparin is attached to a fluorescent dye, FITC. The elution of this colored heparin can also be easily detected visually instead of by other tedious spectroscopic methods. In order to methodically determine the exact binding efficiency of heparin to the prepared column, fluorescence spectroscopy is useful. A question might arise if the heparin molecule is actually binding to the attached HB-peptide or it is just physically adsorbed onto the resin itself, so a column (deemed “negative”) is prepared without HB-peptide. Since the “negative” column does not contain HB-peptide, it is not expected to bind FITC-heparin. As seen in the fluorescence spectra for all of the FITC-heparin fractions that elute from the HB-column (Figure 4.6), the majority of FITC-heparin is present in the 350 mM and 500 mM NaCl fractions. In contrast, the “negative” column elutes heparin after the first round of binding, suggesting that heparin is actually binding to the coupled peptide and not just adsorbed on the resin.

A.



B.

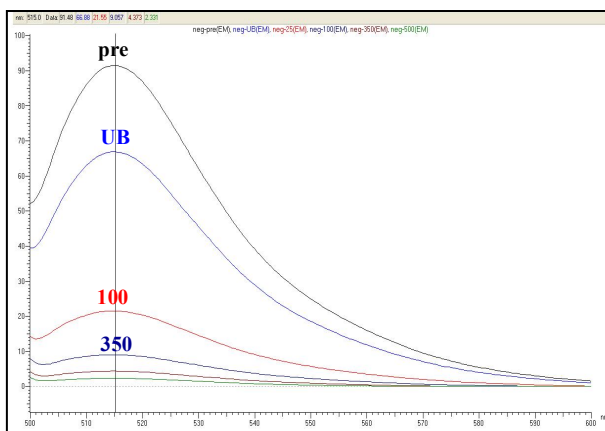


**Figure 4.6** – Fluorescence spectra of FITC-heparin (in 10 mM Tris buffers, pH 8) elution from HB-coupled-Sepharose (Panel-A) and “negative” column of NHS-Sepharose (Panel-B).

On average, about 60% of FITC-heparin is retained on the HB-column (elutes between 350 mM and 500 mM NaCl), which is promising for large-scale heparin binding studies (Figure 4.7). The

majority of FITC-heparin did not bind to the “negative” column, with approximately 75% eluted in the unbound state.

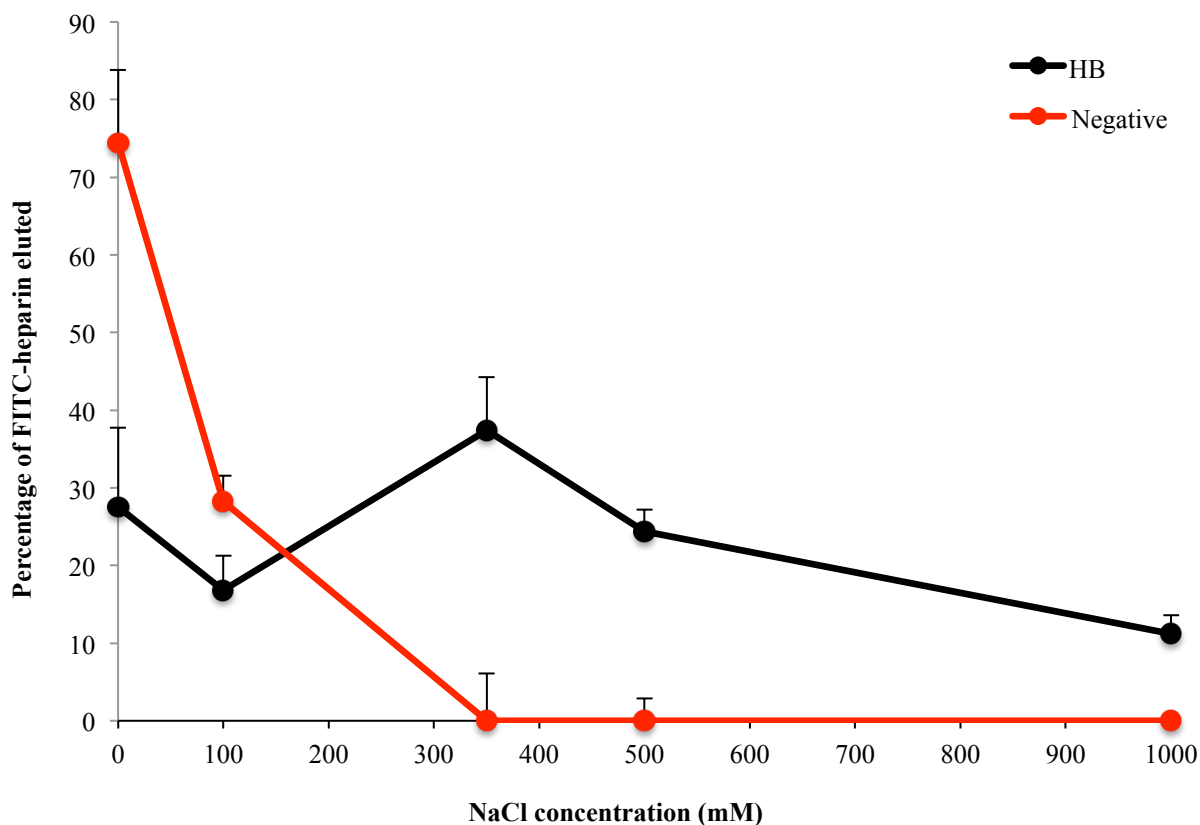


**Figure 4.7** – Plot of elution of FITC-heparin from HB-coupled-Sepharose (black line) and “negative” column, NHS-Sepharose (red line).

The binding studies of FITC-heparin are normally performed using centrifugation of the resin and decanting of the supernatant from the resin, which could result in a loss of FITC-heparin and resin after every elution. For more in-depth binding studies, other methods such as flow chromatography should be employed to avoid loss of FITC-heparin and resin in the future.

Another promising find is that even after several days of storage at 4°C, the affinity resin shows only a slight decrease in binding efficiency (60% to 50%). It is desired to employ this HB-affinity column to separate heparin from the other GAGs (Figure 4.8), but a dye would not be

present on naturally occurring heparin samples that contain other GAGs. In this case, there needs to be another efficient method of detection of the GAGs without attaching a dye. It is expected that CS, then DS, then heparin would elute from the HB-affinity column, based on the binding affinity studies performed by ITC; heparin has greatest binding, then DS, then lastly CS.

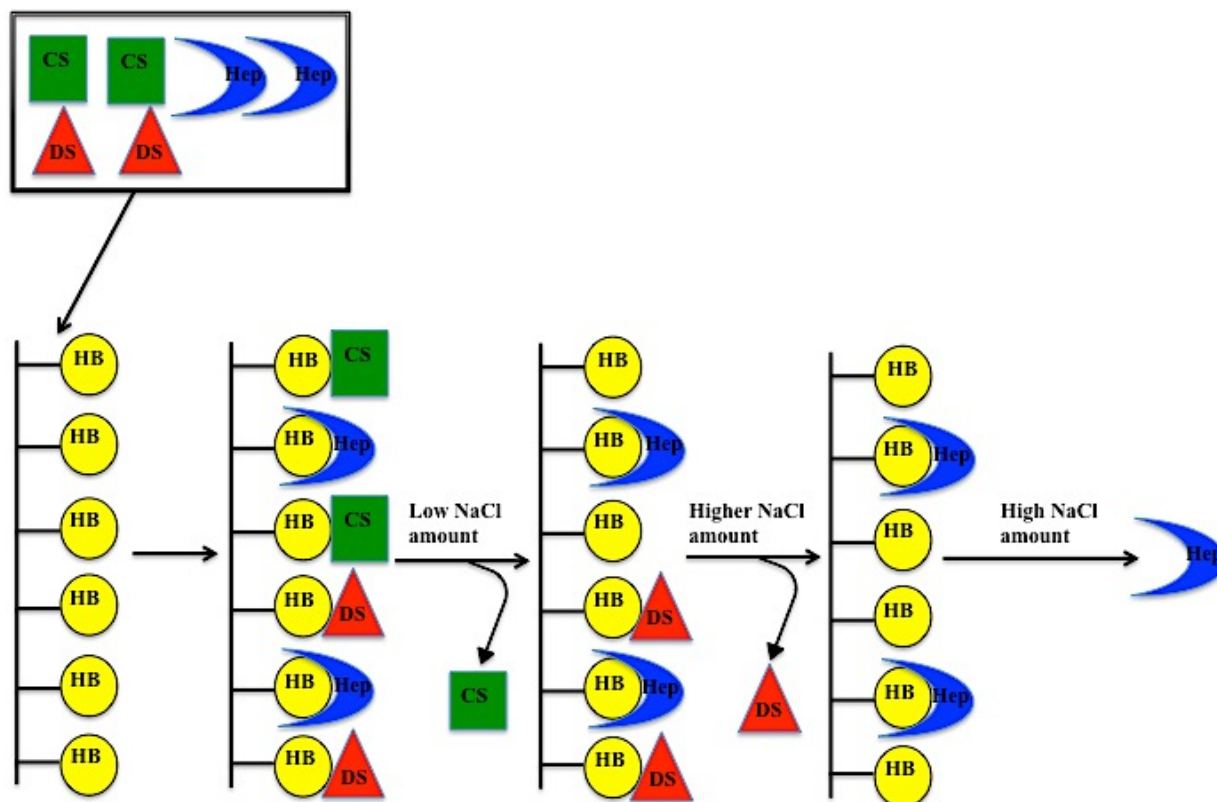


**Figure 4.8** – Cartoon representation of the separation of CS, DS, and heparin using HB-affinity column and NaCl step-wise gradient.

***Each glycosaminoglycan has specific fingerprint in proton NMR spectroscopy:*** NMR

spectroscopy, especially  $^1\text{H}$  NMR, has been used to successfully differentiate various GAGs as well as identify OSCS and DS contaminants in heparin samples<sup>35,44</sup>. There are various “standard” peaks that each GAG contains to identify it from the others. For example, Lee et al has shown that the acetyl group in a proton spectrum ( $\sim 2.0$  ppm) can be used as a fingerprint for the various GAGs<sup>45</sup>. There is however caution required when identifying the GAGs based on



this peak alone because it is such a narrow range. For example, heparin's methyl resonance is around 2.05 ppm, CS has one from 2.00 to 2.06 ppm, and DS contains one from 2.07 to 2.09 ppm<sup>46,47</sup>. Again, the exact chemical shifts can change depending on the solvent used. The presence of OSCS in heparin samples produces a peak at 2.15 ppm<sup>46</sup>. This extreme shift of 0.15 ppm from the corresponding 2.00 ppm methyl proton of the acetyl group in heparin would actually be useful for the detection of OSCS impurity in heparin. For the other GAGs that still need to be removed from heparin, other peaks need to be identified as markers. Based on the analysis of several heparins, other peaks that are always present are 5.42, 5.23, 5.01, 4.82, 4.60, 4.40, 4.34, 4.27, 4.12, 4.03, 3.87, 3.77, 3.67, 3.40, and 3.28<sup>46</sup>. These peaks are extremely helpful in identifying important peaks present in heparin. When comparing heparin to the other GAGs, the NMR spectrum of each GAG needs to be measured in order to determine similarities and differences in the GAG structures. The NMR spectra of all three GAGs are overlaid to visually identify unique peaks of interest for each GAG (Figure 4.9).

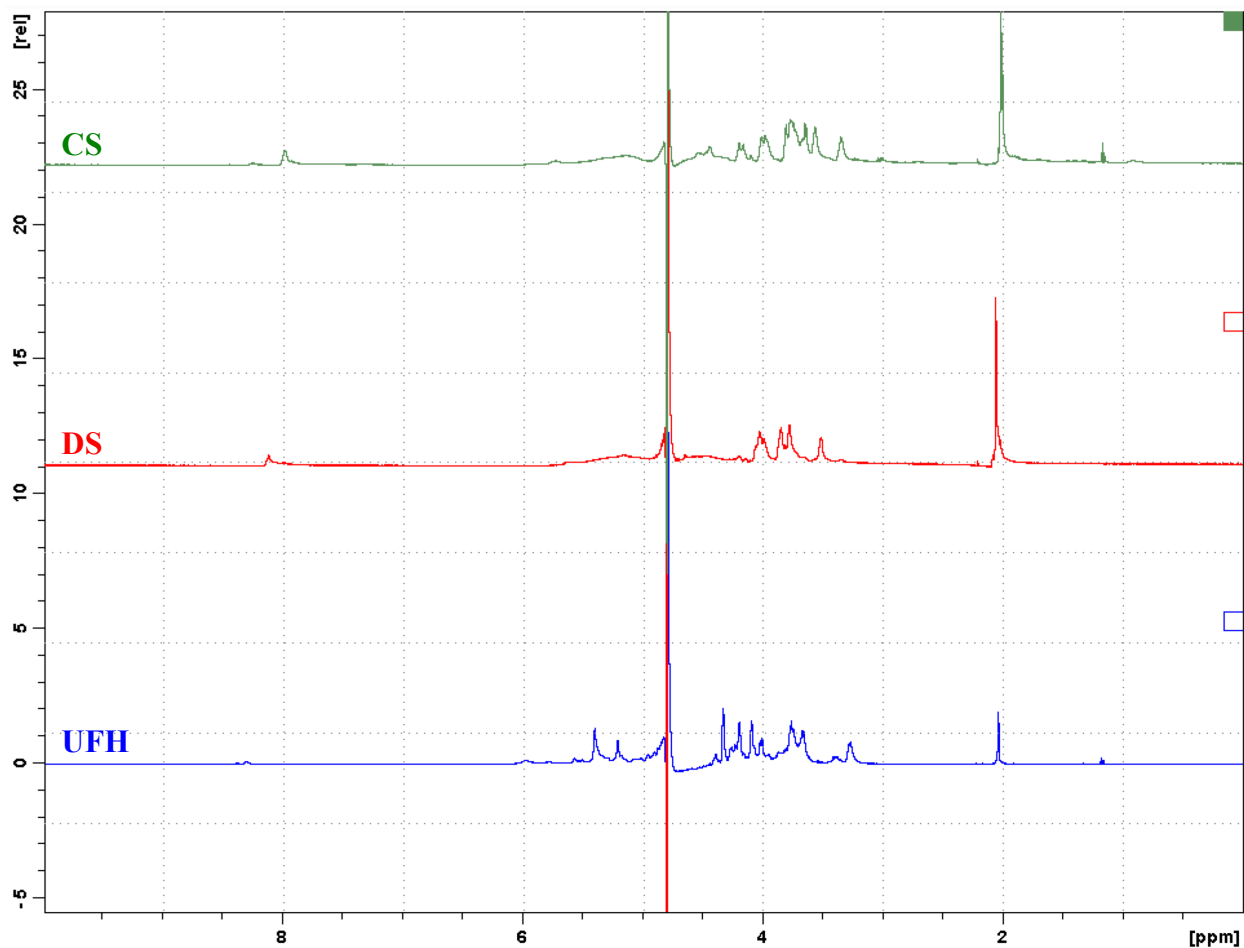


**Figure 4.9** – The <sup>1</sup>H NMR spectra of CS (green), DS (red), and UFH (blue) in 10 mM phosphate buffer, 100 mM NaCl, pH 7.2 in 10% D<sub>2</sub>O at 298 K.

By obtaining all of the peaks that are present in each GAG, the peaks that are within 0.02 ppm of each other are discarded. After this is performed, the peaks that are uniquely found in UFH, CS, or DS alone were identified as important peaks in heparin (Figures 4.10, 4.11, 4.12).

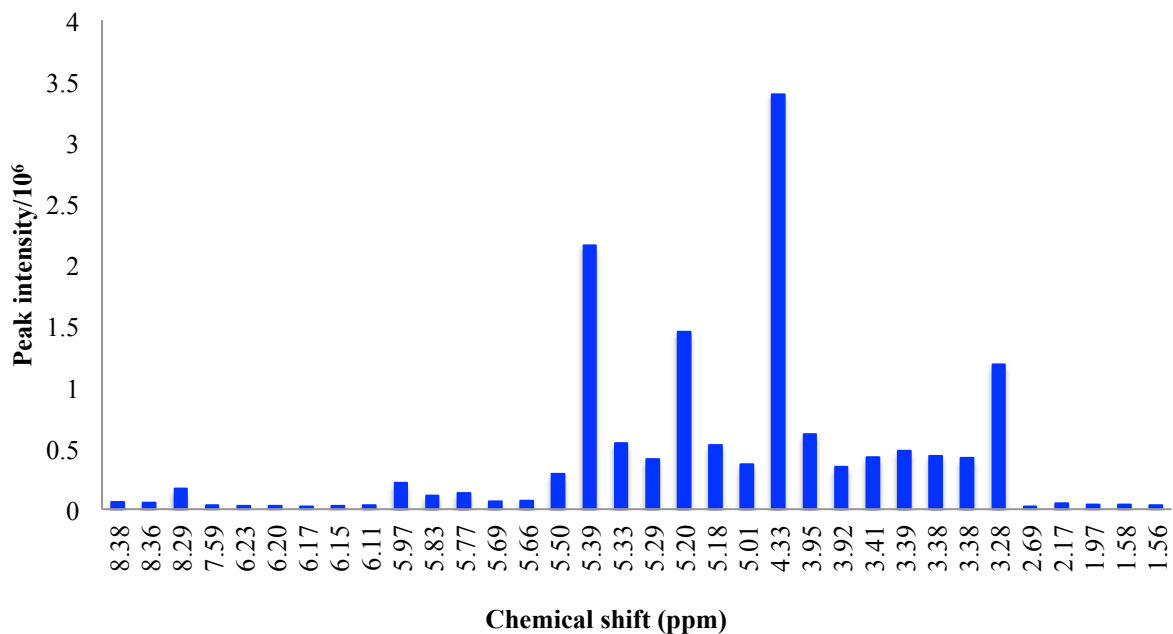


**Figure 4.10** – Plot of the unique <sup>1</sup>H NMR peaks present in the standard UFH sample.

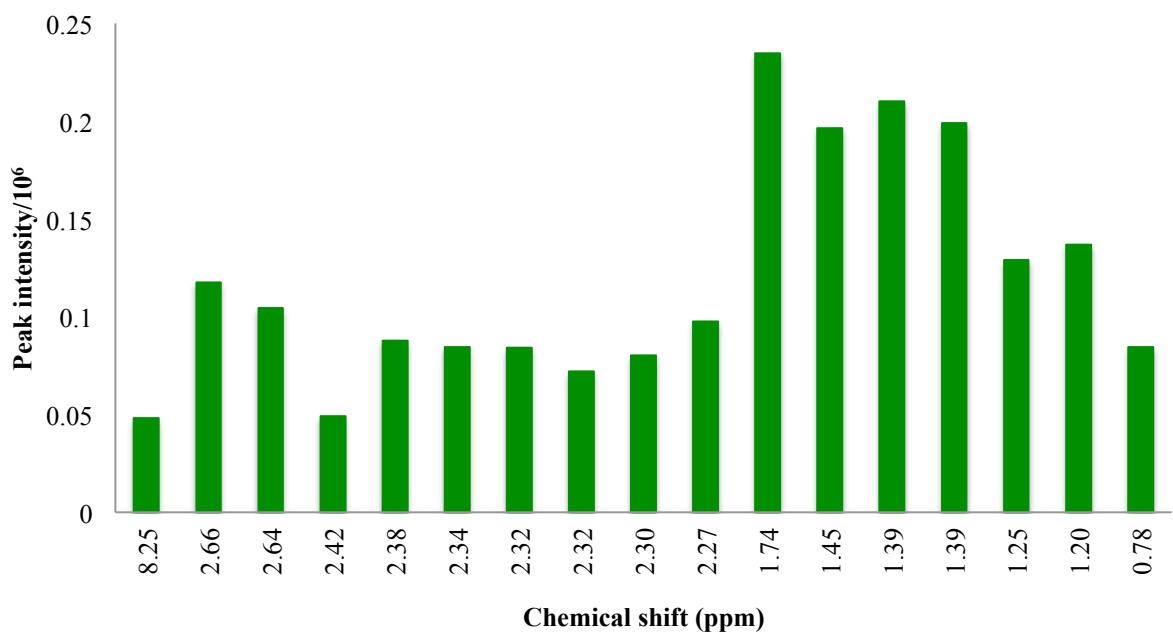


**Figure 4.11** – Plot of the unique <sup>1</sup>H NMR peaks present in the standard CS sample.

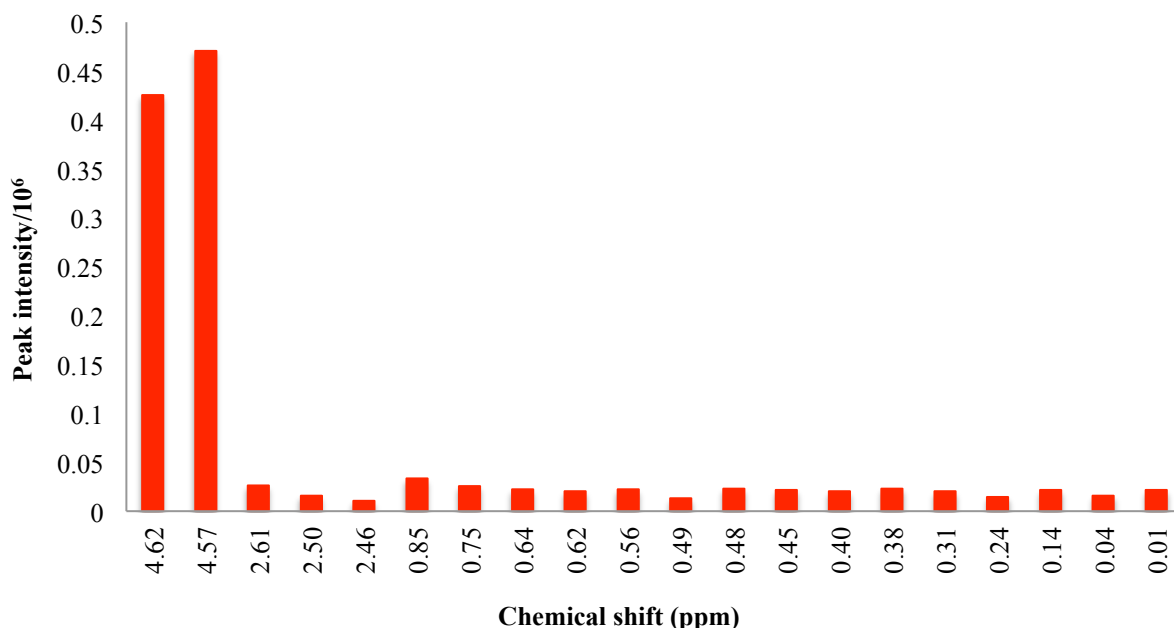


**Figure 4.12** – Plot of the unique <sup>1</sup>H NMR peaks present in the standard DS sample.

These unique peaks can now be used to identify GAGs that are present in eluted fractions once binding of a GAG mixture to HB-affinity column occurs. The few peaks that elicit a stronger signal are used for detection of UFH, CS, and DS in the fractions collected from the affinity column (Table 4.3). The peaks observed in both CS and DS are indistinguishable from each other and are identified as strictly an impurity if found in the UFH sample.

Unique peaks in UFH	Unique peaks in CS	Unique peaks in DS	Unique peaks in CS and DS
5.39	2.66	4.62	5.1
5.33	2.64	4.57	5.14
5.29	-	-	5.15
5.2	-	-	-
5.01	-	-	-
3.41	-	-	-
3.39	-	-	-
3.28	-	-	-

**Table 4.3** – Isolated peaks used for identification of GAGs during binding studies on HB-affinity column.

***Slight separation of GAGs is observed using HB-affinity column:*** After these “standard” peaks are detected, they were then searched for in all of the fractions collected from the HB-affinity column. Even though the methyl proton in the acetyl group around 2.0 ppm is a good marker for most heparin samples, this peak is only present in fractions from 0 mM to 300 mM NaCl, and not beyond this point. After 300 mM NaCl, this peak cannot be used to obtain information about each GAG. Based on the ITC experiments, DS and CS do bind to HB-peptide but not as tightly as heparin does. Binding of these GAGs is expected once applied to the affinity column, but not tight binding that would require the addition of high salt concentrations to elute. DS has a better binding affinity than CS, so DS would be expected to elute at higher salt concentration than CS. Due to the polydispersity of the GAGs, the various-sized chains would have a propensity to bind with different affinities to the HB-peptide. This phenomenon would most likely result in elution of various chains of each GAG in each fraction. The main objective of this experiment is as heparin is eluting (at high salt concentration), it would not contain any other GAG impurity. From the NMR spectra different eluted fractions, heparin is present in all the fractions (Figure 4.13). Because of its heterogeneity in molecular weight, this finding is not unexpected. The amount of sulfation is dependent on the polydispersity of the heparin sample, which leads to a variation in negative charge for each chain. Unfractionated heparin contains chains of varying lengths, which would bind to the HB-peptide with different strengths and behaviors, causing them to be eluted in varying concentrations of salt. This phenomenon leads to a loss of heparin during the purification process because some of the chains elute at lower salt concentrations. The heparin sample is bound to the HB-affinity resin with different affinities, which does not allow all of the heparin sample to elute only at high salt concentration. If the heparin sample

consists of chains of the same molecular weight, we would ensure all of heparin would elute only at high salt concentration.

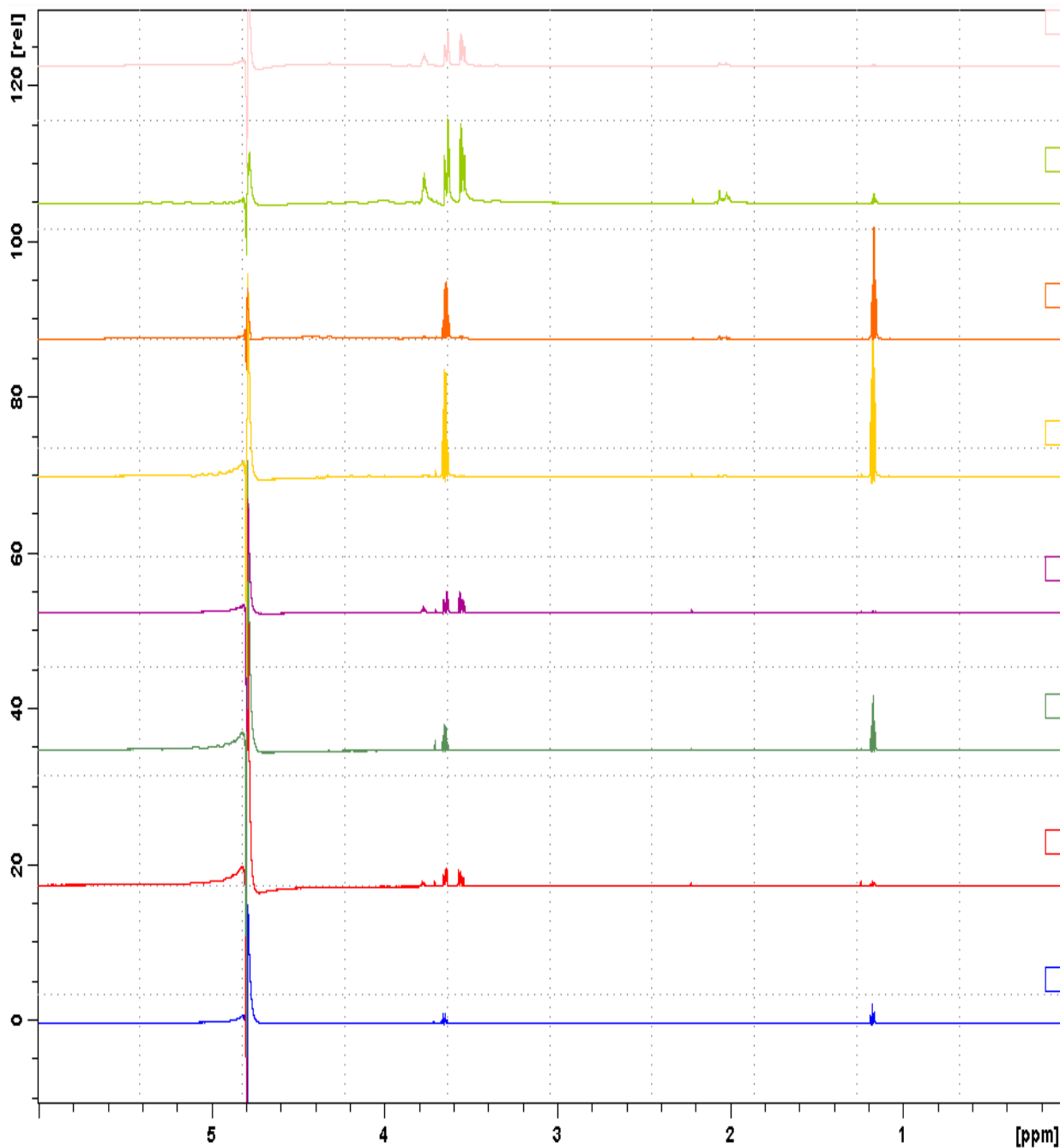


**Figure 4.13** – Overlay of  $^1\text{H}$  NMR spectra of all GAG fractions collected from the HB-affinity column. Unbound is light pink, 0 mM NaCl is lime green, 100 mM NaCl is orange, 200 mM NaCl is yellow, 300 mM NaCl is purple, 400 mM NaCl is green, 500 mM NaCl is red, and 2 M NaCl is blue.

From the unbound state to 100 mM NaCl, there is a reasonably good distribution of all three GAGs (Figure 4.14, 4.15, 4.16). This is promising because CS and DS impurities in heparin samples would elute at lower NaCl concentration, leaving pure heparin in fractions that elute at higher NaCl (300 mM to 500 mM). Before the 2008 contamination scare, very small trace amounts of impurities of GAGs were present in heparin samples, but they did not interfere with the biological activity of pharmaceutical heparin.

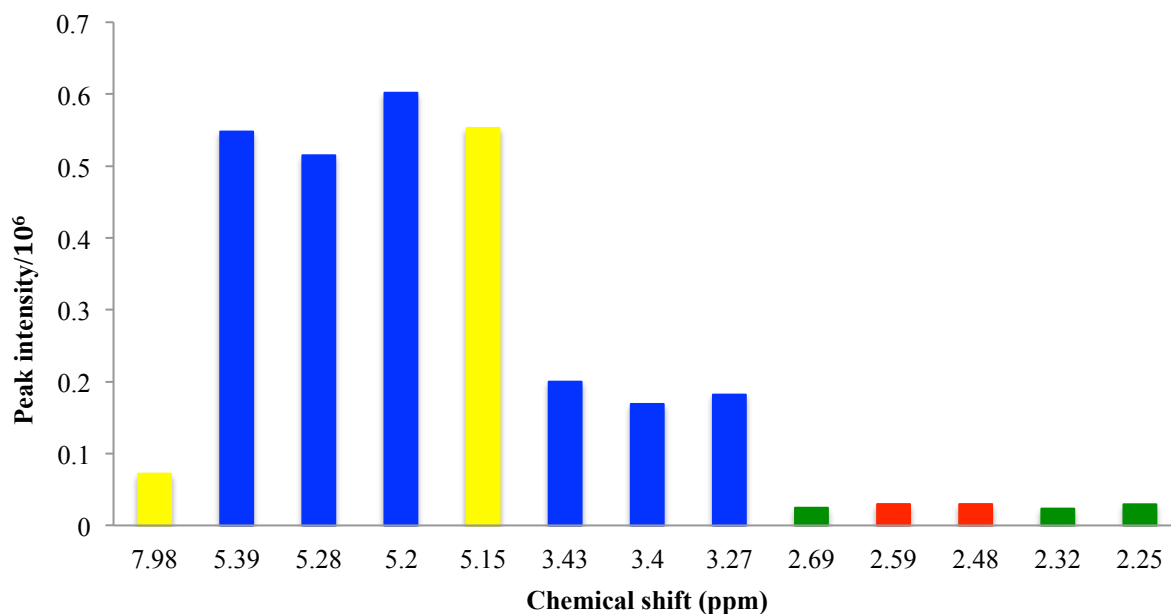


**Figure 4.14** – Plot of “standard” peaks identified in the unbound fraction from HB-affinity column. Heparin peaks are in blue, CS peaks are in green, DS peaks are in red, and the peaks in both CS and DS denoted as “impurities” are in yellow.

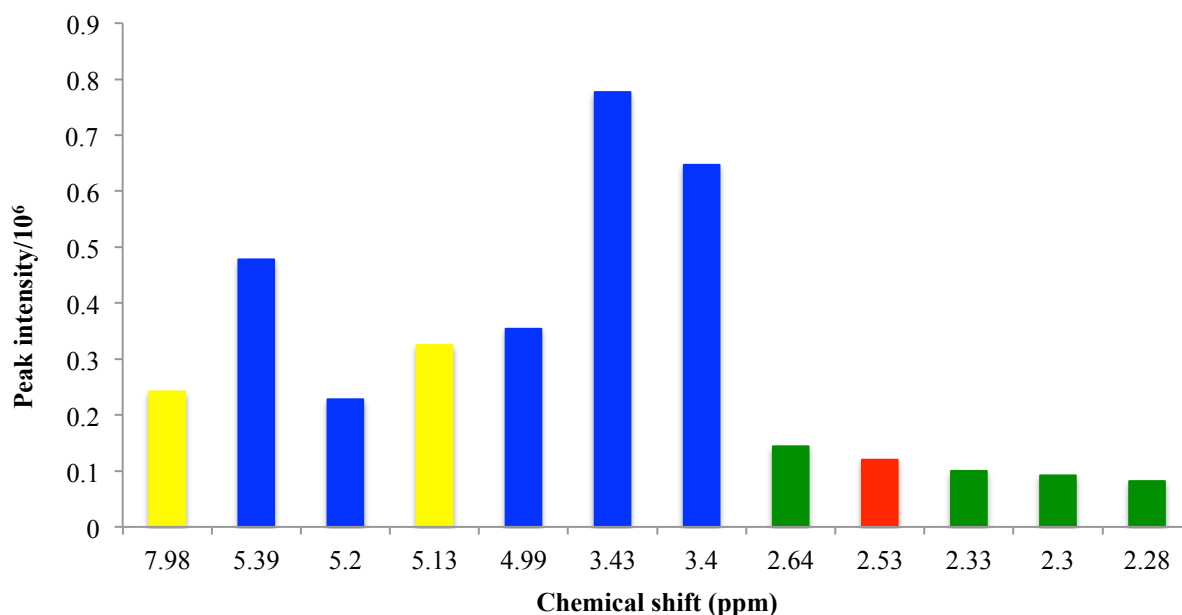


**Figure 4.15** – Plot of “standard” peaks identified in the 0 mM NaCl fraction from HB-affinity column. Heparin peaks are in blue, CS peaks are in green, DS peaks are in red, and the peaks in both DS and CS denoted “impurities” are in yellow.

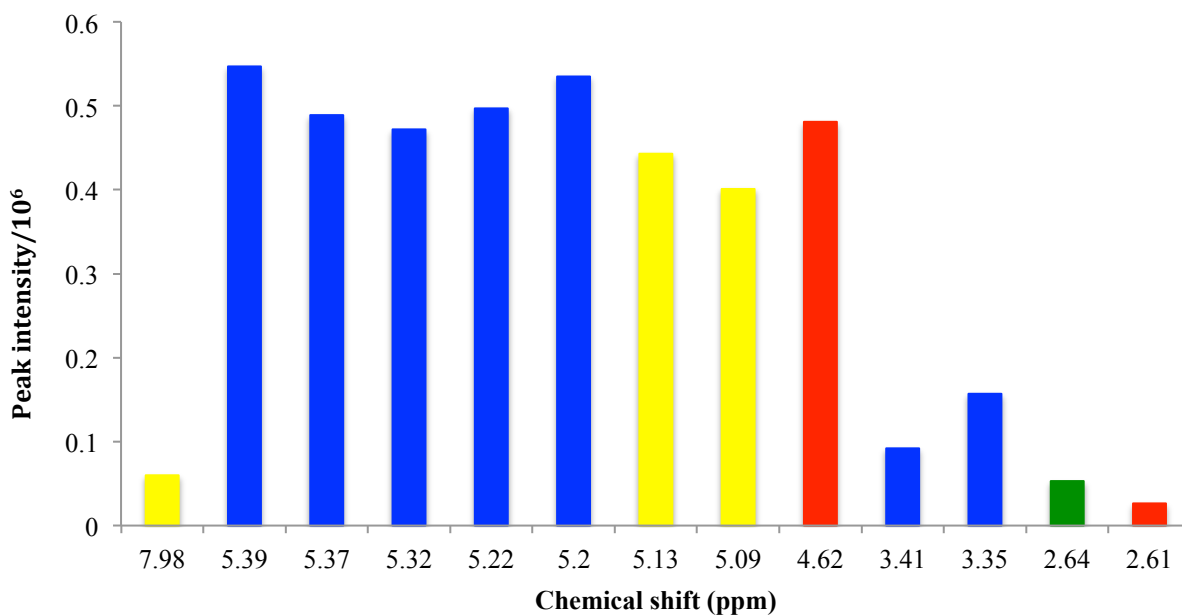


**Figure 4.16** – Plot of “standard” peaks identified in the 100 mM NaCl fraction from HB-affinity column. Heparin peaks are in blue, CS peaks are in green, DS peaks are in red, and the peaks in both DS and CS denoted as “impurities” are in yellow.



As the salt concentration increases all the way to 400 mM, heparin continues to be eluted with high peak intensities but there are also peaks corresponding to the “impurities” peaks present in both CS and DS. At this point it is still difficult to determine which GAG these yellow peaks represent. It is interesting to observe larger peaks corresponding to heparin in the 200 mM NaCl fraction (Figure 4.17), but it does not necessarily equate to larger yield of the heparin sample. This finding could be due to the heparin chains that elute at 200 mM NaCl containing more individual structural groups having more yield. For example, a longer chain of heparin contains more individual groups than a shorter chain, which in turn, produces more signals in the NMR spectrum. It is interesting to note that at 300 mM NaCl (Figure 4.18), two peaks representing CS are present, even though it would be expected that CS would elute at a lower NaCl concentration. After this point, however, there are no unique peaks corresponding to CS alone that are discovered in the higher salt concentrations (>400 mM NaCl). Again, at 400 mM NaCl (Figure 4.19), the mysterious “impurity” peak exists along with peaks corresponding to heparin.

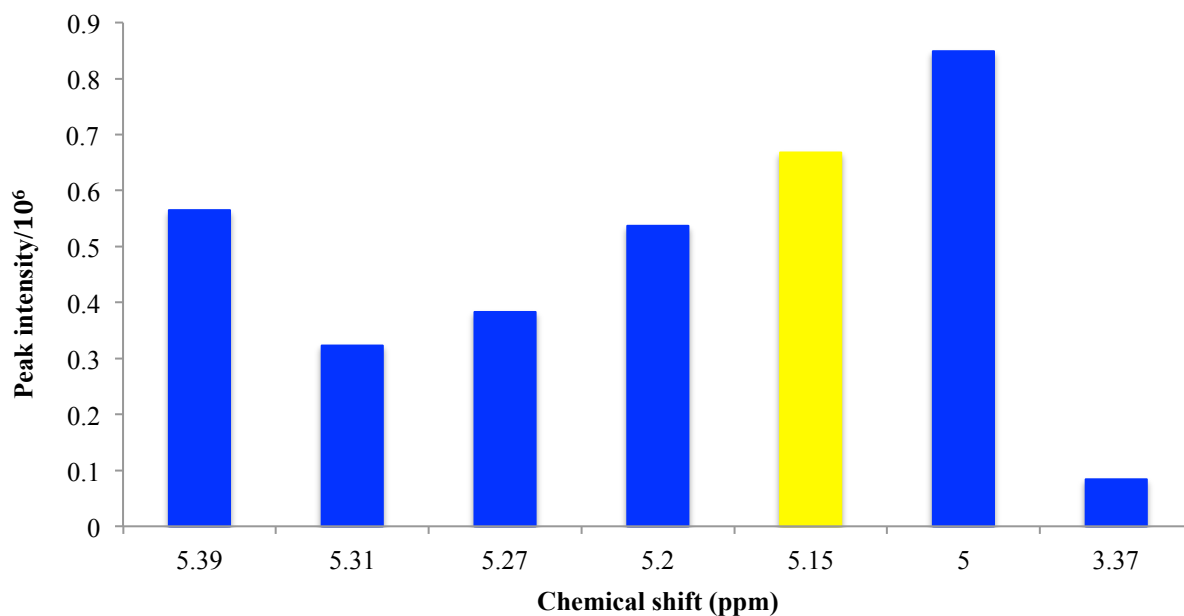


**Figure 4.17** – Plot of “standard” peaks identified in the 200 mM NaCl fraction from HB-affinity column. Heparin peaks are in blue and the peak in both DS and CS denoted as “impurity” is in yellow.

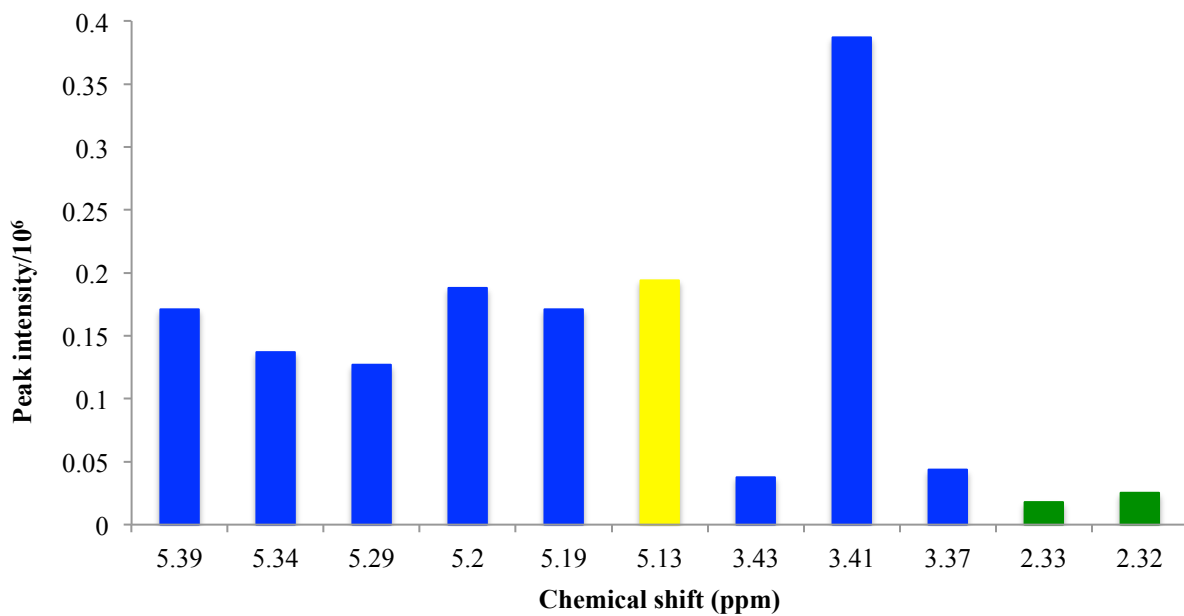


**Figure 4.18** – Plot of “standard” peaks identified in the 300 mM NaCl fraction from HB-affinity column. Heparin peaks are in blue and the peak in both DS and CS denoted as “impurity” is in yellow.

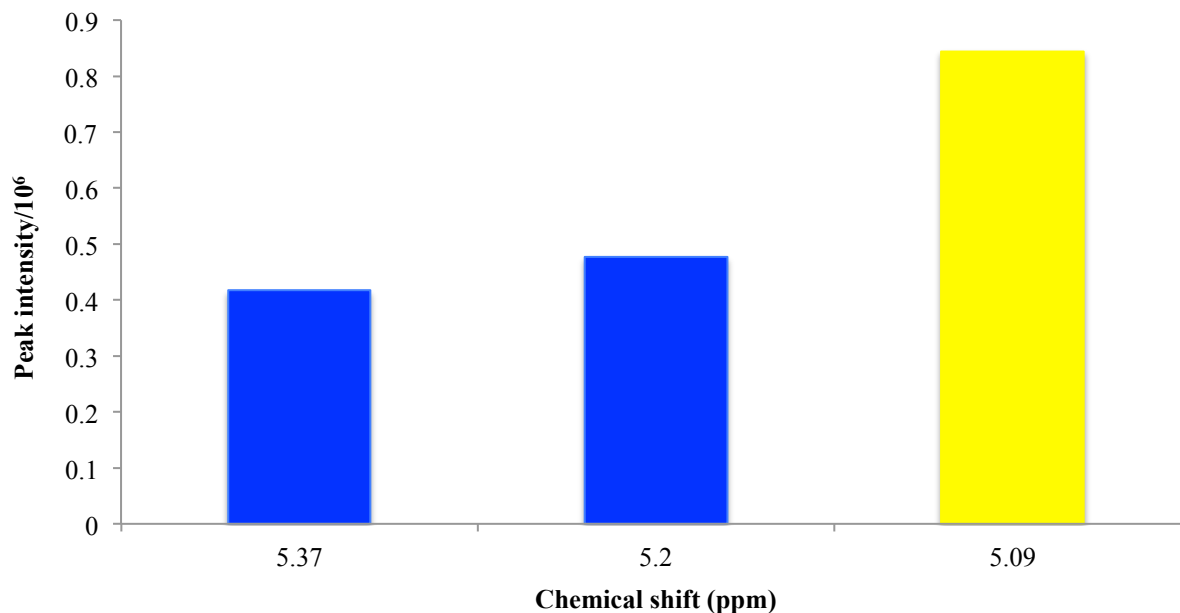


**Figure 4.19** – Plot of “standard” peaks identified in the 400 mM NaCl fraction from HB-affinity column. Heparin peaks are in blue and the peak in both DS and CS denoted as “impurity” is in yellow.

At 500 mM NaCl (Figure 4.20), the majority of peaks isolated are from heparin, which is expected since through binding studies with ITC, heparin displayed a high binding affinity (nM range) compared to the other GAGs. Also, FITC-heparin elutes from HB-affinity column at 350 mM and 500 mM NaCl, which is in agreement with the NMR data presented here. There are residual peaks uncovered in the 2 M NaCl fraction (Figure 4.21), but their intensities are extremely low compared to the other fractions (only trace amounts present). This could be due to some small chains getting trapped in the resin beads, causing them to elute slower.

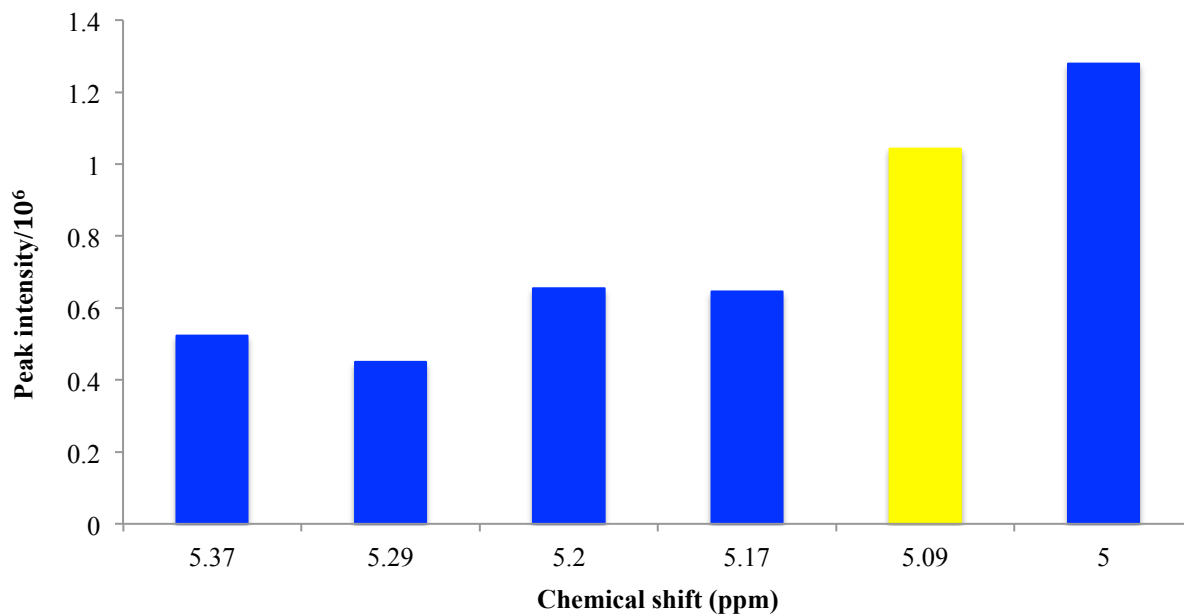


**Figure 4.20** – Plot of “standard” peaks identified in the 500 mM NaCl fraction from HB-affinity column. Heparin peaks are in blue and the peak in both DS and CS denoted as “impurity” is in yellow.

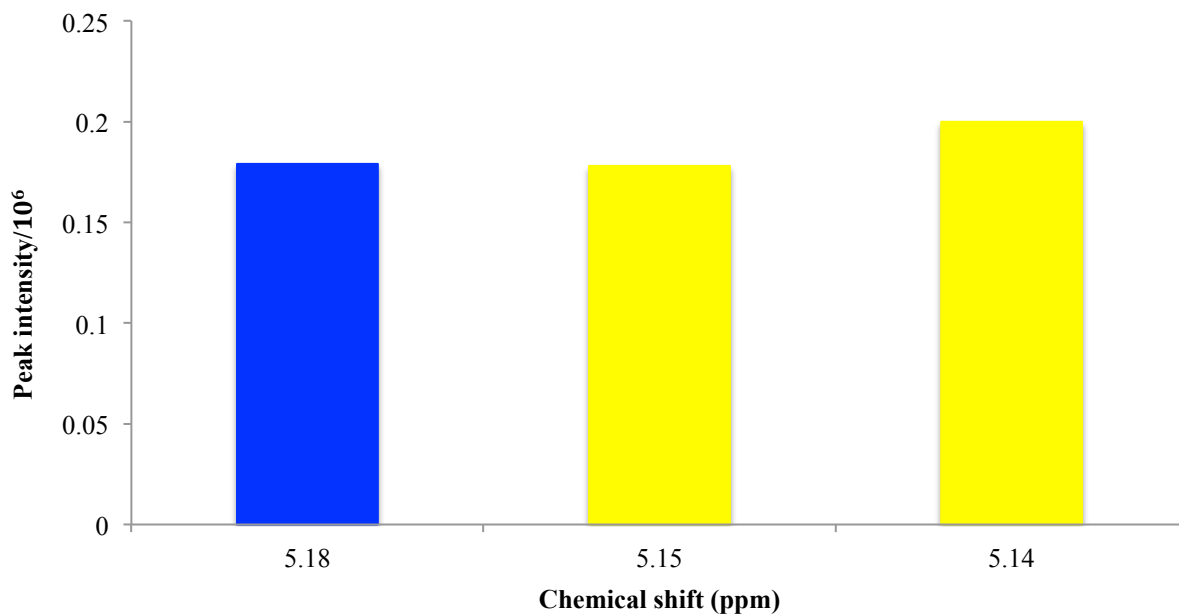


**Figure 4.21** – Plot of “standard” peaks identified in the 2 M NaCl fraction from HB-affinity column. Heparin peak is in blue and the peaks in both DS and CS denoted as “impurities” are in yellow.

As the mysterious peaks of “impurities” still exist in the 500 mM and 2 M NaCl fractions, it can be concluded that they belong to DS instead of CS. DS has a stronger binding affinity for the HB-peptide, as observed from the ITC curves. CS, due to its moderate but less binding affinity than DS, is expected to elute at lower salt concentration and especially in less than 500 mM and 2 M NaCl. As heparin is eluted from the column in each fraction and there were still some impurities in the higher salt concentrations, further mutations need to be performed on the HB-peptide to enable it to selectively bind to heparin alone and not to the other GAGs.

***Glycosaminoglycans can be isolated from chicken intestines:*** After the GAG elution is assessed using HB-peptide as an affinity column, a commercial use of this peptide is desirable. It needs to be examined if the HB-affinity resin can be used to isolate heparin in animal tissues. Normally, heparin is isolated and purified from porcine intestines or bovine lungs<sup>48</sup>. Mad cow disease became an issue early on, and it is difficult to distinguish heparin from pig and cow. To combat this problem, other animal tissue sources need to be investigated for the isolation of heparin in large yields. In order to obtain heparin in a cost-effective manner, the Kumar lab is examining the possibility of isolating heparin from other animal tissue sources. Avian species, such as turkey and chicken, have been shown to contain heparin<sup>49,9</sup>. With Tyson Inc. (with headquarters in Northwest Arkansas) being the largest company dealing with chicken products, it may be a viable proposition to develop methods to isolate and purify heparin from chicken intestines. Contaminants are also present along with the proteoglycans and GAGs in chicken intestines that interfere with the binding affinity of GAGs to the HB-affinity column. These contaminants, such as DNA, proteins, and lipids need to be removed before heparin can be purified on the HB-affinity column. DNase is used to remove DNA, and thermolysin is chosen to remove proteins.

DNA needs to be completely degraded because it is a negatively-charged molecule, which could have some nonspecific binding affinity for HB-peptide. This would in turn interfere with the GAG binding to HB-affinity column. DNase is used first because if thermolysin were used first, it would completely inactivate DNase once it is added. In the next step, the thermostable metalloproteinase cleaves proteins found in the sample. This enzyme preferentially cleaves the N-terminal end of hydrophobic side chains (i.e. Leu, Phe, Ile, Val) as well as Met, His, Tyr, Ala, Asn, Ser, Thr, Gly, Lys, Glu or Asp<sup>50,51</sup>. This enzyme is often times, and in our case, used as a nonspecific proteinase to hydrolyze peptide bonds<sup>52</sup>. A flow chart (Figure 4.22) is provided detailing the steps that are employed for the isolation of GAGs in chicken intestines.

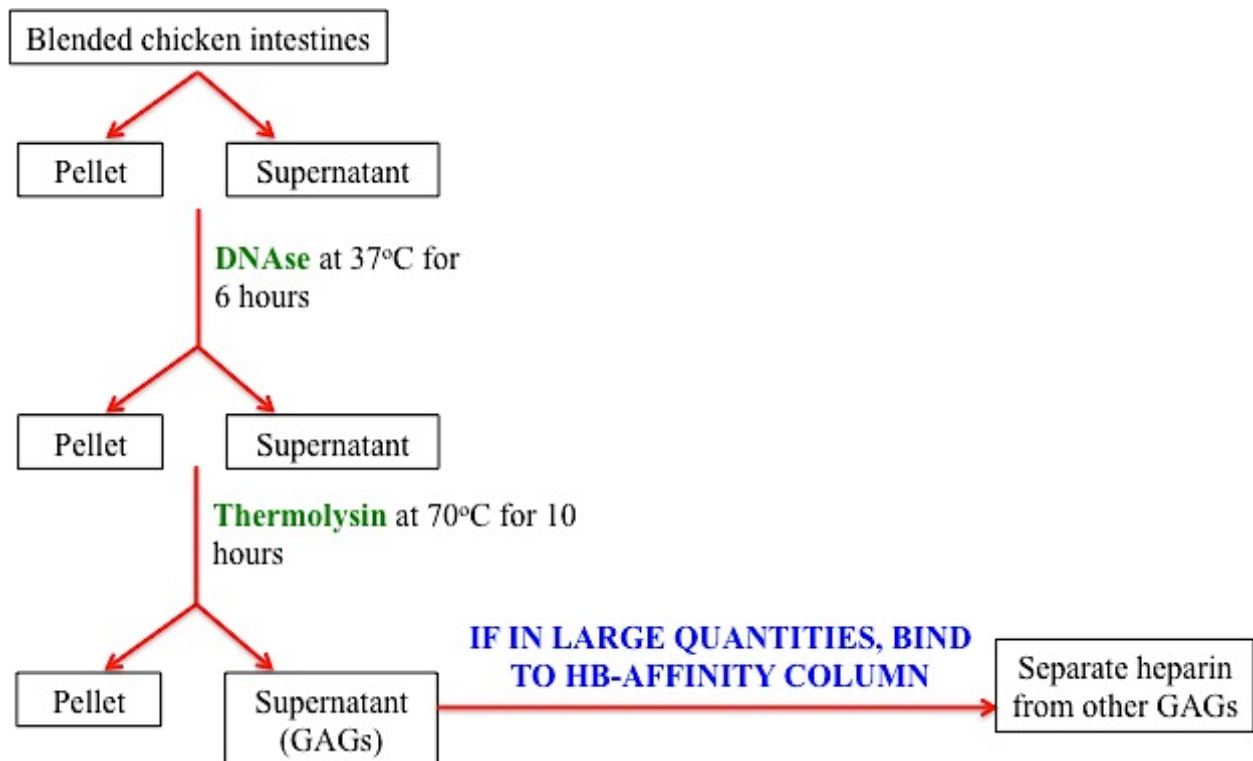


**Figure 4.22** – Flow-chart outlining steps for isolation of GAGs and pure heparin from chicken intestines.

The first step of this process is to determine if DNase is capable of removing DNA before the removal of proteins is implemented. Agarose gel electrophoresis is used to detect DNA that is present in various samples, which aids in determining if the DNase treatment is successful or not. The use of DNase (Figure 4.23) removes the DNA present in the chicken samples (lane 1), as seen on the agarose gel (lane 3), which is successful compared to the “control” sample that had no enzyme present.

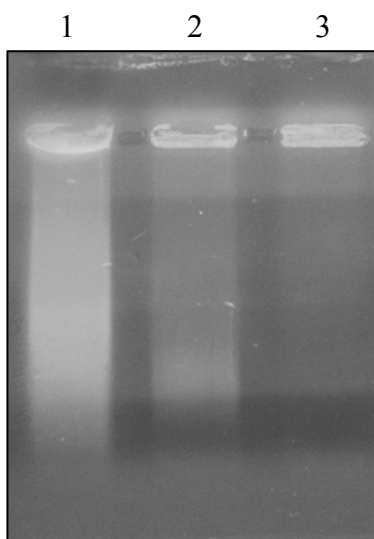


**Figure 4.23** – DNase treatment of chicken sample after homogenization by blender occurred. Lane 1, chicken sample—pre DNase treatment; Lane 2, “control” sample—post 37°C treatment (no DNase addition); Lane 3, “test” sample—post DNase treatment.

Proteins are removed by thermolysin by its ability to degrade proteins at very nonspecific sites, resulting in very small bits of peptides. The high temperature of 70°C also acts as alternative method of denaturing other proteins not susceptible to thermolysin cleavage, because most proteins are not stable at such high temperatures as thermolysin. This enzyme can also be used to degrade the protein portion of the proteoglycan, resulting in GAG liberation from the cell surface. GAGs that would have been lost as proteoglycans on the cell surface are now released as free negatively-charged GAG molecules, ready to be separated on the HB-affinity column.

All proteins in the “test” sample are degraded by thermolysin and heat as seen in lane 4, whereas the “control” sample (lane 6) still contains some protein bands on the gel (Figure 4.24).

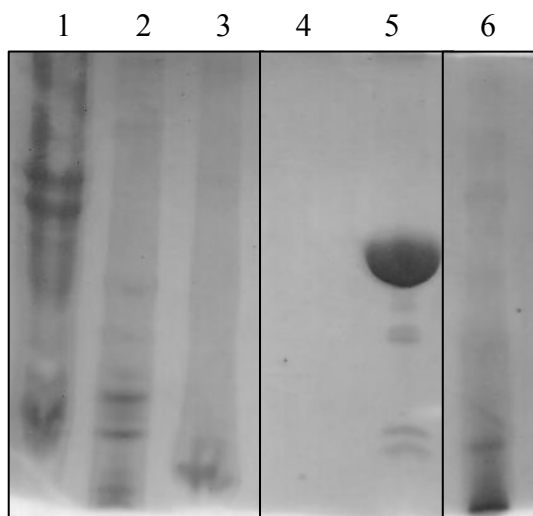


**Figure 4.24** – Thermolysin cleavage of proteins in the chicken sample after DNase treatment occurred. Lane 1, chicken sample—pre thermolysin or DNase treatment; Lane 2, “test” sample—post DNase treatment (supernatant); Lane 3, “test” sample—post DNase treatment (pellet); Lane 4, “test” sample—post DNase (supernatant), post thermolysin; Lane 5, “test” sample—post DNase (pellet), post thermolysin; Lane 6, “control” sample—post 37°C, post 70°C treatment (no enzyme addition).

There is a decrease in the protein bands in the “control” sample, suggesting that the temperature used (70°C) is optimal to denature proteins. Both enzyme treatments result in a cloudy mixture that contains white debris as the top layer, characteristic of lipids. Using the heat and enzyme process, lipids seem to also be removed without the use of an additional enzyme. This process also removes cell debris and other proteins as seen by lane 3 even prior to proteolytic cleavage. If thermolysin is still present in the supernatant even after centrifugation, passing the chicken sample over the HB-affinity column would result in the enzyme’s removal from the GAGs because it is not expected to have any affinity for the HB-peptide.



*Azure A* assay shows only a small amount of GAGs are isolated from chicken intestines: Once all the unnecessary contaminating components are removed, the amount of GAGs that are isolated can be determined by the metachromatic properties of Azure A when bound to the negatively-charged GAGs. Standard plots are generated, based on the absorbance of Azure A at 620 nm for known concentrations of heparin. The metachromasia of Azure A is sensitive to the time of incubation. As seen in the plot of absorbance of the Azure A in the presence of heparin, the absorbance at 620 nm decreases slightly as the time of incubation increases (Figure 4.25). To obtain accurate results, an incubation period of 30 minutes is chosen to account for the slight changes in the Azure A behavior over time.

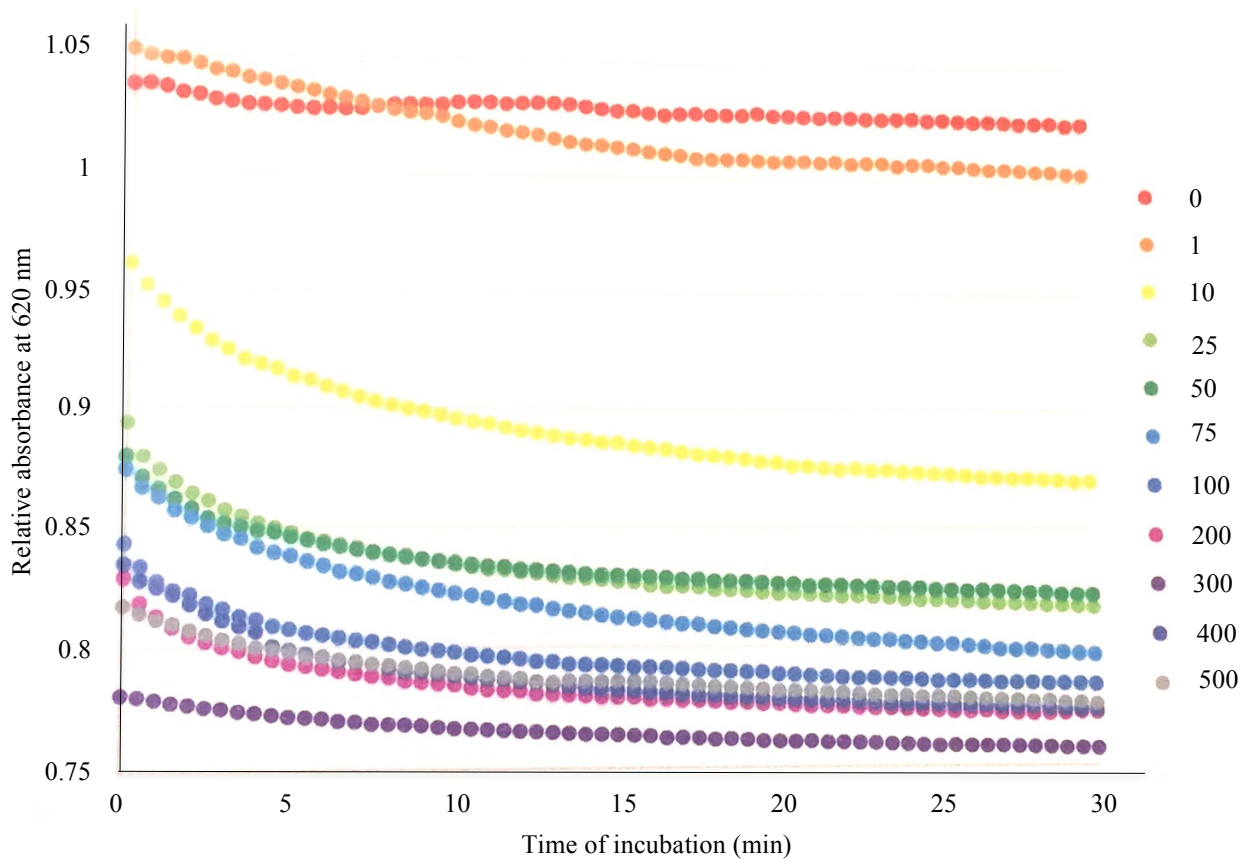


**Figure 4.25** – Plot of the time course incubation of Azure A with varying amounts of heparin. Each color represents a different amount of heparin ( $\mu\text{g/mL}$ ).

The absorbance of Azure A changes slightly over time but reaches a plateau from 20 minutes to 30 minutes. A longer incubation time removes the inaccuracy in absorbance reading that occurs when less time is used (less than 20 minutes).

A standard plot is then developed showing the change in the absorbance of Azure A as a function of the amount of heparin present in the sample at 30 minutes incubation (Figure 4.26). The y-axis was plotted as percentage of absorbance displayed because the starting point (no heparin present) does vary from sample to sample.

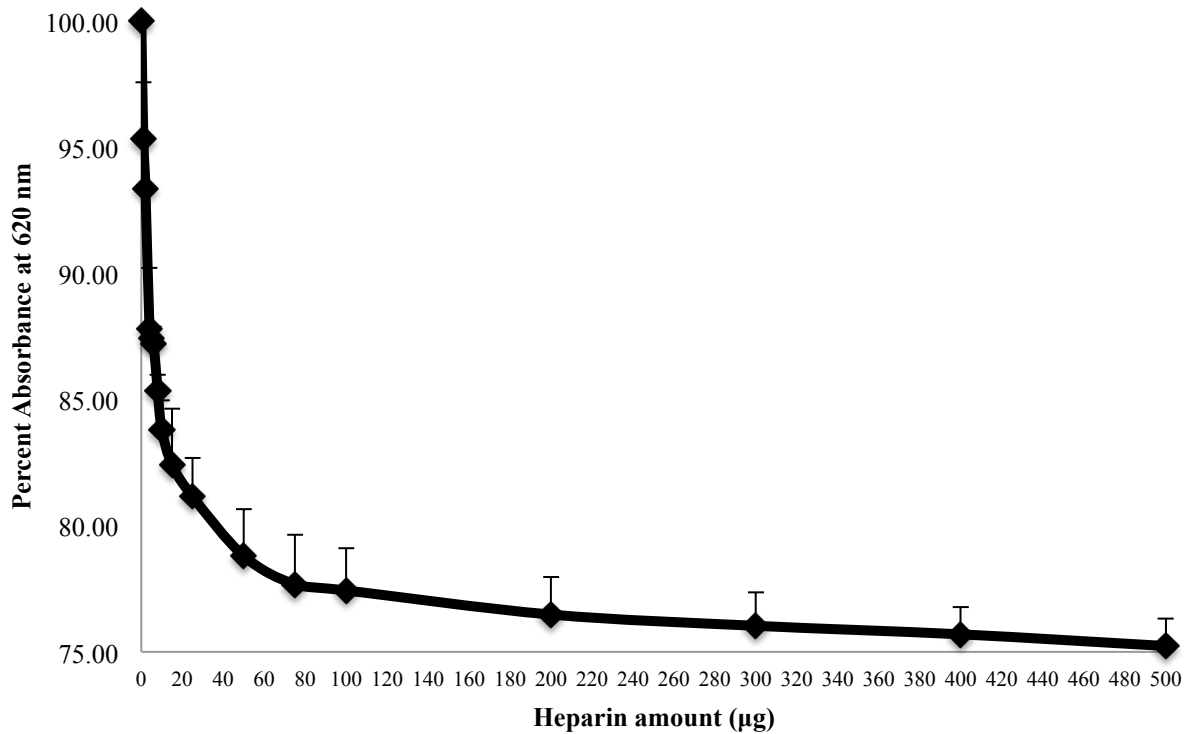


**Figure 4.26** – Plot of the percentage of Azure A absorbance at 620 nm as a function of the amount of heparin present in the sample.

As seen in the plot, there is a linear portion of the curve from 0-10 µg heparin, but beyond this amount, the linearity is lost, and the curve plateaus. The linear component is used to estimate the

amount ( $\mu\text{g}$ ) of heparin is present in the test samples. The isolation of GAGs from the chicken sample is such a small-scale process so it is not expected that a large amount of GAGs be obtained. This reasoning is why the smaller range of heparin can be utilized. A log/log curve was prepared for the range of 0-10  $\mu\text{g}$  heparin to obtain more linearity for the curve (Figure 4.27).

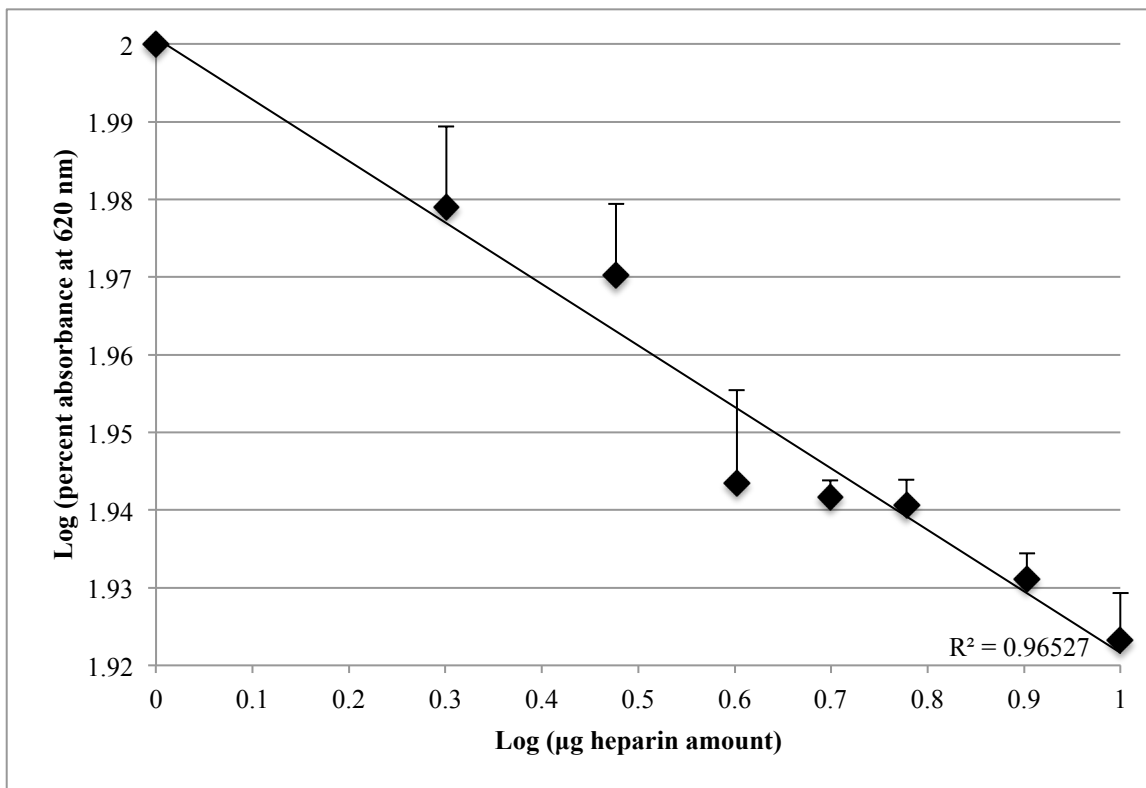


**Figure 4.27** – Linear portion of standard Azure A assay curve obtained as a function of amount of heparin.

Azure A detects sulfated GAGs and cannot distinguish between CS, DS, KS, and heparin. The absorbance reading that is obtained from the chicken sample includes all GAGs present, not just heparin. From the absorbance spectrum, the chicken sample gave an absorbance reading that was about 91% of the initial reading (no heparin present) (Figure 4.28). Based on this value, the amount of heparin that corresponds to this percentage on the standard graph is approximately 3.5  $\mu\text{g}$ . This finding means the chicken sample contains about 3.5  $\mu\text{g}$  of total GAG, not just heparin,

which means the true amount of heparin present is less than this amount. Even though the chicken sample did not produce a better quantity of GAGs, it is promising that the method employed did yield some GAGs.

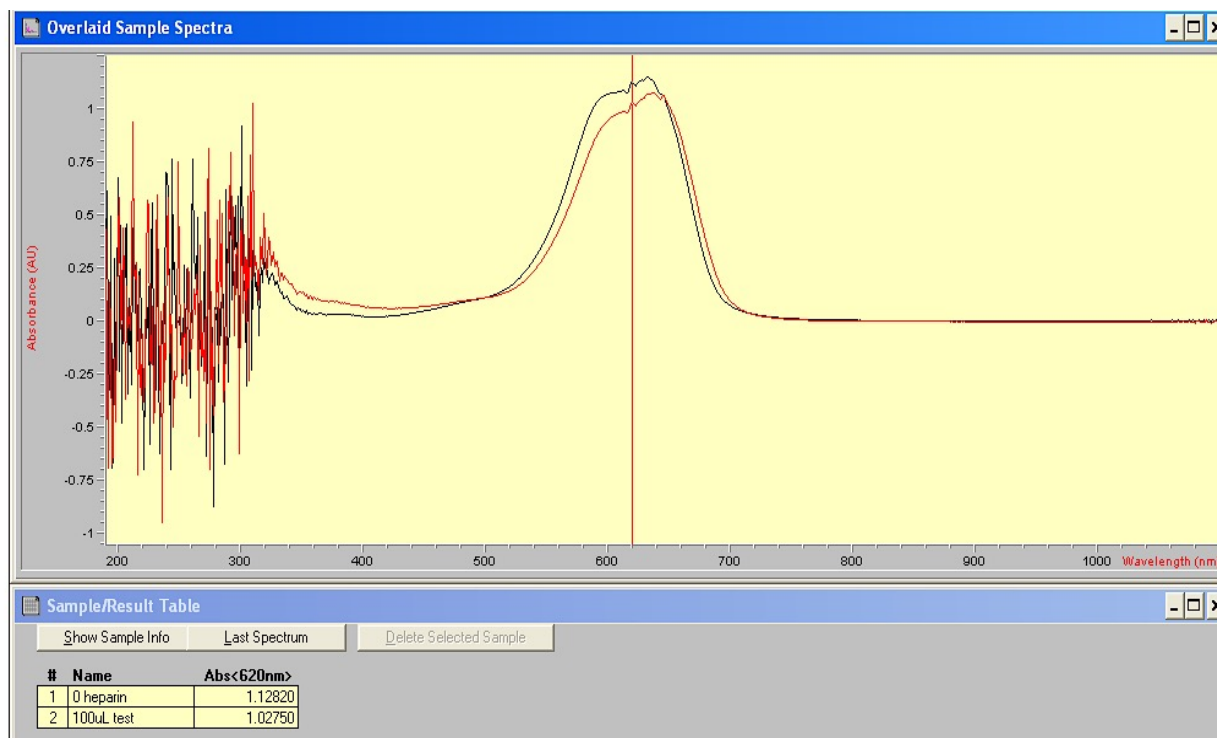


**Figure 4.28** – UV-vis spectrum of Azure A absorbance with the chicken intestine sample after DNase and thermolysin treatment.

The primary goal of this project is to isolate GAGs from chicken intestines, and if enough were isolated, they would then be applied to the HB-affinity column. The preliminary procedure that is accomplished is the isolation of GAGs, but only on a microgram level, and therefore is not sufficient to separate by the HB-affinity column. As the preliminary isolation of GAGs is on a small scale, future endeavors include a large-scale attempt to successfully isolate GAGs using the simple and cost-effective process our lab has developed.

#### 4.5. References

1. Masuko, S.; Linhardt, R. J., Chemoenzymatic synthesis of the next generation of ultralow MW heparin therapeutics. *Future Med. Chem.* **2012**, *4* (3), 289-296.
2. Hwang, S. R.; Seo, D.-H.; Al-Hilal, T. A.; Jeon, O.-C.; Kang, J. H.; Kim, S.-H.; Kim, H. S.; Chang, Y.-T.; Kang, Y. M.; Yang, V. C.; Byun, Y., Orally active desulfated low molecular weight heparin and deoxycholic acid conjugate, 6ODS-LHbD, suppresses neovascularization and bone destruction in arthritis. *J. Controlled Release* **2012**, *163* (3), 374-384.
3. Beni, S.; Limtiaco, J. F. K.; Larive, C. K., Analysis and characterization of heparin impurities. *Anal. Bioanal. Chem.* **2011**, *399* (2), 527-539.
4. Guerrini, M.; Beccati, D.; Shriver, Z.; Naggi, A.; Viswanathan, K.; Bisio, A.; Capila, I.; Lansing, J. C.; Guglieri, S.; Fraser, B.; Al-Hakim, A.; Gunay, N. S.; Zhang, Z.; Robinson, L.; Buhse, L.; Nasr, M.; Woodcock, J.; Langer, R.; Venkataraman, G.; Linhardt, R. J.; Casu, B.; Torri, G.; Sasisekharan, R., Oversulfated chondroitin sulfate is a contaminant in heparin associated with adverse clinical events. *Nat. Biotechnol.* **2008**, *26* (6), 669-675.
5. Kishimoto, T. K.; Viswanathan, K.; Ganguly, T.; Elankumaran, S.; Smith, S.; Pelzer, K.; Lansing, J. C.; Sriranganathan, N.; Zhao, G.; Galcheva-Gargova, Z.; Al-Hakim, A.; Bailey, G. S.; Fraser, B.; Roy, S.; Rogers-Cotrone, T.; Buhse, L.; Whary, M.; Fox, J.; Nasr, M.; Dal Pan, G. J.; Shriver, Z.; Langer, R. S.; Venkataraman, G.; Austen, K. F.; Woodcock, J.; Sasisekharan, R., Contaminated heparin associated with adverse clinical events and activation of the contact system. *N. Engl. J. Med.* **2008**, *358* (23), 2457-2467.
6. Li, B.; Suwan, J.; Martin, J. G.; Zhang, F.; Zhang, Z.; Hoppensteadt, D.; Clark, M.; Fareed, J.; Linhardt, R. J., Oversulfated chondroitin sulfate interaction with heparin-binding proteins: New insights into adverse reactions from contaminated heparins. *Biochem. Pharmacol.* **2009**, *78* (3), 292-300.
7. Maruyama, T.; Toida, T.; Imanari, T.; Yu, G.; Linhardt, R. J., Conformational changes and anticoagulant activity of chondroitin sulfate following its O-sulfonation. *Carbohydr. Res.* **1998**, *306* (1-2), 35-43.
8. Ruiz-Calero, V.; Saurina, J.; Hernandez-Cassou, S.; Galceran, M. T.; Puignou, L., Proton nuclear magnetic resonance characterisation of glycosaminoglycans using chemometric techniques. *Analyst (Cambridge, U. K.)* **2002**, *127* (3), 407-415.
9. Warda, M.; Gouda, E. M.; Toida, T.; Chi, L.; Linhardt, R. J., Isolation and characterization of raw heparin from dromedary intestine: evaluation of a new source of pharmaceutical heparin. *Comp. Biochem. Physiol., Part C Toxicol. Pharmacol.* **2003**, *136C* (4), 357-365.

10. Griffin, C. C.; Linhardt, R. J.; Van Gorp, C. L.; Toida, T.; Hileman, R. E.; Schubert, R. L., II; Brown, S. E., Isolation and characterization of heparan sulfate from crude porcine intestinal mucosal peptidoglycan heparin. *Carbohydr. Res.* **1995**, *276* (1), 183-97.
11. Neville, G. A.; Mori, F.; Holme, K. R.; Perlin, A. S., Monitoring the purity of pharmaceutical heparin preparations by high-field proton nuclear magnetic resonance spectroscopy. *J. Pharm. Sci.* **1989**, *78* (2), 101-4.
12. Ruiz-Calero, V.; Saurina, J.; Galceran, M. T.; Hernandez-Cassou, S.; Puignou, L., Potentiality of proton nuclear magnetic resonance and multivariate calibration methods for the determination of dermatan sulfate contamination in heparin samples. *Analyst (Cambridge, U. K.)* **2000**, *125* (5), 933-938.
13. Pomin, V. H., NMR Chemical Shifts in Structural Biology of Glycosaminoglycans. *Anal. Chem. (Washington, DC, U. S.)* **2014**, *86* (1), 65-94.
14. McEwen, I.; Mulloy, B.; Hellwig, E.; Kozerski, L.; Beyer, T.; Holzgrabe, U.; Wanko, R.; Spieser, J. M.; Rodomonte, A., Determination of Oversulphated Chondroitin Sulphate and Dermatan Sulphate in unfractionated heparin by (1)H-NMR - Collaborative study for quantification and analytical determination of LoD. *Pharmeuropa Bio* **2008**, *2008* (1), 31-9.
15. Limtiaco John, F. K.; Jones Christopher, J.; Larive Cynthia, K., Characterization of heparin impurities with HPLC-NMR using weak anion exchange chromatography. *Anal Chem* **2009**, *81* (24), 10116-23.
16. Zhang, Z.; Weiwer, M.; Li, B.; Kemp, M. M.; Daman, T. H.; Linhardt, R. J., Oversulfated Chondroitin Sulfate: Impact of a Heparin Impurity, Associated with Adverse Clinical Events, on Low-Molecular-Weight Heparin Preparation. *J. Med. Chem.* **2008**, *51* (18), 5498-5501.
17. Petitou, M.; Jacquinet, J.-C.; Sinay; Pierre; Choay; Jean; Lormeau; Jean-Claude; Nassr; Mahmoud Preparation of oligosaccharide uronates, corresponding to fragments of natural mucopolysaccharides, and their biological applications. 1987-115593  
4818816, 19871026., 1989.
18. Lin, F.; Lian, G.; Zhou, Y., Synthesis of Fondaparinux: modular synthesis investigation for heparin synthesis. *Carbohydr. Res.* **2013**, *371*, 32-39.
19. Chen, C.; Yu, B., Efficient synthesis of Idraparinux, the anticoagulant pentasaccharide. *Bioorg. Med. Chem. Lett.* **2009**, *19* (14), 3875-3879.
20. Bhaskar, U.; Hickey, A. M.; Li, G.; Mundra, R. V.; Zhang, F.; Fu, L.; Cai, C.; Ou, Z.; Dordick, J. S.; Linhardt, R. J., A purification process for heparin and precursor polysaccharides using the pH responsive behavior of chitosan. *Biotechnol. Prog.* **2015**, *31* (5), 1348-1359.

21. Saravanan, R.; Shanmugam, A., Isolation and characterization of low molecular weight glycosaminoglycans from marine mollusc *Amusium pleuronectus* (Linne) using chromatography. *Appl. Biochem. Biotechnol.* **2010**, *160* (3), 791-799.
22. Yayon, A.; Klagsbrun, M.; Esko, J. D.; Leder, P.; Ornitz, D. M., Cell surface, heparin-like molecules are required for binding of basic fibroblast growth factor to its high affinity receptor. *Cell (Cambridge, Mass.)* **1991**, *64* (4), 841-8.
23. Ornitz, D. M.; Yayon, A.; Flanagan, J. G.; Svahn, C. M.; Levi, E.; Leder, P., Heparin is required for cell-free binding of basic fibroblast growth factor to a soluble receptor and for mitogenesis in whole cells. *Mol Cell Biol* **1992**, *12* (1), 240-7.
24. Spivak-Kroizman, T.; Lemmon, M. A.; Dikic, I.; Ladbury, J. E.; Pinchasi, D.; Huang, J.; Jaye, M.; Crumley, G.; Schlessinger, J.; Lax, I., Heparin-induced oligomerization of FGF molecules is responsible for FGF receptor dimerization, activation, and cell proliferation. *Cell (Cambridge, Mass.)* **1994**, *79* (6), 1015-24.
25. Aboulaich, N.; Chung, W. K.; Thompson, J. H.; Larkin, C.; Robbins, D.; Zhu, M., A novel approach to monitor clearance of host cell proteins associated with monoclonal antibodies. *Biotechnol. Prog.* **2014**, *30* (5), 1114-1124.
26. Luo, M.; Guan, Y.-X.; Yao, S.-J., On-column refolding of denatured lysozyme by the conjoint chromatography composed of SEC and immobilized recombinant DsbA. *J. Chromatogr. B Anal. Technol. Biomed. Life Sci.* **2011**, *879* (28), 2971-2977.
27. Scopes, R. K., Measurement of protein by spectrophotometry at 205 nm. *Anal Biochem* **1974**, *59* (1), 277-82.
28. Nagasawa, K.; Uchiyama, H., Preparation and properties of biologically active fluorescent heparins. *Biochim. Biophys. Acta, Gen. Subj.* **1978**, *544* (2), 430-40.
29. Laurent, T. C.; Laurent, U. B.; Fraser, J. R., Functions of hyaluronan. *Ann Rheum Dis* **1995**, *54* (5), 429-32.
30. Noble, P. W., Hyaluronan and its catabolic products in tissue injury and repair. *Matrix Biol.* **2002**, *21* (1), 25-29.
31. Taylor, K. R.; Rudisill, J. A.; Gallo, R. L., Structural and Sequence Motifs in Dermatan Sulfate for Promoting Fibroblast Growth Factor-2 (FGF-2) and FGF-7 Activity. *J. Biol. Chem.* **2005**, *280* (7), 5300-5306.
32. Trowbridge, J. M.; Gallo, R. L., Dermatan sulfate: new functions from an old glycosaminoglycan. *Glycobiology* **2002**, *12* (9), 117R-125R.
33. Esko, J.; Linhardt, R., Proteins that Bind Sulfated Glycosaminoglycans. In *Essentials of Glycobiology*, 2nd ed.; Varki, A. e. a., Ed. Cold Spring Harbor: New York, 2009.

34. Raman, R.; Venkataraman, G.; Ernst, S.; Sasisekharan, V.; Sasisekharan, R., Structural specificity of heparin binding in the fibroblast growth factor family of proteins. *Proc. Natl. Acad. Sci. U. S. A.* **2003**, *100* (5), 2357-2362.
35. Linhardt, R. J.; Al-Hakim, A.; Liu, J.; Hoppensteadt, D.; Mascellani, G.; Bianchini, P.; Fareed, J., Structural features of dermatan sulfates and their relationship to anticoagulant and antithrombotic activities. *Biochem. Pharmacol.* **1991**, *42* (8), 1609-19.
36. Igarashi, N.; Takeguchi, A.; Sakai, S.; Akiyama, H.; Higashi, K.; Toida, T., Effect of molecular sizes of chondroitin sulfate on interaction with L-selectin. *Int. J. Carbohydr. Chem.* **2013**, 856142, 9 pp.
37. Linhardt, R. J.; Rice, K. G.; Kim, Y. S.; Engelken, J. D.; Weiler, J. M., Homogeneous, structurally defined heparin-oligosaccharides with low anticoagulant activity inhibit the generation of the amplification pathway C3 convertase in vitro. *J. Biol. Chem.* **1988**, *263* (26), 13090-6.
38. Hileman, R. E.; Fromm, J. R.; Weiler, J. M.; Linhardt, R. J., Glycosaminoglycan-protein interactions: definition of consensus sites in glycosaminoglycan binding proteins. *Bioessays* **1998**, *20* (2), 156-67.
39. Osmond, R. I. W.; Kett, W. C.; Skett, S. E.; Coombe, D. R., Protein-heparin interactions measured by BIAcore 2000 are affected by the method of heparin immobilization. *Anal. Biochem.* **2002**, *310* (2), 199-207.
40. Gray, E.; Mulloy, B.; Barrowcliffe, T. W., Heparin and low-molecular-weight heparin. *Thromb. Haemostasis* **2008**, *99* (5), 807-818.
41. Tao, H.; Liu, W.; Simmons, B. N.; Harris, H. K.; Cox, T. C.; Massiah, M. A., Purifying natively folded proteins from inclusion bodies using sarkosyl, triton X-100, and CHAPS. *BioTechniques* **2010**, *48* (1), 61-62, 64.
42. Hung, Y.-F.; Valda, O.; Schuenke, S.; Stern, O.; Koenig, B. W.; Willbold, D.; Hoffmann, S., Recombinant production of the amino terminal cytoplasmic region of dengue virus non-structural protein 4A for structural studies. *PLoS One* **2014**, *9* (1), e86482/1-e86482/10, 10 pp.
43. Guan, Y.-X.; Fei, Z.-Z.; Luo, M.; Jin, T.; Yao, S.-J., Chromatographic refolding of recombinant human interferon gamma by an immobilized sht GroEL191-345 column. *J. Chromatogr. A* **2006**, *1107* (1-2), 192-197.
44. Beyer, T.; Diehl, B.; Randel, G.; Humpfer, E.; Schaefer, H.; Spraul, M.; Schollmayer, C.; Holzgrabe, U., Quality assessment of unfractionated heparin using <sup>1</sup>H nuclear magnetic resonance spectroscopy. *J. Pharm. Biomed. Anal.* **2008**, *48* (1), 13-19.
45. Lee, S. E.; Chess, E. K.; Rabinow, B.; Ray, G. J.; Szabo, C. M.; Melnick, B.; Miller, R. L.; Nair, L. M.; Moore, E. G., NMR of heparin API: investigation of unidentified signals in the USP-specified range of 2.12-3.00 ppm. *Anal. Bioanal. Chem.* **2011**, *399* (2), 651-662.



46. Zhang, Z.; Li, B.; Suwan, J.; Zhang, F.; Wang, Z.; Liu, H.; Mulloy, B.; Linhardt, R. J., Analysis of pharmaceutical heparins and potential contaminants using <sup>1</sup>H-NMR and PAGE. *J. Pharm. Sci.* **2009**, *98* (11), 4017-4026.
47. Ustun, B.; Sanders, K. B.; Dani, P.; Kellenbach, E. R., Quantification of chondroitin sulfate and dermatan sulfate in danaparoid sodium by (<sup>1</sup>H) NMR spectroscopy and PLS regression. *Anal Bioanal Chem* **2011**, *399* (2), 629-34.
48. Linhardt, R. J.; Gunay, N. S., Production and chemical processing of low molecular weight heparins. *Semin. Thromb. Hemostasis* **1999**, *25* (Suppl. 3), 5-16.
49. Bianchini, P.; Liverani, L.; Mascellani, G.; Parma, B., Heterogeneity of unfractionated heparins studied in connection with species, source, and production processes. *Semin Thromb Hemost* **1997**, *23* (1), 3-10.
50. Ligne, T.; Pauthe, E.; Monti, J.-P.; Gacel, G.; Larreta-Garde, V., Additional data about thermolysin specificity in buffer- and glycerol-containing media. *Biochim. Biophys. Acta, Protein Struct. Mol. Enzymol.* **1997**, *1337* (1), 143-148.
51. Heinrikson, R. L., Applications of thermolysin in protein structural analysis. *Methods Enzymol.* **1977**, *47* (Enzyme Struct., Part E), 175-89.
52. Adekoya, O. A.; Sylte, I., The thermolysin family (M4) of enzymes: Therapeutic and biotechnological potential. *Chem. Biol. Drug Des.* **2009**, *73* (1), 7-16.

**Chapter 5**  
**Conclusions**

Heparin is an extremely important molecule that is naturally present in the body. Exogenous heparin is also used as an anticoagulant during heart bypass surgeries and also to prevent blood clot formation. In 2008, heparin became contaminated with GAGs that are structurally similar to heparin. These contaminants activated various pathways that led to anaphylactic shock, hypotension, and death for many around the world. There is a need for the purification of heparin, which prompted our lab to delve into what molecules naturally bind to heparin to hopefully separate this crucial GAG from the contaminants.

HBPs are a large class of very diverse proteins that specifically bind to heparin for their activity to occur in the body. These unique proteins have distinct regions in their sequence (HBR) responsible for their ability to bind tightly to heparin. The ability for HBPs to bind to heparin for their function is not solely dependent on the amino acid sequence of the HBR, but also on the spatial orientation of the residues once the protein folds correctly. Having the positively-charged residues facing a certain direction enables them to come in contact with the negatively-charged heparin molecule. Many studies have been performed on the structural components of these regions to determine in exactly what manner they bind to heparin. Our lab has constructed a heparin-binding peptide that is modeled after the structural features of the HBPs, which enables the peptide to bind to heparin with high affinity.

The first use of this HB-peptide is as an affinity tag for the purification of various recombinant proteins by heparin-Sepharose affinity chromatography. The proteins chosen (C2A, CALb3, and S100A13) are not known to naturally bind to heparin, which allows the HB-peptide to hold all of the heparin-binding capability. These proteins were expressed and purified to homogeneity under native and denaturing conditions (urea, not guanidine hydrochloride). HB-fused C2A, CALb3, and S100A13A eluted from heparin-Sepharose in 500 mM NaCl, 1 M NaCl,

and 1 M to 2 M NaCl, respectively. The promising find was the expression and purification of CA1b3 because in previous attempts, this protein has not been expressed or purified to homogeneity in good yield. The affinity tag was also successfully removed by proteolytic cleavage (thrombin and TEV protease). Preliminary studies have also revealed that HB-peptide does indeed interact with heparin. Binding studies by ITC showed that HB-peptide binds with a good affinity to heparin in a two-site binding model ( $K_d \sim 0.8$  and  $17 \mu\text{M}$ ). HB-peptide also adopts an alpha helical structure in the presence of heparin, which is also seen in other HBP consensus motifs. There is a moderate change in structure once heparin binds to the peptide, as seen by the shift in crosspeaks in  $^1\text{H}$ - $^{15}\text{N}$  HSQC spectroscopy.

Detection of the expression and purification profiles of the various HB-fusion proteins is desirable, especially if the yield of proteins is too low to visually observe by SDS-PAGE. Polyclonal antibodies generated against the first 12 amino acid residues in the HB-peptide allowed for successful detection of HB-fusion proteins in crude cell samples during expression and purification. The use of secondary antibodies oftentimes leads to nonspecific interactions to occur, resulting in false signals on the nitrocellulose membrane. As we increased the salt concentration from 150 mM NaCl to 750 mM NaCl, the nonspecific bands were successfully removed from the membrane, enabling a more reliable detection method using the anti-HB polyclonal antibodies. The antibodies were able to detect HB-fused C2A down to 10 ng in 150 mM NaCl and 50 ng when the salt concentration is increased. These antibodies were proven to be specific towards the epitope in HB-peptide, whereas the target protein shows no binding to the antibodies. This was seen in the antibodies detecting only the HB-fusion protein and HB-peptide, but not GST alone. These antibodies can also be used to detect HB-fusion proteins in other crude cell lines, such as bacteria, yeast, and mammal.

The original reason this HB-peptide was designed was for the separation of heparin from other GAGs, ultimately leading to its purification. It needed to be determined that HB-peptide binds specifically to heparin, compared to the other GAGs. Based on ITC measurements, the peptide has stronger binding affinity for heparin ( $K_d \sim \text{nM}$ ), then DS ( $K_d \sim \text{low } \mu\text{M}$ ), then CS ( $K_d \sim \text{higher } \mu\text{M}$ ), and lastly HA (no binding observed). This finding is promising that heparin would bind the tightest to the HB-affinity column, allowing heparin to be separated from the other GAGs. This affinity column works in a similar fashion as HBPs are purified on heparin-Sepharose. HB-peptide was successfully coupled onto NHS-Sepharose resin with efficiency as high as 70%. This HB-affinity column was then used to monitor the elution profile of FITC-heparin for initial binding studies. FITC-heparin eluted from the affinity column from 350 mM to 500 mM NaCl, whereas the “negative” column that contained no HB-peptide did not retain FITC-heparin past 0 mM NaCl. The HB-affinity column was then used to separate a mixture of CS, DS, and heparin from one another fairly well. There were only a few “contaminating” molecules of CS or DS present at higher salt concentrations as heparin eluted (400 mM to 500 mM NaCl), as observed by  $^1\text{H}$  NMR spectroscopy. Certain unique peaks present in each pure GAG were used as identifiers for the specific GAG in a mixture. Another endeavor using HB-affinity column was the attempt to isolate GAGs from chicken intestines. After treatment with DNase (removed DNA), thermolysin (removed proteins), and heat (removed lipids), 4  $\mu\text{g}$  of total GAGs were successfully isolated, as seen by the Azure A assay. This production of GAGs from chicken intestines did not warrant enough yields to try and separate the mixture of GAGs using the HB-affinity column.

Future work that needs to be performed is the modification of the HB-peptide to bind much tighter to heparin (low nM), leading to greater separation of GAGs from one another. If heparin binds extremely tight to the HB-affinity column, and the other GAGs have no comparison in binding affinities, heparin could then be eluted at extremely high salt concentrations (>2 M NaCl). This high of salt concentration would not contain any other GAG contaminant. Isolation of GAGs from chicken intestines needs to be optimized further to obtain larger amounts of GAGs. This would enable the GAG mixture to be loaded onto the HB-affinity column for the purification of heparin. The last modification that needs to occur is improvement of Western blotting technique employed using the anti-HB polyclonal antibodies. There is a need to reduce the nonspecific antibodies-antigen interactions seen by multiple bands on the membrane. Monoclonal antibodies can be used for specific detection of HB-fusion proteins if desired. Overall, this HB-peptide has proved to be a key player in recombinant protein purification, immunoblotting, and heparin purification.

## Biosafety Committee Approval Letter



UNIVERSITY OF  
ARKANSAS

Office of Research Compliance

September 17, 2015

MEMORANDUM

TO: Dr. Suresh Kumar Thallapuram  
FROM: Dr. Ines Pinto  
Institutional BioSafety Committee

RE: IBC Protocol Approval

IBC Protocol #: 13002

Protocol Title: "Purification and characterization of novel affinity tag"

Approved Project Period: Start Date: August 03, 2015  
Expiration Date: August 03, 2018

The Institutional Biosafety Committee (IBC) has approved the Renewal of Protocol 13002, "Purification and characterization of novel affinity tag". You may continue your study.

If further modifications are made to the protocol during the study, please submit a written request to the IBC for review and approval before initiating any changes.

The IBC appreciates your assistance and cooperation in complying with University and Federal guidelines for research involving hazardous biological materials.

## Copyright Permission for Figure 1.5

### JOHN WILEY AND SONS LICENSE TERMS AND CONDITIONS

Apr 19, 2016

---

This Agreement between Jacqueline Morris ("You") and John Wiley and Sons ("John Wiley and Sons") consists of your license details and the terms and conditions provided by John Wiley and Sons and Copyright Clearance Center.

License Number	3852830457780
License date	Apr 19, 2016
Licensed Content Publisher	John Wiley and Sons
Licensed Content Publication	Angewandte Chemie International Edition
Licensed Content Title	Heparin-Protein Interactions
Licensed Content Author	Ishan Capila, Robert J. Linhardt
Licensed Content Date	Jan 29, 2002
Pages	23
Type of use	Dissertation/Thesis
Requestor type	University/Academic
Format	Electronic
Portion	Figure/table
Number of figures/tables	2
Original Wiley figure/table number(s)	Figure 2B, Figure 3
Will you be translating?	No
Title of your thesis / dissertation	Heparin-peptide interactions
Expected completion date	Aug 2016
Expected size (number of pages)	200
Requestor Location	Jacqueline Morris 1235 w mount comfort, 209  FAYETTEVILLE, AR 72703 United States Attn: Jacqueline Morris
Billing Type	Invoice
Billing Address	Jacqueline Morris 1235 w mount comfort, 209  FAYETTEVILLE, AR 72703 United States Attn: Jacqueline Morris



Total

0.00 USD

Terms and Conditions

### TERMS AND CONDITIONS

This copyrighted material is owned by or exclusively licensed to John Wiley & Sons, Inc. or one of its group companies (each a "Wiley Company") or handled on behalf of a society with which a Wiley Company has exclusive publishing rights in relation to a particular work (collectively "WILEY"). By clicking "accept" in connection with completing this licensing transaction, you agree that the following terms and conditions apply to this transaction (along with the billing and payment terms and conditions established by the Copyright Clearance Center Inc., ("CCC's Billing and Payment terms and conditions"), at the time that you opened your RightsLink account (these are available at any time at <http://myaccount.copyright.com>).

#### Terms and Conditions

- The materials you have requested permission to reproduce or reuse (the "Wiley Materials") are protected by copyright.
- You are hereby granted a personal, non-exclusive, non-sub licensable (on a stand-alone basis), non-transferable, worldwide, limited license to reproduce the Wiley Materials for the purpose specified in the licensing process. This license, **and any CONTENT (PDF or image file) purchased as part of your order**, is for a one-time use only and limited to any maximum distribution number specified in the license. The first instance of republication or reuse granted by this license must be completed within two years of the date of the grant of this license (although copies prepared before the end date may be distributed thereafter). The Wiley Materials shall not be used in any other manner or for any other purpose, beyond what is granted in the license. Permission is granted subject to an appropriate acknowledgement given to the author, title of the material/book/journal and the publisher. You shall also duplicate the copyright notice that appears in the Wiley publication in your use of the Wiley Material. Permission is also granted on the understanding that nowhere in the text is a previously published source acknowledged for all or part of this Wiley Material. Any third party content is expressly excluded from this permission.
- With respect to the Wiley Materials, all rights are reserved. Except as expressly granted by the terms of the license, no part of the Wiley Materials may be copied, modified, adapted (except for minor reformatting required by the new Publication), translated, reproduced, transferred or distributed, in any form or by any means, and no derivative works may be made based on the Wiley Materials without the prior permission of the respective copyright owner. **For STM Signatory Publishers clearing permission under the terms of the [STM Permissions Guidelines](#) only, the terms of the license are extended to include subsequent editions and for editions in other languages, provided such editions are for the work as a whole in situ and does not involve the separate exploitation of the permitted figures or extracts**, You may not alter, remove or suppress in any manner any copyright, trademark or other notices displayed by the Wiley Materials. You may not license, rent, sell, loan, lease, pledge, offer as security, transfer or assign the Wiley Materials on a stand-alone basis, or any of the rights granted to you hereunder to any other person.
- The Wiley Materials and all of the intellectual property rights therein shall at all times

remain the exclusive property of John Wiley & Sons Inc, the Wiley Companies, or their respective licensors, and your interest therein is only that of having possession of and the right to reproduce the Wiley Materials pursuant to Section 2 herein during the continuance of this Agreement. You agree that you own no right, title or interest in or to the Wiley Materials or any of the intellectual property rights therein. You shall have no rights hereunder other than the license as provided for above in Section 2. No right, license or interest to any trademark, trade name, service mark or other branding ("Marks") of WILEY or its licensors is granted hereunder, and you agree that you shall not assert any such right, license or interest with respect thereto

- NEITHER WILEY NOR ITS LICENSORS MAKES ANY WARRANTY OR REPRESENTATION OF ANY KIND TO YOU OR ANY THIRD PARTY, EXPRESS, IMPLIED OR STATUTORY, WITH RESPECT TO THE MATERIALS OR THE ACCURACY OF ANY INFORMATION CONTAINED IN THE MATERIALS, INCLUDING, WITHOUT LIMITATION, ANY IMPLIED WARRANTY OF MERCHANTABILITY, ACCURACY, SATISFACTORY QUALITY, FITNESS FOR A PARTICULAR PURPOSE, USABILITY, INTEGRATION OR NON-INFRINGEMENT AND ALL SUCH WARRANTIES ARE HEREBY EXCLUDED BY WILEY AND ITS LICENSORS AND WAIVED BY YOU.
- WILEY shall have the right to terminate this Agreement immediately upon breach of this Agreement by you.
- You shall indemnify, defend and hold harmless WILEY, its Licensors and their respective directors, officers, agents and employees, from and against any actual or threatened claims, demands, causes of action or proceedings arising from any breach of this Agreement by you.
- IN NO EVENT SHALL WILEY OR ITS LICENSORS BE LIABLE TO YOU OR ANY OTHER PARTY OR ANY OTHER PERSON OR ENTITY FOR ANY SPECIAL, CONSEQUENTIAL, INCIDENTAL, INDIRECT, EXEMPLARY OR PUNITIVE DAMAGES, HOWEVER CAUSED, ARISING OUT OF OR IN CONNECTION WITH THE DOWNLOADING, PROVISIONING, VIEWING OR USE OF THE MATERIALS REGARDLESS OF THE FORM OF ACTION, WHETHER FOR BREACH OF CONTRACT, BREACH OF WARRANTY, TORT, NEGLIGENCE, INFRINGEMENT OR OTHERWISE (INCLUDING, WITHOUT LIMITATION, DAMAGES BASED ON LOSS OF PROFITS, DATA, FILES, USE, BUSINESS OPPORTUNITY OR CLAIMS OF THIRD PARTIES), AND WHETHER OR NOT THE PARTY HAS BEEN ADVISED OF THE POSSIBILITY OF SUCH DAMAGES. THIS LIMITATION SHALL APPLY NOTWITHSTANDING ANY FAILURE OF ESSENTIAL PURPOSE OF ANY LIMITED REMEDY PROVIDED HEREIN.
- Should any provision of this Agreement be held by a court of competent jurisdiction to be illegal, invalid, or unenforceable, that provision shall be deemed amended to achieve as nearly as possible the same economic effect as the original provision, and the legality, validity and enforceability of the remaining provisions of this Agreement shall not be affected or impaired thereby.

- The failure of either party to enforce any term or condition of this Agreement shall not constitute a waiver of either party's right to enforce each and every term and condition of this Agreement. No breach under this agreement shall be deemed waived or excused by either party unless such waiver or consent is in writing signed by the party granting such waiver or consent. The waiver by or consent of a party to a breach of any provision of this Agreement shall not operate or be construed as a waiver of or consent to any other or subsequent breach by such other party.
- This Agreement may not be assigned (including by operation of law or otherwise) by you without WILEY's prior written consent.
- Any fee required for this permission shall be non-refundable after thirty (30) days from receipt by the CCC.
- These terms and conditions together with CCC's Billing and Payment terms and conditions (which are incorporated herein) form the entire agreement between you and WILEY concerning this licensing transaction and (in the absence of fraud) supersedes all prior agreements and representations of the parties, oral or written. This Agreement may not be amended except in writing signed by both parties. This Agreement shall be binding upon and inure to the benefit of the parties' successors, legal representatives, and authorized assigns.
- In the event of any conflict between your obligations established by these terms and conditions and those established by CCC's Billing and Payment terms and conditions, these terms and conditions shall prevail.
- WILEY expressly reserves all rights not specifically granted in the combination of (i) the license details provided by you and accepted in the course of this licensing transaction, (ii) these terms and conditions and (iii) CCC's Billing and Payment terms and conditions.
- This Agreement will be void if the Type of Use, Format, Circulation, or Requestor Type was misrepresented during the licensing process.
- This Agreement shall be governed by and construed in accordance with the laws of the State of New York, USA, without regards to such state's conflict of law rules. Any legal action, suit or proceeding arising out of or relating to these Terms and Conditions or the breach thereof shall be instituted in a court of competent jurisdiction in New York County in the State of New York in the United States of America and each party hereby consents and submits to the personal jurisdiction of such court, waives any objection to venue in such court and consents to service of process by registered or certified mail, return receipt requested, at the last known address of such party.

#### **WILEY OPEN ACCESS TERMS AND CONDITIONS**

Wiley Publishes Open Access Articles in fully Open Access Journals and in Subscription journals offering Online Open. Although most of the fully Open Access journals publish open access articles under the terms of the Creative Commons Attribution (CC BY) License only, the subscription journals and a few of the Open Access Journals offer a choice of Creative Commons Licenses. The license type is clearly identified on the article.

#### **The Creative Commons Attribution License**

The [Creative Commons Attribution License \(CC-BY\)](#) allows users to copy, distribute and transmit an article, adapt the article and make commercial use of the article. The CC-BY license permits commercial and non-

**Creative Commons Attribution Non-Commercial License**

The [Creative Commons Attribution Non-Commercial \(CC-BY-NC\)License](#) permits use, distribution and reproduction in any medium, provided the original work is properly cited and is not used for commercial purposes.(see below)

**Creative Commons Attribution-Non-Commercial-NoDerivs License**

The [Creative Commons Attribution Non-Commercial-NoDerivs License](#) (CC-BY-NC-ND) permits use, distribution and reproduction in any medium, provided the original work is properly cited, is not used for commercial purposes and no modifications or adaptations are made. (see below)

**Use by commercial "for-profit" organizations**

Use of Wiley Open Access articles for commercial, promotional, or marketing purposes requires further explicit permission from Wiley and will be subject to a fee.

Further details can be found on Wiley Online Library

<http://olabout.wiley.com/WileyCDA/Section/id-410895.html>

**Other Terms and Conditions:**

**v1.10 Last updated September 2015**

**Questions? [customercare@copyright.com](mailto:customercare@copyright.com) or +1-855-239-3415 (toll free in the US) or +1-978-646-2777.**

---

---

## Copyright Permission for Figure 2.32

**Jacqueline Morris** <jagreer@email.uark.edu>  
To: eic@biochem.acs.org

Wed, Apr 20, 2016 at 8:39 AM

Hi,

I am writing my dissertation and I wanted to compare an NMR spectrum I have acquired to one from a Biochemistry Journal article. The citation of the article is as follows:

Rajalingam, D.; Graziani, I.; Prudovsky, I.; Yu, C.; Kumar, T. K. S., Relevance of Partially Structured States in the Non-Classical Secretion of Acidic Fibroblast Growth Factor. *Biochemistry* **2007**, *46* (32), 9225-9238

I wanted to reproduce an NMR spectrum (Figure 7) of C2A, just the NMR spectrum. Please let me know what I need to do to acquire permission to reproduce this without modifying the figure. Thanks,

Jacqueline Morris  
PhD Candidate, University of Arkansas

---

**Currey Courtney** <eic@biochem.acs.org>  
To: Jacqueline Morris <jagreer@email.uark.edu>

Wed, Apr 20, 2016 at 10:34 AM

Dear Ms. Morris,

Thank you for your inquiry. Yes, you may reproduce the NMR spectrum from this paper in your dissertation.

Best of luck in your future endeavors.

Best regards,

Currey Courtney  
Journal office administrator, Biochemistry